Synthesis of Natural Product-Based Probes for the Central Nervous System

By

Andrew P. Riley

Submitted to the graduate degree program in Chemistry and the Graduate Faculty of the University of Kansas in partial fulfillment of the requirements for the degree of Doctor of Philosophy.

_____

Chairperson: Dr. Thomas E. Prisinzano

_____

Dr. Jeffrey Aubé

_____

Dr. Michael D. Clift

_____

Dr. Paul R. Hanson

_____

Dr. Jon A. Tunge

Date Defended: April 28, 2015

The Dissertation Committee for Andrew P. Riley

certifies that this is the approved version of the following dissertation:

Synthesis of Natural Product-Based Probes for the Central Nervous System

_____

Chairperson: Dr. Thomas E. Prisinzano

Date approved: May 6, 2015

**Abstract**

The number of individuals affected by a central nervous system disorder continues to steadily increase. Unfortunately, in many cases the available therapeutic options leaves these diseases undertreated and additional molecular probes are needed to fully understand these conditions. Historically, natural products have served as a rich source of new molecular scaffolds for developing these probes due to their complex structures and unique ability to perturb biological pathways through diverse mechanisms.

With this in mind, the kappa opioid receptor (KOR) agonist salvinorin A, the mu opioid receptor (MOR) agonist herkinorin, and the anti-tau diarylheptanoid myricanol were identified as potential probes for investigating substance abuse, pain, and Alzheimer's Disease, respectively. To determine how the unique neoclerodane structure of salvinorin A interacts with the KOR, methods to chemical modify the steric and electronic properties of the furan ring were developed. The resulting structure-activity relationships (SAR) identified three compounds that successfully attenuated drug seeking behavior in an animal model of drug relapse. In a separate study, a simple modification to the A-ring of herkinorin was found to drastically increase the potency and selectivity for the MOR, thus increasing the potential in vivo utility of the probe. Additional SAR studies also resulted in the first sub-nanomolar diterpene MOR agonist. Finally, an enantioselective route to both enantiomers of myricanol was developed to provide the necessary material for more extensive biological investigations into the compound's tau degradation mechanism. The three studies described herein, highlight the importance of using chemical synthesis to modify and build complex natural products scaffolds in order to probe biological systems.

**Acknowledgements**

I would first like to thank my family whose unconditional love has helped make this work possible. To my parents, thank you for raising me to be so inquisitive and for always being there to provide answers to my endless questions. Sarah, Jonathon, and Keegan I thank you all for your love and support throughout the years. And to Sara, thank you for being a constant source of encouragement and for always believing in me when I needed it the most.

I would also like to thank my extended family at the University of Kansas. It has been a blessing to be surrounded by the faculty members of the departments of chemistry and medicinal chemistry who have a true passion for both teaching and learning. Particular thanks are due to my advisor Tom who despite my constant struggle has worked to develop me into a scientist rather than simply a chemist. And finally, thank you to my laboratory mates Kim, Karrie, Tammi, Mike, Mark, Marci, Rachel, Chad, Alex, and Stephanie as well as my friends throughout Malott Hall; you have turned the constant grind of graduate school into a truly enjoyable experience.

## Table of Contents

## List of Figures

## List of Schemes

## List of Tables

# I. Introduction

*Challenges in Treating Central Nervous System Disorders*

The central nervous system (CNS), made up of the brain and spinal cord, is arguable the most complex system in the human body. Signals initiated in the brain's 100 billion neurons are transduced through $10^{14}$ synapses to the rest of the central and peripheral nervous systems and control nearly every aspect of life from cognition to the biological events necessary for survival.[1] However, due to the high complexity present in the CNS, diseases causing even small perturbations from normal function often result in severe, life-altering symptoms. Currently, it is estimated that as many as 1.5 billion people suffer from a CNS-related disorder, representing approximately a third of all diagnosed diseases.[2,3] Furthermore, the debilitating nature of many of these diseases creates a significant burden to provide care for those affected, resulting in annual cost totaling more than $317 billion from health care expenditures, loss of earnings, and disability benefits.[4] This amount can only be expected to grow as the average population age continues to rise since the incidence of many CNS diseases increases exponentially after the age of 65.[5] Clearly diseases affecting the CNS represent a serious health care concern and novel therapies are needed to treat this growing problem.

Traditionally the pharmaceutical industry has fulfilled the need for new CNS therapeutics, resulting in several very successful drugs including 21 of the 100 top selling prescription pharmaceutics of 2013 (Table 1.1). Despite this historic success, many pharmaceutical companies have begun reducing and eliminating their CNS discovery

programs.[6] This defunding can largely be attributed to the challenges in bringing a CNS drug to market. Among these challenges are the difficulties in attaining proper brain

**Table 1.1**. List of CNS Pharmaceuticals Found in the 100 Top Selling Pharmaceutical Product List of 2013.

| Rank | Drug | Medical Use | Sales ($, in millions) |
|---|---|---|---|
| 1 | Abilify | Psychosis, depression | 1,600 |
| 7 | Cymbalta | Depression, anxiety | 1,000 |
| 10 | Copaxone | Multiple sclerosis | 851 |
| 18 | Lyrica | Neuropathic pain | 624 |
| 19 | OxyContin | Pain | 585 |
| 26 | Lucentis | Macular degeneration | 460 |
| 27 | Vyvanse | Attention deficit hyperactivity disorder | 447 |
| 29 | Namenda | Alzheimer's Disease | 434 |
| 38 | Methylphenidate | Attention deficit hyperactivity disorder | 327 |
| 39 | Suboxone | Pain, opioid addiction | 321 |
| 46 | Seroquel XR | Psychosis, depression | 291 |
| 48 | Avonex | Multiple sclerosis | 281 |
| 50 | Rebif | Multiple sclerosis | 280 |
| 52 | Gilenya | Multiple sclerosis | 272 |
| 57 | Acetaminophen/ hydrocodone | Pain | 264 |
| 66 | Amphetamine/ dextroamphetamine | Attention deficit hyperactivity disorder; narcolepsy | 240 |
| 71 | Lidocaine | Pain | 225 |
| 72 | Lunesta | Insomnia | 225 |
| 74 | Zytiga | Shift work sleep disorder, narcolepsy | 222 |
| 97 | Afinitor | Attention deficit hyperactivity disorder | 180 |
| 99 | Adderall XR | Attention deficit hyperactivity disorder | 177 |

Based upon data from Q 2013 found at http://www.drugs.com/stats/top100/sales.

penetration, the increased risk of side effects, and poor target identification and validation. Taken together, these challenges result in a decreased approval rate for clinical candidates and increased development times compared to other therapeutic areas.[7,8]

For a compound to exert a biological effect in the brain, it must first transverse the blood brain barrier (BBB). The BBB is a series of capillary endothelial cells connected by tight junctions that form a barrier between the circulating blood and the intracellular fluid of the CNS. This protective barrier allows for the passage of nutrients and hormones into the brain and limits the access of xenobiotics.[9] The majority of CNS drugs gain access to the brain via intercellular passive diffusion (Figure 1.1).[10] Furthermore, transmembrane transporters, such as p-glycoprotein, act as a second layer of defense and actively efflux compounds out of the CNS.[11] Conversely, some molecules, such as glucose and amino acids, are actively shuttled across the BBB via influx transporters. An effort has been made to design drugs that achieve proper brain penetration via active transport,[12] however these design principles are still under development.

The existence of the BBB requires that in addition to classical pharmacokinetic values, such as bioavailability and plasma concentration, other parameters must be used to measure brain penetration. Historically, the total brain concentration ($C_b$) and the brain-to-plasma ratio ($C_b/C_p$) have been used for this purpose due to the relative

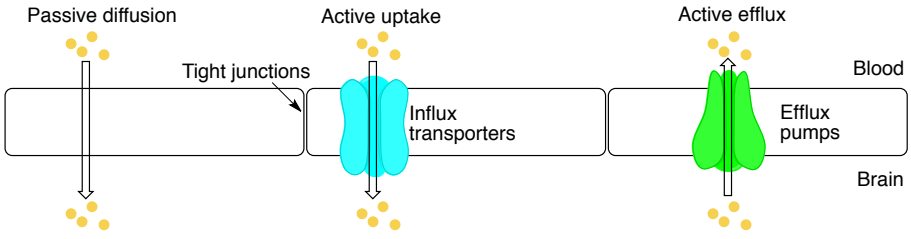


**Figure 1.1.** Schematic representation of mechanisms controlling BBB penetration.

simplicity in their measurements.[13] However, when used alone, these measurements can be misleading as they do not accurately describe the amount of free drug available to interact with the target. Receptor occupancy, which measure the percent of total receptors being occupied by the drug, is a more useful parameter, however these tests are time consuming and costly.[14] Therefore, they are typically reserved only for compounds late in the drug development process.

Several studies have sought to use these and other parameters to correlate brain penetration with certain physicochemical properties. A retrospective analysis performed at Pfizer revealed that CNS-active drugs are typically smaller (median MW=305.3), less lipophilic (median clogP=2.8), have fewer hydrogen bond donors (median=1), and smaller polar surface areas (median TPSA=44.8 $Å^2$) than non-CNS drugs.[15] Although this and other related studies have provided optimal ranges for these physiochemical parameters,[15-17] much like Lipinski's Rule of Five, these are only guidelines for developing a successful CNS drug.

In addition to the difficulties faced through brain penetration, the complexity of the CNS also creates significant problems in identifying and validating reliable biological targets. In many CNS disorders, especially those involving psychosis and neurodegeneration, this is the direct result of a poor understanding of the underlying cause of the disease. Historically target identification was a somewhat serendipitous process and the mechanisms of action for many drugs were only determined after a favorable phenotype had been discovered.[18] The sequencing of the human genome has recently resulted in a shift to a more genetic-based approach, however this has been met with only limited success.[19]

Even when potential targets have been proposed, the complexity of CNS disorders also results in poor preclinical animal models.[8] The models that do exist typically are the result of one of two approaches.[7] When the pathophysiology cause is well understood, genetically modified animals are created to emulate these effects and allow for the investigation of novel therapeutics. The second approach relies on the use of already approved drugs to build a behavioral or pharmacodynamics model. This model can then be used to identify novel compounds that produce similar results. Unfortunately, in several CNS disorders—particularly for those diseases where there are no approved drugs and the underlying cause is not well defined—these approaches have yet to produce a reliable animal model. Furthermore, useful predictive and prognostic biomarkers for many CNS diseases are virtually non-existent.[18] This ultimately results in poor translation of preclinical successes into clinical results leading to increased pessimism for the pharmaceutical industry.

The combination of increasing incidences of CNS diagnoses and decreased interest of the pharmaceutical industry toward the development of novel therapies has the potential to lead to a very bleak future. It is therefore necessary to continue research efforts that will validate proposed targets, improve upon existing treatments, and to provide probe molecules that assist in the understanding the basic pathophysiological causes of diseases. This is particularly true in the areas of: (1) drug abuse therapies where several biological targets have been proposed but current treatment is limited; (2) pain management where all approved therapies possess undesirable side effects; and (3) Alzheimer's Disease where the underlying cause of the disease remains unknown.

*Substance Abuse and Dependence*

Illicit drug use and addiction represents a serious and growing problem in the United States and much of the developed world. The National Survey on Drug Use and Health (NSDUH) conducted by the Substance Abuse and Mental Health Services Administration indicates approximately 23.9 million Americans aged 12 or older have used an illicit substance within the last year.[20] This number represents 9.3% of the population, which has increased nearly an entire percent over the last decade. Because of the addicting and rewarding nature of many illicit drugs, this increased level of drug use has also resulted in increased levels of those suffering from substance abuse or dependency. According to the NSDUH, in 2012 an estimated 22.2 million individuals were classified as abusing or dependent upon an illicit drug or alcohol. However, of these affected individuals only 4 million received treatment, clearly demonstrating a severe treatment gap. While the majority of these treatments consist of psychotherapy, either in a group or individual setting, pharmacological interventions also exist for opiate and alcohol abuse.[21] These therapies assist in preventing relapse and easing withdrawal symptoms by correcting the biochemical changes that take place in the brain during addiction.[22]

There are currently four FDA-approved drugs used for the treatment of opioid dependence, all of which act at the mu-opioid receptor (MOR)—the site of action for abused opiates such as heroin (Figure 1.2). Methadone and buprenorphine are used in replacement therapy in which a prescription drug is used to take the place of the drug of abuse. This prescription eases the withdrawal symptoms and reduces intense drug cravings by providing low levels of receptor activation.[23] The prescribed dose is then

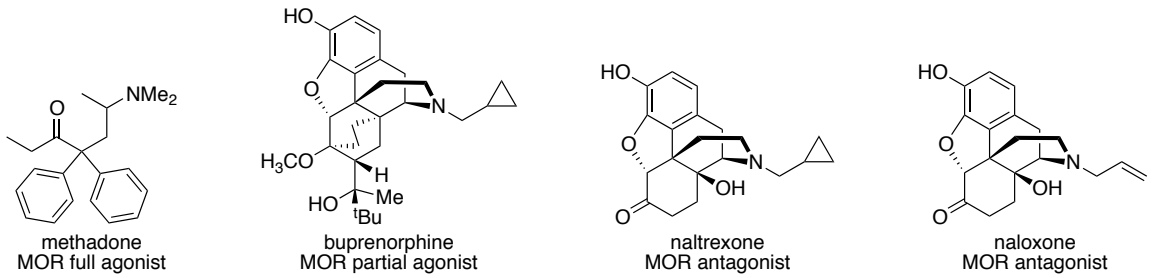


**Figure 1.2.** FDA-approved drugs used in the treatment of opiate addiction and their action at the MOR.

typically reduced over a period of 4 weeks in specialized methadone clinics or longer periods of time during outpatient care.[21] Although methadone replacement therapy has been used successfully for several decades, it has been criticized as simply replacing illicit opiate addicts with methadone addicts and methadone detoxification is an arduous process in itself. Furthermore, as a MOR full agonist, the possibility of methadone overdose still exists, a problem that is exacerbated by methadone's long duration of action. As a partial agonist at the MOR, buprenorphine is less prone to overdose, however evidence exists that buprenorphine may not be as effective as methadone.[24]

The other two medications approved to treat opioid dependence are the MOR antagonists naltrexone and naloxone. As antagonists, these drugs block the action of abused opiates, however they also induce acute opiate withdrawal. For this reason, naltrexone or naloxone is sometimes used to induce rapid opioid detoxification while the patient is under general anesthesia. However, this process introduces inherit risk and numerous deaths have been reported from this procedure.[25] Furthermore, antagonist-based therapies require continued patient compliance as even a single skipped dose allows for illicit opiates to have an effect if the patient relapses. So while these MOR agonist- and antagonist-based treatments have found some clinical utility, they are far from ideal and additional research into novel therapies is well warranted.

Although not illicit, nicotine found in tobacco products is extremely addicting. Nicotine derives its rewarding effects by activating nicotinic acetylcholine receptors (nAChR), leading to a increase in dopamine in the nucleus accumbens[26]—a portion of the brain heavily involved in motivation, reward, and reinforcement learning.[27] The cessation of nicotine use, therefore, results in a decrease in dopamine and the onset of withdrawal symptoms. Nicotine replacement therapy in the form of patches, sprays, gums, and lozenges are used mitigate these symptoms by providing enough nicotine to reduce cravings.

As an alternative to nicotine replacement therapy, varenicline and bupropion can be prescribed to aid in overcoming nicotine addictions (Figure 1.3). Varenicline is a partial nAChR agonist developed by Pfizer based upon the naturally occurring partial agonist cytisine[28]—which is also used to aid in smoking cessation in parts of Europe and Russia.[29] As partial agonists, varenicline and cytisine provide consistent, low levels of dopamine to reduce withdrawal symptoms and occupy the nAChR binding sites thus preventing nicotine from producing a rewarding effect.

The other medication prescribed for smoking cessation is the antidepressant bupropion, which is a nAChR antagonist and norepinephrine/dopamine reuptake inhibitor.[30] Much like the partial agonists, bupropion blocks the effects of nicotine by antagonizing the nAChR. However, rather than increasing dopamine by activating


nicotine
nAChR full agonist

varenicline
nAChR partial agonist

cytisine
nAChR partial agonist

bupropion
nAChR antagonist
catecholamine reuptake inhibitor

**Figure 1.3.** Drugs prescribed to assist in smoking cessation and their relevant pharmacology.

nAChR, bupropion raises levels of dopamine by inhibiting the uptake of norepinephrine and dopamine. These clinically approved medications for nicotine addiction highlight an important feature for drug abuse therapies: to properly treat addiction and abuse an effective treatment must not only limit the rewarding action of the drug, but also mitigate the negative symptoms associated with its discontinuation.

In comparison to opiates and nicotine, the effects of ethanol on the CNS are considerably more complex, affecting both lipid membrane composition as well as several excitatory and inhibitory neurotransmitter receptors.[31] Additionally, the MOR is at least partially responsible for the rewarding affects of alcohol[32] and the MOR antagonist naltrexone is prescribed for the management of alcohol dependence (Figure 1.4). The rewarding affects of alcohol and the potential for relapse are also successfully mitigated with acamprosate, although its mechanism of action is still debated.[33,34]

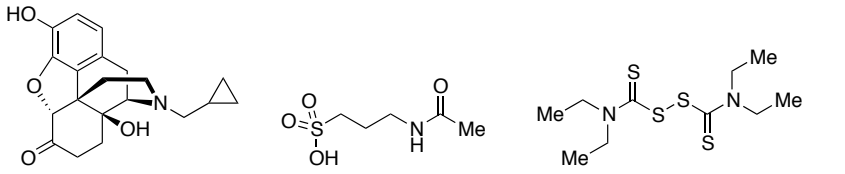


**Figure 1.4.** Treatment options for alcohol abuse and their known mechanisms of action.

The oldest medication used to treat alcohol abuse, disulfiram, has a less direct effect on the CNS but instead inhibits acetaldehyde dehydrogenase. In the liver, ethanol is first converted to acetaldehyde, which is in turn converted to acetic acid by acetaldehyde dehydrogenase. While on disulfiram, the consumption of alcohol leads to a buildup of acetaldehyde resulting in a number of negative effects including nausea, vomiting, and headaches. Although largely effective in preventing alcohol use when in a controlled setting, disulfiram does not control cravings and patient compliance is often an issue.[35]

With the exception of alcohol abuse therapies, all approved treatments for substance abuse act at the same receptor as the drug of abuse. However, for many abused substances, including alcohol and CNS stimulants like cocaine and methamphetamine, the cause of the rewarding properties is either too complex or is not amenable to targeting for a drug abuse therapy. In these cases, if a viable therapeutic option is to be developed alternative strategies to mitigating the rewarding effects must be explored. The dopamine hypothesis of drug addiction states that the rewarding properties of drugs of abuse are produced by increased levels of dopamine in the brain, especially in the nucleus accumbens and ventral tegmental area.[36] Therefore the reduction of dopamine in these areas may reduce drug-seeking behavior.

Of the many targets that have been explored to develop a novel drug abuse therapy, the kappa opioid receptor (KOR) shows particular promise. Unlike the MOR, activation of the KOR results in decreased levels of dopamine.[37] Although initially developed by the Upjohn Company as potentially non-addictive analgesics, the arylacetamide class of KOR agonist represented by U69,693, U50,488h, and enadoline (Figure 1.5), has shown considerable efficacy in in various animal models of addiction.[38-45] Unfortunately these traditional KOR agonists suffer from several side effects including dysphoria, depression, and sedation thus preventing their utility as drug abuse treatments.[46,47] More recently, several other KOR agonists, including those based on the naturally occurring neoclerodane diterpene salvinorin A, have renewed interest in targeting the KOR, largely due to their ability to decrease cocaine-induced drug-seeking behavior with an improved side-effect profile.[44,48-50] Ongoing research in this field is

focused on elucidting the reason for these differences, which could potentially validate the KOR as a therapeutic target for treating drug addiction and abuse.

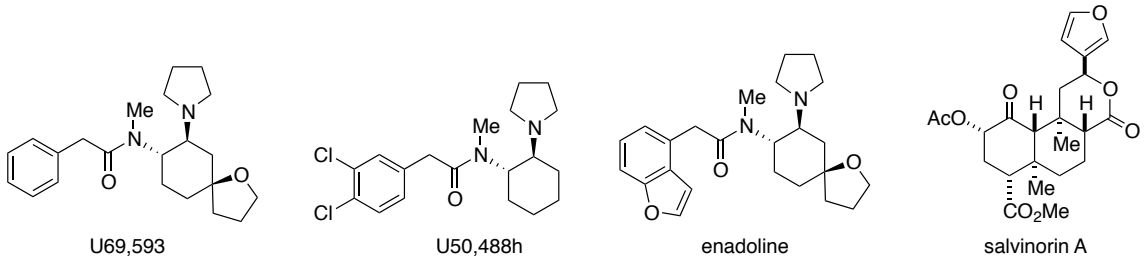


**Figure 1.5.** Representative arylacetamide KOR agonists and the naturally occurring KOR agonist salvinorin A.

*Chronic and Severe Pain*

Approximately 100 million Americans suffer from chronic or reoccurring pain, representing nearly half of the adult population and more than all cancer, heart disease, and diabetes patients combined.[51] This can largely be attributed to the comorbidity of chronic pain with several major disease states including cancer, arthritis, and diabetes.[52] For example, approximately 50-70% cancer patients suffer from some degree pain.[53] As a result of this prevalence, pain is the leading reason for seeking medical care and approximately $635 billion annually are lost to health care costs and decreases in productivity.[52] The analgesics used today can be divided in two general classes: non-steroid anti-inflammatory drugs (NSAIDs) and opiates.

NSAID analgesics, such as ibuprofen and aspirin (Figure 1.6), are amongst the most commonly used drugs for the treatment of pain and as their name implies are particularly effective in controlling pain associated with inflammation. In 1971, Vane determined the anti-inflammatory affects of aspirin and other NSAIDs arise from the disruption of prostaglandin synthesis via the inhibition of the cyclooxygenase (COX) enzyme.[54] The COX enzyme exists in at least two separate isoforms: COX-1 and COX-

2.[55,56] COX-1 is constitutively expressed and serves a protective role by synthesizing the prostaglandins found in the gastric mucosa. Under normal conditions, COX-2 is found in only low levels, however its expression is rapidly induced by pro-inflammatory stimuli.[57] Because aspirin and other traditional NSAIDs non-selectively inhibit COX-1/2, their chronic use can result in ulcers do to decreased production of protective prostaglandins found in the stomach lining.[58] In response to the discovery of the inducible isoform COX-2, several COX-2 selective NSAIDs, including celecoxib, rofecoxib, and valdecoxib, were developed that possess minimal gastrointestinal side effects.[58] Despite this improvement, the use of COX-2 inhibitors does increase the risk of cardiovascular complications,[59] which has ultimately resulted in the costly removal of rofecoxib and valdecoxib from the market.[60]

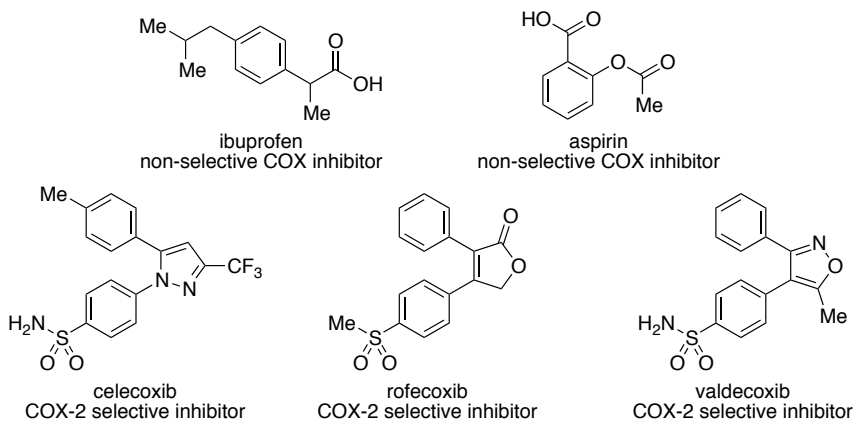


**Figure 1.6.** NSAIDs used in the treatment of pain.

The more powerful opioid class of analgesics is often used to treat severe and chronic pain, sometimes in combination with NSAIDs. Opioids provide pain relief by activating the opioid receptors, a group of three related G-protein coupled receptors (GPCRs) found throughout the body. The activation of the opioid receptors by their endogenous peptide ligands or exogenous agonists initiates numerous downstream effects including the inhibition adenylate cyclase, the opening of potassium channels, and the inhibition of N-type $Ca^{2+}$ channels.[61] These effects ultimately inhibit neurotransmitter

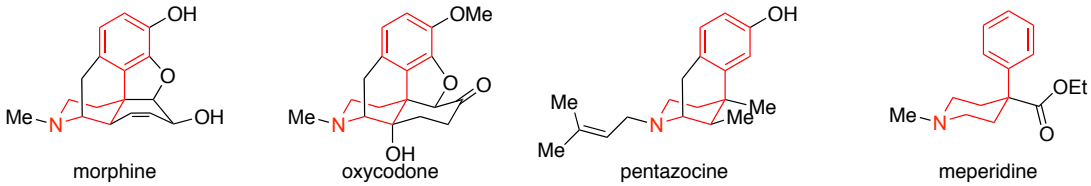


**Figure 1.7.** Structures of opioid analgesics highlighting their shared phenylpiperidine structure.

release thereby preventing the neurons from transmitting the signals of pain to the brain. Through this mechanism, all three opioid receptors have analgesic potential, however most clinically used opioids, such as morphine, oxycodone, pentazocine, and meperidine (Figure 1.7) are either synthetic or semi-synthetic derivatives of morphine and therefore act at the MOR.[62]

Despite being the "gold standard" for pain management, all opioid analgesics suffer from a similar side effect profile that includes sedation, respiratory depression, constipation, tolerance, and depression.[63] These "on target" side effects are the direct result of the opioids action at the MOR. The exact mechanism by which opioids induce sedation is not fully understood, however it is believed to be related to a decrease in sensory input.[64] Similarly, respiratory depression is caused by a reduction in the brain's responsiveness to $CO_2$.[65] Respiratory depression is especially dangerous as it is the leading cause of death from opioid overdose.[66] Sedation and respiratory depression are primarily related to the opioids effect on the nervous system, however the presence of MOR in the gastrointestinal tract results in decreased intestinal motility following opioid treatment.[67] In some instances, this constipation can be overcome by co-administering peripherally restricted MOR antagonist such as melthylnaltrexone, however this side effect often remains a dose limiting consideration.

In addition to these side effects that can be observed after acute opioid treatment,

the chronic use of opioids results in significant biochemical adaptations within the nervous system. This leads to increased levels of drug being required to produce analgesia (tolerance) and normal function (dependence). Tolerance is particularly concerning as the increased doses are more likely to cause other side effects. Due to the widespread use of opioid analgesics and the frequency of their side effects, a significant effort has been made to separate the analgesic properties of opioids from their negative effects.

Although several theories have been proposed to account for these observed side effects increasing evidence indicates that β-arrestin-2 plays a critical role in their development.[68] Most importantly, genetically modified mice lacking β-arrestin-2 show increased and prolonged morphine analgesia and decreased tolerance, constipation and respiratory suppression.[69] β-Arrestins are a small family of proteins involved in GPCR regulation and desensitization. Upon activation, a GPCR can be phosphorylated by one of several GPCR kinases, which leads to β-arrestin recruitment and eventual internalization and desensitization of the receptor.[70] In addition to this desensitization mechanism, it is now apparent that the GPCR/β-arrestin complex is also capable of initiating unique signal transduction pathways.[71] For many receptors, including the MOR, it is possible for a ligand to activate the receptor without recruiting β-arrestins, a phenomenon known as functional selectivity. Therefore, MOR agonists that are able to activate the receptor without causing β-arrestin-2 recruitment may produce analgesia without the accompanying β-arrestin-dependent side effects. The identification of functionally selective agonists will likely require that novel ligands not based upon the traditional

morphine scaffold be identified and their interactions with the MOR thoroughly investigated.

*Alzheimer's Disease*

According to the World Health Organization (WHO), dementia represents a major health care problem affecting the entire global population.[72] Defined by a general decline in cognitive ability that interferes with daily life, dementia was estimated to effect 35.6 million individuals worldwide in 2010. However, as healthcare advances continue to raise the average life expectancy, this number is expected to nearly double every 20 years with an estimated 66 million suffers by 2030 and 115 million by 2050.[73] In addition to those personally diagnosed with dementia, a significant burden is also placed on caregivers. This burden is both social and financial, with estimated annual healthcare cost reaching $604 billion in 2012.[74] Clearly the WHO is correct in stating that developing a cure must become a global priority. Since Alzheimer's Disease (AD) represents approximately 60-80% of all dementia cases, understanding and developing a treatment for AD is a logical, albeit difficult, first step.[75]

The first reported case of AD, was described by Alois Alzheimer in 1906.[76] In his study, Alzheimer correlated the now stereotypical dementia of a patient, Auguste Deter, with two abnormal deposits discovered during his posthumous histological examination of her brain. These deposits were later identified as extracellular senile plaques composed of the peptide beta-amyloid (Aβ)[77,78] and intracellular neurofibrillary tangles (NFT) made up of the microtubule-associated protein tau.[79-81] The presence of these deposits in the brains of all AD patients suggests that either one or both of them are responsible for the

neuronal degeneration associated with AD. However, the exact role that Aβ plaques and NFT play is still debated and several theories have been proposed.

The oldest hypothesis, the cholinergic hypothesis, proposes that AD is caused by decreased levels of the neurotransmitter acetylcholine (ACh) in the brain.[82] This is primarily based upon reports that detailed decreased levels of choline acetyltransferase—an enzyme responsible for the biosynthesis of acetylcholine—in the AD patients' brains.[83-85] ACh has also been shown to be involved in learning and memory,[86] further supporting the hypothesis that a decrease in ACh would lead to the observed dementia. Research into the cholinergic hypothesis ultimately produced four of the approved treatment options for AD (Figure 1.8). Tacrine, donepezil, rivastigmine, and galantamine are inhibitors of acetylcholine esterase—an enzyme responsible for the breakdown of ACh.[87] Unfortunately, these treatment options are only marginally effective at treating the symptoms of AD and do not halt its progress. This has led a decline in the support of the cholinergic hypothesis.[88]

The other approved treatment option for AD is the *N*-methyl-D-aspartate (NMDA) receptor antagonist memantine (Figure 1.8). Activation of NMDA receptors

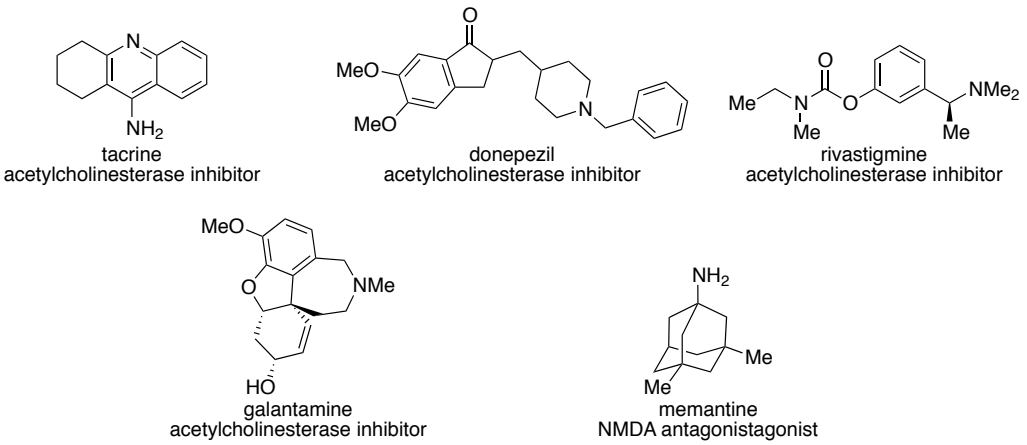


**Figure 1.8.** Approved treatment options for Alzheimer's Disease and their mechanisms of action.

with endogenous glutamate results in an influx of calcium into the neuron, which is necessary for proper neuronal function and plasticity.[89] However, over activation of NMDA receptors leads to calcium overload and cell death. Memantine is thought to operate by partially blocking the influx of calcium and prevent this excitotoxicity. Once again, memantine only appears to treat the symptoms of AD and does not provide an answer to the underlying cause.[90]

In 1991, the amyloid cascade hypothesis was proposed to attempt to account for the formation of plaques and NFT and establish how they lead to dementia in AD (Figure 1.9).[91] This theory postulates that dysregulation of the machinery that processes the amyloid precursor protein (APP) into Aβ leads to the formation of plaques. These plaques are toxic themselves but also lead to the hyperphosphorylation of tau protein. This hyperphosphorylation causes tau to aggregate leading to neuronal degeneration and ultimately dementia. It is important to note that the amyloid cascade hypothesis accounts for both Aβ plaques and NFT however, the exact mechanism through which plaques induce the formation of NFT is not established.[92] This theory is supported by the fact that genetic mutations that lead to early onset familial AD (EOFAD) have been identified in the genes that encode APP[93-95] and two proteins responsible for APP's cleavage to Aβ.[96-98] This evidence has led researchers to develop inhibitors of the enzymes responsible for Aβ production as a potential cure for AD.

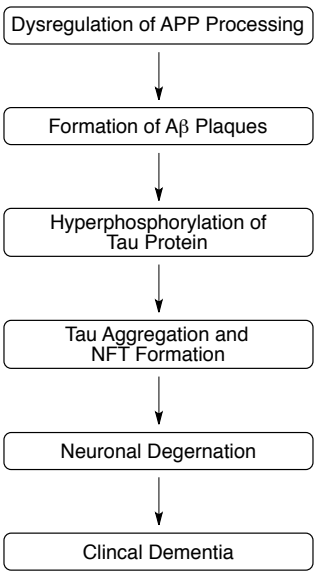


**Figure 1.9.** Amyloid cascade hypothesis, adapted from Ref 91.

APP is an integral membrane protein found largely in the synapses of neurons. APP is first cleaved by one of two proteases: α-secretase or β-secretase. Processing of APP by α-secretase produces soluble N-terminal APP (APPSα) that is not amyloidogenic and thus does not produce AD.[99] Cleavage of APP by β-secretase produces a membrane bound fragment referred to as C99,[100] which is further processed by γ-secretase to give Aβ.[101] However, both β-secretase and γ-secretase are involved in other physiological functions. Most notably, β-secretase is involved in the nerve myelination through the processing of neuregulin 1[102] and γ-secretase processes Notch receptors—an important receptor in multiple cell signaling systems.[103] Several "Notch sparing" γ-secretase inhibitors have and are currently being developed to avoid potential side effects. However the NSAID (*R*)-flurbiprofen, a γ-secretase inhibitor that does not effect Notch processing, was shown to be ineffective in Phase 3 clinical trials.[104] Similarly, several β-secretase inhibitors are also being investigated[105] including the Merck compound MK-8931, which is currently in Phase 2/3 clinical trials for the treatment of mild to moderate AD.[106]

The other major lesion found in the brains of AD patients are composed of the protein tau.[107] Tau normally binds to and stabilizes microtubules and promotes their assembly and polymerization, thereby promoting axonal function and viability.[108-110] However, in AD—and at least 20 other neurodegenerative disease known collectively as tauopathies—tau is hyperphosphorylated leading to its dissociation from microtubules and aggregation into paired helical filaments (PHF) or straight filaments (SF). These PHFs and SF make up the NFT lesions. Thus it appears as though tau-induced neurodegeneration arises from a combination of a toxic gain of function through the

formation of NFT and a toxic loss of function through the destabilization of microtubules. Proponents of this tau-hypothesis are supported by the fact that the location and formation of NFT correlates more strongly with disease progression than Aβ plaque formation.[111] Furthermore, transgenic mice lacking tau protein are protected from Aβ-induced toxicity[112,113] and tau dysfunction alone is sufficient to produce dementia.[114] This mounting evidence clearly establishes tau's central role in AD pathology.

Accordingly, a significant effort has been made toward developing a tau-targeting therapy for AD.[115] Since tau protein is phosphorylated by members of several kinase families including GSK-3,[116] MARK[117], PKA[118], and Cdk5[119], inhibitors of these proteins have been thoroughly investigated. Although several have shown promise in animal models, the GSK-3 inhibitor tideglusib showed no clinical benefit in patients with AD or progressive paranuclear palsy, another tauopathy.[120]

Other studies have sought not to inhibit phosphorylation but to prevent tau aggregation. A high-throughput screen of over 200,000 compounds revealed several rhodanines, anthraquinones, *N*-phenylamines, and phenylthiazolylhydrazides are effective tau aggregation inhibitors (TAI).[121] The oldest known TAI, methylene blue, has recently completed a successful phase 2 clinical trial and will be advancing into phase 3 studies with a more stable reduced analogue.[122] Although these results with TAI appear promising, pre-aggregation forms of tau have also been shown to be neurotoxic and affect memory.[123] Thus the decrease in the overall concentration of tau protein may be more beneficial. On the other hand, completely eliminating tau protein may have negative effects due to a loss of microtubule stabilization. Transgenic mice deficient in tau, however, are not only viable but also do not show obvious signs of neurodegeneration.[124]

Several studies have investigated the potential of decreasing tau concentrations by activating the proteasome[125] or autophagosome.[126] Nevertheless, there remains a desperate need for the discovery and pharmacological characterization of additional small molecules that are able to affect tau concentrations in order to validate this therapeutic option.

*Natural Products*

Prior to written history, humans have been using plants and other natural substances in the treatment of a variety of human ailments, including several CNS disorders. For instance, the oldest medical text from ancient Mesopotamia dated to about 2600 BC describes the use of opium poppy (*Papaver somniferum*) to treat pain.[127] Historically these medicines consisted of the complex mixtures of compounds that were isolated from the natural source. However the isolation of pure morphine from the poppy plant in 1804 marked a new era of natural product chemistry in which the beneficial effects could be attributed to a single chemical component.[128] Several decades later another monumental step was taken when Felix Hoffmann prepared acetyl salicylic acid (aspirin) from salicylic acid, providing the first example of a chemical modification used to improve the biological properties of a natural product.[129] Natural products have continued to play a major role in drug development and up until relatively recently, these compounds represented the largest source of lead compounds. However, in the 1980s the advent of combinatorial chemistry allowed access to large libraries of completely synthetic compounds. Nevertheless, natural products still remain incredibly influential in

drug development and 34% of currently approved small molecules are natural products or derivatives derived from them.[130]

The influence of natural products on drug design can be attributed to the many advantages natural products have over other small molecules. Principal among these is the structural diversity and complexity of natural products that often provides high degrees of specificity and potency. Several millennia of evolutionary pressures have forced the producing organisms to develop secondary metabolites finely tuned to perform a specific biological function. In many cases, these functions are defensive in nature, which explains why a particularly high percentage of anti-cancer and anti-infective drugs are natural product based.[130] By comparison, combinatorial libraries are oftentimes driven by the ease in which compounds can be synthesized rather than being driven by a specific biological need. This has resulted in libraries filled with molecules with less than ideal drug-like properties and multiple violations of drug design principles such as Lipinski's Rule of Five. On the other hand, natural products are often cited as exceptions to Lipinski's rules, partially due to their ability to take advantage of active uptake mechanisms.[131] The recent efforts to develop "natural product-like" libraries made up of more structurally complex scaffolds will, hopefully, produce more promising lead compounds.[132-136]

In addition to the complex structure found in many natural products, their identification through ethnobotanical studies provides another unique benefit. Ethnobotany can be described as the study of the relationship between plants and people. Due to the long history of utilizing plants for a medicinal purpose, countless traditional remedies have been developed to treat a variety of ailments. Over the last several

decades, natural product chemists have begun searching for the individual chemical components found in these remedies that may be exerting the beneficial effects. This approach often narrows the potential biological targets to those that could produce the observed biological effect or conversely, narrow the plants to investigate to identify a desired biological response. Alternatively, natural products discovered in this manner may lead to the identification of novel biological pathways or molecular targets. Perhaps the best example of this is the identification of the opioid receptors, whose discover was highly dependent upon radioligands derived from naturally occurring opiates. Additionally, ethnobotanical studies can provide preliminary toxicity and pharmacokinetic information. This is particularly useful in CNS disorders where brain penetration can be a significant hurdle (*vide supra*). Thus if a plant is used to produce an altered mental state (ex: hallucination, sedation, etc.) it is likely doing so by acting directly in the brain. These advantages clearly indicate that the use of ethnobotany to guide isolation studies is a powerful tool to the natural products chemist.

Despite the many advantages provided by natural products in early drug discovery there are several challenges associated with their use. Among these are the difficulties in isolation and reisolation of the active component. Since many secondary metabolites are produced in only minute quantities, isolation of significant amounts for biological studies is often problematic. This can be particularly true since secondary metabolites synthesis can vary depending upon environmental cues. Although efforts to provide this material through total synthesis or molecular biology have proven successful in some cases, these studies are often time consuming and laborious. Furthermore, natural products often need significant structure optimization to modulate their pharmacokinetic properties for use as

drugs. The complex structure and high functional group density found in many natural products necessitate the use of mild or carefully optimized reaction conditions to achieve selective transformations.

Finally, the enactment of the Convention on Biological Diversity in 1993 and the Nagoya Protocol in 2010 has introduced considerable legal complications in natural product field. These treaties outline specific guidelines for the conservation of biological diversity including "the fair and equitable sharing of the benefits arising out of the utilization of genetic resources."[137,138] While these measures are morally and ethically valuable, the added regulations has deterred or slowed some pharmaceutical and academic research interests.[139] Nevertheless difficulties arising from accessibility, intellectual property and structure modification are common to many drug discovery efforts, regardless of the source of the initial lead.

Natural products clearly represent an important starting point for investigating complex biological systems. In particular, the numerous benefits of natural products are often well suited to overcome the many challenges faced in CNS drug discovery. For instance, the neoclerodane diterpene salvinorin A (Figure 1.10) is a naturally occurring KOR agonist that appears to have unique pharmacological properties when compared to traditional, synthetic KOR agonists. Therefore salvinorin A has promising potential as a probe of the KOR's role in drug addiction. Similarly, a semi-synthetic derivative of salvinorin A, herkinorin, is a MOR agonist structurally unlike all other MOR agonist, which suggests it may not possess the same side-effect profile as the opioid analgesics. Finally, the diarylheptanoid myricanol has recently been shown to decrease cellular concentrations of tau protein making it an attractive scaffold for investigating

Alzheimer's Disease. While these three compounds are useful leads for developing CNS probe molecules, a detailed understanding of their interactions with their biological targets is still needed. Such an understanding will only be possible through the synthesis or chemical manipulation of the structures of these natural products.

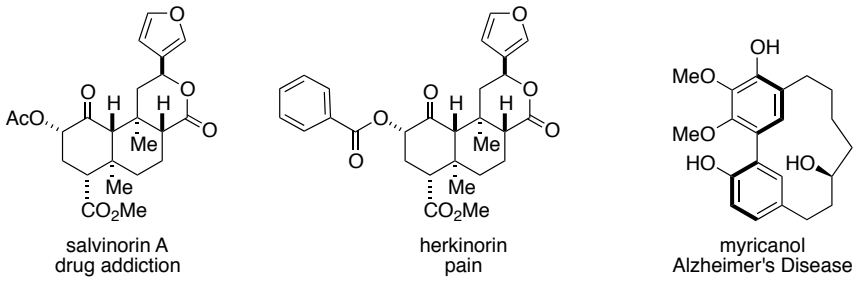


**Figure 1.10.** Naturally derived compounds with potential to probe several CNS disorders.

**References:**

(1) Palmer, A. M.; Alavijeh, M. S. Translational CNS medicines research. *Drug Discovery Today* **2012**, *17*, 1068.

(2) Palmer, A. M. The role of the blood-CNS barrier in CNS disorders and their treatment. *Neurobiol. Dis.* **2010**, *37*, 3.

(3) Rankovic, Z. Drug design: balancing physicochemical properties for optimal brain exposure. *J. Med. Chem.* **2015**, *58*, 2584.

(4) Insel, T. R. Assessing the economic costs of serious mental illness. *American J. Psychiatry* **2008**, *165*, 663.

(5) Alavijeh, M. S.; Chishty, M.; Qaiser, M. Z.; Palmer, A. M. Drug metabolism and pharmacokinetics, the blood-brain barrier, and central nervous system drug discovery. *NeuroRx* **2005**, *2*, 554.

(6) Chandler, D. J. Something's got to give: psychiatric disease on the rise and novel drug development on the decline. *Drug Discovery Today* **2013**, *18*, 202.

(7) Pangalos, M. N.; Schechter, L. E.; Hurko, O. Drug development for CNS disorders: Strategies for balancing risk and reducing attrition, *Nat. Rev. Drug Discov.* **2007**, *6*, 521.

(8) Kola, I.; Landis, J. Can the pharmaceutical industry reduce attrition rates? *Nat. Rev. Drug Discov.* **2004**, *3*, 711.

(9) Abbott, N. J.; Patabendige, A. A.; Dolman, D. E.; Yusof, S. R.; Begley, D. J. Structure and function of the Blood-brain barrier. *Neurobiol. Dis.* **2010**, *37*, 13.

(10) Di, L.; Artursson, P.; Avdeef, A.; Ecker, G. F.; Faller, B.; Fischer, H.; Houston, J. B.; Kansy, M.; Kerns, E. H.; Kramer, S. D.; Lennernas, H.; Sugano, K. Evidence-based Approach to assess passive diffusion and carrier-mediated drug transport. *Drug Discovery Today* **2012**, *17*, 905.

(11) Mahar Doan, K. M.; Humphreys, J. E.; Webster, L. O.; Wring, S. A.; Shampine, L. J.; Serabjit-Singh, C. J.; Adkison, K. K.; Polli, J. W. Passive permeability and P-glycoprotein-mediated efflux differentiate central nervous system (CNS) and non-CNS marketed drugs, *J. Pharmacol. Exp. Ther.* **2002**, *303*, 1029.

(12) Malakoutikhah, M.; Teixido, M.; Giralt, E. Shuttle-mediated drug delivery to the brain. *Angew. Chem. Int. Ed.* **2011**, *50*, 7998.

(13) Rankovic, Z. Designing CNS Drugs for Optimal Brain Exposure. In *Blood-Brain Barrier in Drug Discovery : Optimizing Brain Exposure of CNS Drugs and Minimizing Brain Side Effects for Peripheral Drugs;* Di, L.; Kerns, E. H., ed.; Wiley: New York, 2015.

(14) Read, K. D.; Braggio, S. Assessing brain free fraction in early drug discovery. *Exp. Opin. on Drug Metab. Toxicol.* **2010**, *6*, 337.

(15) Wager, T. T.; Chandrasekaran, R. Y.; Hou, X.; Troutman, M. D.; Verhoest, P. R.; Villalobos, A.; Will, Y. Defining desirable central nervous system drug space through the alignment of molecular properties, *in vitro* ADME, and safety attributes. *ACS Chem. Neurosci.* **2010**, *1*, 420.

(16) Wager, T. T.; Hou, X.; Verhoest, P. R.; Villalobos, A. Moving beyond rules: the development of a central nervous system multiparameter optimization (CNS MPO) approach to enable alignment of druglike properties. *ACS Chem. Neurosci.* **2010**, *1*, 435.

(17) Ghose, R. A measured approach: determining the PLCgamma1 docking site on Itk using a biochemical ruler. *J. Mol. Bio.* **2013**, *425*, 679.

(18) Nutt, D.; Goodwin, G. ECNP Summit on the future of CNS drug research in Europe 2011. *Eur. Neuropsychopharmacol.* **2011**, *21*, 495.

(19) Cacabelos, R.; Martinez-Bouza, R.; Carril, J. C.; Fernandez-Novoa, L.; Lombardi, V.; Carrera, I.; Corzo, L.; McKay, A. Genomics and pharmacogenomics of brain disorders. *Curr. Pharm. Biotechnol.* **2012**, *13*, 674.

(20) Substance Abuse and Mental Health Services Administration, Results from the 2012 National Survey on Drug Use and Health: Summary of National Findings, **2012**.

(21) Diaper, A. M.; Law, F. D.; Melichar, J. K. Pharmacological strategies for detoxification. *Br.. J. Clin. Pharmacol.* **2014**, *77*, 302.

(22) Hyman, S. E.; Malenka, R. C. Addiction and the brain: the neurobiology of compulsion and its persistence. *Nat. Rev. Neurosci.* **2001**, *2*, 695.

(23) Kreek, M. J.; Vocci, F. J. History and current status of opioid maintenance treatments: blending conference session. *J. Sub. Abuse Treat.* **2002**, *23*, 93.

(24) Mattick, R. P.; Breen, C.; Kimber, J.; Davoli, M. Buprenorphine maintenance versus placebo or methadone maintenance for opioid dependence. *The Cochrane Database of Systematic Reviews* **2014**, *2*, CD002207.

(25) Hamilton, R. J.; Olmedo, R. E.; Shah, S.; Hung, O. L.; Howland, M. A.; Perrone, J.; Nelson, L. S.; Lewin, N. L.; Hoffman, R. S. Complications of ultrarapid opioid detoxification with subcutaneous naltrexone pellets. *Acad. Emerg. Med.* **2002**, *9*, 63.

(26) Pontieri, F. E.; Tanda, G.; Orzi, F.; Di Chiara, G. Effects of nicotine on the nucleus accumbens and similarity to those of addictive drugs. *Nature* **1996**, *382*, 255.

(27) Koob, G. F. Neural mechanisms of drug reinforcement. *Ann. N. Y. Acad. Sci.* **1992**, *654*, 171.

(28) Coe, J. W.; Brooks, P. R.; Vetelino, M. G.; Wirtz, M. C.; Arnold, E. P.; Huang, J.; Sands, S. B.; Davis, T. I.; Lebel, L. A.; Fox, C. B.; Shrikhande, A.; Heym, J. H.; Schaeffer, E.; Rollema, H.; Lu, Y.; Mansbach, R. S.; Chambers, L. K.; Rovetti, C. C.; Schulz, D. W.; Tingley, F. D., 3rd; O'Neill, B. T. Varenicline: an $\alpha_4\beta_2$ nicotinic receptor partial agonist for smoking cessation. *J. Med. Chem.* **2005**, *48*, 3474.

(29) Tutka, P.; Zatonski, W. Cytisine for the treatment of nicotine addiction: from a molecule to therapeutic efficacy. *Pharm. Rep.* **2006**, *58*, 777.

(30) Stahl, S. M.; Pradko, J. F.; Haight, B. R.; Modell, J. G.; Rockett, C. B.; Learned-Coughlin, S. A Review of the Neuropharmacology of Bupropion, a Dual

Norepinephrine and Dopamine Reuptake Inhibitor. *Prim. Care Comp. J.Clin. Psych.* **2004**, *6*, 159.

(31) Harris, R. A. Ethanol actions on multiple ion channels: which are important? *Alcohol.: Clin. Exp. Res.* **1999**, *23*, 1563.

(32) Heyser, C. J.; Roberts, A. J.; Schulteis, G.; Koob, G. F. Central administration of an opiate antagonist decreases oral ethanol self-administration in rats. *Alcohol.: Clin. Exp. Res.* **1999**, *23*, 1468.

(33) De Witte, P.; Littleton, J.; Parot, P.; Koob, G. Neuroprotective and abstinence-promoting effects of acamprosate: elucidating the mechanism of action. *CNS Drugs* **2005**, *19*, 517.

(34) Reilly, M. T.; Lobo, I. A.; McCracken, L. M.; Borghese, C. M.; Gong, D.; Horishita, T.; Harris, R. A. Effects of acamprosate on neuronal receptors and ion channels expressed in Xenopus oocytes. *Alcohol.: Clin. Exp. Res.***2008**, *32*, 188.

(35) Brewer, C. Patterns of compliance and evasion in treatment programmes which include supervised disulfiram. *Alcohol Alcoho.***1986**, *21*, 385.

(36) Pierce, R. C.; Kumaresan, V. The mesolimbic dopamine system: the final common pathway for the reinforcing effect of drugs of abuse? *Neurosci. Biobehav. Rev.* **2006**, *30*, 215.

(37) Di Chiara, G.; Imperato, A. Opposite effects of mu and kappa opiate agonists on dopamine release in the nucleus accumbens and in the dorsal caudate of freely moving rats. *J Pharmacol. Exp. Ther.* **1988**, *244*, 1067.

(38) Bolanos, C. A.; Garmsen, G. M.; Clair, M. A.; McDougall, S. A. Effects of the kappa-opioid receptor agonist U-50,488 on morphine-induced place preference conditioning in the developing rat. *Eur. J. Pharmacol.* **1996**, *317*, 1.

(39) Crawford, C. A.; McDougall, S. A.; Bolanos, C. A.; Hall, S.; Berger, S. P. The effects of the kappa agonist U-50,488 on cocaine-induced conditioned and unconditioned behaviors and Fos immunoreactivity. *Psychopharmacology* **1995**, *120*, 392.

(40) Funada, M.; Suzuki, T.; Narita, M.; Misawa, M.; Nagase, H. Blockade of morphine reward through the activation of kappa-opioid receptors in mice. *Neuropharmacology* **1993**, *32*, 1315.

(41) Glick, S. D.; Maisonneuve, I. M.; Raucci, J.; Archer, S. Kappa opioid inhibition of morphine and cocaine self-administration in rats. *Brain Res.* **1995**, *681*, 147.

(42) Negus, S. S.; Mello, N. K.; Portoghese, P. S.; Lin, C. E. Effects of kappa opioids on cocaine self-administration by rhesus monkeys. *J Pharmacol. Exp. Ther.* **1997**, *282*, 44.

(43) Schenk, S.; Partridge, B.; Shippenberg, T. S. U69593, a kappa-opioid agonist, decreases cocaine self-administration and decreases cocaine-produced drug-seeking. *Psychopharmacology* **1999**, *144*, 339.

(44) Morani, A. S.; Kivell, B.; Prisinzano, T. E.; Schenk, S. Effect of kappa-opioid receptor agonists U69593, U50488H, spiradoline and salvinorin A on cocaine-induced drug-seeking in rats. *Pharmaco., Biochem. Behav.* **2009**, *94*, 244.

(45) Schenk, S.; Partridge, B.; Shippenberg, T. S. Reinstatement of extinguished drug-taking behavior in rats: effect of the kappa-opioid receptor agonist, U69593. *Psychopharmacology* **2000**, *151*, 85.

(46) Walsh, S. L.; Strain, E. C.; Abreu, M. E.; Bigelow, G. E. Enadoline, a selective kappa opioid agonist: comparison with butorphanol and hydromorphone in humans. *Psychopharmacology* **2001**, *157*, 151.

(47) Rimoy, G. H.; Wright, D. M.; Bhaskar, N. K.; Rubin, P. C. The cardiovascular and central nervous system effects in the human of U-62066E. A selective opioid receptor agonist. *Eur. J. Clin. Pharmacol.* **1994**, *46*, 203.

(48) Simonson, B.; Morani, A. S.; Ewald, A. W.; Walker, L.; Kumar, N.; Simpson, D.; Miller, J. H.; Prisinzano, T. E.; Kivell, B. M. Pharmacology and anti-addiction effects of the novel kappa opioid receptor agonist Mesyl Sal B, a potent and long-acting analogue of salvinorin A. *Br. J. Pharmacol.* **2015**, *172*, 515.

(49) Morani, A. S.; Ewald, A.; Prevatt-Smith, K. M.; Prisinzano, T. E.; Kivell, B. M. The 2-methoxy methyl analogue of salvinorin A attenuates cocaine-induced drug seeking and sucrose reinforcements in rats. *Eur. J. Pharmacol.* **2013**, *720*, 69.

(50) Riley, A. P.; Groer, C. E.; Young, D.; Ewald, A. W.; Kivell, B. M.; Prisinzano, T. E. Synthesis and kappa-Opioid Receptor Activity of Furan-Substituted Salvinorin A Analogues. *J. Med. Chem.* **2014**, *57*, 10464.

(51) Prisinzano, T. E. Neoclerodanes as atypical opioid receptor ligands. *J. Med. Chem.* **2013**, *56*, 3435.

(52) Davis, J. A.; Robinson, R. L.; Le, T. K.; Xie, J. Incidence and impact of pain conditions and comorbid illnesses. *J. Pain Res.* **2011**, *4*, 331.

(53) Nersesyan, H.; Slavin, K. V. Current aproach to cancer pain management: Availability and implications of different treatment options. *Ther. Clin. Risk Manage.* **2007**, *3*, 381.

(54) Vane, J. R. Inhibition of prostaglandin synthesis as a mechanism of action for aspirin-like drugs. *Nature New Biol.* **1971**, *231*, 232.

(55) Fu, J. Y.; Masferrer, J. L.; Seibert, K.; Raz, A.; Needleman, P. The induction and suppression of prostaglandin H2 synthase (cyclooxygenase) in human monocytes. *J. Biol. Chem.* **1990**, *265*, 16737.

(56) Xie, W. L.; Chipman, J. G.; Robertson, D. L.; Erikson, R. L.; Simmons, D. L. Expression of a mitogen-responsive gene encoding prostaglandin synthase is regulated by mRNA splicing. *Proc. Natl. Acad. Sci. U. S. A.* **1991**, *88*, 2692.

(57) Seibert, K.; Zhang, Y.; Leahy, K.; Hauser, S.; Masferrer, J.; Perkins, W.; Lee, L.; Isakson, P. Pharmacological and biochemical demonstration of the role of cyclooxygenase 2 in inflammation and pain. *Proc. Natl. Acad. Sci. U. S. A.* **1994**, *91*, 12013.

(58) Marnett, L. J. The COXIB experience: a look in the rearview mirror *Annu. Rev. Pharmacol. Toxicol.* **2009**, *49*, 265.

(59) Cannon, C. P.; Cannon, P. J. Physiology. COX-2 inhibitors and cardiovascular risk. *Science* **2012**, *336*, 1386.

(60) Payne, R. *J. Pain* **2000**, Limitations of NSAIDs for pain management: toxicity or lack of efficacy? *1*, 14.

(61) Stein, C. *Opioids in pain control : basic and clinical aspects*; Cambridge University Press: Cambridge, UK ; New York, NY, USA, 1999.

(62) Casy, A. F.; Parfitt, R. T. *Opioid analgesics : chemistry and receptors*; Plenum Press: New York, 1986.

(63) Cherny, N.; Ripamonti, C.; Pereira, J.; Davis, C.; Fallon, M.; McQuay, H.; Mercadante, S.; Pasternak, G.; Ventafridda, V.; Expert Working Group of the European Association of Palliative Care, N. Strategies to manage the adverse effects of oral morphine: an evidence-based report. *J. Clin. Oncol.* **2001**, *19*, 2542.

(64) Young-McCaughan, S.; Miaskowski, C. Definition of and mechanism for opioid-induced sedation. *Pain Manage. Nurs.* **2001**, *2*, 84.

(65) Bourke, D. L.; Warley, A. The steady-state and rebreathing methods compared during morphine administration in humans. *J. Phys.* **1989**, *419*, 509.

(66) White, J. M.; Irvine, R. J. Mechanisms of fatal opioid overdose. *Addiction* **1999**, *94*, 961.

(67) Massi, P.; Giagnoni, G.; Basilico, L.; Gori, E.; Rubino, T.; Parolaro, D. Intestinal effect of morphine 6-glucuronide: in vivo and in vitro characterization. *Eur. J. Pharmacol.* **1994**, *253*, 269.

(68) Raehal, K. M.; Schmid, C. L.; Groer, C. E.; Bohn, L. M. Functional selectivity at the mu-opioid receptor: implications for understanding opioid analgesia and tolerance. *Pharmacol. Rev.* **2011**, *63*, 1001.

(69) Raehal, K. M.; Walker, J. K.; Bohn, L. M. Morphine side effects in beta-arrestin 2 knockout mice. *J. Pharmacol. Exp. Ther.* **2005**, *314*, 1195.

(70) Moore, C. A.; Milano, S. K.; Benovic, J. L. Regulation of receptor trafficking by GRKs and arrestins. *Annu. Rev. Physiol.* **2007**, *69*, 451.

(71) Lefkowitz, R. J.; Shenoy, S. K. Transduction of receptor signals by beta-arrestins. *Science* **2005**, *308*, 512.

(72) World Health Organization; Alzheimer's Disease International. *Dementia: a Public Health Priority* **2012**, 112.

(73) Alzheimer's Disease International World Alzheimer Report 2010: The Global Economic Impact of Dementia **2010**.

(74) Wortmann, M. Dementia: a global health priority—highlights from an ADI and World Health Organization report *Alzheimers Res. Ther.* **2012**, *4*.

(75) Burns, A.; Iliffe, S. Alzheimer's disease. *BMJ* **2009**, *338*, b158.

(76) Hippius, H.; Neundorfer, G. The discovery of Alzheimer's disease. *Dial. Clin. Neurosci.* **2003**, *5*, 101.

(77) Glenner, G. G.; Wong, C. W. Initial report of the purification and characterization of a novel cerebrovascular amyloid protein. *Biochem. Bioph. Res. Co.* **1984**, *120*, 885.

(78) Joachim, C. L.; Duffy, L. K.; Morris, J. H.; Selkoe, D. J. Protein chemical and immunocytochemical studies of meningovascular beta-amyloid protein in Alzheimers-disease and normal aging. *Brain Res.* **1988**, *474*, 100.

(79) Grundkeiqbal, I.; Iqbal, K.; Quinlan, M.; Tung, Y. C.; Zaidi, M. S.; Wisniewski, H. M. Microtubule-associated protein-tau: a component of Alzheimer paired helical filaments. *J. Biol. Chem.* **1986**, *261*, 6084.

(80) Kosik, K. S.; Joachim, C. L.; Selkoe, D. J. Microtubule-associated protein tau (tau) is a major antigenic component of paired helical filaments in Alzheimer Disease. *Proc. Natl. Acad. Sci. U. S. A.* **1986**, *83*, 4044.

(81) Nukina, N.; Kosik, K.; Selkoe, D.; Ihara, Y. Tau protein Is integrated into paired helical filaments in Alzheimers disease. *J. Neuropath. Exp. Neur.* **1986**, *45*, 338.

(82) Francis, P. T.; Palmer, A. M.; Snape, M.; Wilcock, G. K. The cholinergic hypothesis of Alzheimer's disease: a review of progress. *J. Neurol. Neurosur.* **1999**, *66*, 137.

(83) Bowen, D. M.; Smith, C. B.; White, P.; Davison, A. N. Neurotransmitter-related enzymes and indexes of hypoxia in senile dementia and other abiotrophies. *Brain* **1976**, *99*, 459.

(84) Davies, P.; Maloney, A. J. F. Selective loss of central cholinergic neurons in Alzheimers disease. *Lancet*. **1976**, *2*, 1403.

(85) Perry, E. K.; Gibson, P. H.; Blessed, G.; Perry, R. H.; Tomlinson, B. E. Neurotransmitter enzyme abnormalities in senile dementia—choline-acetyltransferase and glutamic-acid decarboxylase activities in necropsy brain-tissue. *J. Neurol. Sci.* **1977**, *34*, 247.

(86) Drachman, D. A.; Leavitt, J. Human memory and cholinergic system-relationship to aging. *Arch. Neurol-Chicago* **1974**, *30*, 113.

(87) Anand, P.; Singh, B. A review on cholinesterase inhibitors for Alzheimer's disease. *Arch. Pharm. Res.* **2013**, *36*, 375.

(88) Morris, J. C. Challenging assumptions about Alzheimer's disease: mild cognitive impairment and the cholinergic hypothesis. *Ann. Neurol.* **2002**, *51*, 143.

(89) Gilling, K.; Jatzke, C.; Wollenburg, C.; Vanejevs, M.; Kauss, V.; Jirgensons, A.; Parsons, C. G. A novel class of amino-alkylcyclohexanes as uncompetitive, fast, voltage-dependent, N-methyl-D-aspartate (NMDA) receptor antagonists - in vitro characterization. *J. Neural. Transm.* **2007**, *114*, 1529.

(90) Zemek, F.; Drtinova, L.; Nepovimova, E.; Sepsova, V.; Korabecny, J.; Klimes, J.; Kuca, K. Outcomes of Alzheimer's disease therapy with acetylcholinesterase inhibitors and memantine. *Exp. Opin. drug Saf.* **2014**, *13*, 759.

(91) Selkoe, D. J. The molecular pathology of Alzheimers disease. *Neuron* **1991**, *6*, 487.

(92) Mudher, A.; Lovestone, S. Alzheimer's disease-do tauists and baptists finally shake hands? *Trends in Neurosci.* **2002**, *25*, 22.

(93) Chartier-Harlin, M. C.; Crawford, F.; Houlden, H.; Warren, A.; Hughes, D.; Fidani, L.; Goate, A.; Rossor, M.; Roques, P.; Hardy, J.; et al. Early-onset Alzheimer's disease caused by mutations at codon 717 of the beta-amyloid precursor protein gene. *Nature* **1991**, *353*, 844.

(94) Goate, A.; Chartier-Harlin, M. C.; Mullan, M.; Brown, J.; Crawford, F.; Fidani, L.; Giuffra, L.; Haynes, A.; Irving, N.; James, L.; et al. Segregation of a missense mutation in the amyloid precursor protein gene with familial Alzheimer's disease. *Nature* **1991**, *349*, 704.

(95) Murrell, J.; Farlow, M.; Ghetti, B.; Benson, M. D. A mutation in the amyloid precursor protein associated with hereditary Alzheimer's disease. *Science* **1991**, *254*, 97.

(96) Rogaev, E. I.; Sherrington, R.; Rogaeva, E. A.; Levesque, G.; Ikeda, M.; Liang, Y.; Chi, H.; Lin, C.; Holman, K.; Tsuda, T.; et al. amilial Alzheimer's disease in kindreds with missense mutations in a gene on chromosome 1 related to the Alzheimer's disease type 3 gene. *Nature* **1995**, *376*, 775.

(97) Sherrington, R.; Rogaev, E. I.; Liang, Y.; Rogaeva, E. A.; Levesque, G.; Ikeda, M.; Chi, H.; Lin, C.; Li, G.; Holman, K.; Tsuda, T.; Mar, L.; Foncin, J. F.; Bruni, A.

C.; Montesi, M. P.; Sorbi, S.; Rainero, I.; Pinessi, L.; Nee, L.; Chumakov, I.; Pollen, D.; Brookes, A.; Sanseau, P.; Polinsky, R. J.; Wasco, W.; Da Silva, H. A.; Haines, J. L.; Perkicak-Vance, M. A.; Tanzi, R. E.; Roses, A. D.; Fraser, P. E.; Rommens, J. M.; St George-Hyslop, P. H. Cloning of a gene bearing missense mutations in early-onset familial Alzheimer's disease. *Nature* **1995**, *375*, 754.

(98) Levy-Lahad, E.; Wijsman, E. M.; Nemens, E.; Anderson, L.; Goddard, K. A.; Weber, J. L.; Bird, T. D.; Schellenberg, G. D. A familial Alzheimer's disease locus on chromosome 1. *Science* **1995**, *269*, 970.

(99) Lammich, S.; Kojro, E.; Postina, R.; Gilbert, S.; Pfeiffer, R.; Jasionowski, M.; Haass, C.; Fahrenholz, F. Constitutive and regulated alpha-secretase cleavage of Alzheimer's amyloid precursor protein by a disintegrin metalloprotease. *Proc. Natl. Acad. Sci. U. S. A.* **1999**, *96*, 3922.

(100) Vassar, R.; Bennett, B. D.; Babu-Khan, S.; Kahn, S.; Mendiaz, E. A.; Denis, P.; Teplow, D. B.; Ross, S.; Amarante, P.; Loeloff, R.; Luo, Y.; Fisher, S.; Fuller, L.; Edenson, S.; Lile, J.; Jarosinski, M. A.; Biere, A. L.; Curran, E.; Burgess, T.; Louis, J. C.; Collins, F.; Treanor, J.; Rogers, G.; Citron, M. Beta-secretase cleavage of Alzheimer's amyloid precursor protein by the transmembrane aspartic protease BACE. *Science* **1999**, *286*, 735.

(101) Wolfe, M. S.; Xia, W. M.; Ostaszewski, B. L.; Diehl, T. S.; Kimberly, W. T.; Selkoe, D. J. Two transmembrane aspartates in presenilin-1 required for presenilin endoproteolysis and gamma-secretase activity. *Nature* **1999**, *398*, 513.

(102) Willem, M.; Garratt, A. N.; Novak, B.; Citron, M.; Kaufmann, S.; Rittger, A.; DeStrooper, B.; Saftig, P.; Birchmeier, C.; Haass, C. Control of peripheral nerve myelination by the beta-secretase BACE1. *Science* **2006**, *314*, 664.

(103) De Strooper, B.; Annaert, W.; Cupers, P.; Saftig, P.; Craessaerts, K.; Mumm, J. S.; Schroeter, E. H.; Schrijvers, V.; Wolfe, M. S.; Ray, W. J.; Goate, A.; Kopan, R. A presenilin-1-dependent gamma-secretase-like protease mediates release of Notch intracellular domain. *Nature* **1999**, *398*, 518.

(104) Green, R. C.; Schneider, L. S.; Amato, D. A.; Beelen, A. P.; Wilcock, G.; Swabb, E. A.; Zavitz, K. H.; Grp, T. P. S. Effect of Tarenflurbil on Cognitive Decline and Activities of Daily Living in Patients With Mild Alzheimer Disease A Randomized Controlled Trial. *JAMA* **2009**, *302*, 2557.

(105) Menting, K. W.; Claassen, J. A. H. R. Beta-secretase inhibitor; a promising novel therapeutic drug in Alzheimer's disease. *Front. Aging Neurosci.* **2014**, *6*.

(106) Merck Sharp & Dohm Corp. A Phase III, Randomized, Placebo-Controlled, Parallel-Group, Double-Blind Clinical Trial to Study the Efficacy and Safety of MK-8931 (SCH 900931) in Subjects With Amnestic Mild Cognitive Impairment Due to Alzheimer's Disease. In: ClinicalTrials.gov [Internet]. Bethesda (MD): National Library of Medicine (US). 2000-[cited 2015 April 3]. Available from: https://www.clinicaltrials.gov/ct2/show/NCT01953601 NLM Identifier: NCT 01953601

(107) Wolfe, M. S. Therapeutic strategies for Alzheimer's disease. *Nat Rev Drug Discov* **2002**, *1*, 859.

(108) Weingarten, M. D.; Lockwood, A. H.; Hwo, S. Y.; Kirschner, M. W. A protein factor essential for microtubule assembly. *Proc. Natl. Acad. Sci. U. S. A.* **1975**, *72*, 1858.

(109) LoPresti, P.; Szuchet, S.; Papasozomenos, S. C.; Zinkowski, R. P.; Binder, L. I. Functional implications for the microtubule-associated protein tau: localization in oligodendrocytes. *Proc. Natl. Acad. Sci. U. S. A.* **1995**, *92*, 10369.

(110) Cleveland, D. W.; Hwo, S. Y.; Kirschner, M. W. *J.* Physical and chemical properties of purified tau factor and the role of tau in microtubule assembly. *Mol. Biol.***1977**, *116*, 227.

(111) Arriagada, P. V.; Growdon, J. H.; Hedley-Whyte, E. T.; Hyman, B. T. Neurofibrillary tangles but not senile plaques parallel duration and severity of Alzheimer's disease. *Neurology* **1992**, *42*, 631.

(112) Rapoport, M.; Dawson, H. N.; Binder, L. I.; Vitek, M. P.; Ferreira, A. Tau is essential to beta-amyloid-induced neurotoxicity. *Proc. Natl. Acad. Sci. U. S. A.* **2002**, *99*, 6364.

(113) Roberson, E. D.; Scearce-Levie, K.; Palop, J. J.; Yan, F.; Cheng, I. H.; Wu, T.; Gerstein, H.; Yu, G. Q.; Mucke, L. Reducing endogenous tau ameliorates amyloid beta-induced deficits in an Alzheimer's disease mouse model. *Science* **2007**, *316*, 750.

(114) Goedert, M.; Jakes, R. Mutations causing neurodegenerative tauopathies. *Biochem. Biophys. Acta* **2005**, *1739*, 240.

(115) Spillantini, M. G.; Goedert, M. Tau pathology and neurodegeneration. *The Lancet. Neurol.* **2013**, *12*, 609.

(116) Llorens-Martin, M.; Jurado, J.; Hernandez, F.; Avila, J. GSK-3beta, a pivotal kinase in Alzheimer disease. *Front. Mol. Neurosci.* **2014**, *7*, 46.

(117) Drewes, G.; Ebneth, A.; Preuss, U.; Mandelkow, E. M.; Mandelkow, E. MARK, a novel family of protein kinases that phosphorylate microtubule-associated proteins and trigger microtubule disruption. *Cell* **1997**, *89*, 297.

(118) Zheng-Fischhofer, Q.; Biernat, J.; Mandelkow, E. M.; Illenberger, S.; Godemann, R.; Mandelkow, E. Sequential phosphorylation of Tau by glycogen synthase kinase-3beta and protein kinase A at Thr212 and Ser214 generates the Alzheimer-specific epitope of antibody AT100 and requires a paired-helical-filament-like conformation. *Eur. J. Biochem.* **1998**, *252*, 542.

(119) Kimura, T.; Ishiguro, K.; Hisanaga, S. Physiological and pathological phosphorylation of tau by Cdk5. *Front. Mol. Neurosci.* **2014**, *7*, 65.

(120) Medina, M.; Avila, J. New perspectives on the role of tau in Alzheimer's disease. Implications for therapy. *Biochem. Pharmacol.* **2014**, *88*, 540.

(121) Bulic, B.; Pickhardt, M.; Schmidt, B.; Mandelkow, E. M.; Waldmann, H.; Mandelkow, E. Development of tau aggregation inhibitors for Alzheimer's disease. *Angew. Chem. Int. Ed.* **2009**, *48*, 1740.

(122) Wischik, C. M.; Staff, R. T.; Wischik, D. J.; Bentham, P.; Murray, A. D.; Storey, J. M.; Kook, K. A.; Harrington, C. R. Tau aggregation inhibitor therapy: an exploratory phase 2 study in mild or moderate Alzheimer's disease. *J. Alzheimer's Dis.* **2015**, *44*, 705.

(123) Berger, Z.; Roder, H.; Hanna, A.; Carlson, A.; Rangachari, V.; Yue, M.; Wszolek, Z.; Ashe, K.; Knight, J.; Dickson, D.; Andorfer, C.; Rosenberry, T. L.; Lewis, J.;

Hutton, M.; Janus, C. Accumulation of pathological tau species and memory loss in a conditional model of tauopathy. *J. Neurosci.* **2007**, *27*, 3650.

(124) Ke, Y. D.; Suchowerska, A. K.; van der Hoven, J.; De Silva, D. M.; Wu, C. W.; van Eersel, J.; Ittner, A.; Ittner, L. M. Lessons from tau-deficient mice. *Int. J. Alz. Dis.* **2012**, *2012*, 873270.

(125) Dickey, C. A.; Dunmore, J.; Lu, B.; Wang, J. W.; Lee, W. C.; Kamal, A.; Burrows, F.; Eckman, C.; Hutton, M.; Petrucelli, L. HSP induction mediates selective clearance of tau phosphorylated at proline-directed Ser/Thr sites but not KXGS (MARK) sites. *FASEB* **2006**, *20*, 753.

(126) Berger, Z.; Ravikumar, B.; Menzies, F. M.; Oroz, L. G.; Underwood, B. R.; Pangalos, M. N.; Schmitt, I.; Wullner, U.; Evert, B. O.; O'Kane, C. J.; Rubinsztein, D. C. Rapamycin alleviates toxicity of different aggregate-prone proteins. *Hum. Mol. Genet.* **2006**, *15*, 433.

(127) Ji, H. F.; Li, X. J.; Zhang, H. Y. Natural products and drug discovery. Can thousands of years of ancient medical knowledge lead us to new and powerful drug combinations in the fight against cancer and dementia? *EMBO Rep.* **2009**, *10*, 194.

(128) Hartmann, T. From waste products to ecochemicals: fifty years research of plant secondary metabolism. *Phytochemistry* **2007**, *68*, 2831.

(129) Sneader, W. The discovery of aspirin: a reappraisal. *BMJ* **2000**, *321*, 1591.

(130) Newman, D. J.; Cragg, G. M. Natural products as sources of new drugs over the 30 years from 1981 to 2010. *J. Nat. Prod.* **2012**, *75*, 311.

(131) Ganesan, A. The impact of natural products upon modern drug discovery. *Curr. Opin. Chem. Bio.* **2008**, *12*, 306.

(132) Balthaser, B. R.; Maloney, M. C.; Beeler, A. B.; Porco, J. A., Jr.; Snyder, J. K. Remodelling of the natural product fumagillol employing a reaction discovery approach. *Nature Chem.* **2011**, *3*, 969.

(133) Burke, M. D.; Schreiber, S. L. A planning strategy for diversity-oriented synthesis. *Angew. Chem. Int. Ed.* **2004**, *43*, 46.

(134) Huigens, R. W., 3rd; Morrison, K. C.; Hicklin, R. W.; Flood, T. A., Jr.; Richter, M. F.; Hergenrother, P. J. A ring-distortion strategy to construct stereochemically complex and structurally diverse compounds from natural products. *Nature Chem.* **2013**, *5*, 195.

(135) McLeod, M. C.; Singh, G.; Plampin, J. N., 3rd; Rane, D.; Wang, J. L.; Day, V. W.; Aubé, J. Probing chemical space with alkaloid-inspired libraries. *Nature Chem.* **2014**, *6*, 133.

(136) Pelish, H. E.; Westwood, N. J.; Feng, Y.; Kirchhausen, T.; Shair, M. D. Use of biomimetic diversity-oriented synthesis to discover galanthamine-like molecules with biological properties beyond those of the natural product. *J. Am. Chem. Soc.* **2001**, *123*, 6740.

(137) United Nations Convention on Biological Diversity. *J. Ethnopharmacol.* **1996**, *51*, 287.

(138) Morgera, E.; Buck, M.; Tsioumani, E. *The 2010 Nagoya Protocol on Access and Benefit-sharing*; M. Nijhoff Pub.: Leiden ; Boston, 2013.

(139) Drahl, C. Navigating Nagoya. *Chemical & Engineering News Archive* **2011**, *89*, 50.

## II. Modifications to the Furan Ring of Salvinorin A

*Introduction*

The psychoactive plant *Salvia divinorum* found in Oaxaca, Mexico has been used by Mazatec shamans for centuries in traditional divination rituals due to the vivid hallucinations experienced following ingestion of the plant's leaves.[1] In addition to its use to induce divination, *S. divinorum* was also used in the treatment for constipation, diarrhea, headache, and rheumatism.[1] The hallucinatory effects of *S. divinorum*, have more recently attracted the attention of recreational drug users seeking a "legal high."[2,3] However, several state and national legislatures have responded by outlawing the sale of the plant.[4] In 1982, the neoclerodane diterpene salvinorin A (Figure 2.1, **1**) was isolated from *S. divinorum*[5] and was later determined to be responsible for the plant's hallucinatory actions.[6]

Following the identification and structure elucidation of **1**, its pharmacological target was identified through the NIH Psychoactive Drug Screening Program.[7] In a screen of 50 targets consisting of receptors, transporters, and ion channels, **1** was found to bind selectively and potently activate the kappa opioid receptor (KOR). These actions are particularly noteworthy for several

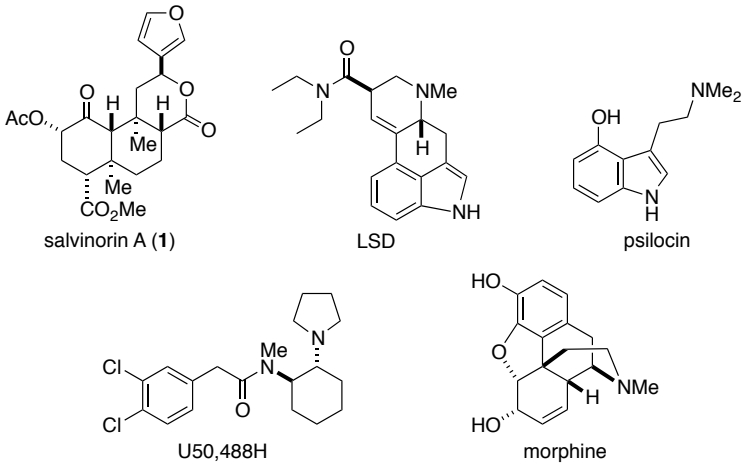


**Figure 2.1.** Structures of salvinorin A (**1**) and structurally dissimilar hallucinogens LSD and psilocin and opioid ligands U50,488H and morphine.

reasons. First, **1** does not derive its psychoactive effects from the 5-$HT_{2a}$ receptor, the target of traditional hallucinogens such as psilocin and LSD (Figure 2.1). This involvement of the KOR in perception provides support for the notion that the KOR could serve as a potential target for a number of diseases where perception is altered, for example schizophrenia or dementia.[8] Secondly, the terpenoid structure of **1** makes it structurally distinct from other known opioid ligands such as the arylacetamide U50,488H and opiates like morphine (Figure 2.1). A basic nitrogen was previously believed to be a structural requirement for binding to a highly conserved aspartate residue within the binding site of the opioid receptors.[9,10] However, the isolation of **1** as the first non-nitrogenous opioid has led to a crucial rethinking of this hypothesis and the development of novel non-nitrogenous ligands.[11]

Due to the structural distinctiveness of **1**, several models have been developed in an attempt to understand how it interacts with the KOR (Figure 2.2). Historically, most opioid receptor models begin with the creation of an *in silico* salt-bridge between a basic nitrogen and the conserved aspartate residue in TMIII.[12] However, the lack of basic nitrogen in **1** requires alternative approaches to be taken. Using a molecular model original built for the KOR agonist U69,598, Roth *et. al.* proposed a model with key hydrogen bonding interactions taking place at the furan ring (Q115), lactone carbonyl oxygen (Y139), carbomethoxy carbonyl oxygen (Y312) and the acetate carbonyl oxygen (Y313) (Figure 2.2A).[7] Based upon subsequent site-directed mutagenesis, covalent labeling, and substituted-cysteine accessibility method (SCAM) studies this model was later adjusted to revise the H-bonding interactions at the furan ring (Y119 and Y320) and

to include hydrophobic iterations with the methyl ester (I294 and E297) and C2 acetate (Y313) (Figure 2.2B).[13,14]

Using chimeric opioid receptors and site-directed mutagenesis, an additional model was proposed by Kane.[12] Here the key interactions consisted of hydrophobic interaction with the C2 acetate (Y312 and Y313), H-bonding interactions with the lactone carbonyl oxygen (Q115), and pi-stacking interactions with the furan (Y320) (Figure

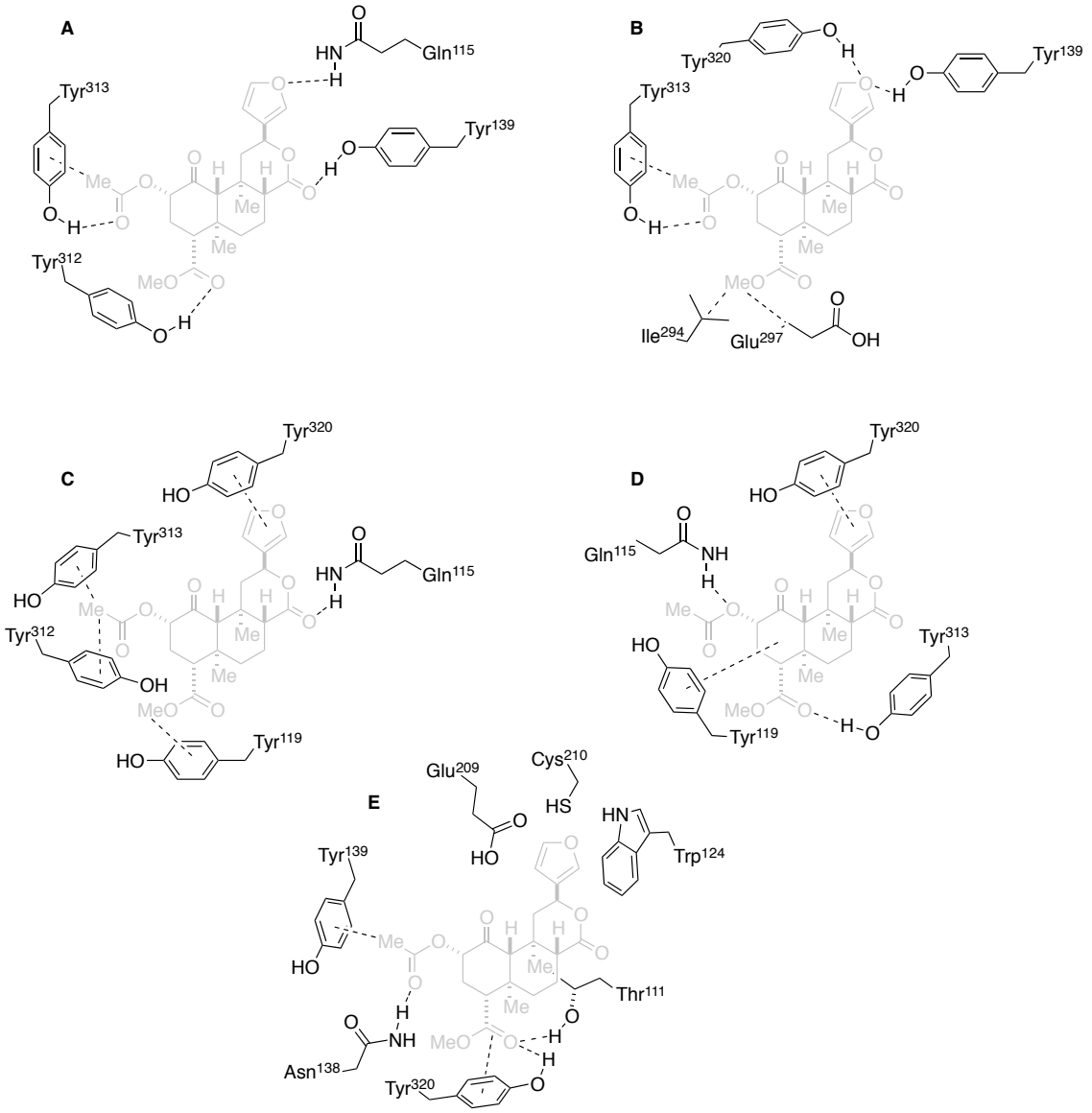


**Figure 2.2.** Putative binding modes for **1** with key residues as proposed by A)Roth[7] B)Yan[13,14] C) Kane[12] D)Singh[15] E)Vardy[18].

2.2C). In an alternative approach to incorporate data from structure-activity relationship studies, this group also utilized a training set of 15 derivatives of **1** to develop a virtual model. This model was shown to be reasonable accurate at predicting the activity of other analogues of **1**. Similar pi-stacking with the furan ring (Y320) was proposed however the role of the amino acid residues Q115, Y119, and Y313 were adjusted to interact with the C2 ester, diterpene backbone, and carbomethoxy carbonyl, respectively (Figure 2.2D).[15] Although the four models discussed above are slightly different, all the residues invoked are in close proximity within the three-dimensional structure of the receptor. This is particularly impressive considering that the antagonist-bound structure of the KOR was not solved until 2012,[16] several years after these models were developed.

The advent of the crystal structure of the KOR is likely to have a profound impact upon future ligand development. It is, however, important to note that because the KOR antagonist JD-Tic was bound in the active site, the receptor is in the inactive state. Nevertheless, virtual library screening using this inactive state has produced novel agonist leads[17] suggesting that binding models for **1** based upon this structure may be useful. Following the solving of the structure, a model was developed for the endogenous peptide dynorphin A, the arylacetamide U69,593, the octahydroisoquinolinone carboxamide 1xx, and **1**.[18,19] The model for **1** proposes a very detailed list of the amino acid residues that are in close proximity to the ligand (Figure 2.2E). Among these are the pocket created by Glu209, Cys210, and Trp124 to accommodate the furan ring without any clear H-bond or pi-stacking interactions. The C4 methyl ester is proposed to interact through both H-bonding interactions (Thr111 and Tyr320) and potentially through a pi-stacking interaction (Tyr320). Finally, the acetoxy moeity is suggested to interact through

both a hydrophobic interaction via the acetyl methyl (Tyr139) and an H-bond interaction via the carbonyl oxygen (Arg138). Although this latest model differs the most from the other four, because it is based upon the KOR crystal structure rather than that of rhodopsin, it likely provides the clearest picture of the true interactions. However this cannot be definitively known until a crystal structure of the **1**-KOR complex is solved.

Until this time, further elucidation of how **1** binds with the KOR will require the continued use of structure-activity relationship (SAR) studies through the development of semi-synthetic probe molecules. Historically these studies have been important in determining the functionality in **1** required for proper binding and activation. This topic has been eloquently reviewed,[20] and some general trends are highlighted in Figure 2.3. However two positions have attracted the majority of the attention and deserve additional comment. Removal of the C2 acetyl moiety results in the alcohol salvinorin B, a diterpene also found in the leaves of *S. divinorum*, that is devoid of KOR activity.[21] Largely due to the ease and reproducibility of this hydrolysis, numerous studies have explored this position ultimately leading to several important findings. These include the discovery of methanesulfonyl (Ms), ethoxymethyl (EOM), and methoxymethyl (MOM) substituted salvinorin B which all show equal or increased affinity at the KOR (Figure 2.4). Because of their increased metabolic stability these compounds have served as excellent probe molecules for examining the KOR *in vivo*.[22-25]

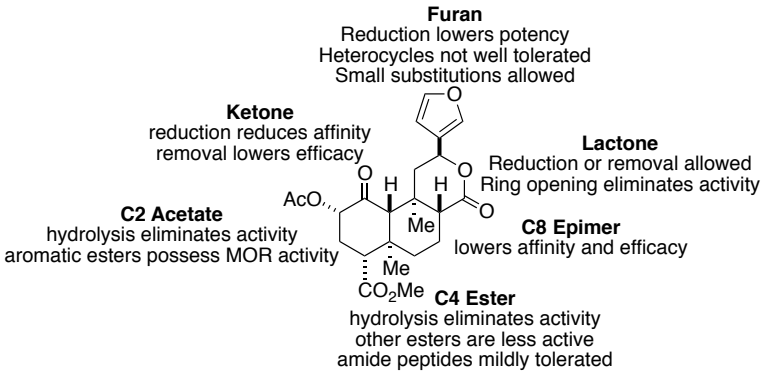


**Figure 2.3.** Established structure activity relationships for **1** at the KOR.

An equally important finding was that C2 aromatic esters possess significantly less activity at KOR but increased activity at the mu opioid receptor (MOR), making these probes attractive leads for novel treatments for pain.

The other well-studied position is the furan moiety appended at C12. Primarily due to the metabolic toxicity associated with furan rings,[26] most of these investigations have focused on its replacement. Heterocycles such as oxazolines, oxazoles, pyrroles, triazoles, benzothiophenes, and benzofurans have been explored however these analogues ultimately result in poor affinity. A ligand bearing a 2-methyl-1,3,5-oxazdiazole (**3**) did however result in only a modest 30-fold reduction in binding relative to **1** (Figure 2.4). Therefore the preparation of additional heterocyclic isosteres may be worthwhile to improve the metabolic stability of **1**.

Prior to 2013, significantly less work had been done to investigate the effects of substitutions on the furan ring itself. The lone examples in the literature, 16-bromosalvinorin A (**4**) and 16-vinylsalvinorin A (**5**), showed only small differences in

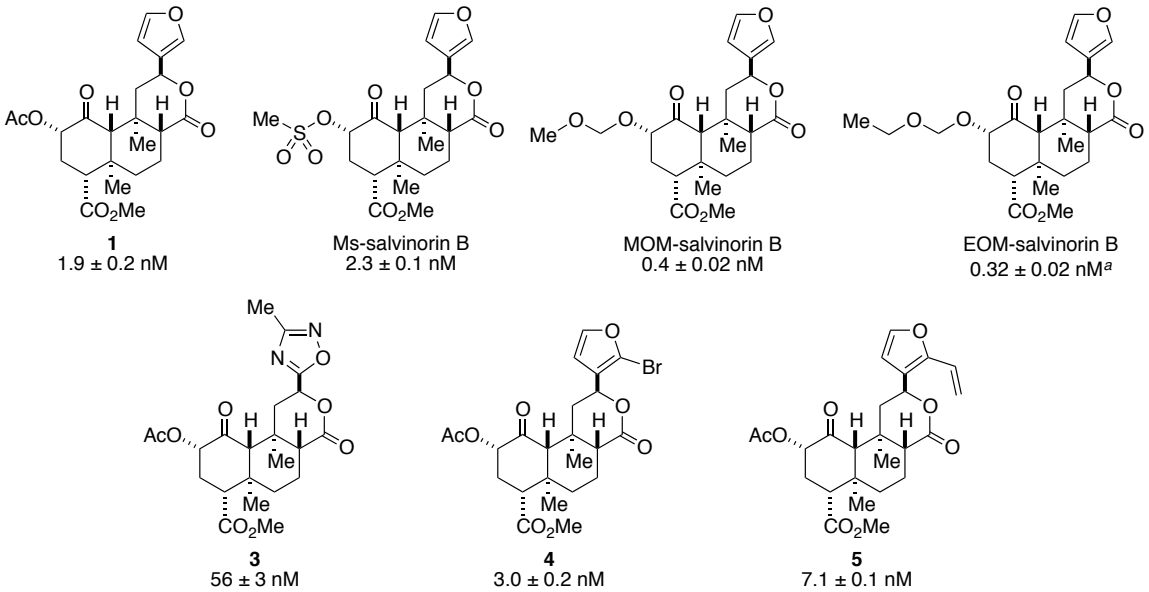


**Figure 2.4.** Salvinorin A and several derivatives and their corresponding $K_i$ values.[20]

binding at the KOR in comparison to **1**,[27] indicating other substitutions may also be tolerated. Because the furan ring is implicated in every proposed binding model (Figure 2.2) substitutions that effect the steric or electronic character of the furan ring may be useful in determining how **1** interacts with its molecular target.

*Synthesis of Analogues*

*Replacement of Furan with Isoxazoles*

Based upon the limited success of previous studies utilizing heterocycles that differed significantly from furan, it was envisioned that isoxazoles appended to the neoclerodane core at the 3-position would serve as better probes. These heterocycles differ from furan by the replacement of the C16 methine with a nitrogen and allow for substitutions at C15. This additional nitrogen is expected to cause increased *in vivo* stability due to differences in metabolism. The toxicity associated with furans is the result of their CYP450-mediated oxidation, which eventually results in enonals that can undergo bioconjugation either via a Michael addition or through attack of the aldehyde (Scheme 2.1). The pi system of the isoxazole is less electron rich due to the additional heteroatom, therefore isoxazoles undergo reductive ring openings. Hydrolysis of the resulting imine results in a diketone that is more metabolically stable.[26] The ability to include substitutions at C15 will allow for additional probing of the KOR binding pocket.

**Scheme 2.1.** Differences in metabolism of furans and isoxazoles

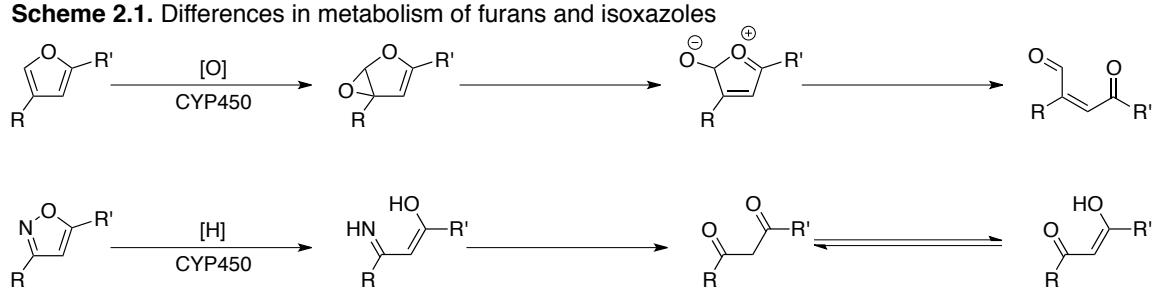

The synthesis of the isoxazole probes begins with the known three step protocol to convert the furan ring of **1** to an aldehyde (Scheme 2.2).[28] Briefly, ruthenium-catalyzed oxidative degradation of the furan produces the carboxcylic acid that is then converted to an ethyl thioester. Selective reduction of the thioester in the presence of four other carbonyls is accomplished using a mild Fukuyama reduction. Through this process gram quantities of the aldehyde **7** can be synthesized with only a single chromatographic purification step. Condensation of **7** with hydroxylamine in refluxing methanol and pyridine produces the oxime **8** as separable mixture of *cis* and *trans* isomers. This mixture is then oxidized to the nitrile oxide with (bis(trifluoracetoxy)iodo)benzene (PIFA) which undergoes a [3+2] dipolar cycloaddition with a number of terminal alkynes.[29] The resulting isoxazoles were isolated in moderate yields and as a single regioisomer. In this initial study, both aromatic and aliphatic alkynes were used to investigate potential effects on activity at the KOR.

**Scheme 2.2**. Synthesis of isoxazloes via [3+2] cycloaddition reactions[a]

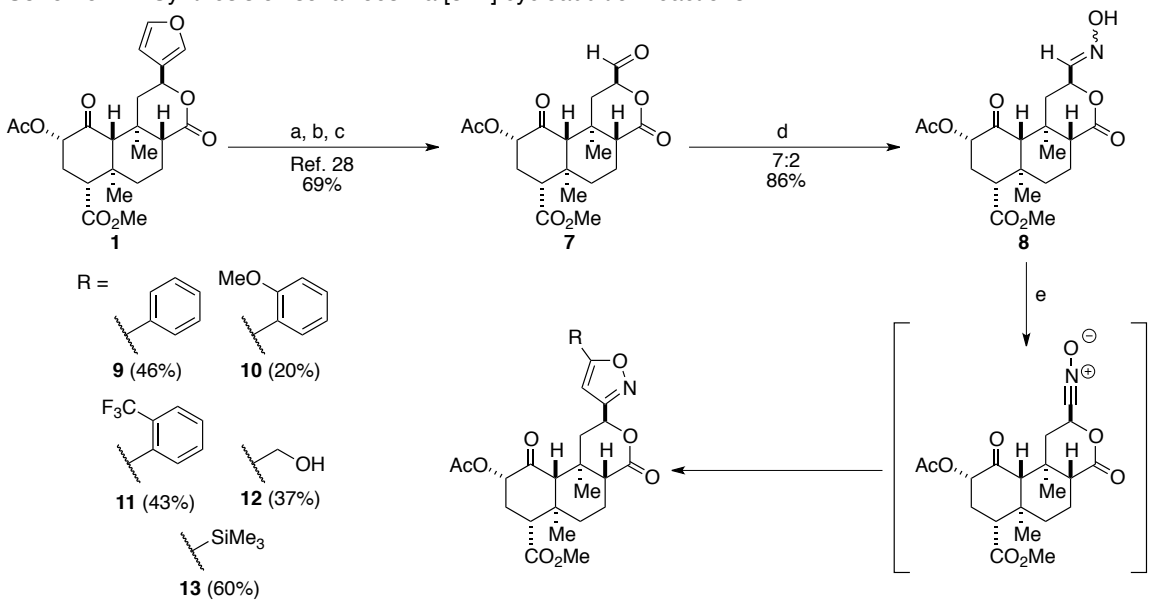


[a]Reagents and condidtions: a) $RuCl_3 \cdot H_2O$ (0.03 equiv), $NaIO_4$ (12 equiv), $CCl_4$, $Ch_3CN$, $H_2O$, RT, 3 h; b) CDMT (3 equiv), NMM (6 equiv), EtSH (3 equiv), THF, RT, 48 h; c) Pd/C (0.10 equiv), $Et_3SiH$ (3 equiv), $CH_2Cl_2$, 16 h; d) $NH_2OH \cdot HCl$ (4 equiv), pyr. (10 equiv), MeOH, 65 °C, 4 h; e) $PhI(TFA)_2$ (1.5 equiv), HC≡CR (5 equiv), MeCN, $H_2O$ 16 h.

To access the unsubstituted isoxazole, ethynyltrimethylsilane was employed in the cycloaddition reaction to produce **13**. Unfortunately attempts to remove the silyl protecting group using either CsF[30] or TBAF resulted in a formal loss of ketene to produce the nitrile **14** (Scheme 2.3). This structural assignment was confirmed by comparison to a sample of **14** prepared via the tosylchloride-mediated dehydration of **8**. A careful examination of the literature reveals that this fluoride-promoted fragmentation of the isoxazole ring is known and thought to occur via the corresponding anion.[31] Recently, similar fragmentations have been used for the installation of acetonitriles moieties to aromatic systems.[32,33]

**Scheme 2.3**. Attempt to desilylate **13** results in nitrlie formation[a]

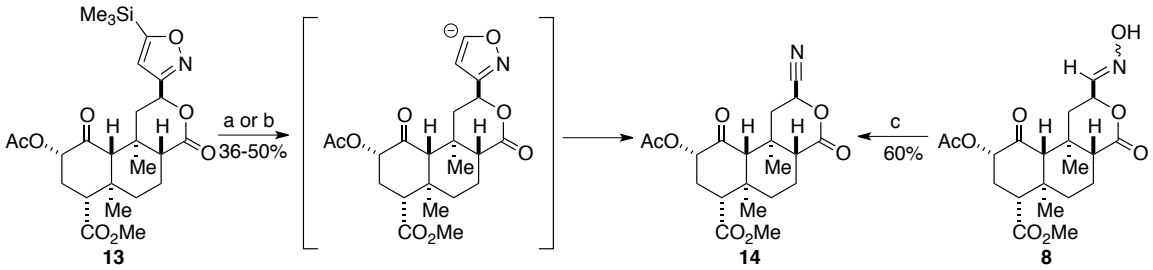


[a]Reagents and condidtions: a) CsF (1.4 equiv), MeCN, EtOH, RT, 30 min; b) TBAF (1.0 equiv), $CH_2Cl_2$, 0 °C, 30 min; c) TsCl (1.0 equiv), $Et_3N$ (2.0 equiv), $CH_2Cl_2$, RT, 24 h.

*Substitutions to the Furan Ring*

In order to probe the steric and electronic effects in the furan ring binding pocket of the KOR, a series of probe molecules with modifications to the furan ring was needed. The methods that were developed to provide these substitutions drew heavily upon the selective bromination of the C16 position and subsequent palladium-catalyzed Stille coupling that had been previously reported. However both of these processes would require significant improvement in order to expand the number of substitutions that could be accessed.

**Scheme 2.4.** Mono- and di-bromination of **1**.[a]

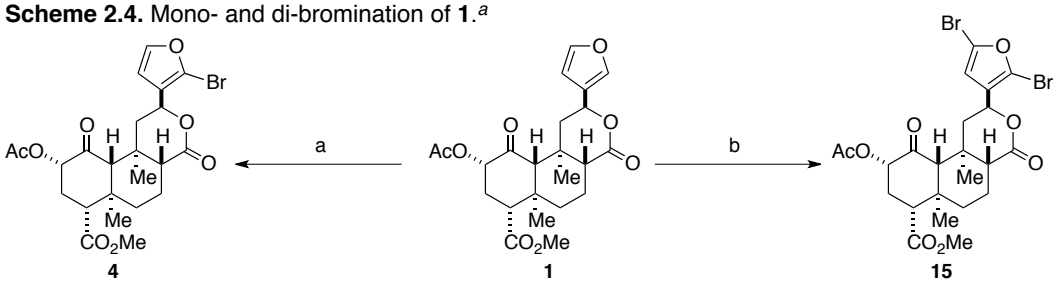


[a] Reagents and conditions: a) NBS (1.4 equiv), $Br_2$ (cat.), $CH_2Cl_2$, RT, 30 min; b) NBS (1.4 equiv), $Br_2$ (1.0 equiv), $CH_2Cl_2$, RT, 30 min.

The bromination of **1** with NBS has been reported several times in the literature,[27,34,35] however under these conditions the reaction requires extended reaction times leading to decomposition of **1** and yields that vary between 10-61%. A brief screen of several additives found that the addition of a catalytic amount of $Br_2$ led to complete conversion after only 30 minutes and consistent yields of 49% (Scheme 2.4).[36] The arylbromide product (**4**) was spectroscopically identical to that isolated from the uncatalyzed reaction and for the first time the regiochemistry was confirmed by single-crystal X-ray diffraction (Figure 2.5). The mechanism by which $Br_2$ affects the reaction remains to be elucidated however $Br_2$ may simply be serving as a source of catalytic HBr. Interestingly, the use of stoichiometric amount of $Br_2$ results in the dibromide **15**.

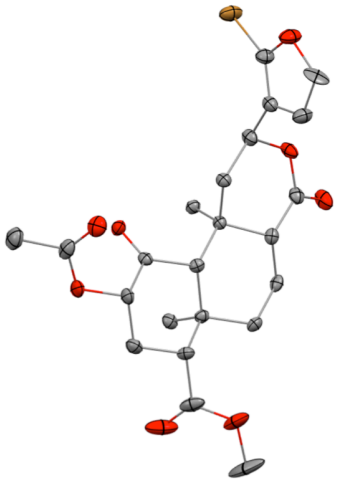

**Figure 2.5**. X-ray crystal structure of **4** confirming substitution at C16.

With rapid and reliable access to **4,** investigations into using this arylbromide as a functional handle to introduce other substitutions to the furan ring were now possible. This has previously be demonstrated with a Stille coupling in the synthesis of **5**, however the significant toxicity associated with organotin reagents makes this process less than ideal. The limited toxicity of boronic acids makes Suzuki-Miyaura couplings an attractive

alternative. Furthermore, the number of commercially available boronic acids now greatly outnumbers that of stannanes (14,601 and 1,097, respectively).[37]

To determine whether a Suzuki-Miyaura coupling could be applied to introduce substitution to the furan ring of **1** the cross-coupling of **4** and phenylboronic acid was first explored. The biaryl phosphine ligand SPhos developed by Buchwald has been shown to be quite successful in challenging Suzuki-Miyaura reactions and was therefore selected for the first attempt.[38,39] Employing the literature precedented reaction conditions led to full conversion of **4**, however two isomeric products were isolated from the reaction mixture. Detailed analysis of the $^{1}H$ and $^{13}C$ NMR spectra revealed these two compounds to be the C8 epimers **16** and **17** (Table 2.1). Epimerization at this alpha center is well documented in both semi-synthetic and total synthesis efforts and occurs under both basic and acid conditions.[40,41] Additionally, C8-epi-**1** is found in the smoke of pyrolysed *S. divinorum* leaves.[42,43] Unfortunately this epimerization results in a loss of nearly all activity at the KOR and evaluation of the **16** and **17** using a calcium mobilization assay indicated that **17** was nearly 50 times less potent that **16**. Therefore careful optimization of these reaction conditions was necessary to avoid this deleterious side reaction.

Noting that the epimerization is likely due to either the basic or thermal conditions used during the reaction, optimization studies focused primarily around these two variables (Table 2.1). Reducing the amount of base present did successfully reduce the amount of epimerization (Entry 1-3), however this also significantly reduced the conversion rate for the reaction. This proved to be particularly negative because **4** could not be easily removed from **16** by simple silica gel chromatography. Fortunately reducing the temperature from 100 °C to 60 °C with 3.0 equivalents of base resulted in full

conversion of **4** without any observable epimerization. Interestingly, decreasing the amount of base at this temperature resulted in lower conversion and increased levels of epimerization. Cooling the reaction to room temperature was unsuccessful and produced less than <10% conversion. Full conversion of **4** was observed in both THF and 1,4-dioxane but with increased levels of epimerization indicating toluene was the optimal solvent.

With these optimized conditions in hand, the full scope of potential substitutions was explored using a variety of commercially available boronic acids (Scheme 2.5). Substitutions were well-tolerated at all three positions to the phenyl ring producing

**Table 2.1.** Optimization of Suzuki-Miyaura Reaction Conditions.[a]

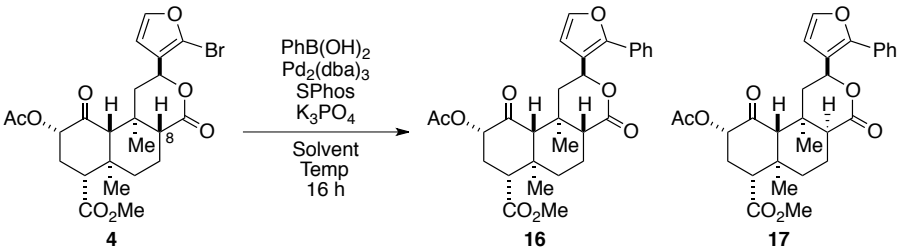


| Entry | Equiv Base | Temp (°C) | Solvent | % Conversion[b] | Ratio **16/17**[c] |
|---|---|---|---|---|---|
| 1 | 3.0 | 100 | PhMe | 100 | 12:1 |
| 2 | 2.5 | 100 | PhMe | 92 | 80:1 |
| 3 | 2.0 | 100 | PhMe | 17 | >99:1 |
| **4** | **3.0** | **60** | **PhMe** | **100** | **>99:1** |
| 5 | 2.5 | 60 | PhMe | 96 | 25:1 |
| 6 | 3.0 | RT | PhMe | <10 | --[d] |
| 7 | 2.5 | RT | PhMe | <10 | --[d] |
| 8 | 2.5 | 60 | 1,4-Diox | 100 | 19:1 |
| 9 | 2.5 | 60 | THF | 100 | 5:1 |

[a] General reaction conditions: $PhB(OH)_2$ (2 equiv), $Pd_2(dba)_3$ (0.04 equiv), SPhos (0.16 equiv). [b] Conversion based on the consumption of **4** as measured by GC–MS. [c] Ratio of **15**/**16** measure by HPLC. [d] Not measured due to lack of product formation.

products in moderate to excellent yield. As expected, boronic acids bearing electron-donating groups generally produced higher yields than electron-deficient boronic acids. Furans substituted at either the 2- or 3-position and the 3-thiophene were successfully appended to C16, however the 2-thiophene boronic acid was unsuccessful. These heterocyclic boronic acids are prone to protodeborylation.[44] This was somewhat overcome through the use of the MIDA-boronate technology developed by Burke however low reaction yields were still observed after 24 hours.[45] The incorporation of alkyl or alkenyl moieties was somewhat more challenging and the only successful products isolated were **39**-**42**. With all other alkyl boronic acids (such as cyclohexyl or isopropyl) and partially with phenethylboronic acid, the major product was **1**, from

**Scheme 2.5.** Substitutions to C16 through Suzuki-Miyaura reactions.[a]

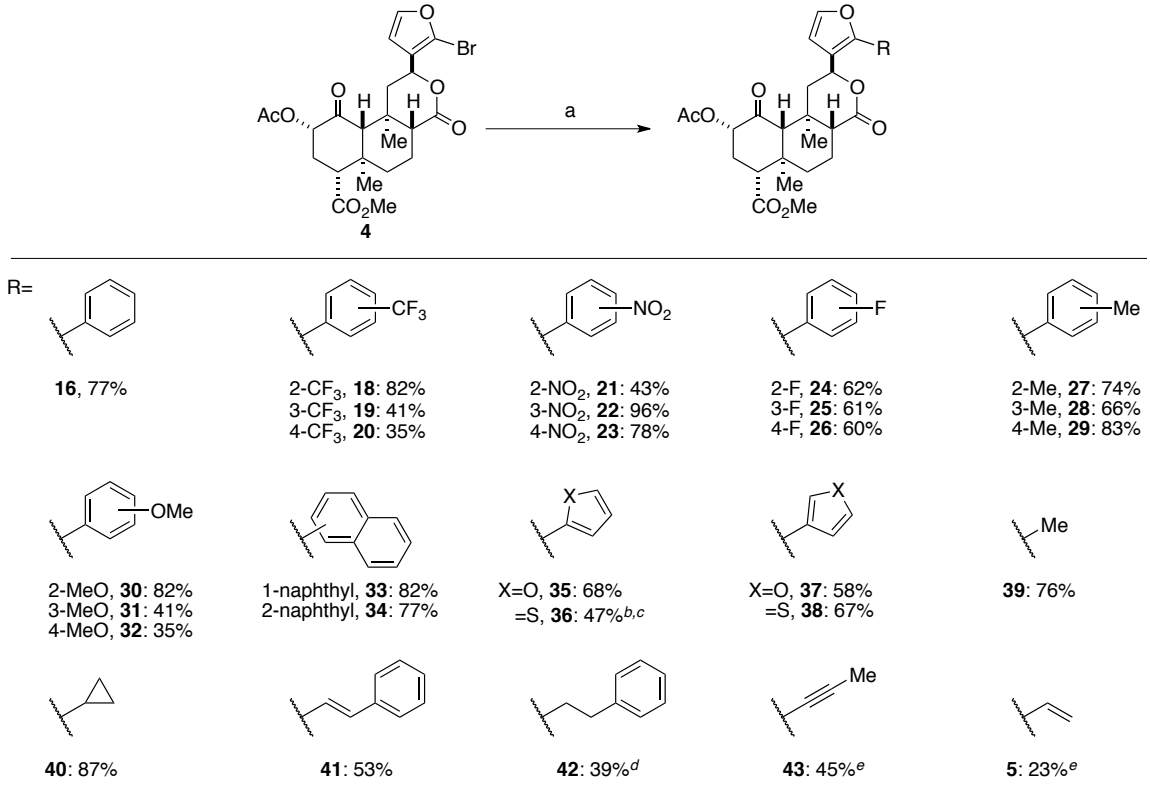


[a] Reagents and conditions: a) $RB(OH)_2$ (2.0 equiv), $K_3PO_4$ (3.0 equiv), $Pd_2(dba)_3$ (0.04 equiv), SPhos (0.16 equiv), PhMe, 60 °C, 16 h. bAlternate condition: 2-thiopheneboronic acid MIDA ester (1.2 equiv), $K_3PO_4$ (7.5 equiv), $Pd(OAc)_2$ (0.05 equiv), SPhos (0.10 equiv), diox/$H_2O$ (5:1), 60 °C, 24 h. c 69% BRSM. [d] 13% of **1** recovered. e Alternate condition: $RBF_3K$ (1.1 equiv), $Cs_2CO_3$ (3.0 equiv), $Pd(dppf)\cdot CH_2Cl_2$ (0.09 equiv), THF/$H_2O$ (20:1), 65 °C.

protodebromination of **4**. General access to alkyl substitutions was, however, made possible via the selective reduction of an olefin precursor. For example, the vinyl group in **5**, was easily reduced with Pd/C to an ethyl moiety (**44**) without the over reduction of the furan ring that had been previously reported (Scheme 2.6).[35,46] Under these conditions the nitro-substituted analogues **21**-**23** were also reduced to the corresponding anilines **45**-**47**, which were also unobtainable with Suzuki-Miyaura couplings.

**Scheme 2.6.** Selective reduction of olefin and nitro moieties.[a]

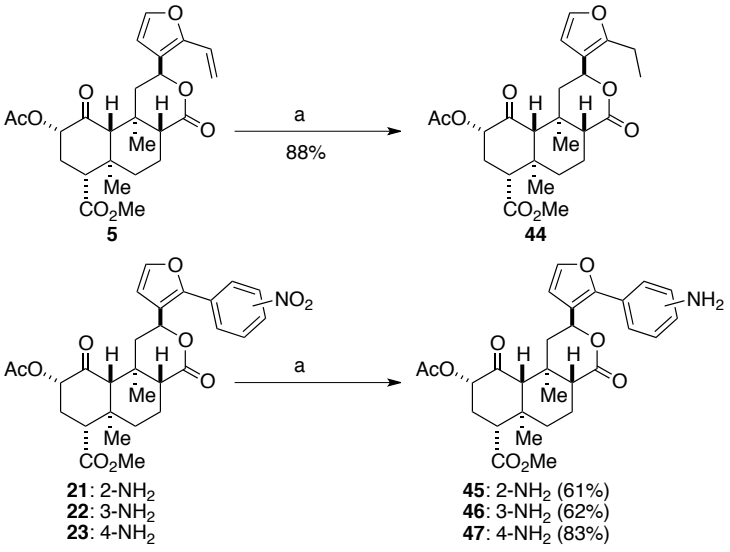


[a] Reagents and conditions: a) Pd/C (10%), $H_2$ (balloon), MeOH/THF (3:2).

To complement the $sp^2$- and $sp^3$-hybridzed substitutions made possible by the Suzuki-Miyaura couplings, terminal alkynes were introduced through a Sonogashira

**Scheme 2.7.** Introduction of alkyne substitutions via Sonogashira reactions.[a]

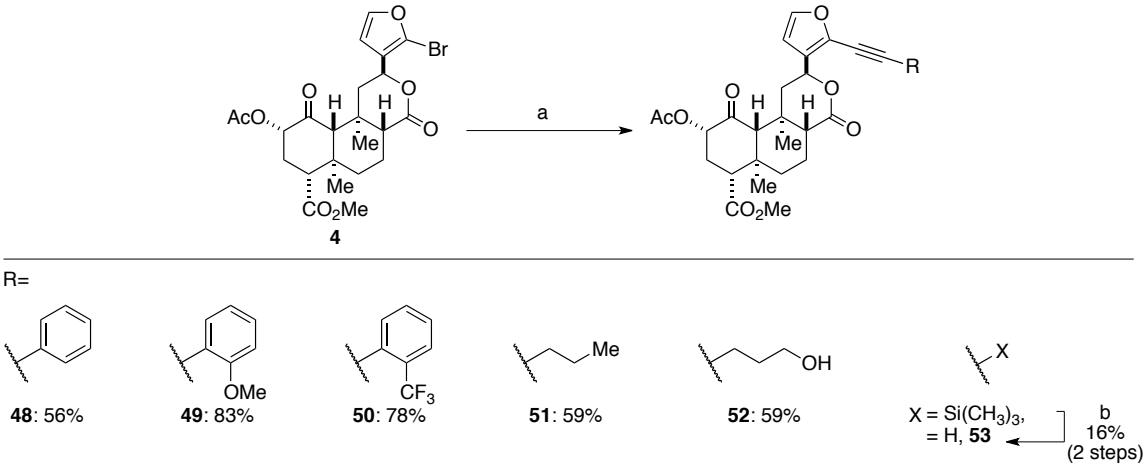


[a] Reagents and conditions: a) appropriate terminal alkyne (2.0 equiv), $PdCl_2(PPh_3)_2$ (0.05 equiv), CuI (0.1 equiv), THF/$Et_3N$ (1:1), 80 °C, 16 h; b) TBAF (2.0 equiv), $CH_2Cl_2$, RT, 30 min.

reaction (Scheme 2.7). In this case standard conditions proved successful without the need for optimization and no epimerization was observed despite the use of excess triethylamine at elevated temperatures. Using these conditions a more focused series was synthesized to access the effects of alkyl and aromatic groups at the end of the alkyne. The gaseous nature of propyne did prevent the use of a Sonogashira coupling however performing a Suzuki-Miyaura reaction with a trifluoroborate salt produced **43** in acceptable yields (Scheme 2.5). Similar conditions also allowed for the synthesis of the vinyl-substituted **5**.

The dibromide **16** was also a compatible partner in cross-coupling reactions, albeit a less efficient one. At first, the reaction was performed with a single equivalent of phenyl boronic acid to determine if there was any preference in regioselectivity, which could potentially allow access to C15-substituted analogues (Scheme 2.8). Interestingly the reaction resulted in a mixture of recovered starting material and the diarylated product **54**. The lack of a monoarylated product suggests that the second coupling reaction occurs faster than the first. Dimethylation of **16** with excess methylboronic acid resulted in **55** in

**Scheme 2.8.** Disubstitutions to the furan ring via Suzuki-Miyaura reactions.[a]

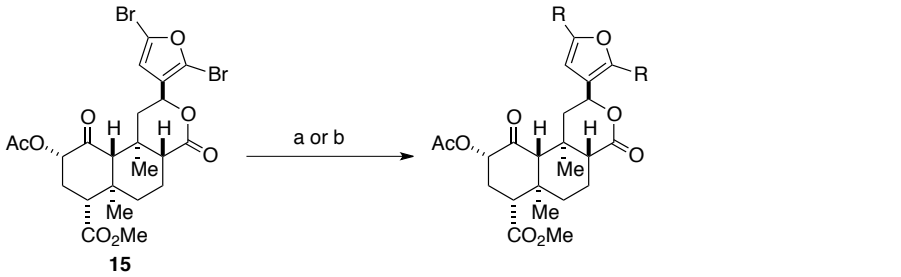


R=

**54**: 40%[b,c]


**55**: 46%[d]

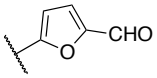


**56**: 14%[d]

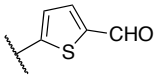


**57**: 13%[d]

[a] Reagents and conditions: a) $PhB(OH)_2$ (1.0 equiv.), $K_3PO_4$ (3.0 equiv), $Pd_2(dba)_3$ (0.04 equiv), SPhos (0.16 equiv), PhMe, 60 ° C, 16 h; b) a) $RB(OH)_2$ (4.0 equiv.), $K_3PO_4$ (3.0 equiv), $Pd_2(dba)_3$ (0.04 equiv), SPhos (0.16 equiv), PhMe, 60 °C, 16 h. [b]Condition (a) used. [c]72% BRSM. [d]Condition (b) used.

only 46%, which corresponds to less than 68% yield for each methylation. By comparison, the methylation of **5** was achieved in 76% yield, indicating that **16** is either less reactive or less stable in the cross-coupling reactions. The diarylation with 5-formyl-2-furanboronic acid and 5-formyl-2-thiopheneboronic acid was also briefly explored as a potential opportunity to convert the furan ring into heterocyclic triads. These motifs have recently attracted attention due to their ability to induce apoptosis.[47] Although an interesting notion, the low yields of these transformations limited the exploration of converting **1** into an apoptosis-inducing chemical probe.

As an alternative method to alter the steric and electronic parameters of the furan ring, trifluoromethyl groups were introduced as shown in Scheme 2.9. Using recently developed conditions developed for the trifluormethylation of various arenes and heteroarenes,[48] **1** was efficiently converted into a easily separable mixture of **58** and **59**. The position of each substitution was assigned through a combination of 2D NMR and C-F coupling constants. The HMBC spectra of **58** and **59** show strong correlations between the C12 proton and carbons C13, C14, and C16. This allowed for the assignment of the remaining aromatic carbon signal to C15. This C15 signal in the $^{13}C$ spectrum of **58** appeared as a quartet ($^{2}J_{CF}$ = 43 Hz) indicating it was directly appended to a trifluoromethyl group. COSY experiments were used to confirm this assignment however were less conclusive due to weak coupling of the C14 and C15 protons of **59**. Of these two probes, **58** is particularly useful because only one other report has illustrated the monosubstitution of this position.[49]

**Scheme 2.9.** Trifluoromethylation of **1** using photoredox catalysis.[a]

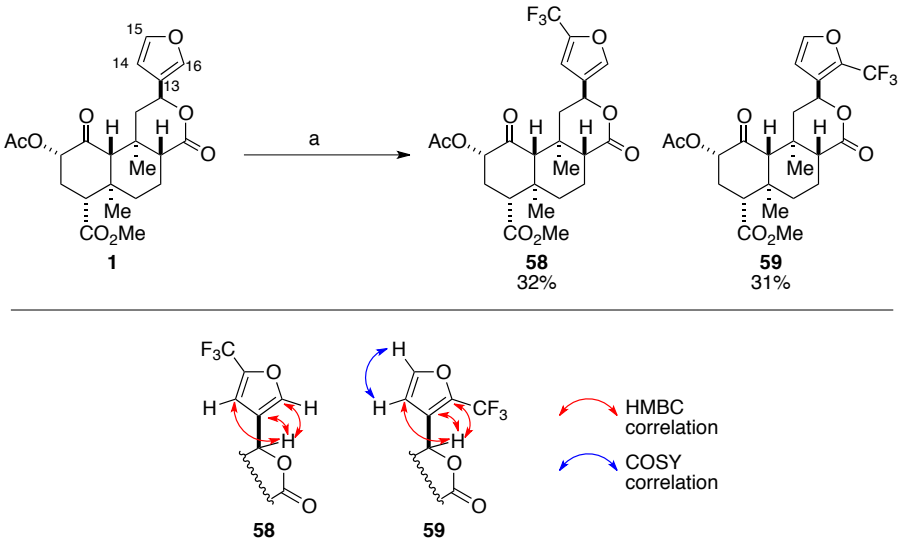


[a] Reagents and conditions: a) $Ru(phen)_3Cl_2 \cdot H_2O$ (0.02 equiv), $CF_3SO_2Cl_2$ (4.0 equiv), $KH_2PO_4$ (3.0 equiv), *hv*, MeCN, RT, 48 h.

This other report also details the synthesis of **60** and **61** by heating **1** with paraformaldehyde in acetic acid (Scheme 2.10). An attempt to reproduce this result yielded a complex mixture of the mono- and bis-acetoxymethylated products (**62** and **63**, respectively) in addition to **60** and **61**. All efforts to improve the selectivity or yield of this reaction using Lewis acids (such as $BF_3 \cdot OEt_2$ and LiCl), increasing the reaction times and temperatures, or through slow addition of the paraformaldehyde were unsuccessful. The primary alcohol of **61** was, however, successful oxidized to the aldehyde **64** under Swern conditions. Condensation of **64** with hydroxylamine led to the intermediate oxime, which was converted directly to **65** without further purification. This three compound series (**60**, **64**, and **65**) was expected to complement the corresponding all carbon series (**44**, **5**, and **53**) and provide useful insight into how electron density in the furan ring affects interactions with the KOR.

**Scheme 2.10.** Synthesis of hydroxymethyl-, formyl-, and cyano-substituted analogues.[a]

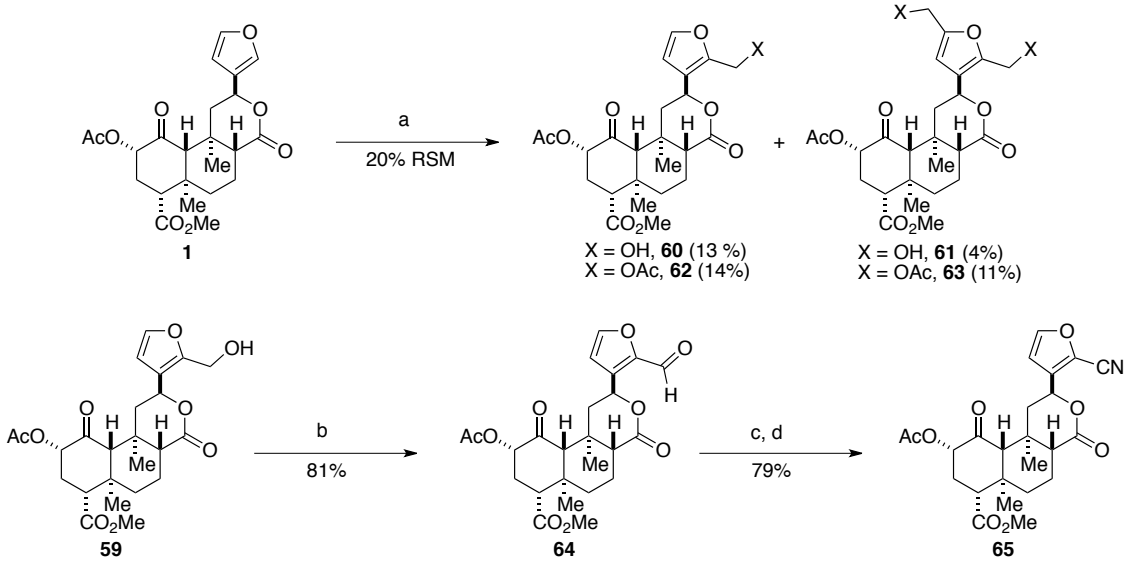


[a] Reagents and conditions: a) $(CH_2O)_n$ (5.43 equiv), AcOH, 75 °C, 20 h; b) DMSO (27 equiv), $(COCl)_2$ (14 equiv), $Et_3N$ (5.2 equiv), $CH_2Cl_2$, -78 °C to rt, 4 h; c) $NH_2OH{\cdot}HCl$ (4.0 equiv), pyr (9.3 equiv), MeOH, 65 °C, 5 h; d) TsCl (1.1 equiv), DIPEA (2.6 equiv), $CH_2Cl_2$, RT, 12 h.

*In Vitro Studies*

To assess how the modifications that had been made to the furan ring of **1** would affect activity at the KOR, compounds **4**-**65** were screened using a DiscoveRx HitHunter® cAMP Assay Platform. This *in vitro* measure of receptor activation utilizes CHO cells overexpressing the KOR on the cell surface. Activation of the receptors with KOR agonists leads to a release of the $G\alpha_i$ that inhibits the forskolin-induced formation of cAMP by adenylate cyclase. These levels of cAMP are then quantified using a competitive immunosassay.[50] Using this assay the $EC_{50}$ and $E_{max}$ values of **4**-**64** were obtained to measure their potencies and efficacies, respectively. Although most of these compounds retained full efficacy at the KOR—indicating they are full agonists—compounds **21**, **47**, and **49** appear to be partial agonists with $E_{max}$ values of 84%, 65%, and 88%, respectively. However, their relatively low potencies ($EC_{50}$ = 360 ± 60 nM, 620

± 140 nM, and 6,000 ± 2000 nM, respectively) hampers their potential utility. A comparison of the $EC_{50}$ values for the remaining compounds was used to determine how changes to the steric and electronic properties of the furan ring affects KOR activation, which should provide additional insight into the furan ring binding pocket.

*Isoxazoles Series*

The replacement of the furan ring with an isoxazole resulted in a drastic decrease in activity (Table 2.2). The least potent of these compounds, **9**, contained an unsubstituted phenyl ring and was almost 5 orders of magnitude less potent than **1** at the KOR. It is somewhat interesting that substitution of this phenyl ring did lead to a slight increase in potency. This effect does not seem to be electronic in nature as both the electron-donating methoxy group (**10**) and electron-withdrawing trifluormethyl group (**11**) produced similar effects. The most active in this series was the trimethylsilyl-

**Table 2.2**. KOR Activity of Isoxazole Series.

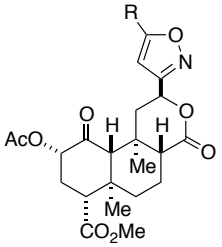


| Entry | Compound | R= | $EC_{50}$[a] (nM) | $E_{max}$[b] (%) |
|---|---|---|---|---|
| **1** | Salvinorin A (**1**) | -- | 0.042 ± 0.005 | 101 |
| 2 | **9** | $C_6H_5$ | 4000 ± 1000 | 110 |
| 3 | **10** | 2-$MeOC_6H_4$ | 300 ± 50 | 106 |
| 4 | **11** | 2-$CF_3C_6H_4$ | 581 ± 8 | 110 |
| 5 | **12** | $CH_2OH$ | 770 ± 80 | 107 |
| 6 | **13** | $Si(CH_3)_3$ | 15 ± 2 | 104 |

[a] $EC_{50}$ = Effective concentration to produce 50% of the maximal response as measured by inhibition of cAMP accumulation in CHO cells. Mean ± standard error of the mean; n = 4. [b] $E_{max}$ = % of maximal response produced by U69,593.

substituted **13** that was intended to serve as a precursor to the unsubstituted ring with an $EC_{50}$ = 15 ± 2 nM, however the compound is still more than 300 times less potent than the parent natural product. Whether these drops in potency relative to **1** are the result of substitution at the C15 position or from the electronic differences between furan and isoxazole is currently unclear. This will remain difficult to determine until a route to the unsubstituted isoxazole is discovered or a general process to introduce substitutions to the C15 position of **1** is made possible.

*Substituted Series*

The latest binding model of **1** based on the recent antagonist bound crystal structure of the KOR predicts the furan ring to bind in a small pocket composed of Trp124, Glu209, and Cys 210.[18,19] The substitution of the furan ring has now provided the necessary probes needed to validate these claims. Evaluation of these compounds reveals that, in general, substituting the furan ring led to a decrease in potency at the KOR, which supports the hypothesis that **1** binds in a sterically encumbering portion of the binding pocket. Several of the sterically less demanding

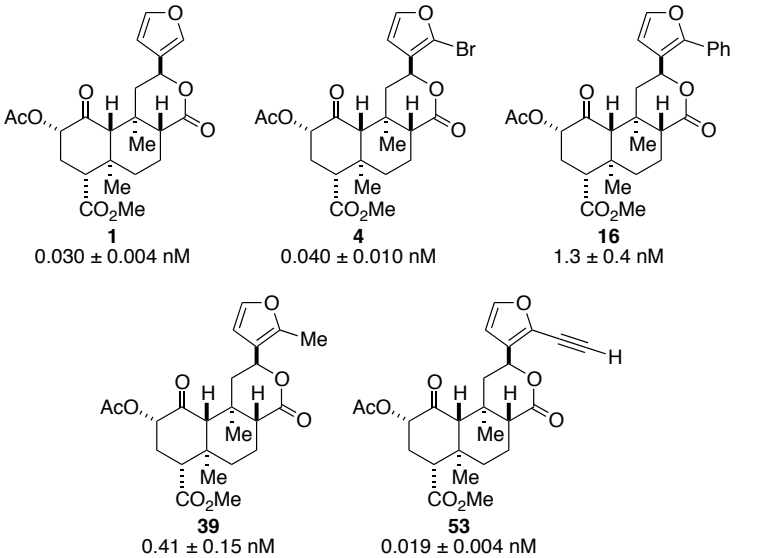


**Figure 2.6.** Compounds containing small substitutions to C16 and their corresponding potencies at the KOR.

substitutions, however, did give rise to compounds with low to sub-nanomolar potencies (Figure 2.6). These compounds would serve as the basis to elucidate additional SAR.

The introduction of a phenyl group to the C16 position of the furan ring did result in an approximate 40-fold decrease in potency at the KOR. However using **16** as a point of comparison, additional ligand-receptor interactions could be identified. Such an interaction would be observed as an increase in potency relative to **16**. Therefore, trifluoromethyl- and fluoro-substitutions were introduced to the phenyl to probe for halogen bonding interactions (**18**-**20**, **24**-**26**). The methoxy-, nitro-, and amino-phenyl rings as well as the 5-membered heterocycles were included to observe potential hydrogen bonding. Given the relative frequency of the "methyl effect," tolyl-substitutions were also examined.[51] Finally the pi-system of the substitutions was extended with naphthyl analogues in an attempt to gain additional pi-stacking interactions. Despite the wide range of functionality that was introduced, screening of the 24 compounds (**16**, **18**-**35**, **36**-**37**, **45**-**47**) containing aromatic rings appended to C16 unfortunately revealed no increase in potency relative to **16** (Table 2.3). Furthermore, neither substitution position nor electron density appeared to have a profound effect on activity. Instead, the activity of the ligands appeared to be highly dependent upon the steric properties of the substitutions.

A similar dependence upon steric size was observed in the bromo-, alkyl-, alkenyl-, and alkynyl-substituted analogues (Table 2.4). Bromination of the furan ring had an insignificant effect upon activity, which is consistent with previous results.[27,35] However, replacement of the bromine with small alkyl groups such as methyl, ethyl or

**Table 2.3**. KOR Activity of Aromatic-substituted Series

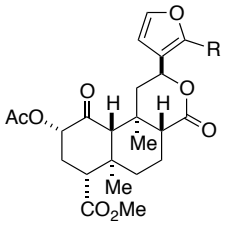


| Entry | Compound | R= | $EC_{50}$ [a] (nM) | $E_{max}$ [b] (%) |
|---|---|---|---|---|
| 1 | **1** | H | 0.030 ± 0.004 | 101 |
| 2 | **16** | Ph | 1.3 ± 0.4 | 101 |
| 3 | **18** | 2-$CF_3$-$C_6H_4$ | 8.4 ± 2.3 | 102 |
| 4 | **19** | 3-$CF_3$-$C_6H_4$ | 27 ± 6.0 | 101 |
| 5 | **20** | 4-$CF_3$-$C_6H_4$ | 1020 ± 250 | 102 |
| 6 | **21** | 2-$NO_2$-$C_6H_4$ | 360 ± 60 | 84 |
| 7 | **22** | 3-$NO_2$-$C_6H_4$ | 450 ± 100 | 108 |
| 8 | **23** | 4-$NO_2$-$C_6H_4$ | 170 ± 50 | 106 |
| 9 | **24** | 2-$FC_6H_4$ | 1.2 ± 0.1 | 102 |
| 10 | **25** | 3-$FC_6H_4$ | 12.0 ± 3.0 | 93 |
| 11 | **26** | 4-$FC_6H_4$ | 54.0 ± 7.0 | 97 |
| 12 | **27** | 2-$MeC_6H_4$ | 5.4 ± 1.1 | 101 |
| 13 | **28** | 3-$MeC_6H_4$ | 3.4 ± 1.1 | 102 |
| 14 | **29** | 4-$MeC_6H_4$ | 2.3 ± 0.4 | 101 |
| 15 | **30** | 2-$MeOC_6H_4$ | 10 ± 2.0 | 104 |
| 16 | **31** | 3-$MeOC_6H_4$ | 8.6 ± 2.6 | 104 |
| 17 | **32** | 4-$MeOC_6H_4$ | 16.0 ± 5.0 | 107 |
| 18 | **45** | 2-$NH_2$-$C_6H_4$ | 430 ± 60 | 97 |
| 19 | **46** | 3-$NH_2$-$C_6H_4$ | 630 ± 160 | 103 |
| 20 | **47** | 4-$NH_2$-$C_6H_4$ | 620 ± 140 | 65 |
| 21 | **33** | 1-naphthyl | 37.0 ± 9.0 | 98 |
| 22 | **34** | 2-naphthyl | 25.0 ± 7.0 | 98 |
| 23 | **35** | 2-furyl | 6.7 ± 1.6 | 99 |
| 24 | **37** | 3-furyl | 6.5 ± 1.3 | 105 |
| 25 | **38** | 3-thienyl | 4.3 ± 0.5 | 105 |

[a] $EC_{50}$ = Effective concentration to produce 50% of the maximal response as measured by inhibition of cAMP accumulation in CHO cells. Mean ± standard error of the mean; $n \geq 3$. [b] $E_{max}$ = % of maximal response produced by U69,593.

cyclopropyl led to a 13-33 fold decrease in potency. This potency loss is regained when moving from an ethyl- (**44**, $EC_{50}$ = 2.9 ± 0.6 nM) to vinyl- (**5**, $EC_{50}$ = 0.96 ± 0.24 nM) to ethynyl-substituted (**53**, $EC_{50}$ = 0.019 ± 0.004 nM) furan rings. This effect is directly related to the steric parameters of each substitution (A-values: ethyl: 1.8 kcal/mol; vinyl:

**Table 2.4**. KOR Activity of Bromo-, Alkyl-, Alkenyl-, and Alkynyl-Substituted Series.

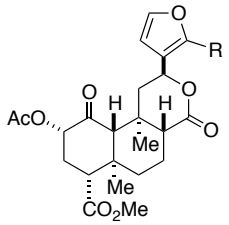


| Entry | Compound | R= | $EC_{50}$ [a] (nM) | $E_{max}$ [b] (%) |
|---|---|---|---|---|
| 1 | **1** | H | 0.030 ± 0.004 | 101 |
| 2 | **4** | Br | 0.040 ± 0.010 | 100 |
| 3 | **39** | Me | 0.41 ± 0.15 | 101 |
| 4 | **40** | cyclopropyl | 1.00 ± 0.03 | 102 |
| 5 | **44** | Et | 2.9 ± 0.6 | 103 |
| 6 | **5** | $CH_2$=C(H) | 0.96 ± 0.24 | 101 |
| 7 | **53** | HC≡C | 0.019 ± 0.004 | 100 |
| 8 | **42** | $PhCH_2CH_2$ | 38.0 ± 5.0 | 102 |
| 9 | **41** | PhC(H)=C(H) | 20.0 ± 2.0 | 102 |
| 10 | **48** | PhC≡C | 100 ± 5 | 102 |
| 11 | **49** | 2-MeO-$C_6H_4$≡C | 6000 ± 2000 | 88 |
| 12 | **50** | 2-$CF_3$-$C_6H_4$≡C | 430 ± 50 | 107 |
| 13 | **43** | MeC≡C | 26.0 ± 10 | 102 |
| 14 | **51** | $Me(CH_2)_2$≡C | 9300 ± 300 | 90 |
| 15 | **52** | $HO(CH_2)_3$≡C | 890 ± 30 | 108 |
| 16 | **59** | $HOCH_2$ | 3.3 ± 0.2 | 102 |
| 17 | **63** | CHO | 7.3 ± 2.5 | 104 |
| 18 | **64** | CN | 9.4 ± 2.2 | 104 |

[a] $EC_{50}$ = Effective concentration to produce 50% of the maximal response as measured by inhibition of cAMP accumulation in CHO cells. Mean ± standard error of the mean; n ≥ 3. [b] $E_{max}$ = % of maximal response produced by U69,593.

1.7 kcal/mol; ethynyl: 0.5 kcal/mol).[52] Additionally, decreasing the amount of saturation limits the rotational freedom, which could improve binding to and activation of the KOR. The terminal alkyne **53** is particularly interesting as it represents the only modification to the furan ring, to date, that has resulted in an increase in activity at the KOR.

This same trend is not seen when a phenyl group is present at the end of the two-carbon linker. While **41** bearing an alkene is slightly more potent than its saturated variant **42** ($EC_{50}$ = 20 ± 5.0 nM and 38.0 ± 5.0 nM, respectively), the alkyne **48** is considerable less potent than both ($EC_{50}$ = 100 ± 5 nM). This suggests that while decreasing saturation from **42** to **41** does decrease steric bulk in the binding site, the linear alkyne extends the phenyl ring too far into the pocket and prevents proper receptor activation.

A similar trend was observed when alkyl groups were present at the end of the alkyne of **53**. The addition of a methyl group reduced the potency from 0.019 ± 0.004 nM to 26.0 ± 10 nM. This effect was even more pronounced with a propyl group present at the end of the alkyne ($EC_{50}$= 9300 ± 300 nM). The introduction of an alcohol at the end of this propyl chain (**52**) did result in a small increase in potency ($EC_{50}$= 890 ± 30 nM) relative to **51** however these effects are still heavily outweighed by the steric bulk of the substitution.

In addition to these strong steric effects, modulation of the furan rings electronic character also had a measurable effect. The hydroxymethyl, aldehyde and nitrile functionalities in **59**, **63**, and **64**, respectively, were anticipated to be sterically similar to the ethyl, vinyl, and ethynyl moieties of **44**, **5**, and **53**. Therefore, any differences in activity can be mostly attributed to the electron-withdrawing nature of the aldehyde and

nitrile. As expected, **29** and **59**, which are both sterically and electronically similar, were equipotent, however both **63** and **64** were significantly less potent than their all carbon counterparts. This indicates that an electron-rich furan is preferred for KOR activation.

The final series of compounds used to investigate the effects of substituting the furan possessed substituents at the C15 position. Because bromination occurs selectively at the C16 position, substitution at this position was not as straightforward. Fortunately the radical nature of the photoredox catalyzed trifluoromethylation led to an equal mixture of C15- and C16-substituted products, thus allowing for a single point of comparison. Given the steric and electronic effects discussed above, it is unsurprising that both **58** and **59** are significantly less potent than **1** (Table 2.5). However, **58** bearing the trifluoromethyl group at C15 is 10 times more potent at the KOR than **59**. This preference

**Table 2.5**. KOR Activity of C15-substituted Derivatives.

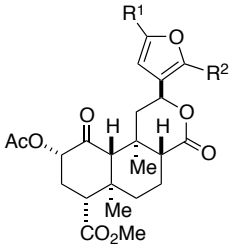


| Entry | Compound | $R^1$= | $R^2$= | $EC_{50}$[a] (nM) | $E_{max}$[b] (%) |
|---|---|---|---|---|---|
| 1 | **1** | H | H | 0.030 ± 0.004 | 101 |
| 2 | **58** | $CF_3$ | H | 3.1 ± 0.3 | 102 |
| 3 | **59** | H | $CF_3$ | 31 ± 11 | 100 |
| 4 | **4** | H | Br | 0.040 ± 0.010 | 100 |
| 5 | **15** | Br | Br | 240 ± 50 | 106 |
| 6 | **39** | H | Me | 0.41 ± 0.15 | 101 |
| 7 | **55** | Me | Me | 250 ± 50 | 105 |

[a] $EC_{50}$ = Effective concentration to produce 50% of the maximal response as measured by inhibition of cAMP accumulation in CHO cells. Mean ± standard error of the mean; n ≥ 3. [b] $E_{max}$ = % of maximal response produced by U69,593.

for C15 substitution suggests the lack of potency in the isoxazole series (**9**-**13**) is likely due to decreased electron density in the heterocycles rather than from steric effects of the substitutions. Since the electronic differences in **58** and **59** are expected to be negligible, the preference for C15 substitution must be primarily due to steric differences in the binding pocket. Potentially the furan ring may be positioned such that C15 is located in a less sterically encumbering portion of the binding pocket. Alternatively, rotation about the C12-C13 bond may allow the furan ring to adopt several different favorable binding modes. The disubstituted probe molecules **15** and **55** were useful in distinguishing between these two possibilities. If the C15 substitution were oriented toward an open pocket then an additional C15 substitution would not be expected to have a large effect. On the other hand, if the furan ring rotates to position the substitutions outside of a narrow pocket, then an additional substitution would be less well tolerated because either C15 or C16 would need to be directed into the binding pocket (Figure 2.7). A comparison of **4** to **15** and **39** to **55** (Table 2.5) clearly shows that the additional substitution results in a 600 and 6,000 fold drop in potency, supporting the notion that the furan ring rotates in order to accommodate the substitutions.

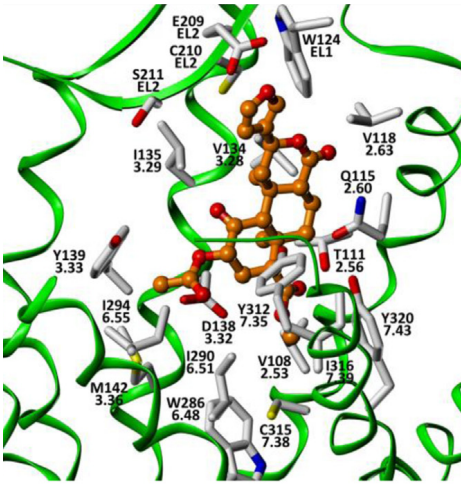


**Figure 2.7**. Proposed binding model of **1** based on the KOR crystal structure. Figure adapted from reference 19.

*In Vivo Studies*

By synthesizing and evaluating 46 novel KOR probe molecules three potent agonists were identified (**4**, **39**, and **53**). Further evaluation of these three compounds indicated they were highly selective for the KOR, possessing no measurable activity at the MOR ($EC_{50}$ > 10 μM). To determine whether these results would translate into *in vivo* efficacies, the agonists' abilities to affect cocaine-primed reinstatement were assessed in collaboration with the Kivell laboratory at Victoria University of Wellington, New Zealand.

This animal model of drug relapse takes place in three phases.[53] In the first phase, Sprague-Dawley rats are trained to self-administer cocaine solution intravenously by depressing a lever. The number of lever presses can be used to quantitate drug seeking behavior. In the second phase of the experiment the cocaine solution is replaced with a saline solution. During this "extinction" phase the number of active lever presses is quickly diminished because the rewarding properties of cocaine have been removed. In the final "reinstatement" phase, the test animals are treated with either test compounds or a vehicle control then given a large dose of cocaine (20 mg/kg). In this final phase the animals' drug seeking behavior increases even though they are only administering saline solutions. Under this paradigm, a number of KOR agonists, including several derivatives of **1**, successfully attenuate the level of drug seeking behavior in the reinstatement phase relative to the vehicle control.[54-56]

The agonists described in this study showed similar results to other KOR agonist in their ability to reduce drug seeking behavior (Figure 2.8A-C).[57] The more potent agonists **4** and **53** both dose-dependently decreased responding during the extinction

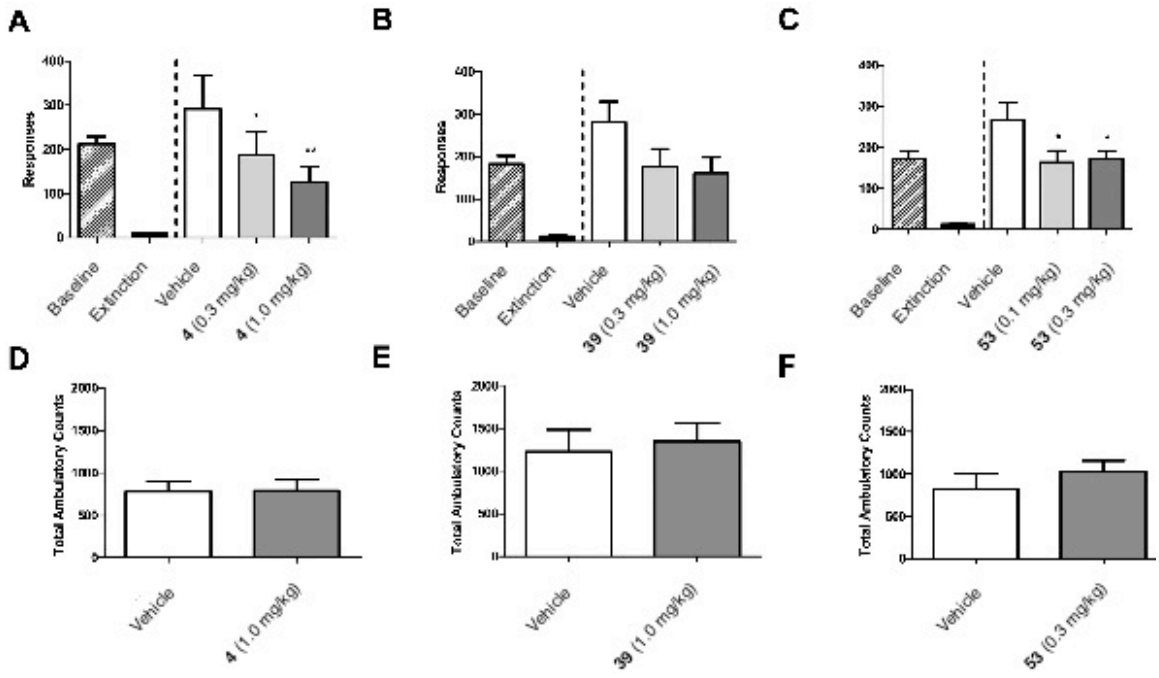


**Figure 2.8.** Effects of salvinorin A derived compounds on drug seeking behavior and cocaine-induced spontaneous locomotion. Active lever responses for cocaine self-administration during baseline and extinction (pretest) and during reinstatement following a priming injection of cocaine (20 mg/kg) for 4 (A), 39 (B), and 53 (C). Repeated measures ANOVA followed by Dunnett's multiple comparison test (*P < 0.05; **P < 0.01) (n = 5 or 6). Effect of 4 (D) (P = 0.9326), 39 (E) (P = 0.7289), and 53 (F) (P = 0.3659) on spontaneous locomotor activity in the rat shown as total

period. Consistent with our *in vitro* results, the more potent agonist **53** was able to induce a statistically significant result at a lower dose (0.1 mg/kg) than that required for **4** (0.3 mg/kg). Additionally, the methyl-substituted **39** appeared to be trending toward decreasing responses at increasing doses but these results were not significantly different from the vehicle treated animals.

These encouraging results clearly indicate that **4** and **53** (and likely **39** at higher doses) are able to decrease drug seeking behavior in an animal model of relapse. Furthermore, the high selectivity of these compounds for the KOR indicates that these effects are KOR-dependent. However, the decreased responding may be the result sedation and decreased motor coordination that has been observed with other KOR agonists.[55,58] To determine if these side-effects were responsible for the decreased

responding, the effects of **4**, **39**, and **53** on cocaine-induced spontaneous locomotion was determined (Figure 2.8D-F). At the highest doses used, no statistical difference from vehicle control was observed for all three compounds, indicating they are not having a sedative effect. This indicates that the decrease in drug seeking behavior is not the result of sedation. Furthermore, these compounds appear to show at least some decrease in side effects in comparison to traditional KOR agonists.

*Conclusion*

Taken together, these results clearly demonstrate that these modified natural products hold promise for validating the KOR as a potential abuse therapy target. Although a number of other KOR agonists have shown similar results in animal models of drug relapse, these and other derivatives of **1** have shown substantially different side effect profiles.[25,58] For this reason, studies aimed at investigating the effects of **4** on drug self-administration and the rewarding effects of drugs of abuse—as well as other potential side effects—are currently being performed. Included within these studies is the use of non-human primates to simultaneously measure activity at the KOR and sedation. Preliminary results indicate that **4** causes similarly levels of KOR activation as **1** but with substantially less sedation. Combined with additional studies using **53**, and potentially **39**, these investigations will provide interesting insight into how substitutions to the furan ring affect *in vivo* activity.

**References:**


(1) Valdes, L. J.; Diaz, J. L.; Paul, A. G. Ethnopharmacology of Ska-Maria-Pastora. *J Ethnopharmacol*. **1983**, *7*, 287.

(2) Casselman, I.; Heinrich, M. Novel use patterns of *Salvia divinorum*: unobtrusive observation using YouTube. *J. Ethnopharmacol*. **2011**, *138*, 662.

(3) Lange, J. E.; Daniel, J.; Homer, K.; Reed, M. B.; Clapp, J. D. *Salvia divinorum*: effects and use among YouTube users. *Drug Alcohol Depend*. **2010**, *108*, 138.

(4) Griffin, O. H.; Miller, B. L.; Khey, D. N. Legally high? Legal considerations of *Salvia divinorum*. *J. Psychoact. Drugs* **2008**, *40*, 183.

(5) Ortega, A.; Blount, J. F.; Manchand, P. S. Salvinorin, a new *trans*-neoclerodane diterpene from *Salvia divinorum*. *J. Chem. Soc. Perk. Trans. 1* **1982**, 2505.

(6) Valdes, L. J.; Butler, W. M.; Hatfield, G. M.; Paul, A. G.; Koreeda, M. Divinorin A, a psychotropic terpenoid, and divinorin B from the hallucinogenic mexican mint *Salvia divinorum*. *J. Org. Chem*. **1984**, *49*, 4716.

(7) Roth, B. L.; Baner, K.; Westkaemper, R.; Siebert, D.; Rice, K. C.; Steinberg, S.; Ernsberger, P.; Rothman, R. B. Salvinorin A: A potent naturally occurring nonnitrogenous kappa opioid selective agonist. *Proc. Natl. Acad. Sci. U. S. A.* **2002**, *99*, 11934.

(8) Tejeda, H. A.; Shippenberg, T. S.; Henriksson, R. The dynorphin/kappa-opioid receptor system and its role in psychiatric disorders. *Cell. Mol. Life Sci*. **2012**, *69*, 857.

(9) Surratt, C. K.; Johnson, P. S.; Moriwaki, A.; Seidleck, B. K.; Blaschak, C. J.; Wang, J. B.; Uhl, G. R. Mu opiate receptor: Charged transmembrane domain amino acids

are critical for agonist recognition and intrinsic activity. *J. Biol. Chem.* **1994**, *269*, 20548.

(10) Mansour, A.; Taylor, L. P.; Fine, J. L.; Thompson, R. C.; Hoversten, M. T.; Mosberg, H. I.; Watson, S. J.; Akil, H. Key residues defining the mu-opioid receptor binding pocket: A site-directed mutagenesis study. *J. Neurochem.* **1997**, *68*, 344.

(11) Weltrowska, G.; Chung, N. N.; Lemieux, C.; Guo, J. X.; Lu, Y. X.; Wilkes, B. C.; Schiller, P. W. "Carba"-analogues of fentanyl are opioid receptor agonists. *J. Med. Chem.* **2010**, *53*, 2875.

(12) Kane, B. E.; Nieto, M. J.; McCurdy, C. R.; Ferguson, D. M. A unique binding epitope for salvinorin A, a non-nitrogenous kappa opioid receptor agonist. *FEBSJ* **2006**, *273*, 1966.

(13) Yan, F.; Bikbulatov, R. V.; Mocanu, V.; Dicheva, N.; Parker, C. E.; Wetsel, W. C.; Mosier, P. D.; Westkaemper, R. B.; Allen, J. A.; Zjawiony, J. K.; Roth, B. L. Structure-based design, synthesis, and biochemical and pharmacological characterization of novel salvinorin A analogues as active state probes of the kappa-opioid receptor. *Biochemistry* **2009**, *48*, 6898.

(14) Yan, F.; Mosier, P. D.; Westkaemper, R. B.; Stewart, J.; Zjawiony, J. K.; Vortherms, T. A.; Sheffler, D. J.; Roth, B. L. Identification of the molecular mechanisms by which the diterpenoid salvinorin A binds to kappa-opioid receptors. *Biochemistry* **2005**, *44*, 8643.

(15) Singh, N.; Cheve, G.; Ferguson, D. M.; McCurdy, C. R. A combined ligand-based and target-based drug design approach for G-protein coupled receptors:

application to salvinorin A, a selective kappa opioid receptor agonist. *J. Comput.-Aided Mol. Des.* **2006**, *20*, 471.

(16) Wu, H.; Wacker, D.; Mileni, M.; Katritch, V.; Han, G. W.; Vardy, E.; Liu, W.; Thompson, A. A.; Huang, X. P.; Carroll, F. I.; Mascarella, S. W.; Westkaemper, R. B.; Mosier, P. D.; Roth, B. L.; Cherezov, V.; Stevens, R. C. Structure of the human kappa-opioid receptor in complex with JDTic. *Nature* **2012**, *485*, 327.

(17) Negri, A.; Rives, M. L.; Caspers, M. J.; Prisinzano, T. E.; Javitch, J. A.; Filizola, M. Discovery of a novel selective kappa-opioid receptor agonist using crystal structure-based virtual screening. *J. Chem. Inf. Model.* **2013**, *53*, 521.

(18) Vardy, E.; Mosier, P. D.; Frankowski, K. J.; Wu, H. X.; Katritch, V.; Westkaemper, R. B.; Aubé, J.; Stevens, R. C.; Roth, B. L. Chemotype-selective modes of action of kappa-opioid receptor agonists. *J. Biol. Chem.* **2013**, *288*, 34470.

(19) Polepally, P. R.; Huben, K.; Vardy, E.; Setola, V.; Mosier, P. D.; Roth, B. L.; Zjawiony, J. K. Michael acceptor approach to the design of new salvinorin A-based high affinity ligands for the kappa-opioid receptor. *Eur. J. Med. Chem.* **2014**, *85*, 818.

(20) Cunningham, C. W.; Rothman, R. B.; Prisinzano, T. E. Neuropharmacology of the naturally occurring kappa-opioid hallucinogen salvinorin A. *Pharmacol. Rev.* **2011**, *63*, 316.

(21) Chavkin, C.; Sud, S.; Jin, W.; Stewart, J.; Zjawiony, J. K.; Siebert, D. J.; Toth, B. A.; Hufeisen, S. J.; Roth, B. L. Salvinorin A, an active component of the hallucinogenic sage salvia divinorum is a highly efficacious kappa-opioid

receptor agonist: structural and functional considerations. *J. Pharmacol. Exp. Ther.* **2004**, *308*, 1197.

(22) Peet, M. M.; Baker, L. E. Salvinorin B derivatives, EOM-Sal B and MOM-Sal B, produce stimulus generalization in male Sprague-Dawley rats trained to discriminate salvinorin A. *Behav. Pharmacol.* **2011**, *22*, 450.

(23) Hooker, J. M.; Munro, T. A.; Beguin, C.; Alexoff, D.; Shea, C.; Xu, Y.; Cohen, B. M. Salvinorin A and derivatives: protection from metabolism does not prolong short-term, whole-brain residence. *Neuropharmacology* **2009**, *57*, 386.

(24) Simonson, B.; Morani, A. S.; Ewald, A. W.; Walker, L.; Kumar, N.; Simpson, D.; Miller, J. H.; Prisinzano, T. E.; Kivell, B. M. Pharmacology and anti-addiction effects of the novel kappa opioid receptor agonist Mesyl Sal B, a potent and long-acting analogue of salvinorin A. *Br. J. Pharmacol.* **2015**, *172*, 515.

(25) Morani, A. S.; Ewald, A.; Prevatt-Smith, K. M.; Prisinzano, T. E.; Kivell, B. M. The 2-methoxy methyl analogue of salvinorin A attenuates cocaine-induced drug seeking and sucrose reinforcements in rats. *Eur. J. Pharmacol.* **2013**, *720*, 69.

(26) Dalvie, D. K.; Kalgutkar, A. S.; Khojasteh-Bakht, S. C.; Obach, R. S.; O'Donnell, J. P. Biotransformation reactions of five-membered aromatic heterocyclic rings. *Chem. Res. Toxicl.* **2002**, *15*, 269.

(27) Beguin, C.; Duncan, K. K.; Munro, T. A.; Ho, D. M.; Xu, W.; Liu-Chen, L. Y.; Carlezon, W. A., Jr.; Cohen, B. M. Modification of the furan ring of salvinorin A: identification of a selective partial agonist at the kappa opioid receptor. *Bioorg. Med. Chem.* **2009**, *17*, 1370.

(28) Simpson, D. S.; Lovell, K. M.; Lozama, A.; Han, N.; Day, V. W.; Dersch, C. M.; Rothman, R. B.; Prisinzano, T. E. Synthetic studies of neoclerodane diterpenes from *Salvia divinorum*: role of the furan in affinity for opioid receptors. *Org. Biomol. Chem.* **2009**, *7*, 3748.

(29) Jawalekar, A. M.; Reubsaet, E.; Rutjes, F. P.; van Delft, F. L. Synthesis of isoxazoles by hypervalent iodine-induced cycloaddition of nitrile oxides to alkynes. *Chem. Comm.* **2011**, *47*, 3198.

(30) Padwa, A.; Macdonald, J. G. Cycloaddition of benzonitrile oxide with vinylsilanes. *Tetrahedron Lett.* **1982**, *23*, 3219.

(31) Kitamura, T.; Mansei, Y.; Fujiwara, Y. 1,3-Dipolar cycloaddition of alkynyliodonium salts with a nitrile oxide: Synthesis and reactivity of isoxazolyliodonium salts. *J. Organomet. Chem.* **2002**, *646*, 196.

(32) Lindsay-Scott, P. J.; Clarke, A.; Richardson, J. Two-step cyanomethylation protocol: Convenient access to functionalized aryl- and heteroarylacetonitriles. *Org. Lett.* **2015**, *17*, 476.

(33) Velcicky, J.; Soicke, A.; Steiner, R.; Schmalz, H. G. Palladium-catalyzed cyanomethylation of aryl halides through domino suzuki coupling-isoxazole fragmentation. *J. Am. Chem. Soc.* **2011**, *133*, 6948.

(34) Harding, W. W.; Schmidt, M.; Tidgewell, K.; Kannan, P.; Holden, K. G.; Gilmour, B.; Navarro, H.; Rothman, R. B.; Prisinzano, T. E. Synthetic studies of neoclerodane diterpenes from Salvia divinorum: Semisynthesis of salvinicins A and B and other chemical transformations of salvinorin A. *J. Nat. Prod.* **2006**, *69*, 107.

(35) Simpson, D. S.; Katavic, P. L.; Lozama, A.; Harding, W. W.; Parrish, D.; Deschamps, J. R.; Dersch, C. M.; Partilla, J. S.; Rothman, R. B.; Navarro, H.; Prisinzano, T. E. Synthetic studies of neoclerodane diterpenes from *Salvia divinorum*: Preparation and opioid receptor activity of salvinicin analogues. *J. Med. Chem.* **2007**, *50*, 3596.

(36) Riley, A. P.; Day, V. W.; Navarro, H. A.; Prisinzano, T. E. Palladium-catalyzed transformations of salvinorin A, a neoclerodane diterpene from *Salvia divinorum*. *Org. Lett.* **2013**, *15*, 5936.

(37) SciFinder Search performed on April 29, 2015 for commerically available, single component stannanes and boronic acids.

(38) Walker, S. D.; Barder, T. E.; Martinelli, J. R.; Buchwald, S. L. A rationally designed universal catalyst for Suzuki-Miyaura coupling processes. *Angew. Chem. Int. Ed.* **2004**, *43*, 1871.

(39) Barder, T. E.; Walker, S. D.; Martinelli, J. R.; Buchwald, S. L. Catalysts for Suzuki-Miyaura coupling processes: Scope and studies of the effect of ligand structure. *J. Am. Chem. Soc.* **2005**, *127*, 4685.

(40) Munro, T. A.; Duncan, K. K.; Staples, R. J.; Xu, W.; Liu-Chen, L. Y.; Beguin, C.; Carlezon, W. A., Jr.; Cohen, B. M. 8-epi-Salvinorin B: Crystal structure and affinity at the kappa opioid receptor. *Beilstein J. Org. Chem.* **2007**, *3*, 1.

(41) Scheerer, J. R.; Lawrence, J. F.; Wang, G. C.; Evans, D. A. Asymmetric synthesis of salvinorin A, a potent kappa opioid receptor agonist. *J. Am. Chem. Soc.* **2007**, *129*, 8968.

(42) Ma, Z.; Deng, G.; Lee, D. Y. Novel neoclerodane diterpene derivatives from the smoke of salvinorin A. *Tetrahedron Lett*. **2010**, *51*, 5207.

(43) Ma, Z. Z.; Deng, G.; Dai, R. H.; Xu, W.; Liu-Chen, L. Y.; Lee, D. Y. W. Thermal degradation products derived from the smoke of *Salvia divinorum* leaves. *Tetrahedron Lett*. **2010**, *51*, 5480.

(44) Brown, R. D.; Buchanan, A. S.; Humffray, A. A. Protodeboronation of thiophenboronic acids. *Aust. J. Chem*. **1965**, *18*, 1521.

(45) Knapp, D. M.; Gillis, E. P.; Burke, M. D. A general solution for unstable boronic acids: slow-release cross-coupling from air-stable MIDA boronates. *J. Am. Chem. Soc*. **2009**, *131*, 6961.

(46) Munro, T. A.; Rizzacasa, M. A.; Roth, B. L.; Toth, B. A.; Yan, F. Studies toward the pharmacophore of salvinorin A, a potent kappa opioid receptor agonist. *J. Med. Chem*. **2005**, *48*, 345.

(47) Salamoun, J.; Anderson, S.; Burnett, J. C.; Gussio, R.; Wipf, P. Synthesis of heterocyclic triads by Pd-catalyzed cross-couplings and evaluation of their cell-specific toxicity profile. *Org. Let.*. **2014**, *16*, 2034.

(48) Nagib, D. A.; MacMillan, D. W. C. Trifluoromethylation of arenes and heteroarenes by means of photoredox catalysis. *Nature* **2011**, *480*, 224.

(49) Munro, T. A.; Xu, W.; Ho, D. M.; Liu-Chen, L. Y.; Cohen, B. M. Studies toward bivalent kappa opioids derived from salvinorin A: Heteromethylation of the furan ring reduces affinity. *Beilstein J. Org. Chem*. **2013**, *9*, 2916.

(50) Golla, R.; Seethala, R. A homogeneous enzyme fragment complementation cyclic AMP screen for GPCR agonists. *J. Biomol. Screen*. **2002**, *7*, 515.

(51) Leung, C. S.; Leung, S. S. F.; Tirado-Rives, J.; Jorgensen, W. L. Methyl effects on protein-ligand binding. *J. Med. Chem.* **2012**, *55*, 4489.

(52) Carey, F. A.; Sundberg, R. J. *Advanced Organic Chemistry Part A: Structure and Mechanism*; 5 ed.; Springer Science: New York, NY, 2007.

(53) Spealman, R. D.; Barrett-Larimore, R. L.; Rowlett, J. K.; Platt, D. M.; Khroyan, T. V. Pharmacological and environmental determinants of relapse to cocaine-seeking behavior. *Pharm., Biochem. and Behav.* **1999**, *64*, 327.

(54) Schenk, S.; Partridge, B.; Shippenberg, T. S. U69593, a kappa-opioid agonist, decreases cocaine self-administration and decreases cocaine-produced drug-seeking. *Psychopharmacology* **1999**, *144*, 339.

(55) Morani, A. S.; Kivell, B.; Prisinzano, T. E.; Schenk, S. Effect of kappa-opioid receptor agonists U69593, U50488H, spiradoline and salvinorin A on cocaine-induced drug-seeking in rats. *Pharm., Biochem. and Behav.* **2009**, *94*, 244.

(56) Kivell, B. M.; Ewald, A. W.; Prisinzano, T. E. Salvinorin A analogs and other kappa-opioid receptor compounds as treatments for cocaine abuse. *Adv. Pharmacol.* **2014**, *69*, 481.

(57) Riley, A. P.; Groer, C. E.; Young, D.; Ewald, A. W.; Kivell, B. M.; Prisinzano, T. E. Synthesis and kappa-opioid receptor activity of furan-substituted salvinorin A analogues. *J. Med. Chem.* **2014**, *57*, 10464.

(58) Fantegrossi, W. E.; Kugle, K. M.; Valdes, L. J., 3rd; Koreeda, M.; Woods, J. H. Kappa-opioid receptor-mediated effects of the plant-derived hallucinogen, salvinorin A, on inverted screen performance in the mouse. *Behav. Pharmacol.* **2005**, *16*, 627.

## III. Synthesis of Highly Potent and Selective Herkinorin Analogues

*Introduction*

During early investigations into the structure-activity relationships (SAR) of salvinorin A at the opioid receptors, it was discovered that the replacement of the C2 acetate with a benzoate moiety caused a decrease in affinity and potency at the KOR, however increased affinity and potency at the mu opioid receptor (MOR) (Figure 3.1).[1] Much like salvinorin A, the lack of a basic nitrogen in this derivative, deemed herkinorin (**1**), made it unique amongst other known MOR agonists. Additional interest was garnered when more extensive pharmacological investigations revealed that despite being a full MOR agonist, **1** did not recruit β-arrestin-2.[2,3] This functional selectivity is particularly noteworthy since genetically modified mice lacking β-arrestin-2 display prolonged and enhanced antinociception and diminished respiratory depression, constipation, and tolerance following morphine treatment.[4-6] Therefore **1** represents an interesting step toward a more effective treatment option for pain management that lacks the negative side effects associated with opiate analgesics.

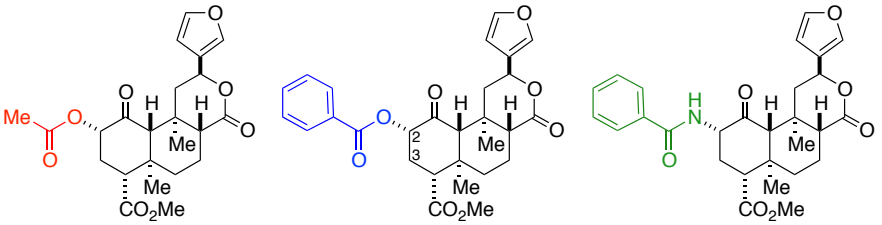


**Figure 3.1.** Structures and binding affinities of salvinorin A, herkinorin, and herkamide.[3]

Unfortunately, there are several problems with **1** that limit its use as an *in vivo* probe. In a competitive binding assay, **1** shows less than 8-fold selectivity for the MOR over the KOR (Figure 3.1) and less than 3-fold selectivity in a [$^{35}$S]GTPγS functional

assay.[3] This marginal selectivity results in significant KOR activation that could potentially make it difficult to attribute any observed effects specifically to MOR activation. This has already been observed in a piglet model where it was demonstrated that **1** causes vasodilation in a KOR-dependent fashion.[7] Additionally, the antinociceptive effects of **1** appear to be limited to the peripheral nervous system. In a rat paw formalin test of antinociception, **1** blocked the effects of a painful stimulus, however these effects appear to be limited to the site of injection.[8] Potentially, rapid of metabolism by esterases to salvinorin B (**3**), which is inactive at all three opioid receptors,[9] may prevent **1** from acting on the central nervous system thus limiting its effects to the periphery.

To address these metabolic issues, the ester of **1** was replaced with a more metabolically stable amide. Interestingly, herkamide (**2**) is significantly more selective than **1** for the MOR (Figure 3.1).[3] Additionally, **2** activates the receptor more potently than **1**.[3] This increase in selectivity and potency suggests that **2** could overcome several of the problems that limit the utility of **1**. Thus a more thorough investigation into the differences of how **1** and **2** interact with the MOR is warranted. Potentially the observed pharmacological differences could be explained by either: (1) the ligands binding at different sites of the MOR; (2) the ligands binding to different states of the receptor; or (3) the ligands inducing different receptor conformations. While it may be difficult to separate the latter two possibilities, the differences in receptor binding sites could be addressed through a parallel series of compounds based upon **1** and **2**. Unfortunately, a lengthy and low yielding route to **2** prevents the synthesis of the large number of compounds that would be necessary for this study. Therefore, a compound that could be readily accessed and possess a similar pharmacological profile to **2** would be desirable.

The design of such a compound would first require an understanding of the structural differences between **1** and **2**.

*Design and Synthesis of Analogues*

The most apparent difference between **1** and **2** is the ability for **2** to participate as a hydrogen bond donor. However, preliminary molecular modeling also indicated a more subtle structural difference: the phenyl ring of **2** appears to lie in plane with the neoclerodane core whereas the corresponding angle in **1** is larger.[3] To provide additional support to the hypothesis that the phenyl ring configuration affects the ligands' selectivities, X-ray quality crystals of **1** and **2** were grown and their structures indicate a similar difference in phenyl ring orientations (Figure 3.2). Although this model represents only two possible conformations, and not necessarily the most biologically relevant confirmations, it does at least suggest the notion that the orientation of the phenyl ring influences the ligands' potencies and selectivities. Furthermore, the modification of the

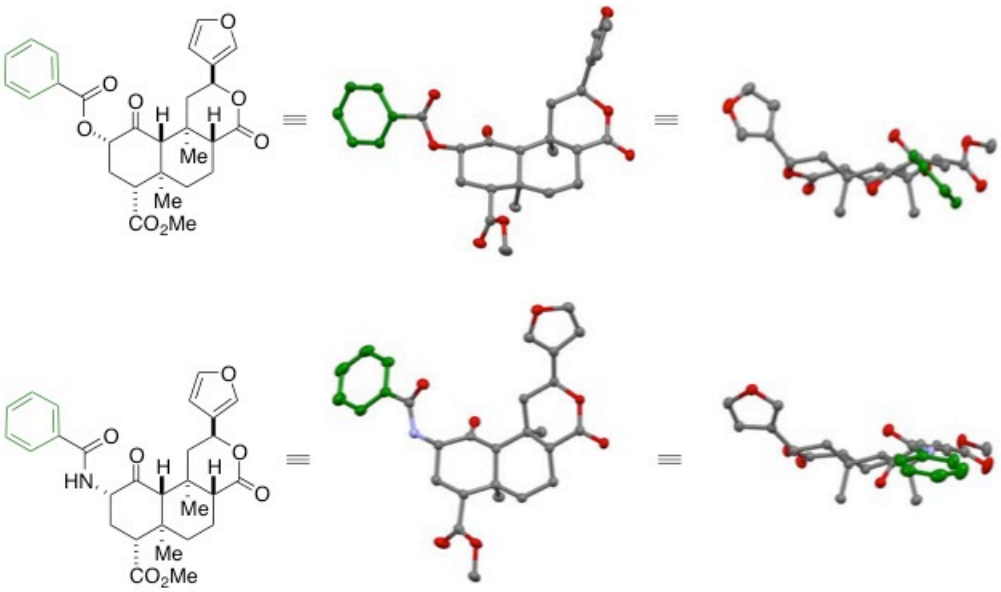


**Figure 3.2.** Crystal structures of **1** and **4** demonstrating differences in phenyl ring orientations.

**Scheme 3.1.** Oxidation and subsequent benzoylation of salvinorin B.[a]

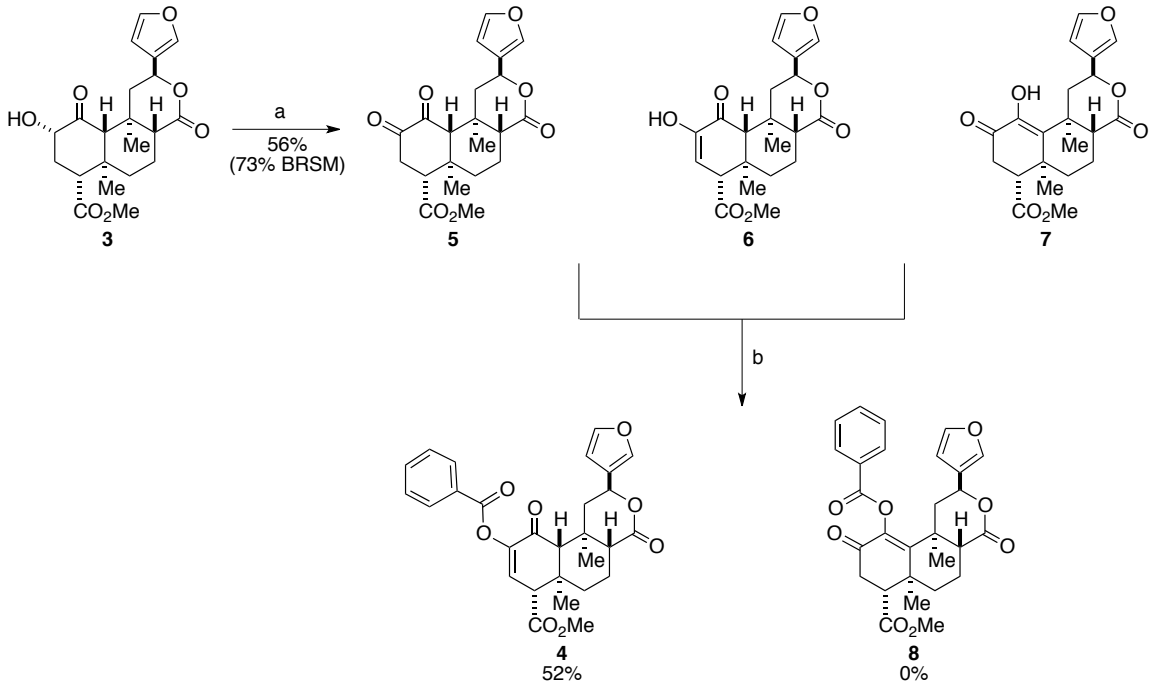


[a]Reagents and conditions: a) $Cu(OAc)_2$ (3.0 equiv), $CH_2Cl_2$/MeOH (1:1), RT, 16 h; b) BzCl (2.0 equiv), DIPEA (2.0 equiv), DMAP (0.1 equiv), $CH_2Cl_2$, RT, 16 h.

C2 position would be expected to affect the potency and selectivity of the ligand. One such modification that has yet to be explored is the introduction of a degree of unsaturation between C2 and C3 as in **4** (Scheme 3.1). In addition to being readily accessible from **3**, the $sp^2$-hybridization of C2 would force the appendant oxygen to be coplanar with the diterpene core, which could in turn lead to a ligand with activity that mimics **2**.

This degree of unsaturation could be introduced via the oxidation of **3** to the α-diketone **5** and subsequent tautomerization to a combination of the diosphenols **6** and **7** (Scheme 3.1). Initial attempts to induce this oxidation under several Swern conditions resulted in only trace amounts of product. However, $Cu(OAc)_2$ accomplished the transformation in an acceptable 56% yield.[10,11] Although remaining **3** (17%) could easily removed from the reaction mixture via simple silica gel chromatography, the product was

isolated as a mixture of **5**, **6**, and **7**, presumably due to rapid equilibrium between the three isomers. Fortunately, acylation with benzoyl chloride led to the selective formation of **4** over the other possible regioisomer **8**.

To provide additional information about how this modification to the structure of **1** would affect activity at the opioid receptors, two parallel series of compounds containing substitutions to the phenyl rings were synthesized (Scheme 3.2). One series was derived from the acylation of **3** (**9a**-**31a)** while the other was derived from **6** (**9b**-**31b**). Due to high variability in the quality of the commercially available acid chlorides,

**Scheme 3.2.** Synthesis of two parallel series of herkinorin derivatives.[a]

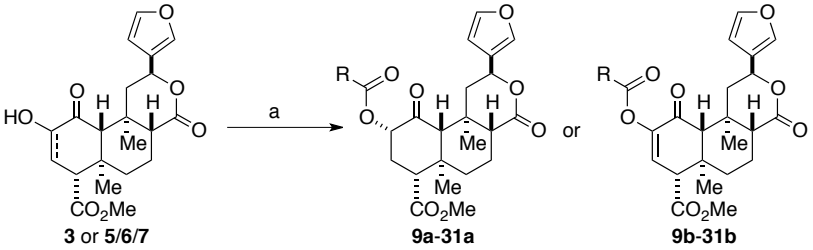


R =

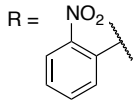
**9a**: 34%
**9b**: 60%

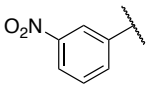
**10a**: 7%
**10b**: 51%

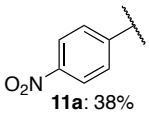
**11a**: 38%
**11b**: 70%

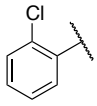
**12a**: 42%
**12b**: 56%

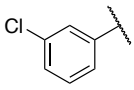
**13a**: 43%
**13b**: 55%

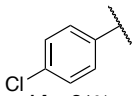
**14a**: 31%
**14b**: 44%

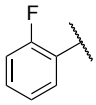
**15a**: 39%
**15b**: 71%

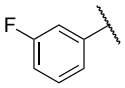
**16a**: 39%
**16b**: 53%

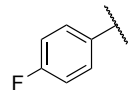
**17a**: 31%
**17b**: 52%

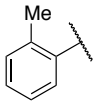
**18a**: 18%
**18b**: 58%

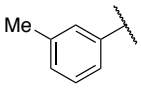
**19a**: 30%
**19b**: 45%

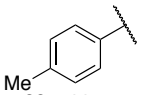
**20a**: 28%
**20b**: 71%

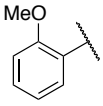
**21a**: 30%
**21b**: 57%

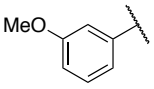
**22a**: 31%
**22b**: 56%

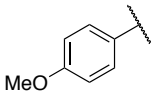
**23a**: 27%
**23b**: 36%


**24a**: 44%
**24b**: 50%


**25a**: 45%
**25b**: 48%

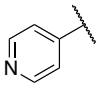
**26a**: 46%
**26b**: 35%


**27a**: 34%
**27b**: 64%


**28a**: 40%
**28b**: 38%

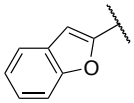
**29a**: 36%
**29b**: 50%


**30a**: 35%
**30b**: 0%[b]


**31a**: 35%
**31b**: 0%[b]

[a]Reagents and conditions: a) $RCO_2H$ (2.0 equiv), ECI·HCl (2.0 equiv), DMAP (2.0 equiv), $CH_2Cl_2$, RT, 16 h. [b]Varying amounts of **7** isolated as the only product.

the acylations were performed by activating the corresponding carboxylic acids *in situ* with EDC·HCl and DMAP. To expedite in the synthesis of these compounds, the reaction were run in parallel on a MiniBlock XT system and purified by mass-directed reverse phase HPLC. Although compounds **9a**-**31a** were successfully prepared in this manner, **9b**-**31b** proved to be unstable to the purification process and were synthesized using standard benchtop chemistry and purified using a combination of silica gel chromatography and semi-preparatory reverse phase HPLC. This method proved successful for introducing substitutions to the phenyl ring as well its replacement with several heterocycles, however the introduction of either a 2- or 3-furan to **6** was unsuccessful. Despite several attempts with alternate coupling reagents, only varying amounts of **7** were isolated from the reaction mixtures. Potentially **30b** and **31b** may have rapidly formed and decomposed leaving the less reactive **7** as the only stable compound.

The carboxylic acids utilized for these series were specifically selected to identify potential interactions with the MOR. The substituents were introduced at the *meta*, *ortho*, and *para* positions as it was likely that any trends that were observed may be dependent upon their location on the ring. The electronic differences in the substitutions spanned from the strongly electron withdrawing nitro moiety to the electron donating methoxy group. The nitro and methoxy moieties were also used to probe for hydrogen bonding between the ligands and the MOR. Similarly, the chloro- and fluoro-substituted rings would be useful in identifying potential halogen bonding interactions. The methyl groups were included to determine the effect that steric parameters would have on the ligands' activities. Finally, the heterocycles were expected to modulate the electron density of the aromatic ring and provide hydrogen bond acceptors without introducing additional steric

**Scheme 3.3.** Inversion of the C2 stereocenter and synthesis of 2-epi-herkinorin.[a]

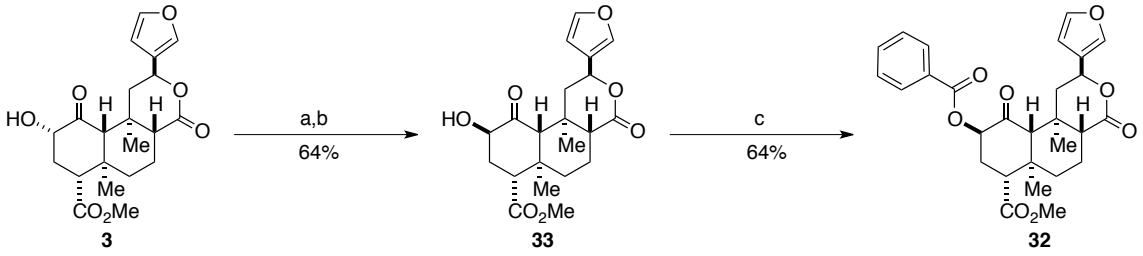


[a]Reagents and conditions: a) 4-$NO_2$-$PhCO_2H$ (3.0 equiv), DIAD (3.0 equiv), $PPh_3$ (3.0 equiv), $CH_2Cl_2$, RT, 16 h. b) $K_2CO_3$ (1.0 equiv), MeOH, 0 °C, 15 min. c) BzCl (2.5 equiv), DIPEA (2.5 equiv), DMAP (0.25 equiv), $CH_2Cl_2$, RT, 16 h.

bulk.

In addition to these two series of compounds, the effects of the configuration of C2 on activity were further explored by inverting the stereochemistry of this position.The synthesis of 2-epi-herkinorin (**32**) has been reported, however its activity at the opioid receptors was not disclosed.[12] Additionally, attempts to obtain **32** directly from **3** using the reported Mitsunobu procedure were unsuccessful. As an alternative, the C2 stereocenter of **3** was first inverted via a Mitsunbou reaction using the more active 4-nitro-benzoic acid (Scheme 3.3). Subsequent ester cleavage with methanolic $K_2CO_3$ produced 2-epi-salvinorin B (**33**).[13] Acylation of **33** with benzoyl chloride produced **32** in good yields.[1]

*In Vitro Studies*

To determine if the additional degree of unsaturation in the core of **1** would affect potency and selectivity at the opioid receptors as predicted, **1, 2, 4**, and the standard MOR agonists morphine and DAMGO were screened for activity at the MOR and the KOR using the same inhibition of forskolin-induced cAMP accumulation assay described in chapter 2 (Table 3.1). The desaturation of the C2-C3 bond resulted in a significant increase in the potency at the MOR. Additionally, all activity at the KOR was eliminated,

**Table 3.1**. MOR and KOR Activities of Diterpene and Standard MOR Agonists.

| Entry | Compound | MOR $EC_{50}$ (nM)[a] | KOR $EC_{50}$ (nM)[a] | Selectivity (MOR/KOR) |
|---|---|---|---|---|
| 1 | **1** | 42 ± 4 | 170 ± 30 | 4.0 |
| 2 | **2** | 3.0 ± 0.4 | >10,000 | >3,300 |
| 3 | **4** | 1.2 ± 0.2 | >10,000 | >8,300 |
| 4 | **32** | >10,000 | --[b] | N/A |
| 4 | morphine | 3.7 ± 0.3 | 140 ± 20 | 38 |
| 5 | DAMGO | 0.6 ± 0.1 | >10,000 | >10,000 |

[a] $EC_{50}$ = Effective concentration to produce 50% of the maximal response as measured by inhibition of cAMP accumulation in CHO cells expressing either MOR or KOR. [b]Not tested.

leading to a substantial increase in selectivity compared to **1**. Inversion of the natural C2 stereochemistry resulted in a complete loss of activity at the MOR, suggesting that the increased potency of **4** is not the result of decreasing the distance to an interaction on the α-face of the A-ring.

It is impressive that the formal removal of two hydrogen atoms from **1**—arguably the simplest modification that could be performed—leads to such a drastic change in activity and results in a compound that is more potent than morphine and with similar potency as the peptidic ligand DAMGO. Taken together, this activity profile is nearly identical to that of **2**, which is also more potent and selective for the MOR than **1**. This would suggest that **2** and **4** bind similarly to the opioid receptors.

To elucidate additional SAR that might lead to a further increase in potency, **9a**-**29a** and **9b**-**29b** were screened for activity at the MOR (Table 3.2). Of all the compounds screened, all but one (**24a**) retained full efficacy at the MOR. A comparison of the two series of compounds indicated that those containing the oxidized A-ring tended to be 1-2 orders of magnitude more potent than the corresponding saturated variant. A scatter plot comparison of the $pEC_{50}$ for unsaturated series versus the $pEC_{50}$ for the saturated series

**Table 3.2.** MOR Potencies of Two Series of Derivatives of Herkinorin Derivatives Bearing Parallel Substitutions.

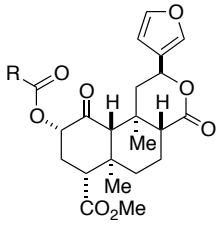


**1**, **9a-29a**

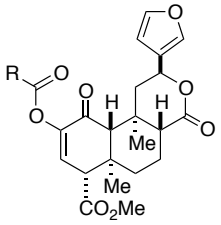


**4**, **9b-29b**

| Entry | Compound | R= | $EC_{50}$ (nM)[a] | $EC_{50}$ (nM)[a] |
|---|---|---|---|---|
| 1 | **1** | $C_6H_5$ | 42 ± 4 | 1.2 ± 0.2 |
| 2 | **9** | 2-$NO_2$-$C_6H_4$ | 2000 ± 1000 | 1900 ± 600 |
| 3 | **10** | 3-$NO_2$-$C_6H_4$ | 3500 ± 200 | 320 ± 10 |
| 4 | **11** | 4-$NO_2$-$C_6H_4$ | 1100 ± 100 | 31 ± 2 |
| 5 | **12** | 2-Cl-$C_6H_4$ | 3400 ± 200 | 290 ± 20 |
| 6 | **13** | 3-Cl-$C_6H_4$ | 2400 ± 100 | 250 ± 30 |
| 7 | **14** | 4-Cl-$C_6H_4$ | 700 ± 100 | 29 ± 8 |
| 8 | **15** | 2-F-$C_6H_4$ | 400 ± 100 | 4.7 ± 0.4 |
| 9 | **16** | 3-F-$C_6H_4$ | 460 ± 80 | 15 ± 2 |
| 10 | **17** | 4-F-$C_6H_4$ | 800 ± 200 | 5 ± 1 |
| 11 | **18** | 2-$CH_3$-$C_6H_4$ | 1600 ± 400 | 240 ± 40 |
| 12 | **19** | 3-$CH_3$-$C_6H_4$ | 1800 ± 300 | 160 ± 30 |
| 13 | **20** | 4-$CH_3$-$C_6H_4$ | 430 ± 10 | 21.8 ± 0.3 |
| 14 | **21** | 2-$CH_3O$-$C_6H_4$ | 3300 ± 300 | 2000 ± 1000 |
| 15 | **22** | 3-$CH_3O$-$C_6H_4$ | 330 ± 20 | 11 ± 2 |
| 16 | **23** | 4-$CH_3O$-$C_6H_4$ | 190 ± 60 | 8 ± 3 |
| 17 | **24** | 2-pyridine | >50,000[b] | 410 ± 50 |
| 18 | **25** | 3-pyridine | 240 ± 20 | 3.3 ± 0.8 |
| 19 | **26** | 4-pyridine | 340 ± 10 | 6 ± 1 |
| 20 | **27** | 2-thiophene | 330 ± 70 | 1.4 ± 0.8 |
| 21 | **28** | 3-thiophene | 23 ± 5 | 1.3 ± 0.9 |
| 22 | **29** | 2-benzofuran | 1050 ± 80 | 31 ± 9 |

[a] $EC_{50}$ = Effective concentration to produce 50% of the maximal response as measured by inhibition of cAMP accumulation in CHO cells expressing either MOR or KOR. [b]No activity observed at 50 μM.

indicates a clear correlation in activity (Figure 3.3). Therefore parallel changes in structure produced parallel changes in activity, which strongly supports the hypothesis

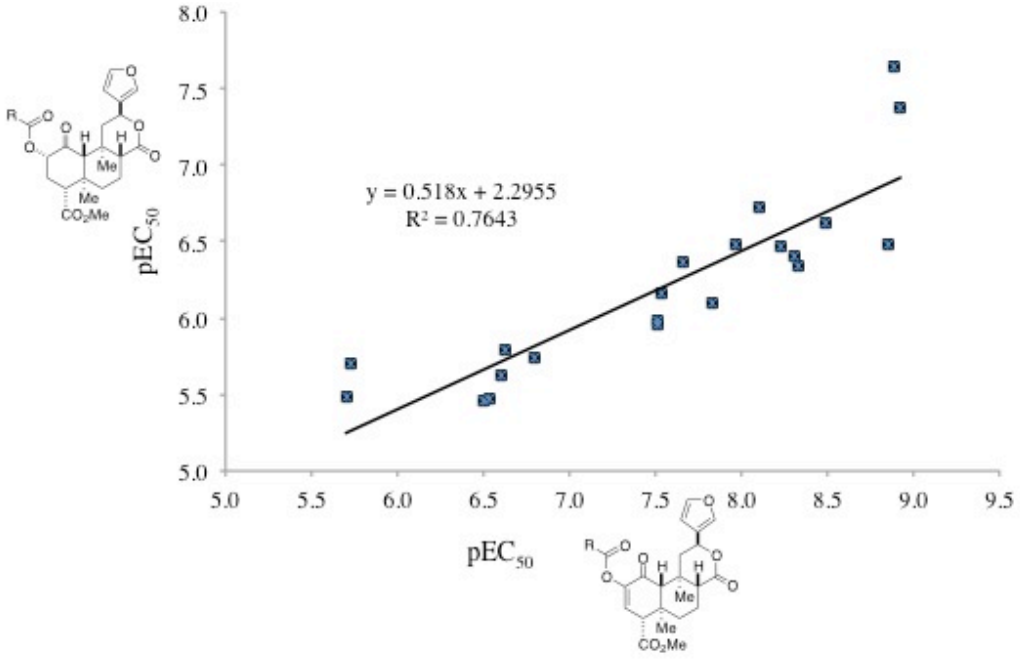


**Figure 3.3.** Scatter plot demonstrating parallel changes in structure produces parallel changes in potency at the MOR.

that compounds **9a**-**29a** and **9b**-**29b** bind in an identical position to the MOR and make similar interactions with the receptor.

The introduction of additional substituents to the phenyl ring of **1** and **4** generally led to a decrease in potency, however by focusing on the more potent set of compounds several useful trends were observed. The activity of the ligand was highly dependent on the position of the substitution on the aromatic ring: the *para* position was strongly preferred over the *meta* which in turn was favored over the *ortho* position. A similar dependence was observed during the limited SAR studies on **1**.[3,14] The lone exception to this trend was the fluoro-substituted rings (Table 3.2, Entries 15-17) where the *ortho* and *para* substituted rings were equipotent to each other and slightly more potent than the *meta* substituted ring. The small fluorine substitutions being the exception to the general trend suggests the effect on substituent position is primarily steric in nature. The electronic properties of the substitutions on the phenyl ring, however, did also have an

impact upon ligand potency. As the electron donating ability of the substitutions at the *meta* and *para* positions increased, a trend of increasing potency was observed. However, this trend once again failed to apply to the fluoro-substituted rings, likely due to their decreased steric properties.

Because of the negative impact of larger substitutions, bioisosteres of the phenyl ring were also explored (Table 3.2, Entries 17-21). Previous SAR studies on **1**, had indicated that replacement of the phenyl ring with a 2-thiophene, 3-thiophene, or 3-pyridine was reasonably tolerated, resulting in only small (1-4 fold) reductions in activity.[3,14] Using the inhibition of forskolin-induced cAMP functional assay, these differences in activity were slightly amplified. Interestingly, in this assay **27a**, bearing a 2-thiophene, was more potent than **1**. In the modified A-ring series (**24b**-**29b)**, several of the heterocycles were also very well tolerated, especially the thiophene-containing derivatives, which were equipotent to **4**. The 3- and 4-substitued pyridines resulted in a mild decrease in potency relative to **4** (2.8-fold and 5-fold, respectively) while both the 2-pyridine and 2-benzofuran were considerable less active than **4** (340-fold and 26-fold, respectively).

Based upon the SAR that had been developed several additional probe molecules were synthesized (Scheme 3.4) and evaluated (Table 3.3) to further probe ligand-receptor interactions and potentially develop more potent MOR ligands. The substitutions to the phenyl ring suggested that small, electron-rich groups at either the *meta* or *para* positions were most tolerated. This prompted the introduction of hydroxy moeties at these positions resulting in the phenols **34** and **35**. Compound **34** was equipotent to **4** at the MOR making it the most potent derivative bearing a *meta* substitution. Consistent with

**Scheme 3.4.** Synthesis of derivatives of **4** based upon initial SAR[a]

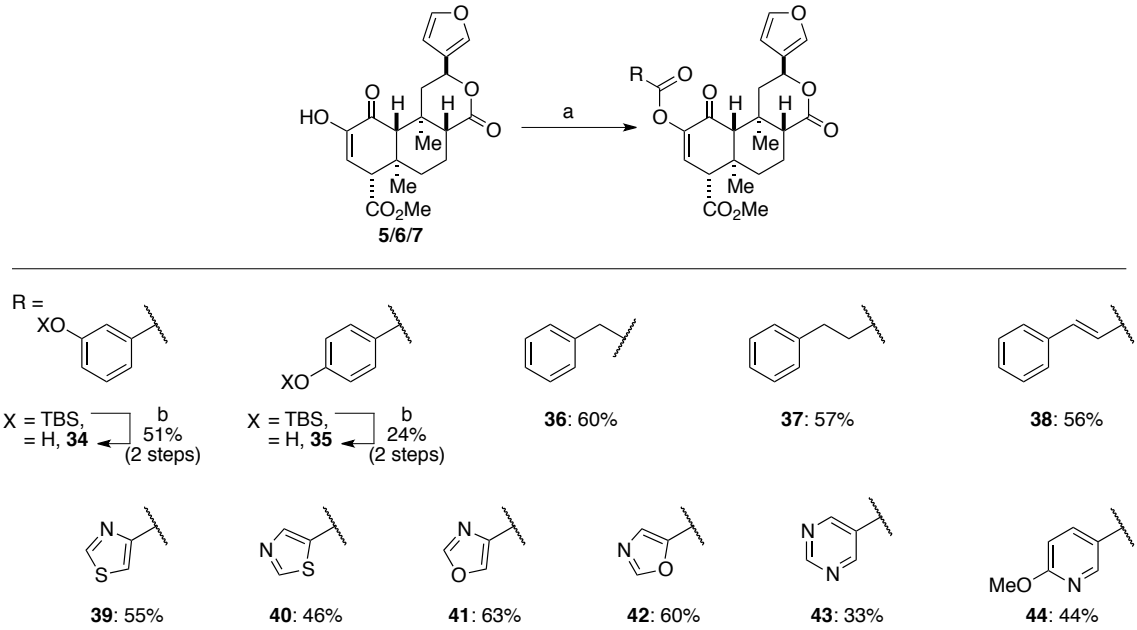


[a]Reagents and conditions: a) $RCO_2H$ (1.5 equiv), ECI·HCl (1.5 equiv), DMAP (1.5 equiv), $CH_2Cl_2$, RT, 16 h. b) TBAF (2.0 equiv), THF, -10 °C, 15 min.

the other substituted rings, the *para* phenol **35** was slightly more potent than **34**, and was the only ligand more potent than **4**. The increased potency of **34** and **35** is particularly encouraging considering the phenols could potentially lead to improved water solubility, especially if halogens were introduced to the phenyl ring to reduce the $pK_a$ of the phenol below 7.

In an attempt to explore the spatial effects within the binding pocket, linkers were introduced between the ester carbonyl and the phenyl ring (**36**-**38**). The alkyl linkers resulted in greater than a 100-fold decrease in activity whereas the alkenyl linker was only moderately less active than **4**. This suggests while there is some additional room in the binding pocket to allow the phenyl ring to extend away from the diterpene core, this increased distance reduces activity. Furthermore, additional rotational freedom in the alkyl linker likely prevents the phenyl ring from adopting the conformation necessary for

**Table 3.3**. MOR Potencies of Additional Analogues Based on Initial SAR.[a]

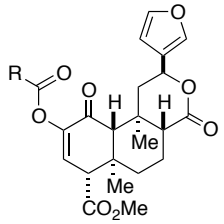


| Entry | Compound | R= | $EC_{50}$ (nM)[a] |
|---|---|---|---|
| 1 | **1** | $C_6H_5$ | 1.2 ± 0.2 |
| 2 | **34** | 3-HO-$C_6H_4$ | 1.3 ± 0.3 |
| 3 | **35** | 4-HO-$C_6H_4$ | 0.83 ± 0.04 |
| 4 | **36** | $C_6H_5$-$CH_2$- | 130 ± 50 |
| 5 | **37** | $C_6H_5$-$CH_2$-$CH_2$- | 500 ± 200 |
| 6 | **38** | $C_6H_5$-CH=C(H)- | 30 ± 10 |
| 7 | **39** | 4-thiazole | 8 ± 3 |
| 8 | **40** | 5-thiazole | >10,000 |
| 9 | **41** | 4-oxazole | 30 ± 2 |
| 10 | **42** | 5-oxazole | >10,000 |
| 11 | **43** | 5-pyrimidine | 6 ± 1 |
| 12 | **44** | 4-$CH_3O$-pyridine | 2.5 ± 0.3 |

[a] $EC_{50}$ = Effective concentration to produce 50% of the maximal response as measured by inhibition of cAMP accumulation in CHO cells expressing either MOR or KOR.

proper MOR activation.

The relative success of the bioisosteric replacement of the phenyl rings with heterocycles also prompted additional heterocycles to be explored. The five-membered thiazoles and oxazoles offered some interesting results. Although the 2-thiophene and 3-thiophene (**27b** and **28b**) were equipotent, a significant difference was observed between the 4-thiazole (**39**, $EC_{50}$ = 8 ± 3 nM) and 5-thiazole (**40**, $EC_{50}$ > 10,000 nM). A similar effect was observed with the 4-oxazole (**41**, $EC_{50}$ = 30 ± 2 nM) and 5-oxazole (**42**, $EC_{50}$ > 10,000 nM). The decrease in potency for **39** and **40** can be explained by the decease in electron density of thiazoles and oxazoles compared to thiophenes. However the

complete loss of activity for **40** and **42** remains somewhat inexplicable. In an attempt to improve upon the most potent pyridine-containing analogue (**25b**) the pyrimidine **43** was synthesized. Additionally, electron density was added to **25b** by incorporating a methoxy moiety at the 4-position (**44**). The additional nitrogen in **43** resulted in a slight decrease in activity, once again supporting the preference for an electron rich ring. **44** was approximately equipotent to **25b**, which is likely due to competing effects between increased steric bulk and increased electron density in the ring.

*Conclusions*

The design of **4** based on key differences identified in the crystal structures of **1** and **2** has led to a new class of neoclerodane diterpene ligands that show remarkable potency and selectivity for the MOR. The additional synthesis and evaluation of two parallel series of compounds was useful not only in identifying that the introduction of an additional degree of unsaturation results in a 10-100 fold increase in potency but also elucidate important SAR trends. By employing these trends, a sub-nanomolar MOR agonist **35** was designed, which could assist in the development of safer analgesics. Toward this goal, **4** is currently being investigated in animal models of antinociception. Preliminary results indicate that **4** produces analgesia and that these effects are no longer limited to the site of injection. Although additional SAR studies and more in depth investigations into the antinociceptive and side-effect profiles of this scaffold are needed, the identification of this modification to the structure of **1** represents a substantial step towards developing a novel class of analgesics.

**References:**


(1) Harding, W. W.; Tidgewell, K.; Byrd, N.; Cobb, H.; Dersch, C. M.; Butelman, E. R.; Rothman, R. B.; Prisinzano, T. E. Neoclerodane diterpenes as a novel scaffold for mu opioid receptor ligands. *J. Med. Chem.* **2005**, *48*, 4765.

(2) Groer, C. E.; Tidgewell, K.; Moyer, R. A.; Harding, W. W.; Rothman, R. B.; Prisinzano, T. E.; Bohn, L. An opioid agonist that does not induce mu-opioid receptor--arrestin interactions or receptor internalization. M. *Mol. Pharm.* **2007**, *71*, 549.

(3) Tidgewell, K.; Groer, C. E.; Harding, W. W.; Lozama, A.; Schmidt, M.; Marquam, A.; Hiemstra, J.; Partilla, J. S.; Dersch, C. M.; Rothman, R. B.; Bohn, L. M.; Prisinzano, T. E. Herkinorin analogues with differential beta-arrestin-2 interactions. *J. Med. Chem.* **2008**, *51*, 2421.

(4) Bohn, L. M.; Lefkowitz, R. J.; Gainetdinov, R. R.; Peppel, K.; Caron, M. G.; Lin, F. T. Enhanced morphine analgesia in mice lacking beta-arrestin 2. *Science* **1999**, *286*, 2495.

(5) Bohn, L. M.; Gainetdinov, R. R.; Lin, F. T.; Lefkowitz, R. J.; Caron, M. G. Mu-opioid receptor desensitization by beta-arrestin-2 determines morphine tolerance but not dependence. *Nature* **2000**, *408*, 720.

(6) Raehal, K. M.; Walker, J. K.; Bohn, L. M. Morphine side effects in beta-arrestin 2 knockout mice. *J. Pharmacol. Exp. Ther.* **2005**, *314*, 1195.

(7) Ji, F.; Wang, Z.; Ma, N.; Riley, J.; Armstead, W. M.; Liu, R. Herkinorin dilates cerebral vessels via kappa opioid receptor and cyclic adenosine monophosphate (cAMP) in a piglet model. *Brain Res.* **2013**, *1490*, 95.

(8) Lamb, K.; Tidgewell, K.; Simpson, D. S.; Bohn, L. M.; Prisinzano, T. E. Antinociceptive effects of herkinorin, a MOP receptor agonist derived from salvinorin A in the formalin test in rats: new concepts in mu opioid receptor pharmacology: from a symposium on new concepts in mu-opioid pharmacology. *Drug Alcohol Depend*. **2012**, *121*, 181.

(9) Chavkin, C.; Sud, S.; Jin, W.; Stewart, J.; Zjawiony, J. K.; Siebert, D. J.; Toth, B. A.; Hufeisen, S. J.; Roth, B. L. Salvinorin A, an active component of the hallucinogenic sage salvia divinorum is a highly efficacious kappa-opioid receptor agonist: structural and functional considerations. *J. Pharmacol. Exp. Ther*. **2004**, *308*, 1197.

(10) Shigehisa, H.; Mizutani, T.; Tosaki, S. Y.; Ohshima, T.; Shibasaki, M. Formal total synthesis of (+)-wortmannin using catalytic asymmetric intramolecular aldol condensation reaction. *Tetrahedron* **2005**, *61*, 5057.

(11) Kotoku, N.; Sumii, Y.; Kobayashi, M. Stereoselective synthesis of core structure of cortistatin A. *Org. Lett*. **2011**, *13*, 3514.

(12) Harding, W. W.; Schmidt, M.; Tidgewell, K.; Kannan, P.; Holden, K. G.; Gilmour, B.; Navarro, H.; Rothman, R. B.; Prisinzano, T. E. Synthetic studies of neoclerodane diterpenes from *Salvia divinorum*: semisynthesis of salvinicins A and B and other chemical transformations of salvinorin A. *J. Nat. Prod*. **2006**, *69*, 107.

(13) Beguin, C.; Richards, M. R.; Li, J. G.; Wang, Y. L.; Xu, W.; Liu-Chen, L. Y.; Carlezon, W. A.; Cohen, B. M. Synthesis and *in vitro* evaluation of salvinorin A

analogues: effect of configuration at C(2) and substitution at C(18). *Bioorg. Med. Chem. Lett.* **2006**, *16*, 4679.

(14) Tidgewell, K.; Harding, W. W.; Lozama, A.; Cobb, H.; Shah, K.; Kannan, P.; Dersch, C. M.; Parrish, D.; Deschamps, J. R.; Rothman, R. B.; Prisinzano, T. E. Synthesis of salvinorin A analogues as opioid receptor probes. *J. Nat. Prod.* **2006**, *69*, 914.

## IV. Synthesis of the *meta,meta*-Bridged Diarylheptanoid Myricanol

*Introduction*

Compounds that are able to reduce tau protein pharmacologically would be useful in gaining a more complete understanding of tau's role in neurodegenerative diseases and could potentially be developed into a treatment for Alzheimer's Disease (AD). Although such compounds are scarce, natural products have historically been a good source of lead compounds, particularly in the field of AD.[1,2] During a recent campaign aimed at identifying novel anti-tau compounds, an extract from the bayberry plant (*Myrica cerifera*) was shown to decrease the concentration of tau protein in four different cell lines while remaining non-toxic.[3] These results were further confirmed in *ex vivo* studies using murine brain slices. Bioassay-guided fractionation revealed the major component of the extract responsible for the activity was a scalemic mixture (86% ee, dextrorotatory in excess) of myricanol (**1**, Figure 4.1).

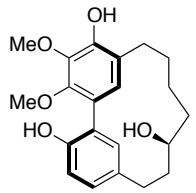

**Figure 4.1**. Structure of (+)-a*R*,11*S*-myricanol (**1**).

This *meta,meta*-bridged diarylheptanoid is found in several plants in the myrica genus, however **1** is typically isolated as a racemate or with the levorotatory enantiomer in excess.[4-7] In addition to the point stereocenter at C11, the di*ortho* substitution of the aromatic rings and the conformational constraint induced by the macrocycle prevent free-rotation about the C1-C2 bond, leading to distinct atropisomers. Crystallographic and computational studies indicate the axial chirality of the C1-C2 bond is greatly influenced by the C11 stereocenter and 11-epi-**1** is 2.72 kcal/mol higher in energy than the natural enantiomer.[6] This potentially explains why diastereomers of **1** have not been isolated

from natural sources. These stereochemical issues are an important consideration because while the scalemic mixture of **1** isolated from *M. cerifera* was able to lower the levels of tau, a commercially available racemate was nearly inactive.[3]

In a recent report occurring concurrently with the synthetic studies detailed below, this interesting stereochemical dependence was further explored with a synthetic racemate.[8] This mixture was active in reducing tau levels, suggesting that the commercially available racemate originally used was impure or not truly composed of **1**. Following separation of the two enantiomers using chiral HPLC, it was shown that (-)-**1** was the active enantiomer. This is rather surprising considering it is the minor enantiomer in *M. cerifera* extracts. More extensive mode of action studies indicated that (-)-**1** decreases both phosphorylated and total tau concentrations and does not affect tau synthesis. Using results from stable isotope labeling with amino acids in cell culture (SILAC) it was proposed that (-)-**1** reduces tau levels via a similar mechanism to rapamycin: by activating autophagy.

These studies have provided some answers regarding the stereochemistry of **1** and its importance in tau clearance, however several questions still remain. Importantly, the assignment of the activity to the minor enantiomer is curious and confirmation of the absolute stereochemistry through asymmetric synthesis would be beneficial. Additionally, although a mode of action was proposed, the specific molecular target of **1** remains unknown. The synthesis of analogues will be useful not only in identifying this target but also in elucidating additional structural-activity relationships (SAR) for this scaffold. And while it is feasible that these analogues could be synthesized using the route outlined by Martin *et. al.*,[8] the overall yields (0.63% over 12 steps) and use of chiral HPLC are less

than ideal. Thus, a synthetic route to **1** that would provide access to both enantiomers in an efficient manner is essential to fully understanding the effects of diarylheptanoids on tau. Furthermore, the macrocyclic strain and axial chirality present in **1** offer interesting synthetic challenges that have not been fully explored.

In the first reported synthesis of **1**, Whiting and Wood addressed these synthetic challenges through a biomimetic approach (Figure 4.2).[9,10] In the biosynthesis of **1**, the linear diarlyheptanoid **2** is proposed to undergo oxidative cyclization via a biradical intermediate.[4] However, despite extensive screening of oxidants, this transformation could not be reproduced in the laboratory. Reductive macrocyclization was accomplished from the bis-iodide **3** using stoichiometric Ni(0), however in only 7% yield. By comparison, dimethylalnusone was formed from **4** in 56% yield under nearly identical conditions.[11] This difference in reactivity is potential the result of increased steric bulk at the aryl-aryl bond of dibenzyl myricanol acetate, however the presence of three $sp^3$ carbons in the chain of dimethylalnusone may also improve cyclization by

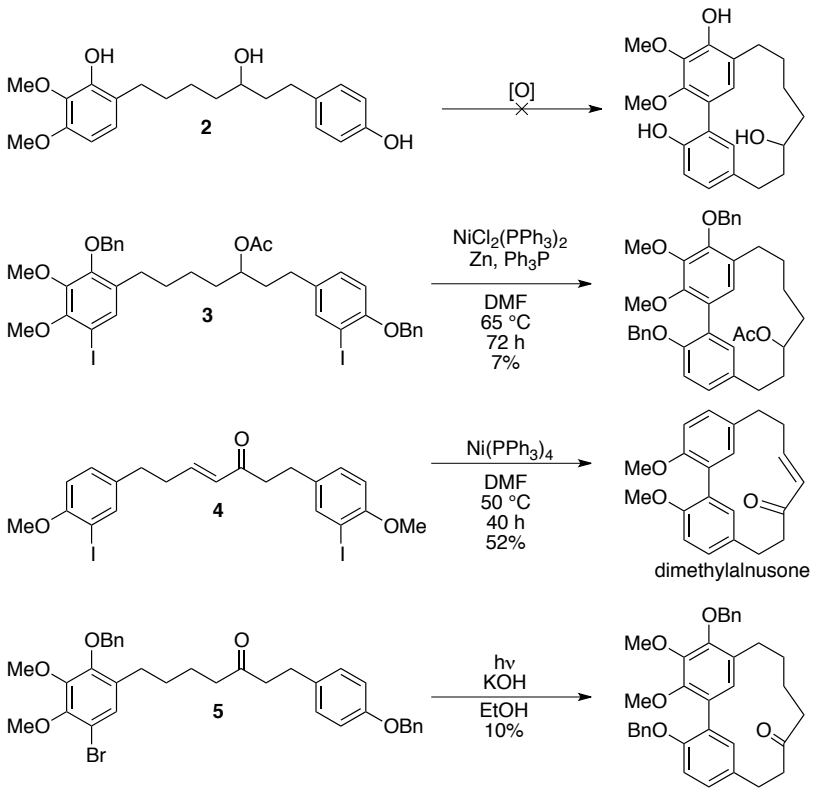


**Figure 4.2.** Approaches to *meta,meta*-bridged diarylheptanoids.

reducing ring strain and free rotation within the tether. Whiting also reported that the bromide **5** underwent successful photochemical cyclization in basic ethanol, but once again in only approximately 10% yield. These low yields are a clear demonstration of the difficulty often encountered in synthesizing cyclophane natural products.[12]

*First Generation Approach*

The biomimetic nature of the Whiting synthesis required that the macrocyclization and biaryl coupling occur simultaneously. However these two events also represent the two most challenging steps in the synthesis. If these two transformations could be separated, the overall yield of the synthesis may be improved. Furthermore, as demonstrated by dimethylalnusone, the presence of multiple $sp^2$-hybridized carbons in the tethering chain may be beneficial to ring closure. Therefore, the initial synthetic target for this improved synthesis was dibenzyl-$\Delta^{7,8}$-myricanone (Figure 4.3, **6**). Based upon recent advances in ring closing metathesis (RCM) methodology and its utility in numerous natural product total syntheses,[13,14] **6** was envisioned to be derived from the diene **7**. Retrosyntethic cleavage of the aryl-aryl bond and olefin chain of **7** through a Suzuki-Miyaura reaction and Weinreb ketone synthesis, respectively, revealed the simple styrene **8** and boronic ester **9** as the first synthons to be targeted.

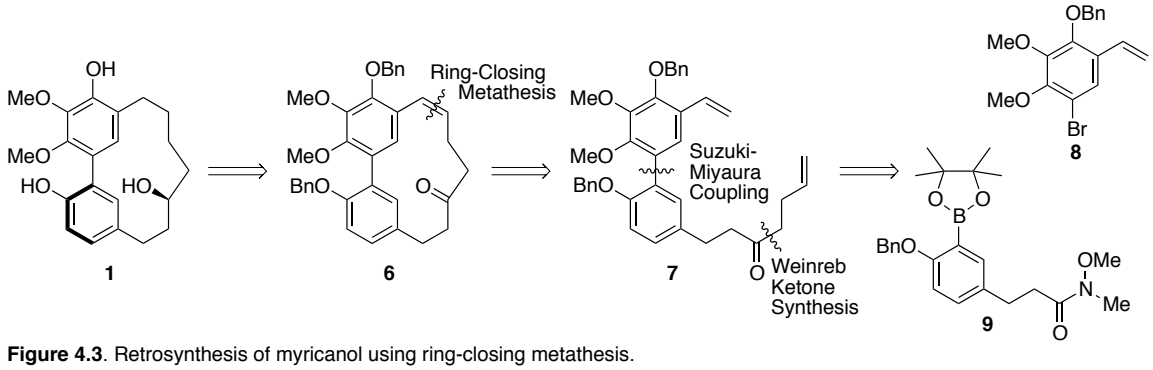


**Figure 4.3**. Retrosynthesis of myricanol using ring-closing metathesis.

**Scheme 4.1.** Synthesis of styrene **8**.[a]

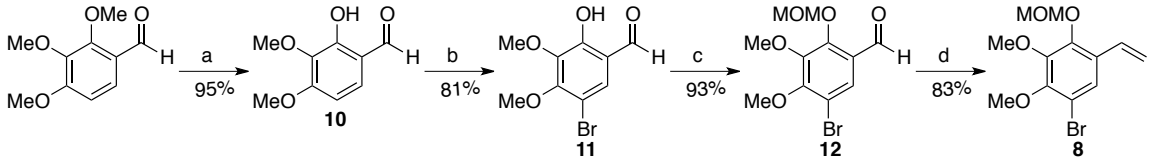


[a] Reagents and conditions: a) $AlCl_3$ (1.0 equiv), PhMe, 75 °C, 5 h; b) $Br_2$ (1.0 equiv), AcOH, RT, 1.5 h; c) MOMCl (2.0 equiv), DIPEA (2.0 equiv), $CH_2Cl_2$, 0 °C, 3.5 h; d)$[Ph_3PCH_3]^+I^-$ (1.9 equiv), n-BuLi (1.8 equiv), THF, 0 °C to RT.

The synthesis of styrene **8** was accomplished in four high yielding steps depicted in Scheme 4.1. Selective mono-demethylation of the commercially available 2,3,4-trimethoxybenzaldehyde was smoothly accomplished with $AlCl_3$ in 95% yield.[15] The preference for demethylation *ortho* to the aldehyde is attributed to the chelation of the Lewis-acidic $AlCl_3$ between the carbonyl oxygen and the adjacent ether, thus activating this position for demethylation. Subsequent bromination of the free phenol **10** with $Br_2$ in acetic acid produced bromophenol **11**, which was protected as a methoxymethyl (MOM-) ether to yield **12** in 75% yield over two steps. Conversion of the aldehyde to a terminal alkene using a Wittig reaction gave **8** in 83% yield. Through this process, **8** was routinely synthesized on multigram-scale.

The synthesis of Weinreb amide **9** was accomplished in an equally efficient manner from the ethyl ester **13** (Scheme 4.2). Bromination and protection of **13** under identical conditions used for the conversion of **10** to **12** produced **15** in similar yields (78% over 2 steps).[16] The ethyl ester **15** was converted directly to Weinreb amide **16** by treatment with the anion generated by the in situ deprotonation of *N,O*-dimethylhydroxylamine with isopropylmagnesium chloride.[17] Alternatively, a two step process involving the saponification of the ester and CDMT-promoted coupling[18] with the *N,O*-dimethylhydroxylamine could be employed. Although the one step process was slightly higher yielding, conversion to the amide via the acid was easily performed on

**Scheme 4.2.** Synthesis of boronate ester **9**.[a]

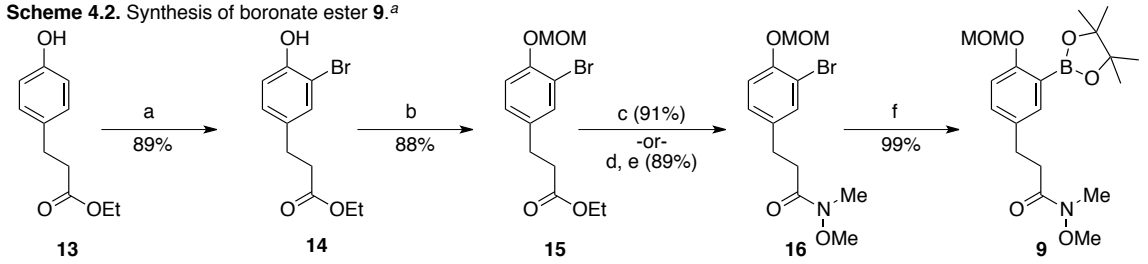


[a] Reagents and conditions: a) $Br_2$ (1.0 equiv), AcOH, RT, 2 h; b) MOMCl (2.0 equiv), DIPEA (2.0 equiv), $CH_2Cl_2$, 0 °C, 3.5 h; c) (MeO)(Me)$NH_2$Cl (1.55 equiv), $^i$PrMgCl (3.0 equiv), THF, -10 °C, 30 min; d) $NaOH_{(aq.)}$, MeOH, RT, 3 h; e) CDMT (1.2 equiv), NMM (3.0 equiv), (MeO)(Me)$NH_2$Cl (1.1 equiv), THF, RT, 16 h; f) HBPin (1.5 equiv), $PdCl_2(MeCN)_2$ (0.02 equiv), SPhos (0.08 equiv), $Et_3N$ (3.0 equiv), 1,4-diox., 110 °C, 4.5 h.

multigram scale. Attempts to borylate **16** under standard palladium-catalyzed Miyaura conditions ($B_2Pin_2$, $PdCl_2$(dppf), KOAc)[19] resulted in incomplete conversion, likely due to the electron-donating MOM-ether moiety deactivating the aryl bromide bond to oxidative addition.[20] However, conditions developed by Buchwald *et. al.* employing the bulky biaryl phosphine ligand SPhos[21] resulted in nearly quantitative yield of the desired product **9**. Excess pinacol borane were detected in the NMR spectra of **9**, however extensive silica gel chromatography did not improve the purity. Fortunately, the impurity did not affect the subsequent reactions and was consumed by treatment with excess Grignard reagent following the Suzuki-Miyaura reaction.

The success of the Buchwald ligands in the palladium-catalyzed borylation of **16** was encouraging for the Suzuki-Miyaura reaction that would be used to join **8** and **9**. Despite the steric encumbrance of *ortho* substituents on both rings and numerous electron-donating groups deactivating the aryl bromide bond to oxidative addition,

**Scheme 4.3.** Synthesis of diene **7**.[a]

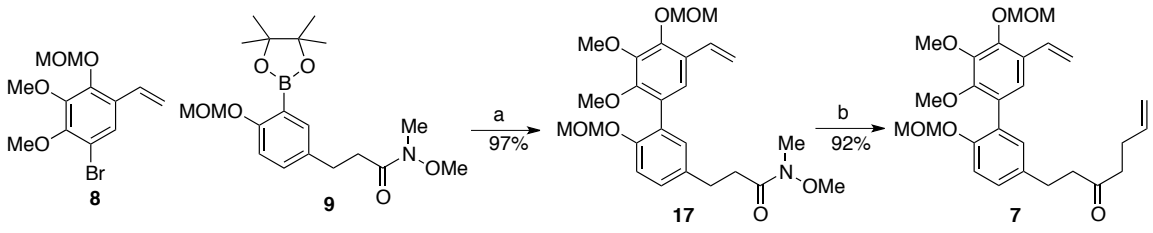


[a] Reagents and conditions: a) **8** (1.0 equiv), **9** (1.3 equiv), $Pd(OAc)_2$ (0.01 equiv), SPhos (0.02 equiv). $K_3PO_4$ (2.0 equiv), PhMe/$H_2O$ (10:1), 100 °C, 16 h; b) $Br(CH_2)_2CH{=}CH_2$ (3.0 equiv), Mg (3.5 equiv), $I_2$ (cat.), THF, 0 °C.

employing a catalyst system composed of $Pd(OAc)_2$ and SPhos resulted in the successful coupling of the two fragments in an impressive 97% yield (Scheme 4.3).[22] The resulting biaryl (**17**) was treated with the Grignard reagent derived from 4-bromobutene to furnish the diene **7** that would serve as the substrate for subsequent RCM investigations.

With **7** in hand, attempts to induce RCM using several ruthenium-based metathesis catalysts ensued (Table 4.1). Initially, exposure of **7** to Grubbs first-generation catalyst (**G-I**) in refluxing $CH_2Cl_2$ resulted in no observed reaction. However, increasing the temperature to 110 °C in toluene resulted in significant decomposition, likely due to the thermal instability of **G-I**. Employing the more active and thermostable Grubbs

**Table 4.1**. Attempted Ring-Closing Metathesis Using Diene **7**.

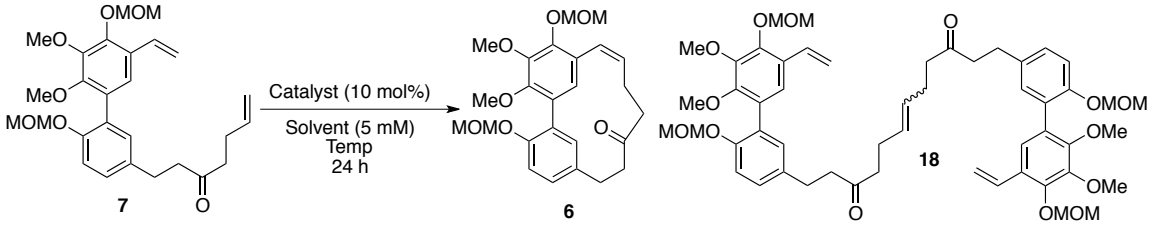


| Entry | Catalyst | Solvent | Temp (°C) | Yield of **6** (%)[a] | Yield of **18** (%)[a] |
|---|---|---|---|---|---|
| 1 | **G-I** | $CH_2Cl_2$ | 40 | 0 | 0 |
| 2 | **G-I** | PhMe | 110 | 0[b] | 0[b] |
| 3 | **G-II** | $CH_2Cl_2$ | 40 | 0 | 26 |
| 4 | **G-II** | PhMe | 110 | 0 | 28 |
| 5 | **HG-II** | PhMe | 110 | 0 | 29 |

[a] Isolated yields. [b] Decomposition of reaction mixture.

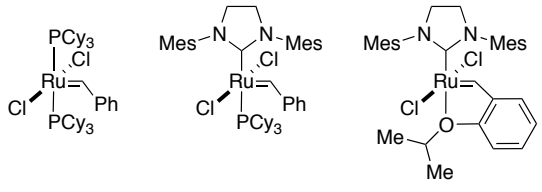

second-generation catalyst (**G-II**) did result in an isolatable product. However, despite highly dilute conditions, no RCM was observed and the sole product was the result of dimerization (**18**). To confirm the assigned structure, **18** was reduced with Pd/C under an atmosphere of $H_2$ and the structure of the resulting product (Figure 4.4, **19**) was determined using COSY NMR. Similar results were seen with **G-II** and Hoveyda-Grubbs second-generation catalyst (**HG-II**) in refluxing toluene.

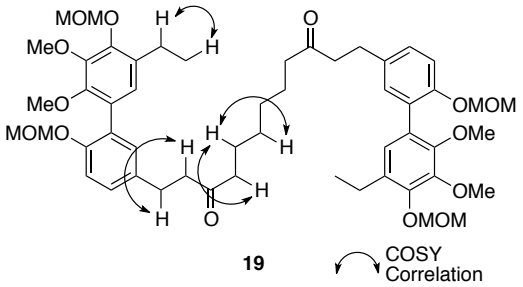


**Figure 4.4**. COSY correlations used to assign the structure of **19**. For clarity, only correlations on half the molecule are shown.

The isolation of **19** as the lone product in the reaction mixture indicated the catalyst was able to bind to the olefin directly attached to the ketone, however, was incapable of completing the RCM process with the styrene. This non-reactive pattern could potentially be the result of: (1) hindered rotation about the aryl-aryl bond preventing the olefins from being in close proximity, or (2) interactions between the MOM-ether protecting group and the catalyst interfering with proper catalytic action. To investigate these two possibilities, the dienes lacking either or both MOM-ethers were synthesized. Additionally, replacement of the MOM-protecting group with a benzyl-protecting group resulted in a substrate devoid of catalyst chelating ability. The model dienes **20**-**24** were prepared from commercially available aldehydes and propionic acids in a similar fashion used to furnish **7** (Scheme 4.4).

With these dienes, the effects from hindered rotation about the aryl-aryl bond could be separated from the effects of the substituent in close proximity to the styrene. With both of the potentially problematic substitutents removed, as in **24**, a macrocycle was formed. However inspection of the mass spectrum of the product indicated that a

dimer had formed rather than the intended monomer (Table 4.2). Attempts to perform the reaction under higher dilution resulted in no reaction after 48 hours. Although disappointing, this result does support that at least one of the MOM-ethers was preventing RCM from occurring. When a MOM-ether was present at $R^3$ (**21**) a similar dimer product was obtained. However, with a MOM-ether present at $R^1$ (**22**) no cyclic products were isolated, suggesting an interaction between the MOM-ether and the catalyst was preventing the reaction from occurring. This was confirmed with substrate **23** bearing only the MOM-ether at the $R^1$ that produced no dimer product. Finally, the benzyl-protected diene **24** was also unable to give the desired monomer and produced the dimer in a low 22% yield, indicating that any substituent at $R^1$ may have an influence on the reaction. However, whether this effect is electronic or steric in nature is unclear.

The results from these model studies indicate that an RCM-based approach to **1** is unlikely to be successful. Synthetic studies on closely related ether-bridge diarylheptenoids have concluded similar difficulties.[23] Due to the reversible nature of

**Scheme 4.4.** Synthesis of dienes for RCM model studies.[a]

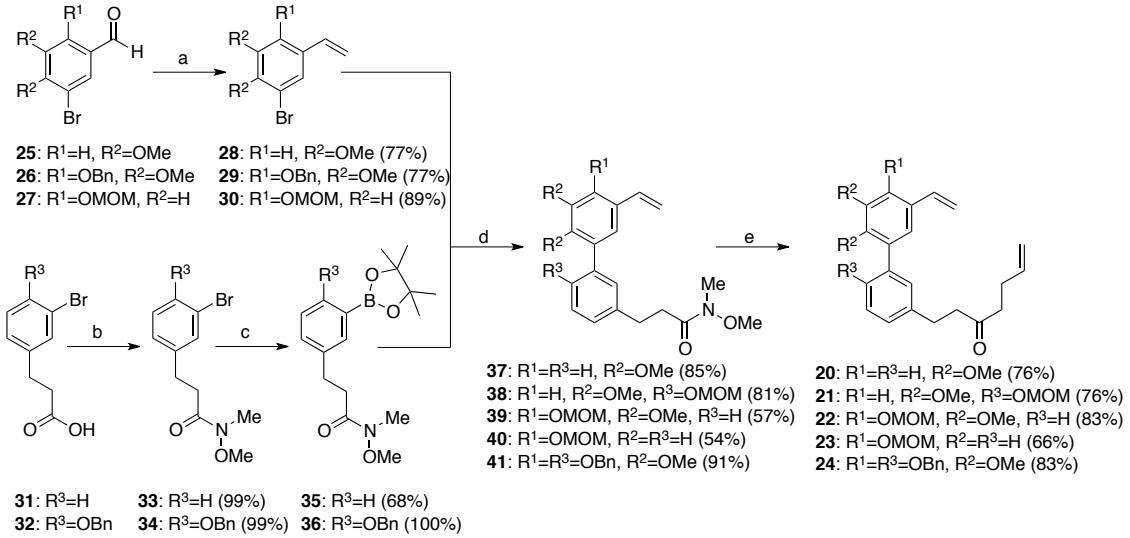


[a] Reagents and conditions: a)$[Ph_3PCH_3]^+I^-$ (1.9 equiv), n-BuLi (1.8 equiv), THF, 0 °C to RT, 3 h; b) CDMT (1.2 equiv), NMM (3.0 equiv), $(MeO)(Me)NH_2Cl$ (1.1 equiv), THF, RT, 16 h; c) HBPin (1.5 equiv), $PdCl_2(MeCN)_2$ (0.02 equiv), SPhos (0.08 equiv), $Et_3N$ (3.0 equiv), 1,4-diox., 110 ° C, 4.5 h; d) $Pd(OAc)_2$ (0.01 equiv), SPhos (0.02 equiv). $K_3PO_4$ (2.0 equiv), PhMe/$H_2O$ (10:1), 100 ° C, e) $Br(CH_2)_2CH{=}CH_2$ (3.0 equiv), Mg (3.5 equiv), $I_2$ (cat.), THF, 0 °C.

**Table 4.2**. RCM Experiments on Model Diene Systems.

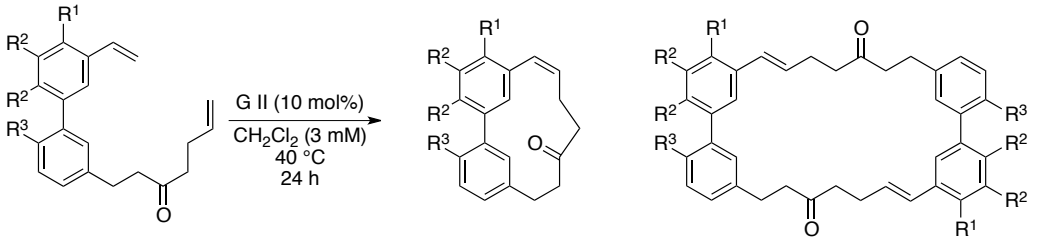


**20-24** **Monomer** **Dimer**

| Entry | Substrate | $R^1$= | $R^2$= | $R^3$= | Monomer Yield (%)[a] | Dimer Yield (%)[a] |
|---|---|---|---|---|---|---|
| 1 | **20** | H | OMe | H | 0 | 31 |
| 2 | **21** | H | OMe | OMOM | 0 | 34 |
| 3 | **22** | OMOM | OMe | H | 0 | 0 |
| 4 | **23** | OMOM | H | H | 0 | 0 |
| 5 | **24** | OBn | OMe | OBn | 0 | 21 |

[a] Isolated yields.

olefin-metathesis,[24] if any monomer were to form during the course of the reaction it could potentially be converted into the dimer products. The observed product ratios would thus reflect their relative thermodynamic stabilities. The increased ring size of the dimers reduces ring stain within the macrocycles, which ultimately increase their stabilities.[25] This suggests that a more irreversible reaction is required for the macrocyclization event.

*Second Generation Approach*

To address the deficiencies of the RCM approach, a revised synthesis to access **1** was initiated. In this second generation synthesis rather than targeting **1** itself, an intermediate utilized in the Whiting synthesis would be the initial focus.[10] Although this approach would be expected to suffer the same low yields for ring closure observed by Whiting, if the synthesis leading up to this intermediate were significantly streamlined, then sufficient quantities of the natural product could still be accessed. With this in mind,

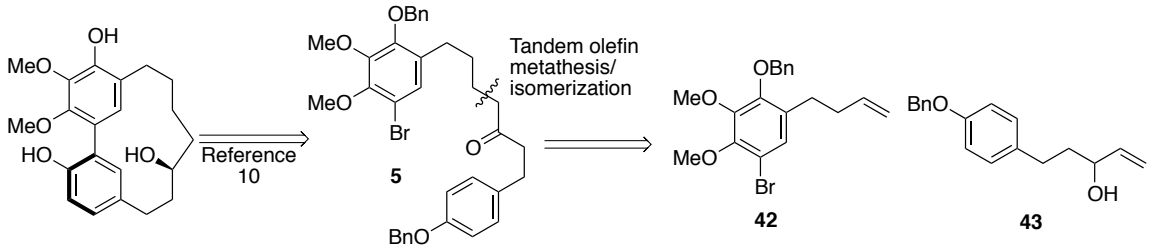


**Figure 4.5.** Retrosynthesis of myricanol using a tandem olefin metathesis/isomerization protocol.

it was determined that bromide **5**, used as a precursor by Whiting, could be potentially accessed through a tandem olefin metathesis/isomerization process (Figure 4.5). The required olefins **42** and **43** could be assembled through elaboration of intermediates from the first generation approach.

The conversion of benzaldehyde **26** to **42** is shown in Scheme 4.5. Addition of the allyl group under aqueous Barbier conditions[26] revealed **44** in excellent yield despite the potential for protodehalogenation.[27] Lewis acid-catalyzed reduction of the benzylic alcohol with triethylsilane yielded **42** in 87%.

The synthesis of allyl alcohol **43** began with protection of the phenol **13** with benzyl bromide (Scheme 4.5). The resulting ester **45** was converted to the corresponding

**Scheme 4.5.** Synthesis of olefins **42** and **43**.[a]

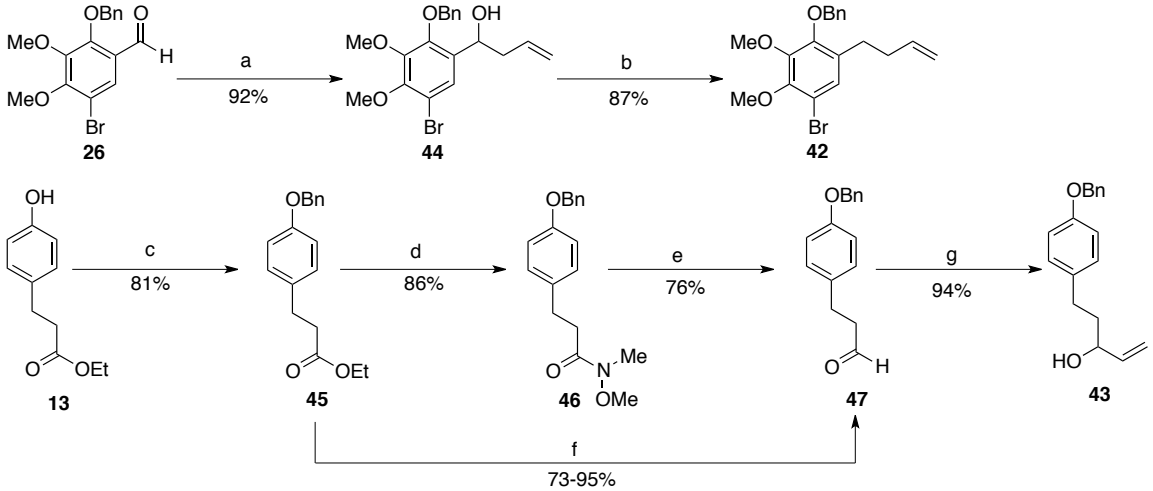


[a] Reagents and conditions: a) allyl bromide (2.0 equiv), Zn (2.0 equiv), THF/$NH_4Cl_{(aq.)}$ (1:2), RT, 6 h; b) $Et_3SiH$ (2.2 equiv), $FeCl_3$ (0.1 equiv), $MeNO_2$, RT, 4 h; c) BnBr (1.1 equiv), $K_2CO_3$ (3.0 equiv), DMF, RT, 16 h; d) (MeO)(Me)$NH_2Cl$ (1.55 equiv), $^i$PrMgCl (3.0 equiv), THF, -10 °C, 30 min; e)$LiAlH_4$ (2.0 equiv), THF, -78 °C, 3 h; f)$^i$$Bu_2AlH$ (1.05 equv), PhMe, -78 °C, 2 h; g)$CH_2$=CHMgBr (2.0 equiv), THF, 0 °C, 5 h

Weinreb amide **51** by again employing (MeO)(Me)NMgCl generated in situ with isopropyl magnesium chloride and *N*,*O*-dimethylhydroxylamine. Reduction with $LiAH_4$ at -78 °C gave **47** in 76% yield. Alternatively this two-step process could be replaced with a high-yielding selective reduction directly from **45** using DIBAl-H, however this reaction was found to be highly dependent upon the quality of commercially available DIBAl-H solution. Exposure of **47** to vinyl magnesium bromide furnished the allyl alcohol **43**.

With **42** and **43** available in only 5 and 4 steps, respectively, from commercially available material, all that remained for a formal synthesis of **1** was the proposed tandem olefin metathesis/isomerization process. Cross-metathesis of **42** and **43** with the **G-II** catalyst in refluxing $CH_2Cl_2$ produced intermediate **48**, which underwent rapid isomerization to enol **49** that in turn tautomerized to the ketone **5** (Scheme 4.6). In addition to **5**, products from the homocoupling of **42** and isomerization of **43** were also isolated from the reaction mixture resulting in the disappointingly low 23% yield for the reaction. However, the synthesis of **5** does represent a formal synthesis of **1**. This streamlined approach to **46** was accomplished in only 9 total steps (6 longest linear sequence) in 10% overall yield, whereas previously, Whiting *et. al.* arrived at this intermediate in 2% yield over 14 total steps (10 longest linear sequence). Unfortunately,

**Scheme 4.6.** Tandem olefin metathesis/isomerization process to access **46**.[a]

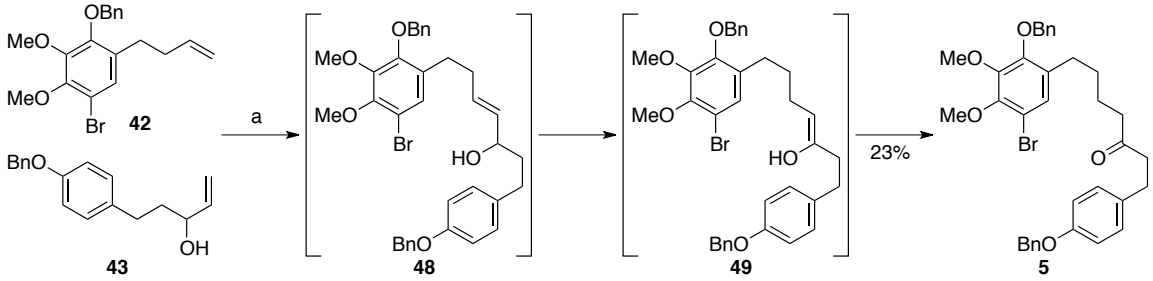


[a] Reagents and conditions: a) **G-II** (0.05 equiv), $CH_2Cl_2$, 40 °C, 16 h.

**Scheme 4.7.** Syntheses dibenzyl myricanone.[a]

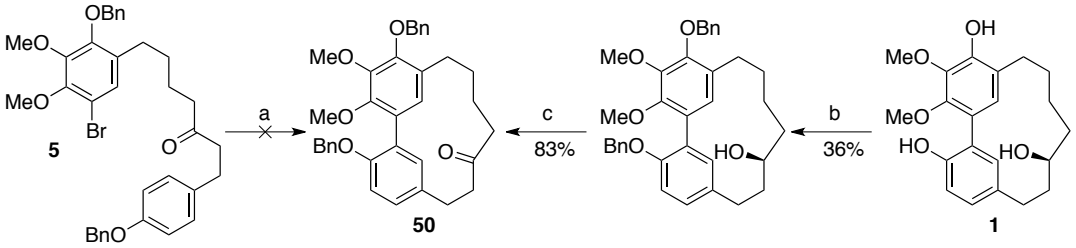


[a] Reagents and conditions: a) hν (254 nm), KOH (6.9 equiv), EtOH, RT, 30 min; b) BnBr (2.0 equiv), $K_2CO_3$ (6.0 equiv), DMF, RT, 16 h; c) PCC (2.0 equiv), $CH_2Cl_2$, RT, 2 h.

attempts to induce radical cyclization via photochemical fragmentation of the aryl bromide bond using the conditions reported by Whiting yielded a very complex reaction mixture (Scheme 4.7). Isolation of the peak with a similar retention time to an authentic sample of dibenzyl myricanone (**50**), using preparative HPLC, resulted in a trace amount of compound that clearly did not correspond to **50** by $^1$H NMR.

*Third Generation Approach*

In a final attempt to complete the synthesis of **1**, a union of the first two generations strategies was conceived. Based upon the success of the palladium-catalyzed biaryl coupling in the first generation synthesis, it was envisioned that an intramolecular Suzuki-Miyaura reaction could be utilized to induce macrocyclization (Figure 4.6). A similar approach was recently utilized in the latest synthesis of myricanol that was reported while these studies were underway.[8] However, in this reported synthesis an achiral ketone was used as the Suzuki-Miyaura substrate forcing the use of chiral HPLC

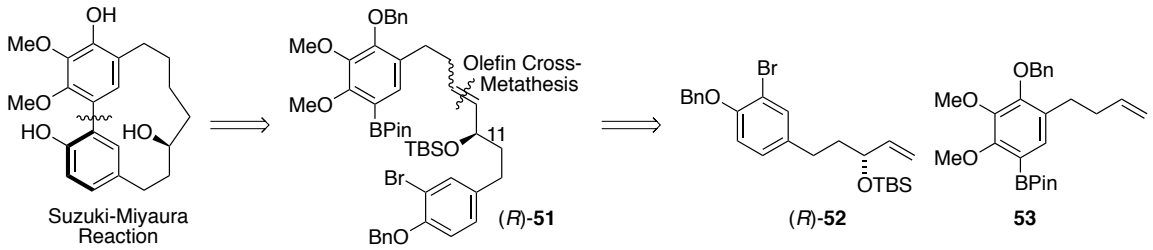


**Figure 4.6**. Retrosynthesis of myricanol utlizing an intramolecular Suzuki-Miyaura reaction.

**Scheme 4.8.** Synthesis and enzymatic resolution of allyl alcohol **56**.[a]

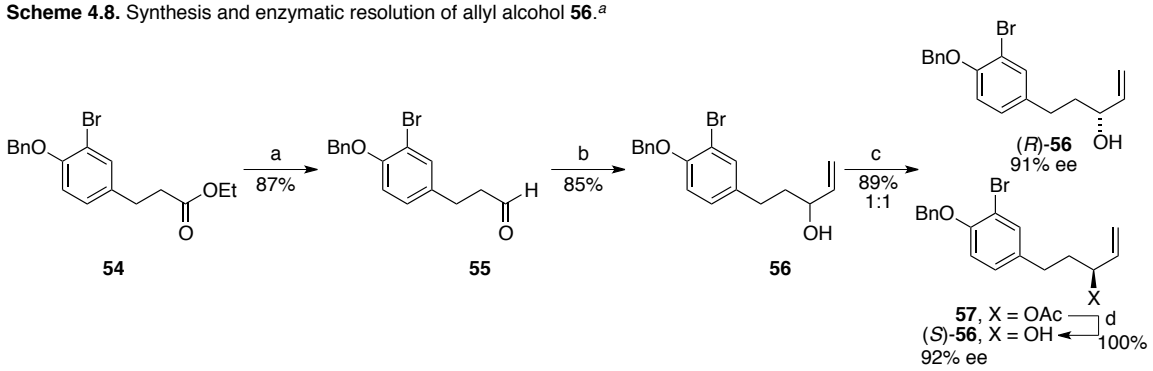


[a] Reagents and conditions: a) $(^{i}Bu)_2AlH$ (1.0 equiv), PhMe, -78 °C; b) $CH_2$=CHMgBr (1.5 equiv), THF, 0 °C c) Amano lipase (50 w/w%), vinyl acetate (1.5 equiv), 4 Å mol. sieves, $^{i}Pr_2O$, RT, 24 h, 57 (44%), 56 (45%); d) $K_2CO_3$ (3.0 equiv), MeOH, 0 °C.

to access enantiopure **1**. Potentially, if a single enantiomer of **51** were employed, the existing C11 stereochemistry might influence the axial chirality of the forming aryl-aryl bond. To test this possibility, the requisite linear precursors would be derived from an olefin cross-metathesis similar to that used in during the second generation approach, employing both enantiomer of the protected allyl alcohol **52** and the pinacol borane **53.**

The synthesis of the allyl alcohols **56** began with the careful reduction of ethyl ester **54** to the aldehyde **55** in 87% yield (Scheme 4.8). Subsequent treatment with vinyl magnesium bromide occurred in 85% yield to furnish the racemic allyl alcohol **56**. Because terminal allyl alcohols are known substrates for lipases,[28] **56** represented an excellent opportunity to separate the two enantiomers through the use of biocatalysis. Thus an amano lipase from *Pseudomonas fluorescens* was used to selectively acetylate the *S*-enantiomer of **56** to provide a ~1:1 mixture (*R*)-**56** and **57**, which was easily deacetylated with methanolic $K_2CO_3$ to produce (*S*)-**56**. Both allyl alcohols were >90% ee as measured by chiral HPLC. The stereochemistry of (*R*)-**56** was determined using Mosher ester analysis[29] and was consistent with results observed with 5-phenylpent-1-en-3-ol.[30]

By providing a separable mixture of substrates containing opposite stereochemical configuration at C11, this enzymatic resolution could potentially allow for the synthesis of both enantiomers of **1** without the need for chiral HPLC separation. If this approach were successful, (*R*)-**56** could be elaborated into (+)-**1**, whereas **57** would provide its enantiomer. However, only one enantiomer of **1** is able to significantly reduce tau protein levels.[8] Therefore, to provide a synthetic route to a specific enantiomer of **1**, a process to interconvert (*R*)-**56** and **57** was developed (Scheme 4.9). Employing AcOH, $PPh_3$, and DIAD, the alcohol of (*R*)-**56** was converted to the acetate with inversion of stereochemistry to provide **57** in 61% yield. The C11 stereocenter in (*S*)-**56** was similarly inverted and the intermediate ester was cleaved to reveal (*R*)-**56**. The use of the more acidic 4-nitrobenzoic acid in the Mitsunobu reaction improved the efficiency of the inversion process to 79% over the two steps. Both (*R*)-**56** and **57** produced through these means were spectroscopically identical to the products of the enzymatic resolution and possessed similar levels of enantiopurity as measured by their optical rotations. Finally, the allyl alcohols were protected as silyl ethers to prevent unwanted isomerization during the subsequent cross-metathesis reaction.

**Scheme 4.9.** Interconversion and protection of allyl alcohols.[a]

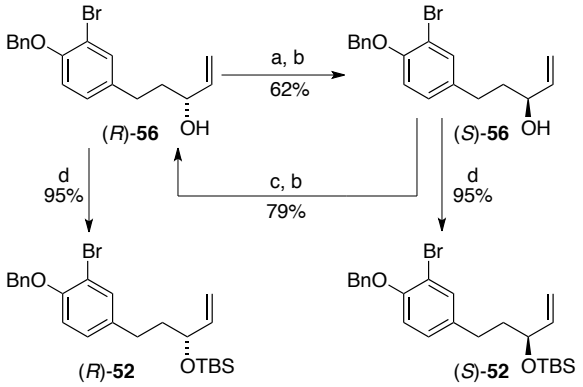


[a] Reagents and conditions: a) AcOH (1.2 equiv), $PPh_3$ (1.2 equiv), DIAD (1.2 equiv), THF, RT, 16 h; b) $K_2CO_3$ (3.0 equiv), MeOH, 0 °C; c) 4-$NO_2$-$C_6H_4CO_2H$ (1.2 equiv), $PPh_3$ (1.2 equiv), DIAD(1.2 equiv), THF, RT, 16 h; d)TBSOTf (1.0 equiv), $Et_3N$ (1.6 equiv), $CH_2Cl_2$, -78 °C, 1 h.

Prior to this cross-metathesis, a procedure for the borylation of **47** needed to be developed. The success of the palladium-catalyzed borylation of **16** (Page 90, Scheme 4.2) employing the Buchwald catalyst system suggested a similar transformation could be

performed on **42**.[21] However these conditions resulted in a complex mixture due to competing hydroboration of the terminal olefin. Significantly cleaner reaction mixtures were observed when bis(pinacolato)diboron ($B_2Pin_2$) was used as the boron source. However, neither $Pd_2dba_3$/XPhos[31] nor $PdCl_2(dppf)$[19] catalyst systems were able to fully convert the starting material. Fortunately, a catalyst system composed of $Pd(dba)_2$ and $PCy_3$, was found to convert **42** to **53** in an acceptable 66% yield (Scheme 4.10).

With gram-scale access to (*R*)-**52**, (*S*)-**52**, and **53**, their union through olefin-metathesis was investigated (Scheme 4.10). The coupling of **52** and **53** proceeded smoothly with **G-II**, to provide the two enantiomers of the linear diarylheptenoid **51** in good yields (79-88%). Cross metathesis of **53** and **57** was also briefly explored, however it was found to be less efficient and produced **58** in only 50% yield. The difference in reactivity between **52** and **57** suggests that **52** is a type II olefin, whereas **57** is type I.[32]

**Scheme 4.10.** Synthesis of linear diarylheptenaoids.[a]

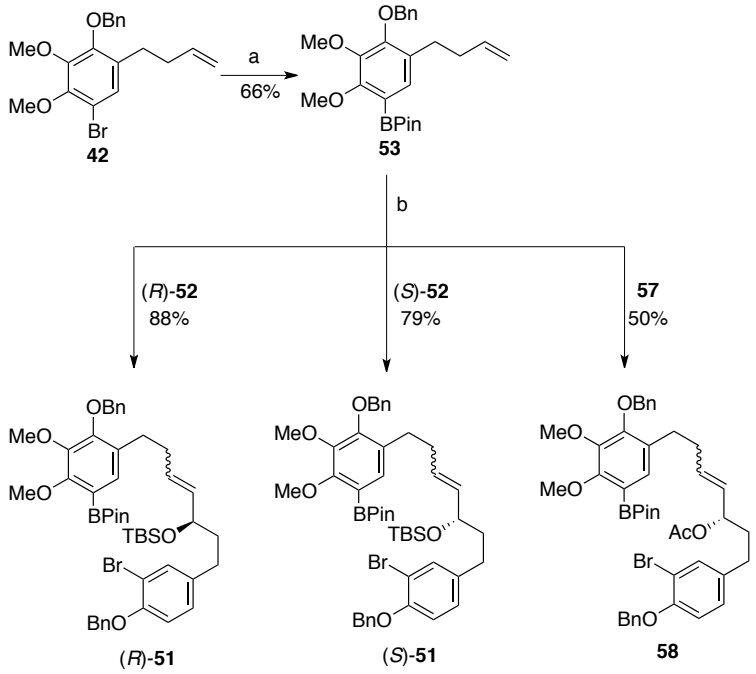


[a] Reagents and conditions: a) $B_2Pin_2$ (1.2 equiv), KOAc (1.5 equiv), $Pd(dba)_2$ (0.03 equiv), $PCy_3$ (0.072 equiv), 1,4-diox., 80 °C, 24 h; b) **G-II** (0.10 equiv), $CH_2Cl_2$, 40 °C, 24 h.

Having synthesized both enantiomers of the bromoborane **51**, investigations into their macrocyclization through Suzuki-Miyaura reactions were possible. Based upon results from similarly strained cyclic peptides and the recent synthesis of myricanone,[8,33-

[35] (*R*)-**51** was exposed to $PdCl_2(dppf)\cdot CH_2Cl_2$ and aqueous $K_2CO_3$ in toluene at 90 °C over 24 hours. With these initial conditions, (*R*)-**51** cyclized to (*R*)-**59** in 18% yield, providing the first evidence that an intramolecular Suzuki-Miyaura reaction would lead to a successful synthesis of **1**.

To explore whether this initial result could be improved, optimization studies were performed by modifying the solvent, concentration, base, and reaction time (Table 4.3). The yields of (*R*)-**59** were slightly improved to 20% by switching from toluene to 1,4-dioxane, however trace amounts of products from the protodehalogenation of (*R*)-**51** were still observed by HRMS of the crude reaction mixtures. Removal of $H_2O$ as the most likely source of protons from the reaction mixture, unfortunately, prevented

**Table 4.3.** Intramolecular Suzuki-Miyaura Optimization Studies.

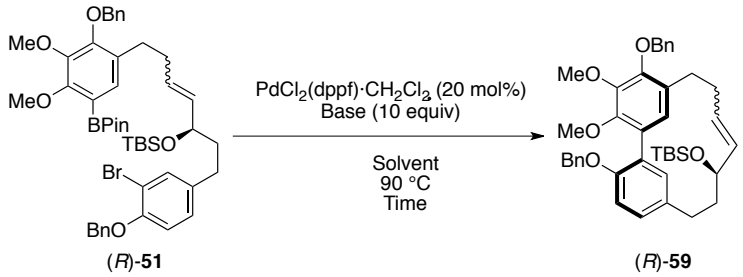


(*R*)-**51** (*R*)-**59**

| Entry | Solvent | Conc (mM) | Base | Time (h) | Yield (%)[a] |
|---|---|---|---|---|---|
| 1 | Tol./$H_2O$ (30:1) | 20 | $K_2CO_3$ | 24 | 18 |
| 2 | Diox./$H_2O$ (30:1) | 20 | $K_2CO_3$ | 24 | 20 |
| 3 | Diox. | 20 | $K_2CO_3$ | 24 | 5 (32)[b] |
| 4 | Diox./$H_2O$ (30:1) | 20 | $K_3PO_4$ | 24 | 26 |
| 5 | Diox./$H_2O$ (30:1) | 2 | $K_3PO_4$ | 24 | 6 |
| 6 | Diox./$H_2O$ (30:1) | 200 | $K_3PO_4$ | 24 | 12 |
| 7 | Diox./$H_2O$ (30:1) | 20 | $K_3PO_4$ | 12 | 23 |
| 8 | Diox./$H_2O$ (30:1) | 20 | $K_3PO_4$ | 48 | 15 |
| 9 | Diox./$H_2O$ (30:1) | 20 | $K_3PO_4$ | 24 | 25[c] |

[a] Isolated yields. [b] BRSM. [c] (*S*)-**51** used as substrate.

hydrolysis of the pinacol ester resulting in recovery of unreacted starting material and significantly reduced yields. Switching to, more basic $K_3PO_4$, did further increase the yields to 26%, although neither increasing nor decreasing the reaction concentration or time had a positive effect (Table 4.3 Entries 5-8). These optimized reaction conditions produced similar yields when applied to (*S*)-**52 (**Entry 9). In all, the reactions carried out during this optimization study, **59** was the only product isolated, with no evidence of intermolecular reactions occurring. Furthermore, the $^{1}H$ and $^{13}C$ NMR spectra indicated the products were a mixture of isomers, however whether these were atropisomers or olefin isomers could not be determined at this point.

All that remained for the synthesis of (+)-**1** and (-)-**1**, was the appropriate manipulation of (*R*)-**59** and (*S*)-**59**, respectively (Scheme 4.11). Simultaneous reduction of the olefin and dihydrogenolysis of the benzyl protecting groups with Pd/C revealed the silyl-protected myricanol **60** in good overall yield (71-78%). The removal of the *tert*-butyldimethyl silyl (TBS) protecting group, unfortunately, proved more troublesome than anticipated. Attempts to desilate (*S*)-**60** with TBAF or CsF as fluoride sources produced no reactions even at elevated temperatures and extended reaction times. The use of $Et_3N{\cdot}3HF$ did lead to some isolated product (40%) however after 1 week, the reaction had yet to reach full conversion.

**Scheme 4.11**. Completetion of the total synthesis of myricanol.[a]

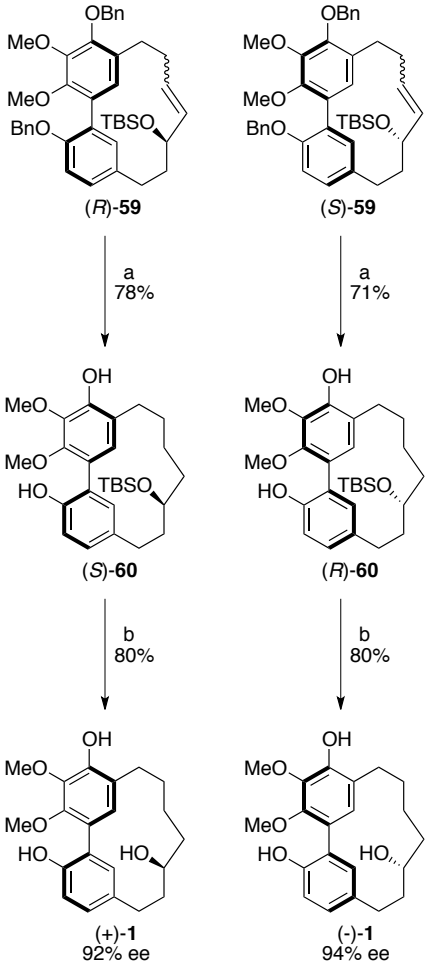


[a] Reagents and conditions: a) 10% Pd/C (20 w/w%), $H_2$ (balloon); b) 1% HCl, EtOH

Fortunately removal of the silyl-protecting group from (*S*)-**60** and (*R*)-**60** with aqueous HCl in ethanol revealed (+)-**1** and (-)-**1** with good levels of enantiopurity (e.e. = 92% for (+)-**1**; e.e. = 94% for (-)-**1**) as determined by chiral HPLC. These levels are significantly higher than that of **1** isolated from *M. cerifera* (Figure 4.7). The two compounds were spectroscopically identical ($^{1}$H NMR, $^{13}$C NMR and HRMS) to each other and to the natural sample. Furthermore, they were isolated as a single atropisomer suggesting that the C11 stereocenter was able to completely control the axial chirality of the forming aryl-aryl bond during the Suzuki-Miyaura cyclization. Alternatively, the barrier of rotation about the aryl-aryl bond may be lower than expected and the isolated atropisomers are the thermodynamically more stable products.

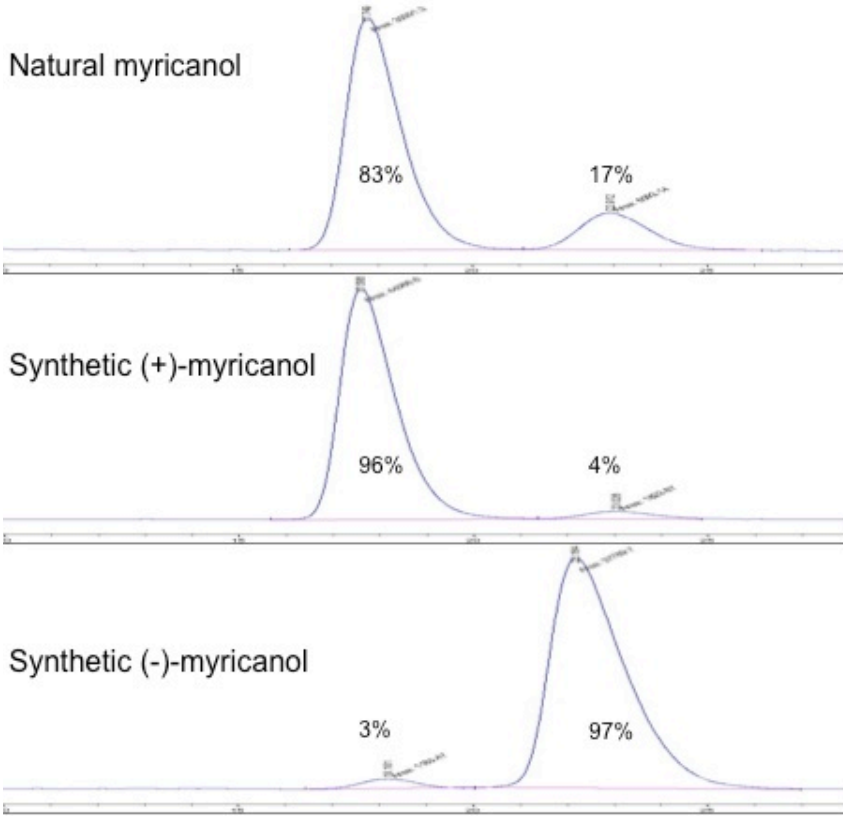


**Figure 4.7.** Chiral HPLC chromatograms demonstrating increased enantiopurity of synthetic **1** compared to natural **1**.

*Conclusions*

The application of strategies developed from two unsuccessful approaches has now resulted in the first asymmetric synthesis of either enantiomer of **1**. In addition to eliminating the need for chiral HPLC to separate the enantiomers, this approach represents a significant improvement over the other reported syntheses of **1** (Table 4.4). Although the step count was similar to that of Whiting's original synthesis and slightly greater than the more recent synthesis by Martin, the overall yield was markedly improved. This can largely be attributed the fact that all but two steps of this synthesis produced products in greater than 75% yield.

This successful synthesis of both enantiomers of **1** will prove useful in determining its biological target by providing substantial material for more extensive studies. Furthermore, this synthetic route should prove amenable to the synthesis of other naturally occurring *meta*,*meta*-bridged diarylheptanoids.[36-42] Many of these compounds have shown a diverse range of biological activities, some of which may be related to the activity of **1**. The synthesis of these and non-naturally occurring analogues will be useful in elucidating SAR, which in turn could provide useful probes for studying the role of tau protein in neurodegenerative tauopathies such as AD.

**Table 4.4**. Comparison of Total Myricanol Syntheses.

| | Current | | Martin[8] | Whiting[10] |
|---|---|---|---|---|
| | (+)-**1** | (-)-**1** | (±)-**1** | (±)-**1** |
| Total step count[a] | 16 | 17 | 12 | 18 |
| Longest linear sequence[a] | 10 | 11 | 9 | 14 |
| Overall yield[a] | 2.7% | 2.1% | 0.63% | ≤0.12%[b] |
| Source of enantioenrichment | enzymatic resolution | enzymatic resolution | chiral HPLC | none |

[a]Yields and step counts from commercially available materials. [b]Yields not reported for final deprotection steps.

**References:**


(1) Fang, L.; Gou, S. H.; Fang, X. B.; Cheng, L.; Fleck, C. Current progresses of novel natural products and their derivatives/analogs as anti-Alzheimer candidates: An update. *Mini-Rev. Med. Chem.* **2013**, *13*, 870.

(2) Calcul, L.; Zhang, B.; Jinwal, U. K.; Dickey, C. A.; Baker, B. J. Natural products as a rich source of tau-targeting drugs for Alzheimer's disease. *Future Med. Chem.* **2012**, *4*, 1751.

(3) Jones, J. R.; Lebar, M. D.; Jinwal, U. K.; Abisambra, J. F.; Koren, J.; Blair, L.; O'Leary, J. C.; Davey, Z.; Trotter, J.; Johnson, A. G.; Weeber, E.; Eckman, C. B.; Baker, B. J.; Dickey, C. A. The diarylheptanoid (+)-a*R*,11*S*-myricanol and two flavones from bayberry (*Myrica cerifera*) destabilize the microtubule-associated protein tau. *J. Nat. Prod.* **2011**, *74*, 38.

(4) Begley, M. J.; Campbell, R. V.; Crombie, L.; Tuck, B.; Whiting, D. A. Constitution and absolute configuration of *meta,meta*-bridged, strained biphenyls from *Myrica nagi*: X-ray analysis of 16-bromomyricanol. *J. Chem. Soc. C* **1971**, 3634.

(5) Inoue, T.; Arai, Y.; Nagai, M. Diarylheptanoids in the bark of *Myrica rubra*. *Yakugaku Zasshi* **1984**, *104*, 37.

(6) Joshi, B. S.; Pelletier, S. W.; Newton, M. G.; Lee, D.; McGaughey, G. B.; Puar, M. S. Extensive 1D, 2D NMR spectra of some [7.0]metacyclophanes and X-ray analysis of (±)-myricanol. *J. Nat. Prod.* **1996**, *59*, 759.

(7) Sun, D. W.; Zhao, Z. C.; Wong, H.; Foo, L. Y. Tannins and other phenolics from *Myrica esculenta* bark. *Phytochemistry* **1988**, *27*, 579.

(8) Martin, M. D.; Calcul, L.; Smith, C.; Jinwal, U. K.; Fontaine, S. N.; Darling, A.; Seeley, K.; Wojtas, L.; Narayan, M.; Gestwicki, J. E.; Smith, G. R.; Reitz, A. B.; Baker, B. J.; Dickey, C. A. Synthesis, stereochemical analysis, and derivatization of myricanol provide new probes that promote autophagic tau clearance. *ACS Chem. Biol.* **2015**, *10*, 1099.

(9) Henleysmith, P.; Whiting, D. A.; Wood, A. F. Methods for the construction of linear 1,7-diarylheptanoids: Synthesis of di-*O*-methylcentrolobol and precursors (synthetic and biosynthetic) to the *meta,meta*-bridged biphenyls myricanol and myricanone. *J. Chem. Soc. Perk., Trans. 1* **1980**, 614.

(10) Whiting, D. A.; Wood, A. F. Total syntheses of the *meta,meta*-bridged biphenyls (±)-myricanol and myricanone, and of an isomeric biphenyl ether, a 14-oxa-[7,1]-metapara-cyclophane. *J. Chem. Soc. Perk., Trans. 1* **1980**, 623.

(11) Semmelhack, M. F.; Ryono, L. S. Nickel-promoted synthesis of cyclic biphenyls—total synthesis of alnusone dimethyl ether. *J. Am. Chem. Soc.* **1975**, *97*, 3873.

(12) Gulder, T.; Baran, P. S. Strained cyclophane natural products: Macrocyclization at its limits. *Nat. Prod. Rep.* **2012**, *29*, 899.

(13) Gradillas, A.; Perez-Castells, J. Macrocyclization by ring-closing metathesis in the total synthesis of natural products: Reaction conditions and limitations. *Angew. Chem. Int. Ed.* **2006**, *45*, 6086.

(14) Hassan, H. M. Recent applications of ring-closing metathesis in the synthesis of lactams and macrolactams. *Chem. Comm.* **2010**, *46*, 9100.

(15) Chan, B. K.; Ciufolini, M. A. Total synthesis of streptonigrone. *J. Org. Chem.* **2007**, *72*, 8489.

(16) Dandepally, S. R.; Williams, A. L. Liebeskind-Srogl cross coupling mediated synthesis of verbenachalcone. *Tetrahedron Lett*. **2010**, *51*, 5753.

(17) Williams, J. M.; Jobson, R. B.; Yasuda, N.; Marchesini, G.; Dolling, U. H.; Grabowski, E. J. J. A new general method for preparation of *N*-methoxy-*N*-methylamides–application in direct conversion of an ester to a ketone. *Tetrahedron Lett*. **1995**, *36*, 5461.

(18) De Luca, L.; Giacomelli, G.; Taddei, M. An easy and convenient synthesis of Weinreb amides and hydroxamates. *J. Org. Chem*. **2001**, *66*, 2534.

(19) Ishiyama, T.; Murata, M.; Miyaura, N. Palladium(0)-catalyzed cross-coupling reaction of alkoxydiboron with haloarenes–a direct procedure for arylboronic esters. *J. Org. Chem*. **1995**, *60*, 7508.

(20) Ishiyama, T.; Ishida, K.; Miyaura, N. Synthesis of pinacol arylboronates via cross-coupling reaction of bis(pinacolato)diboron with chloroarenes catalyzed by palladium(0)-tricyclohexylphosphine complexes. *Tetrahedron* **2001**, *57*, 9813.

(21) Billingsley, K. L.; Buchwald, S. L. An improved system for the palladium-catalyzed borylation of aryl halides with pinacol borane. *J. Org. Chem*. **2008**, *73*, 5589.

(22) Barder, T. E.; Walker, S. D.; Martinelli, J. R.; Buchwald, S. L. Catalysts for Suzuki-Miyaura coupling processes: Scope and studies of the effect of ligand structure. *J. Am. Chem. Soc*. **2005**, *127*, 4685.

(23) Bryant, V. C.; Kumar, G. D. K.; Nyong, A. M.; Natarajan, A. Synthesis and evaluation of macrocyclic diarylether heptanoid natural products and their analogs. *Bioorg. Med. Chem. Lett*. **2012**, *22*, 245.

(24) Furstner, A.; Thiel, O. R.; Ackermann, L. Exploiting the reversibility of olefin metathesis: Syntheses of macrocyclic trisubstituted alkenes and (*R*,*R*)-(-)-pyrenophorin. *Org. Lett.* **2001**, *3*, 449.

(25) Anslyn, E. V.; Dougherty, D. A. *Modern Physical Organic Chemistry*; University Science: Sausalito, CA, 2006.

(26) Einhorn, C.; Luche, J. L. Selective allylation of carbonyl–compounds in aqueous–media *J. Organomet. Chem.* **1987**, *322*, 177.

(27) Hekmatshoar, R.; Sajadi, S.; Heravi, M. M. Reductive dehalogenation of arylhalides and alkylhalides with zinc in THF saturated aqueous ammonium chloride. *J. Chin. Chem. Soc.* **2008**, *55*, 616.

(28) Patel, R. N. *Stereoselective Biocatalysis*; M. Dekker: New York, 2000.

(29) Hoye, T. R.; Jeffrey, C. S.; Shao, F. Mosher ester analysis for the determination of absolute configuration of stereogenic (chiral) carbinol carbons. *Nat. Protoc.* **2007**, *2*, 2451.

(30) Itoh, T.; Nishimura, Y.; Ouchi, N.; Hayase, S. 1-Butyl-2,3-dimethylimidazolium tetrafluoroborate: the most desirable ionic liquid solvent for recycling use of enzyme in lipase-catalyzed transesterification using vinyl acetate as acyl donor. *J. Mol. Catal. B-Enzym.* **2003**, *26*, 41.

(31) Billingsley, K. L.; Barder, T. E.; Buchwald, S. L. Palladium-catalyzed borylation of aryl chlorides: Scope, applications, and computational studies. *Angew. Chem. Int. Ed.* **2007**, *46*, 5359.

(32) Chatterjee, A. K.; Choi, T. L.; Sanders, D. P.; Grubbs, R. H. A general model for selectivity in olefin cross metathesis. *J. Am. Chem. Soc.* **2003**, *125*, 11360.

(33) Roberts, T. C.; Smith, P. A.; Cirz, R. T.; Romesberg, F. E. Structural and initial biological analysis of synthetic arylomycin A(2). *J. Am. Chem. Soc.* **2007**, *129*, 15830.

(34) Shinohara, T.; Deng, H. B.; Snapper, M. L.; Hoveyda, A. H. Isocomplestatin: Total synthesis and stereochemical revision. *J. Am. Chem. Soc.* **2005**, *127*, 7334.

(35) Jia, Y. X.; Bois-Choussy, M.; Zhu, J. P. Synthesis of diastereomers of complestatin and chloropeptin I: Substrate–dependent atropstereoselectivity of the intramolecular Suzuki–Miyaura reaction. *Angew. Chem. Int. Ed.* **2008**, *47*, 4167.

(36) Takeda, Y.; Fujita, T.; Shingu, T.; Ogimi, C. Studies on the bacterial gall of *Myrica rubra*: Isolation of a new [7,0]-metacyclophan from the gall and DL-β-phenylactic acid from the culture of gall-forming bacteria. *Chem. Pharm. Bull.* **1987**, *35*, 2569.

(37) Nagumo, S.; Kaji, N.; Inoue, T.; Nagai, M. Studies on the constituents of aceraceae plants: 2 types of cyclic diarylheptanoid from acer–nikoense. *Chem. Pharm. Bull* .**1993**, *41*, 1255.

(38) Liu, J. X.; Di, D. L.; Huang, X. Y.; Li, C. Two new diarylheptanoids from the pericarps of *Juglans regia* L. *Chin. Chem. Lett.* **2007**, *18*, 943.

(39) Liu, J. X.; Di, D. L.; Wei, X. N.; Han, Y. Cytotoxic diarylheptanoids from the pericarps of walnuts (*Juglans regia*). *Planta medica* **2008**, *74*, 754.

(40) Yang, H.; Sung, S. H.; Kim, J.; Kim, Y. C. Neuroprotective diarylheptanoids from the leaves and twigs of *Juglans sinensis* against glutamate-induced toxicity in HT22 cells. *Planta medica* **2011**, *77*, 841.

(41) Yoshimura, M.; Yamakami, S.; Amakura, Y.; Yoshida, T. Diarylheptanoid sulfates and related compounds from *Myrica rubra* bark. *J. Nat. Prod.* **2012**, *75*, 1798.

(42) Yao, D. L.; Zhang, C. H.; Luo, J.; Jin, M.; Zheng, M. S.; Cui, J. M.; Son, J. K.; Li, G. Chemical constituents from the leaves of *Juglans mandshurica*. *Arch. Pharm. Res.* **2014,** *38*, 480.

## V. Conclusions

Through the use of semi-synthesis to modify the chemical structure of salvinorin A, the preceding studies have shed additional light upon the structure-activity relationships of this fascinating natural product. Additionally, the efforts toward the total synthesis of myricanol have culminated in the first enantioselective route to both enantiomers of the molecule. As is the case in nearly all scientific enquiries, these successes are likely to promote further investigations.

By developing new chemical processes to selectively modify the furan ring of salvinorin A, over 50 novel compounds were synthesized and evaluated at the KOR. These structure-activity relationship studies established that the furan ring binds to a sterically restricted portion of the binding pocket and that an electron rich ring is preferred for optimal receptor activation. Additionally, several compounds were shown to that attenuate drug seeking behavior in an animal model of relapse without inducing sedation (Figure 1). Preliminary studies with 16-bromosalvinorin A also suggested that these compounds are not depressive. Furthermore, studies with rhesus macaques indicate that these results may translate to non-human primates. Because these ligands appear activate the KOR in a way that does not produce the sedation and depression induced by

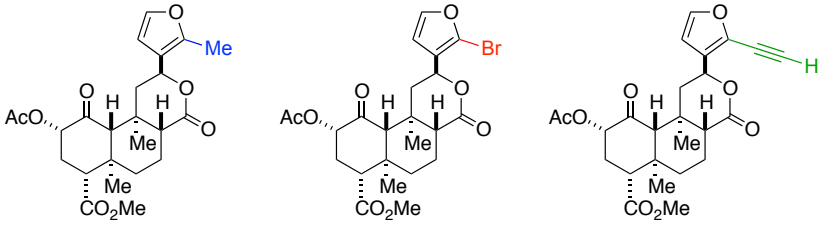


**Figure 1.** C16-substitued derivatives of salvinorin A.

traditional KOR agonists, they will be extremely useful in identifying the signal transduction pathways that produce these side effects.

The investigations aimed at improving the selectivity and potency of herkinorin were also quite successful. Guided by X-ray crystal structures, the introduction of an additional degree of unsaturation to the A-ring of herkinorin was shown to cause a drastic increase in potency at the MOR and eliminate all activity at the KOR. A more detailed exploration of this effect using two parallel series of analogues identified that this increase in potency was not the result of a different binding site. This SAR was also used to design the most potent neoclerodane-based MOR agonist to date, containing a phenol moiety on the phenyl ring. Further analogue development using this SAR will be particularly important in designing ligands with improved PK properties. Of particular interest will be the introduction of a halogen to the phenol ring, which could potentially reduce its $pK_a$ such that it will be ionized at physiological pH. This could potentially improve the water solubility of the compound, but may also negatively effect brain penetration.(*1*) Additionally, further investigations into the in vivo characteristics of these ligands will be crucial since preliminary results indicate that unlike herkinorin, the modified derivative is not peripherally restricted.

Finally, despite several failed approaches to synthesize the cyclophane natural product, an enantioselective route to myricanol has also been accomplished. In addition

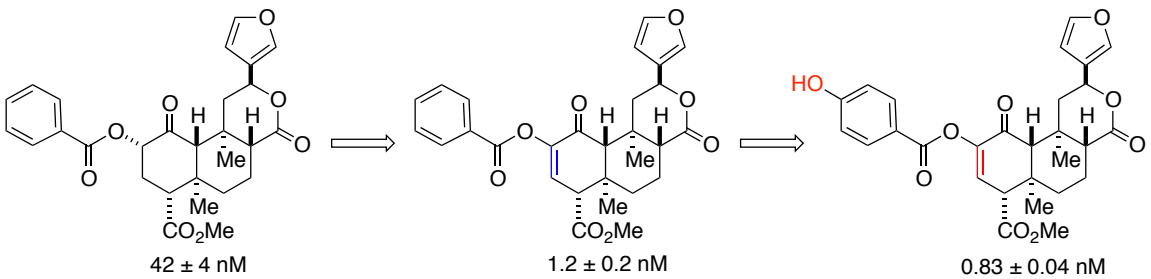


**Figure 2.** Improving MOR potencies through the modification of herkinorin's structure.

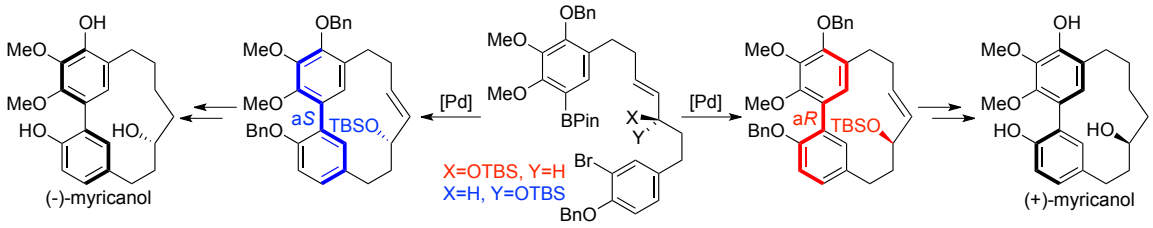


**Figure 3.** Atropselective synthesis of both enantiomers of myricanol.

to being the highest yielding synthesis to date, the difficult macrocyclization event was accomplished with complete substrate control of axial chirality leading to only a single atropisomer. This route will provide the material necessary for more extensive mechanism of action studies and should prove amenable to the synthesis of other natural and unnatural *meta*,*meta*-bridged diarylheptanoid products. Synthetic access to these compounds will be useful in determining how myricanol induces tau degradation, which in turn could assist in identifying a much-needed treatment option for Alzheimer's Disease.

**References:**

(1) Rankovic, Z. CNS drug design: Balancing physicochemical properties for optimal brain exposure. *J. Med. Chem.* **2015**, *58*, 2584.

## VI. Experimentals

**General Experimentals**. All reactions were performed in glassware dried in an oven at 120 °C overnight and cooled under a stream of argon. Solvents were obtained from a dry solvent system that dried solvent by passage through two columns of alumna and degassed by extensive argon sparging. Flash column chromatography (FCC) was performed on silica gel (4-60 μm) from Sorbent Technologies. Reactions and chromatography was monitored by thin-layer chromatography (TLC) on 0.25 mm Analtech GHLF silica gel plates and visualized by UV light (254 nm) and phosphomolybdic or vanillin TLC stain. $^{1}$H and $^{13}$C NMR spectra were acquired on a 500 MHz Bruker AVIII spectrometer equipped with a cryogenically-cooled carbon observe probe or a 400 MHz Bruker AVIIIHD spectrometer. $^{19}$F NMR spectra were acquired on a Bruker 400 AVANCE spectrometer using either fluorobenzene or trifluorotoluene as an internal standard. High resolution mass spectroscopy (HRMS) was performed using a LCT Premier (Micromass Ltd., Manchester UK) time of flight mass spectrometer with an electrospray ion source. Melting points are uncorrected and were measured on a Thomas Hoover Capillary Melting Point Apparatus. HPLC was carried out on a Agilent 1100 series HPLC system with diode array detection at 209 nm on an Agilent Eclipse XDB-C18 column (250 x 10 mm, 5 mm) eluting with 60% MeCN/40% $H_2O$ at 5.0 mL/min. Compounds tested in biological assays were identified as ≥95% pure by HPLC before testing. Commercially available reagents were used directly without further purification. Salvinorin A (**1**) was isolated from *S. divinorum* according to published procedures.[1]

*Experimentals for Chapter II*

Gas chromatography was performed using a Shimadzu QP2010 SE GC fitted with a SHRXI-5MS column (30m x 0.25 mm) with injection temperature set to 260°C and ramping to 320°C over 2 min. Compound **7** was synthesized as reported by Simpson *et. al.*[1] The synthesis of compounds **4**-**5**, **15**, **18**-**64** has been reported.[2,3] Their experimental details are reproduced here for the convenience of the reader.

**General oxime oxidation/cycloaddition reaction.** A solution of the oxime **8** dissolved in MeCN/$H_2O$ (5:1, 50 mM) was treated with a terminal alkyne (5.0 equv). PIFA (1.5 equiv) was added in three portions over 4 hours then stirred overnight. The reaction was concentrated in vacuo and the residue was purified by FCC eluting with 35% EtOAc/Hex.

**General procedure for Table 1**. An oven-dried conical vial was cooled under a stream of argon and charged with a stir bar, **4** (15.0 mg, 29.3 mmol), $Pd_2dba_3$ (1.1 mg, 1.2 mmol), SPhos (1.9 mg, 4.7 mmol), $PhB(OH)_2$ (7.2 mg, 58.7 mmol), and $K_3PO_4$ (18.7 mg, 88.0 mmol). The vial was sealed with a Biotage Reseal cap and flushed with argon for 5 min. Toluene (0.4 mL) was added through the septum and allowed to spin for 5 min. after which the reaction was heated to the indicated temperature for 16 hrs. The reaction was cooled to room temperature and 3.0 mg of 1,10-phenanthroline was added to the reaction, as an internal standard. The mixture was diluted with 1.5 ml of $CH_2Cl_2$ and a portion injected onto a GC-MS. Solvent was removed from the remainder of the solution and diluted to 1 mg/mL with MeCN. The MeCN solution was filtered through a microfilter and a 100 mL portion injected onto a HPLC.

**General Procedure for Suzuki-Miyaura Reaction.** An oven-dried conical vial was cooled under a stream of argon and charged with **4** (60 mg, 0.117 mmol), $Pd_2dba_3$ (4.3 mg, 0.0047 mmol), SPhos (7.7 mg, 0.019 mmol), boronic acid (0.234 mmol), and $K_3PO_4$ (74.7 mg, 0.357 mmol). The vial was sealed with a Biotage Reseal cap and flushed with argon for 5 min before adding toluene (1.6 mL) through the septum. After stirring at room temperature for 5 min., the reaction was heated to 60°C for 16 hrs. The reaction was cooled to room temperature, diluted with EtOAc (2.5 mL) and filtered through a thin pad of silica gel. Solvent was removed *in vacuo* and the residue purified by FCC eluting with 35-45% EtOAc/Pent.

**General Procedure for Sonogashira Reaction.** An oven-dried conical vial was cooled under a stream of argon and charged with **4** (60 mg, 0.117 mmol), $PdCl_2(PPH_3)_2$ (4.1 mg, 0.0059 mmol), and CuI (2.2 mg, 0.012 mmol). The vial was sealed with a Biotage Reseal cap and flushed with argon for 5 min before adding THF (1 mL) and $NEt_3$ (1 mL) through the septum. After stirring at room temperature for 5 min., the terminal alkyne (0.234 mmol) was added and the reaction was heated to 80°C for 16 hrs. The reaction was cooled to room temperature and filtered through Celite, rinsing with EtOAc (70 mL). The filtrate was rinsed with 1 N HCl (~20 mL) and brine (~20 mL). The organic layer was dried over $Na_2SO_4$, decanted and solvent removed *in vacuo*. The residue was purified by FCC eluting with 30-40% EtOAc/Pent.

**General Procedure for reduction.** A solution of the appropriate nitrophenyl/olefin in MeOH/THF (5 mL, 3:2) was treated with Pd/C (10% w/w, 0.10 equiv). The suspension was placed under an atmosphere of $H_2$ by applying a vacuum and backfilling with $H_2$

(3×). After 5 h, the reaction was filtered through a thin pad of Celite and the solvent removed in vacuo. The resulting residue was purified by FCC eluting with EtOAc/Pent.

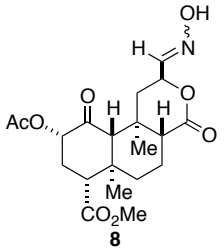

**8**

**(2*S*,4a*R*,6a*R*,7*R*,9*S*,10a*S*,10b*R*)-Methyl 9-acetoxy-2-((hydroxyimino)methyl)-6a,10b-dimethyl-4,10-dioxododecahydro-1*H*-benzo[*f*]isochromene-7-carboxylate**. A solution of **7** (751 mg, 1.90 mmol) in MeOH (30 mL) was treated with $NH_2OH{\cdot}HCl$ (529 mg, 7.62 mmol) and pyridine (1.5 mL, 19.0 mmol). The reaction was heated to reflux for 5 hours then cooled to room temperature. The reaction was concentrated in vacuo and the residue dissolved in EtOAc (25 mL) and $H_2O$ (25 mL). The layers were separated and the aqueous layer extracted with additional EtOAc (2 x 25 mL). The combined organic layers were washed with HCl (2 M, 25 mL), dried over $Na_2SO_4$, and concentrated in vacuo. The residue was purified by FCC eluting with 50% EtoAc/Hex to yield **8** as a 7:2 mixture of *cis*/*trans* isomers. $^1$H NMR (500 MHz, $CDCl_3$) δ 7.58 (s, 1H), 7.42 (d, *J* = 5.71 Hz, 1H), 5.13 (m, 2H), 3.73 (s, 3H), 2.76 (m, 1H), 2.39 (dd, *J* = 5.71, 13.60 Hz, 1H), 2.30 (m, 2H), 2.18 (s, 3H), 2.14 (m, 2H), 2.06 (dd, *J* = 3.15, 11.40 Hz, 1H), 1.78 (m, 1H), 1.60 (m, 3H), 1.40 (s, 3H), 1.10 (s, 3H). $^{13}$C NMR (126 MHz, $CDCl_3$) δ 201.90, 171.55, 170.60, 170.10, 148.94, 75.03, 74.08, 64.05, 53.51, 52.02, 51.09, 42.06, 39.63, 38.04, 35.23, 30.72, 20.61, 18.07, 16.33, 15.55. HRMS calculated for $C_{20}H_{27}NO_8$ $[M+Na]^+$: 432.1634 (calc); 432.1650 (found).

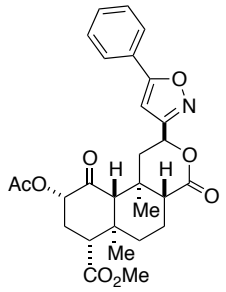

**9**

**(2*S*,4a*R*,6a*R*,7*R*,9*S*,10a*S*,10b*R*)-Methyl 9-acetoxy-6a,10b-dimethyl-4,10-dioxo-2-(5-phenylisoxazol-3-yl)dodecahydro-1*H*-benzo[*f*]isochromene-7-carboxylate.** Prepared from **8** (110 mg, 0.269 mmol) according to general oxime/oxidation/cycloaddition reaction to yield **9** as a white solid (63 mg, 46%). $^{1}$H NMR (500 MHz, $CDCl_3$) δ 7.76 (m, 2H), 7.47 (m, 3H), 6.60 (s, 1H), 5.70 (dd, *J* = 6.19, 10.01 Hz, 1H), 5.18 (dd, *J* = 8.58, 11.66 Hz, 1H), 3.73 (s, 3H), 2.74 (ddd, *J* = 5.61, 12.71, 19.99 Hz, 2H), 2.31 (m, 3H), 2.17 (s, 3H), 2.16 (m, 2H), 1.97 (dd, *J* = 10.16, 13.70 Hz, 1H), 1.79 (dt, *J* = 3.04, 13.27 Hz, 1H), 1.66 (m, 2H), 1.49 (s, 3H), 1.12 (s, 3H). $^{13}$C NMR (126 MHz, $CDCl_3$) δ 201.79, 171.57, 170.91, 170.77, 169.82, 163.86, 130.53, 129.07, 126.98, 125.88, 97.94, 74.89, 71.36, 64.23, 53.48, 51.99, 50.85, 41.99, 40.72, 37.95, 35.44, 30.76, 20.59, 18.13, 16.32, 16.05. HRMS calculated for $C_{28}H_{31}NO_8$: $[M+Na]^+$: 532.1939 (found); 532.1947 (calc).

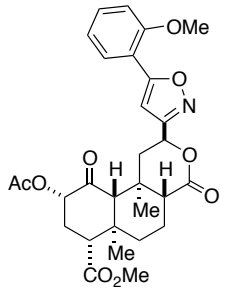

**10**

**(2*S*,4a*R*,6a*R*,7*R*,9*S*,10a*S*,10b*R*)-Methyl 9-acetoxy-2-(5-(2-methoxyphenyl)isoxazol-3-yl)-6a,10b-dimethyl-4,10-dioxododecahydro-1*H*-benzo[*f*]isochromene-7-carboxylate.** Prepared from **8** (50 mg, 0.122 mmol) according to general oxime oxidation/cycloaddition reaction to yield **10** as a white solid (13 mg,

20%). $^1$H NMR (500 MHz, $CDCl_3$) δ 7.96 (dd, *J* = 1.68, 7.79 Hz, 1H), 7.42 (ddd, *J* = 1.72, 7.44, 8.44 Hz, 1H), 7.07 (td, *J* = 0.96, 7.71 Hz, 1H), 7.02 (d, *J* = 8.06 Hz, 1H), 6.86 (s, 1H), 5.71 (dd, *J* = 6.20, 9.92 Hz, 1H), 5.18 (dd, *J* = 8.50, 11.65 Hz, 1H), 3.97 (s, 3H), 3.72 (s, 3H), 2.77 (dd, *J* = 5.09, 11.73 Hz, 1H), 2.69 (dd, *J* = 6.21, 13.81 Hz, 1H), 2.30 (m, 3H), 2.17 (s, 3H), 2.16 (m, 3H), 2.00 (dd, *J* = 10.05, 13.74 Hz, 1H), 1.78 (dt, *J* = 3.04, 13.22 Hz, 1H), 1.66 (m, 1H), 1.49 (s, 3H), 1.12 (s, 3H). $^{13}$C NMR (126 MHz, $CDCl_3$) δ 201.85, 171.62, 171.04, 169.82, 166.88, 163.76, 156.28, 131.55, 127.71, 120.86, 115.95, 111.20, 101.90, 74.90, 71.54, 64.21, 55.56, 53.45, 51.98, 50.76, 41.99, 40.72, 37.93, 35.44, 30.76, 20.59, 18.13, 16.32, 16.11. HRMS calculated for $C_{29}H_{33}NO_9$: $[M+Na]^+$: 562.2039 (found); 562.2053.

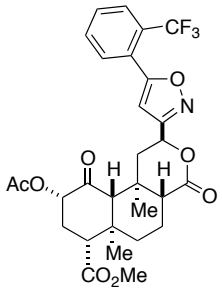

**11**

**(2*S*,4a*R*,6a*R*,7*R*,9*S*,10a*S*,10b*R*)-Methyl 9-acetoxy-6a,10b-dimethyl-4,10-dioxo-2-(5-(2-(trifluoromethyl)phenyl)isoxazol-3-yl)dodecahydro-1*H*-benzo[*f*]isochromene-7-carboxylate.** Prepared from **8** (50 mg, 0.122 mmol) according to general oxime oxidation/cycloaddition reaction to yield **11** as a white solid (30 mg, 43%). $^1$H NMR (500 MHz, $CDCl_3$) δ 7.82 (d, *J* = 7.81 Hz, 1H), 7.75 (d, *J* = 7.70 Hz, 1H), 7.68 (dd, *J* = 4.11, 11.02 Hz, 1H), 7.62 (dd, *J* = 3.92, 11.44 Hz, 1H), 6.62 (s, 1H), 5.73 (dd, *J* = 5.91, 10.61 Hz, 1H), 5.19 (dd, *J* = 8.43, 11.68 Hz, 1H), 3.73 (s, 3H), 2.78 (dd, *J* = 4.99, 11.86 Hz, 1H), 2.71 (dd, *J* = 5.93, 13.75 Hz, 1H), 2.32 (dd, *J* = 4.26, 7.49 Hz, 2H), 2.28 (s, 1H), 2.17 (m, 2H), 2.17 (s, 3H), 1.96 (dd, *J* = 10.78, 13.60 Hz, 1H), 1.80 (dt, *J* =

2.88, 13.21 Hz, 1H), 1.64 (m, 2H), 1.50 (s, 3H), 1.13 (s, 3H). $^{13}$C NMR (126 MHz, $CDCl_3$) δ 201.82, 171.59, 170.64, 169.83, 168.00, 163.48, 132.08, 131.00, 130.45, 128.14 (q, *J* = 31.55 Hz, H), 126.77 (q, *J* = 5.54 Hz, H), 125.79 (q, *J* = 1.84 Hz, H), 123.37 (q, *J* = 273.51 Hz, H), 102.91 (q, *J* = 3.37 Hz, H). 74.90, 71.33, 64.04, 53.45, 51.99, 51.02, 41.98, 40.79, 37.94, 35.46, 30.77, 20.59, 18.11, 16.35, 15.78. HRMS calculated for $C_{29}H_{30}F_3NO_8$: $[M+Na]^+$: 600.1797 (found); 600.1821 (calc).

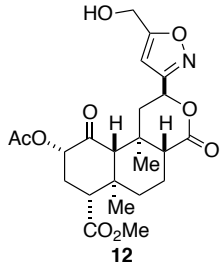

**12**

**(2*S*,4a*R*,6a*R*,7*R*,9*S*,10a*S*,10b*R*)-Methyl 9-acetoxy-2-(5-(hydroxymethyl)isoxazol-3-yl)-6a,10b-dimethyl-4,10-dioxododecahydro-1*H*-benzo[*f*]isochromene-7-carboxylate.** Prepared from **8** (50mg, 0.122 mmol) according to general oxime oxidation/cycloaddition reaction to yield **12** as a white solid (21 mg, 37%). $^1$H NMR (500 MHz, $CDCl_3$) δ 6.32 (s, 1H), 5.64 (dd, *J* = 6.02, 10.44 Hz, 1H), 5.16 (dd, *J* = 8.42, 11.63 Hz, 1H), 4.76 (d, *J* = 4.94 Hz, 2H), 3.73 (m, 3H), 2.77 (dd, *J* = 5.03, 11.81 Hz, 1H), 2.63 (dd, *J* = 6.03, 13.74 Hz, 1H), 2.31 (dd, *J* = 4.14, 7.43 Hz, 3H), 2.27 (d, *J* = 6.46 Hz, 1H), 2.17 (s, 3H), 2.15 (m, 2H), 1.86 (dd, *J* = 10.61, 13.61 Hz, 1H), 1.78 (dd, *J* = 6.55, 9.33 Hz, 1H), 1.67 (m, 1H), 1.46 (s, 3H), 1.11 (s, 3H). $^{13}$C NMR (126 MHz, $CDCl_3$) δ 201.86, 172.44, 171.59, 170.69, 169.93, 163.19, 100.48, 74.94, 71.26, 64.00, 56.50, 53.42, 52.00, 50.88, 41.98, 40.74, 37.91, 35.39, 30.73, 20.60, 18.10, 16.33, 15.80. HRMS calculated for $C_{23}H_{29}NO_9$: $[M+Na]^+$: 486.1738 (found); 486.1740 (calc).

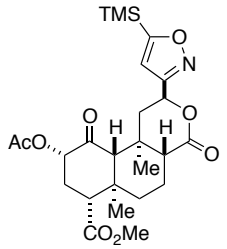

**13**

**(2*S*,4a*R*,6a*R*,7*R*,9*S*,10a*S*,10b*R*)-Methyl 9-acetoxy-6a,10b-dimethyl-4,10-dioxo-2-(5-(trimethylsilyl)isoxazol-3-yl)dodecahydro-1*H*-benzo[*f*]isochromene-7-carboxylate.** Prepared from **8** (171 mg, 0.418 mmol) according to general oxime oxidation/cycloaddition reaction to yield **13** as a white solid (127 mg, 40%). $^{1}$H NMR (500 MHz, $CDCl_3$) δ 6.50 (s, 1H), 5.72 (dd, *J* = 6.05, 10.31 Hz, 1H), 5.15 (m, 1H), 3.72 (s, 3H), 2.75 (dd, *J* = 5.60, 11.24 Hz, 1H), 2.65 (dd, *J* = 6.09, 13.74 Hz, 1H), 2.30 (m, 2H), 2.23 (s, 1H), 2.16 (s, 3H), 2.14 (m, 2H), 1.88 (dd, *J* = 10.43, 13.65 Hz, 1H), 1.78 (dd, *J* = 6.71, 9.37 Hz, 1H), 1.64 (m, 2H), 1.47 (s, 3H), 1.11 (s, 3H), 0.33 (m, 9H). $^{13}$C NMR (126 MHz, $CDCl_3$) δ 201.73, 179.53, 171.56, 170.79, 169.82, 161.43, 110.95, 74.90, 71.28, 64.16, 53.51, 51.98, 50.92, 41.99, 41.34, 37.99, 35.44, 30.74, 20.58, 18.11, 16.32, 15.83, -1.98. HRMS calculated for $C_{25}H_{35}NO_8Si$: $[M+Na]^+$: 528.2009 (found); 528.2030 (calc).

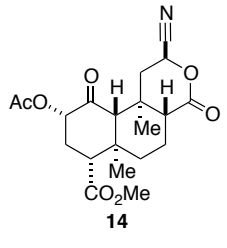

**14**

**(2*S*,4a*R*,6a*R*,7*R*,9*S*,10a*S*,10b*R*)-Methyl 9-acetoxy-2-cyano-6a,10b-dimethyl-4,10-dioxododecahydro-1*H*-benzo[*f*]isochromene-7-carboxylate.**

Method A: A solution **13** (73.7 mg, 0.146 mmol) in MeCN (1 mL) was slowly added to a suspension of CsF (29.9 mg, 0.197 mmol) in MeCN (4 ml) and EtOH (0.2 mL). After 30 min the reaction was quenched with $H_2O$ (10 mL) and extracted with $CH_2Cl_2$ (5 x 15

mL). Combined organic layers were dried over $Na_2SO_4$ and concentrated in vacuo. The esidue was purified by Prep TLC (2 x 40% EtOAc/Hex) to yield **14** (20.4 mg, 36%) as a white solid.

Method B: A solution of TBAF (1 M in THF, 0.10 mmol) was slowly added dropwise to a solution of **14** (50.0 mg, 0.0989 mmol) in $CH_2Cl_2$ (5 mL) cooled to 0 °C. After 30 min at this temperature, the reaction was quenched with H2O (5 mL) and extracted with $CH_2Cl_2$ (3 x 10 mL). The combined organic layers was washed with saturated $NaHCO_3$ (aq.) and brine then dried over $Na_2SO_4$. The solvent was removed in vacuo and residue purified by FCC eluting with 40% EtOAc/Hex to yield **14** (19.4 mg, 50%) as a white solid.

Method C: To a solution of **8** (100 mg, 0.245 mmol) in CH2Cl2 (10 mL) was added TsCl (49 mg, 0.258 mmol) and DIPEA (0.09 mL, 0.503 mmol). After stirring for 24 hours at room temperature, the reaction was diluted with CH2Cl2 (20 mL) and rinsed with HCl (2 M, 10 mL) and brine. The organic layer was dried over Na2SO4 and concentrated in vacuo. The resulting residue was purified by FCC: 40% EtOAc/Hex to yield **14** (58.2 mg, 60%) as a white solid.

$^1$H NMR (500 MHz, $CDCl_3$) δ 5.26 (dd, *J* = 7.36, 8.18 Hz, 1H), 5.17 (m, 1H), 3.73 (s, 3H), 2.79 (dd, *J* = 4.47, 12.33 Hz, 1H), 2.66 (dd, *J* = 7.29, 14.05 Hz, 1H), 2.39 (dd, *J* = 3.13, 11.51 Hz, 1H), 2.32 (dt, *J* = 7.22, 18.64 Hz, 2H), 2.31 (s, 1H), 2.18 (s, 3H), 2.12 (m, 1H), 1.82 (ddd, *J* = 5.68, 9.99, 12.71 Hz, 2H), 1.66 (ddd, *J* = 5.02, 13.66, 25.10 Hz, 2H), 1.35 (s, 3H), 1.08 (s, 3H). $^{13}$C NMR (126 MHz, $CDCl_3$) δ 201.67, 171.38, 169.90, 168.65, 116.81, 74.89, 64.15, 62.92, 53.24, 52.07, 49.65, 41.99, 40.24, 37.51, 35.28, 30.57, 20.55,

18.07, 16.68, 16.21. HRMS calculated for $C_{20}H_{25}NO_7$: $[M+Na]^+$: 414.1529 (found); 414.1544 (calc).

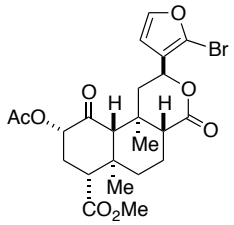

4

**(2*S*,4a*R*,6a*R*,7*R*,9*S*,10a*S*,10b*R*)-Methyl 9-acetoxy-2-(2-bromofuran-3-yl)-6a,10b-dimethyl-4,10-dioxododecahydro-1*H*-benzo[*f*]isochromene-7-carboxylate.** An oven-dried flask was charged with a stir bar, **1** (450 mg, 1.04 mmol), and *N*-bromosuccinimide (260 mg, 1.46 mmol). $CH_2Cl_2$ (50 mL) was added to the reaction followed by a single drop of $Br_2$. After stirring at room temperature for 30 min the reaction mixture was applied directly to a silica gel column and eluted with EtOAc/$CH_2Cl_2$ (0-5%) to yield **4** as a white solid (261 mg, 49%). $^1$H NMR (500 MHz, $CDCl_3$) δ 7.42 (d, *J* = 2.1 Hz, 1H), 6.39 (d, *J* = 2.1 Hz, 1H), 5.43 (dd, *J* = 12.1, 5.1 Hz, 1H), 5.13 (m, 1H), 3.73 (s, 3H), 2.76 (m, 1H), 2.39 (dd, *J* = 13.6, 5.2 Hz, 1H), 2.30 (m, 2H), 2.19 (m, 2H), 2.16 (s, 3H), 2.11 (dd, *J* = 11.5, 2.9 Hz, 1H), 1.81 (m, 1H), 1.62 (m, 3H), 1.47 (s, 3H), 1.12 (s, 3H). $^{13}$C NMR (126 MHz, $CDCl_3$) δ 201.90, 171.53, 170.92, 169.98, 144.66, 122.75, 121.39, 110.75, 75.02, 71.92, 63.91, 53.59, 52.02, 51.59, 42.86, 42.12, 38.16, 35.51, 30.74, 20.58, 18.13, 16.44, 14.98. HRMS calculated for $C_{23}H_{27}BrO_8$: $[M+K]^+$: 549.0499 (found); 549.0526 (calc). Melting point: 195-197 °C.

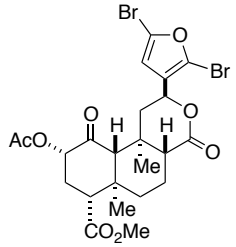


**15**

**(2*S*,4a*R*,6a*R*,7*R*,9*S*,10a*S*,10b*R*)-Methyl 9-acetoxy-2-(2,5-dibromofuran-3-yl)-6a,10b-dimethyl-4,10-dioxododecahydro-1*H*-benzo[*f*]isochromene-7-carboxylate**. An oven-dried flask was charged with a stir bar, **1** (200 mg, 0.462 mmol), and *N*-bromosuccinimide (115 mg, 0.646 mmol). $CH_2Cl_2$ (20 mL) was added to the reaction followed by $Br_2$ (24 mL, 0.46 mmol) dropwise. After stirring at room temperature for 30 min the reaction mixture was applied to a silica gel column and eluted with EtOAc/$CH_2Cl_2$ (0-5%) to yield **15** as a white solid (99 mg, 36%). $^1$H NMR (500 MHz, $CDCl_3$) δ 6.36 (s, 1H), 5.37 (dd, *J* = 12.1, 5.2 Hz, 1H), 5.11 (m, 1H), 3.73 (s, 3H), 2.76 (dd, *J* = 10.3, 6.5 Hz, 1H), 2.38 (dd, *J* = 13.6, 5.2 Hz, 1H), 2.30 (s, 1H), 2.29 (dd, *J* = 13.5, 7.2 Hz, 1H), 2.17 (m, 2H), 2.16 (s, 3H), 2.10 (dd, *J* = 11.3, 2.9 Hz, 1H), 1.80 (m, 1H), 1.59 (m, 3H), 1.45 (s, 3H), 1.11 (s, 3H). $^{13}$C NMR (126 MHz, $CDCl_3$) δ 201.93, 171.51, 170.66, 169.98, 125.95, 123.02, s120.91, 112.59, 75.03, 71.53, 63.80, 53.56, 52.04, 51.53, 42.62, 42.11, 38.12, 35.50, 30.72, 20.58, 18.11, 16.43, 14.98. HRMS calculated for $C_{23}H_{26}O_8Br_2$: $[M+Na]^+$: 626.9626 (found); 626.9632 (calc). Melting point: 202-205°C (dec).

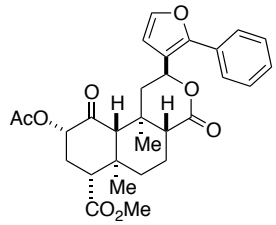

16

**(2*S*,4a*R*,6a*R*,7*R*,9*S*,10a*S*,10b*R*)-Methyl 9-acetoxy-6a,10b-dimethyl-4,10-dioxo-2-(2-phenylfuran-3-yl)dodecahydro-1*H*-benzo[*f*]isochromene-7-carboxylate.** $^{1}$H NMR (500 MHz, $CDCl_3$) δ 7.55 (dd, *J* = 4.4, 3.8 Hz, 2H), 7.45 (m, 3H), 7.38 (m, 1H), 6.49 (d, *J* = 1.9 Hz, 1H), 5.69 (dd, *J* = 12.0, 5.0 Hz, 1H), 5.14 (m, 1H), 3.73 (s, 3H), 2.77 (m, 1H), 2.42 (dd, *J* = 13.7, 5.0 Hz, 1H), 2.30 (s, 1H), 2.29 (m, 1H), 2.21 (m, 2H), 2.15 (m, 1H), 2.14 (s, 3H), 1.81 (m, 1H), 1.69 (m, 3H), 1.44 (s, 3H), 1.12 (s, 3H). $^{13}$C NMR (126 MHz, $CDCl_3$) δ 201.92, 171.57, 171.23, 169.94, 151.72, 142.17, 130.03, 128.84, 128.47, 127.12, 119.24, 110.17, 74.99, 71.97, 64.01, 53.59, 52.00, 51.62, 43.29, 42.12, 38.20, 35.55, 30.75, 20.56, 18.18, 16.45, 15.05. HRMS calculated for $C_{29}H_{32}O_8$: $[M+Na]^+$: 531.1979 (found); 531.1995 (calc). Melting point: 260°C (dec).

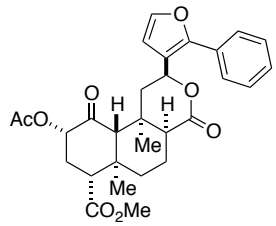

17

**(2*S*,4a*S*,6a*R*,7*R*,9*S*,10a*S*,10b*R*)-Methyl 9-acetoxy-6a,10b-dimethyl-4,10-dioxo-2-(2-phenylfuran-3-yl)dodecahydro-1*H*-benzo[*f*]isochromene-7-carboxylate.** $^{1}$H NMR (500 MHz, $CDCl_3$) δ 7.50 (m, 2H), 7.44 (m, 3H), 7.36 (m, 1H), 6.56 (d, *J* = 1.9 Hz, 1H), 5.42 (dd, *J* = 12.0, 1.4 Hz, 1H), 5.15 (t, 1H), 3.71 (s, 3H), 2.80 (dd, *J* = 8.8, 8.0 Hz, 1H), 2.48 (d, *J* = 3.1 Hz, 1H), 2.39 (dd, *J* = 15.1, 1.9 Hz, 1H), 2.30 (m, 3H), 2.22 (m, 1H), 2.16 (s, 3H), 2.05 (td, *J* = 13.8, 3.9 Hz, 1H), 1.85 (m, 1H), 1.63 (s, 3H), 1.62 (m, 2H), 1.09 (s, 3H). $^{13}$C NMR (126 MHz, $CDCl_3$) δ 202.37, 173.68, 171.89,

169.88, 150.86, 142.18, 130.26, 128.85, 128.31, 126.78, 118.18, 110.49, 75.31, 69.81, 64.33, 52.94, 51.81, 47.96, 45.21, 42.31, 34.70, 34.01, 30.70, 24.55, 20.58, 17.63, 15.26. HRMS calculated for $C_{29}H_{32}O_8$: $[M+Na]^+$: 509.2171 (found); 509.2175 (calc). Melting Point: 116-118°C.

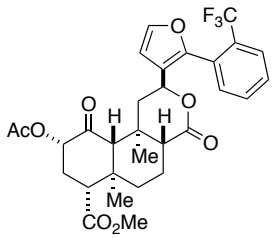

**18**

**(2*S*,4a*R*,6a*R*,7*R*,9*S*,10a*S*,10b*R*)-Methyl 9-acetoxy-6a,10b-dimethyl-4,10-dioxo-2-(2-(2-(trifluoromethyl)phenyl)furan-3-yl)dodecahydro-1*H*-benzo[*f*]isochromene-7-carboxylate.** $^1$H NMR (500 MHz, $CDCl_3$) δ 7.81 (d, *J* = 7.6 Hz, 1H), 7.64 (dd, *J* = 7.5, 6.8 Hz, 1H), 7.57 (t, *J* = 7.5 Hz, 1H), 7.52 (d, *J* = 7.5 Hz, 1H), 7.50 (d, *J* = 1.9 Hz, 1H), 6.49 (d, *J* = 2.0 Hz, 1H), 5.33 (dd, *J* = 11.8, 5.2 Hz, 1H), 5.14 (dd, *J* = 11.9, 8.2 Hz, 1H), 3.73 (s, 3H), 2.76 (dd, *J* = 12.2, 4.7 Hz, 1H), 2.31 (m, 3H), 2.17 (m, 2H), 2.15 (s, 3H), 2.07 (dd, *J* = 11.6, 2.7 Hz, 1H), 1.78 (dd, *J* = 10.0, 2.8 Hz, 1H), 1.63 (m, 3H), 1.33 (s, 3H), 1.09 (s, 3H). $^{13}$C NMR (126 MHz, $CDCl_3$) δ 201.85, 171.57, 171.10, 169.86, 148.75, 143.00, 132.51, 131.75, 130.10 (q, $^2J_{CF}$ = 30.95), 129.60, 127.76 (q, $^3J_{CF}$ = 1.69 Hz), 126.97 (q, $^3J_{CF}$ = 5.15 Hz), 123.53 (q, $^1J_{CF}$ = 273.60 Hz), 121.54, 109.38, 74.90, 71.71, 64.02, 53.55, 52.01, 51.45, 43.23, 42.06, 38.13, 35.47, 30.79, 20.59, 18.15, 16.38, 14.94. $^{19}$F NMR (376 MHz, $CDCl_3$) δ -59.65. HRMS calculated for $C_{30}H_{31}F_3O_8$: $[M+Na]^+$ calcd 599.1869, found 599.1895. Melting point 184-188°C.

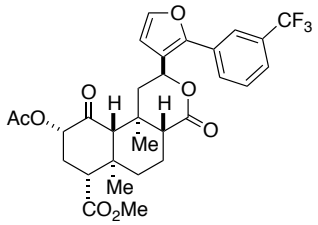

19

**(2*S*,4a*R*,6a*R*,7*R*,9*S*,10a*S*,10b*R*)-Methyl 9-acetoxy-6a,10b-dimethyl-4,10-dioxo-2-(2-(3-(trifluoromethyl)phenyl)furan-3-yl)dodecahydro-1*H*-benzo[*f*]isochromene-7-carboxylate.** $^{1}$H NMR (500 MHz, $CDCl_3$) δ 7.84 (s, 1H), 7.74 (d, *J* = 7.6 Hz, 1H), 7.60 (d, *J* = 17.7 Hz, 1H), 7.60 (t, *J* = 16.6 Hz, 1H), 7.49 (d, *J* = 1.9 Hz, 1H), 6.52 (d, *J* = 1.9 Hz, 1H), 5.67 (dd, *J* = 12.1, 4.9 Hz, 1H), 5.14 (m, 1H), 3.74 (s, 3H), 2.77 (m, 1H), 2.43 (dd, *J* = 13.7, 4.9 Hz, 1H), 2.30 (m, 2H), 2.18 (m, 3H), 2.14 (s, 3H), 1.82 (m, 1H), 1.66 (m, 3H), 1.46 (s, 3H), 1.13 (s, 3H). $^{13}$C NMR (126 MHz, $CDCl_3$) δ 201.82, 171.53, 170.98, 169.99, 149.87, 131.37 (q, $^{2}J_{CF}$ = 32.49 Hz), 130.77, 129.97, 129.42, 124.94 (q, $^{3}J_{CF}$ = 3.70 Hz), 123.87 (q, $^{1}J_{CF}$ = 272.60 Hz), 123.77 (q, $^{3}J_{CF}$ = 3.85 Hz), 120.59, 110.55, 75.00, 71.65, 64.00, 53.62, 52.03, 51.72, 43.14, 42.12, 38.19, 35.56, 30.73, 20.56, 18.16, 16.49, 15.04. $^{19}$F NMR (376 MHz, $CDCl_3$) δ -62.49. HRMS calculated for $C_{30}H_{31}F_3O_8$: $[M+Na]^+$: 599.1885 (found); 599.1869 (calc). Melting point: 167-169°C.

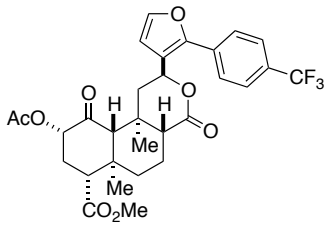

20

**(2*S*,4a*R*,6a*R*,7*R*,9*S*,10a*S*,10b*R*)-Methyl 9-acetoxy-6a,10b-dimethyl-4,10-dioxo-2-(2-(4-(trifluoromethyl)phenyl)furan-3-yl)dodecahydro-1*H*-benzo[*f*]isochromene-7-carboxylate.** $^{1}$H NMR (500 MHz, $CDCl_3$) δ 7.70 (q, *J* = 8.6 Hz, 4H), 7.49 (d, *J* = 1.9 Hz, 1H), 6.53 (d, *J* = 1.9 Hz, 1H), 5.68 (dd, *J* = 12.0, 4.9 Hz, 1H),

5.14 (m, 1H), 3.74 (s, 3H), 2.77 (m, 1H), 2.43 (dd, $J$ = 13.6, 5.0 Hz, 1H), 2.30 (m, 2H), 2.20 (s, 1H), 2.17 (m, 2H), 2.14 (s, 3H), 1.82 (m, 1H), 1.66 (m, 3H), 1.46 (s, 3H), 1.13 (s, 3H). $^{13}$C NMR (126 MHz, $CDCl_3$) δ 201.87, 171.52, 170.98, 169.99, 150.00, 142.98, 133.30, 130.14 (q, $^2J_{CF}$ = 32.81 Hz), 127.09, 125.85 (q, $^3J_{CF}$ = 3.74 Hz), 123.99 (q, $^1J_{CF}$ = 272.10), 120.96, 110.55, 75.00, 71.57, 64.01, 53.62, 52.04, 51.70, 43.12, 42.12, 38.18, 35.56, 30.73, 20.56, 18.17, 16.48, 15.10. $^{19}$F NMR (376 MHz, $CDCl_3$) δ -62.29. HRMS calculated for $C_{30}H_{31}F_3O_8$: $[M+Na]^+$: 599.1873 (found); 599.1869 (calc). Melting point 190-194°C.

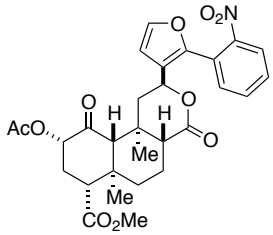

**21**

**(2*S*,4a*R*,6a*R*,7*R*,9*S*,10a*S*,10b*R*)-Methyl 9-acetoxy-6a,10b-dimethyl-2-(2-(2-nitrophenyl)furan-3-yl)-4,10-dioxododecahydro-1*H*-benzo[*f*]isochromene-7-carboxylate.** $^1$H NMR (500 MHz, $CDCl_3$) δ 8.46 (t, $J$ = 1.90 Hz, 1H), 8.21 (ddd, $J$ = 0.99, 2.27, 8.24 Hz, 1H), 7.91 (ddd, $J$ = 1.03, 1.61, 7.77 Hz, 1H), 7.64 (t, $J$ = 8.00 Hz, 1H), 7.52 (d, $J$ = 1.96 Hz, 1H), 6.54 (d, $J$ = 1.94 Hz, 1H), 5.71 (dd, $J$ = 4.86, 12.07 Hz, 1H), 5.13 (m, 1H), 3.74 (s, 3H), 2.77 (m, 1H), 2.45 (dd, $J$ = 4.88, 13.66 Hz, 1H), 2.30 (m, 2H), 2.18 (m, 3H), 2.14 (s, 3H), 1.82 (m, 1H), 1.68 (m, 3H), 1.48 (s, 3H), 1.13 (s, 3H). $^{13}$C NMR (126 MHz, $CDCl_3$) δ 201.81, 171.51, 170.85, 170.01, 148.69, 148.62, 143.15, 132.25, 131.63, 129.97, 122.81, 121.62, 121.49, 110.86, 75.00, 71.50, 64.00, 53.61, 52.04, 51.74, 43.00, 42.12, 38.17, 35.60, 30.72, 20.56, 18.15, 16.50, 15.15. HRMS calculated for $C_{29}H_{31}NO_{10}$: $[M+Na]^+$: 576.1855 (found); 576.1846 (calc). Melting point: 196-198 °C.

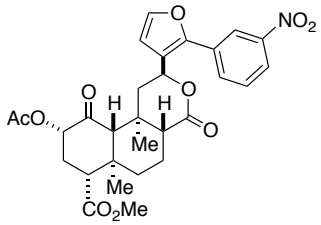

22

**(2*S*,4a*R*,6a*R*,7*R*,9*S*,10a*S*,10b*R*)-Methyl 9-acetoxy-6a,10b-dimethyl-2-(2-(3-nitrophenyl)furan-3-yl)-4,10-dioxododecahydro-1*H*-benzo[*f*]isochromene-7-carboxylate.** $^{1}$H NMR (500 MHz, $CDCl_3$) δ 8.46 (t, *J* = 1.89 Hz, 1H), 8.21 (ddd, *J* = 0.97, 2.26, 8.22 Hz, 1H), 7.91 (ddd, *J* = 1.05, 1.56, 7.77 Hz, 1H), 7.64 (t, *J* = 8.02 Hz, 1H), 7.52 (d, *J* = 1.93 Hz, 1H), 6.54 (d, *J* = 1.93 Hz, 1H), 5.70 (dd, *J* = 4.86, 12.07 Hz, 1H), 5.14 (m, 1H), 3.74 (s, 3H), 2.77 (m, 1H), 2.45 (dd, *J* = 4.87, 13.66 Hz, 1H), 2.30 (m, 2H), 2.19 (m, 3H), 2.14 (s, 3H), 1.82 (m, 1H), 1.70 (m, 3H), 1.48 (s, 3H), 1.13 (s, 3H). $^{13}$C NMR (126 MHz, $CDCl_3$) δ 201.83, 171.51, 170.87, 170.01, 148.68, 148.61, 143.14, 132.24, 131.62, 129.97, 122.80, 121.61, 121.49, 110.86, 75.00, 71.50, 63.97, 53.59, 52.04, 51.72, 42.98, 42.11, 38.16, 35.59, 30.71, 20.56, 18.15, 16.50, 15.15. HRMS calculated for $C_{29}H_{31}NO_{10}$: $[M+Na]^+$: 576.1843 (found); 576.1846 (calc). Melting point:119-123 °C.

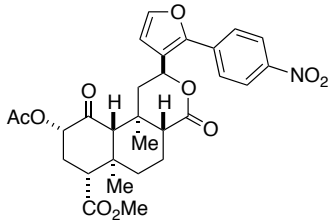

23

**(2*S*,4a*R*,6a*R*,7*R*,9*S*,10a*S*,10b*R*)-Methyl 9-acetoxy-6a,10b-dimethyl-2-(2-(4-nitrophenyl)furan-3-yl)-4,10-dioxododecahydro-1*H*-benzo[*f*]isochromene-7-carboxylate.** $^{1}$H NMR (500 MHz, $CDCl_3$) δ 8.32 (d, *J* = 9.00 Hz, 2H), 7.75 (d, *J* = 9.00 Hz, 2H), 7.54 (d, *J* = 1.86 Hz, 1H), 6.57 (d, *J* = 1.92 Hz, 1H), 5.70 (dd, *J* = 4.89, 12.04 Hz, 1H), 5.13 (m, 1H), 3.74 (s, 3H), 2.77 (m, 1H), 2.45 (dd, *J* =

4.92, 13.64 Hz, 1H), 2.31 (m, 2H), 2.22 (m, 2H), 2.16 (m, 1H), 2.14 (s, 3H), 1.83 (m, 1H), 1.68 (m, 3H), 1.47 (s, 3H), 1.13 (s, 3H). $^{13}$C NMR (126 MHz, $CDCl_3$) δ 201.87, 171.48, 170.81, 170.01, 148.99, 147.14, 143.69, 135.89, 127.18, 124.29, 122.56, 111.03, 75.00, 71.34, 63.96, 53.60, 52.05, 51.72, 42.91, 42.11, 38.14, 35.56, 30.70, 20.55, 18.15, 16.50, 15.14. HRMS calculated for $C_{29}H_{31}NO_{10}$: $[M+Na]^+$: 576.1860 (found); 576.1846 (calc). Melting point: 184-188 °C.

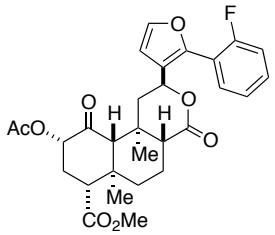


**24**

**(2*S*,4a*R*,6a*R*,7*R*,9*S*,10a*S*,10b*R*)-Methyl 9-acetoxy-2-(2-(2-fluorophenyl)furan-3-yl)-6a,10b-dimethyl-4,10-dioxododecahydro-1*H*-benzo[*f*]isochromene-7-carboxylate.** $^1$H NMR (500 MHz, $CDCl_3$) δ 7.50 (m, 2H), 7.39 (m, 1H), 7.20 (m, 2H), 6.49 (d, *J* = 1.9 Hz, 1H), 5.57 (dd, *J* = 11.9, 5.0 Hz, 1H), 5.13 (m, 1H), 3.73 (s, 3H), 2.76 (dd, *J* = 10.6, 6.3 Hz, 1H), 2.45 (dd, *J* = 13.6, 5.0 Hz, 1H), 2.29 (m, 2H), 2.15 (s, 3H), 2.15 (m, 3H), 1.80 (dd, *J* = 10.0, 3.0 Hz, 1H), 1.62 (m, 3H), 1.42 (s, 3H), 1.11 (s, 3H). $^{13}$C NMR (126 MHz, $CDCl_3$) δ 201.80, 171.60, 171.22, 169.89, 159.20 (d, $^1J_{CF}$ = 249.50 Hz), 145.63, 143.36, 130.68 ($^3J_{CF}$ = 2.23 Hz), 130.64 ($^3J_{CF}$ = 3.35), 124.43 ($^3J_{CF}$ = 3.52 Hz), 121.95, 118.04 ($^2J_{CF}$ = 14.11 Hz), 116.27 ($^2J_{CF}$ = 21.99), 109.96, 74.96, 72.07, 64.06, 53.62, 52.00, 51.62, 43.50, 42.11, 38.23, 35.52, 30.79, 20.59, 18.16, 16.44, 15.02. $^{19}$F NMR (376 MHz, $CDCl_3$) δ -115.25. HRMS calculated for $C_{29}H_{31}FO_8$: $[M+Na]^+$: 549.1891 (found); 549.1901 (calc). Melting point 245-247°C (dec).

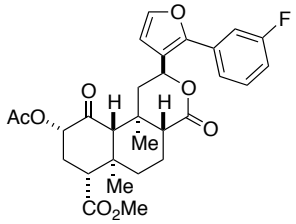

25

**(2*S*,4a*R*,6a*R*,7*R*,9*S*,10a*S*,10b*R*)-Methyl 9-acetoxy-2-(2-(3-fluorophenyl)furan-3-yl)-6a,10b-dimethyl-4,10-dioxododecahydro-1*H*-benzo[*f*]isochromene-7-carboxylate.** $^{1}$H NMR (500 MHz, $CDCl_3$) δ 7.45 (d, *J* = 1.9 Hz, 1H), 7.42 (td, *J* = 8.0, 5.9 Hz, 1H), 7.33 (m, 1H), 7.29 (m, 1H), 7.07 (m, 1H), 6.50 (d, *J* = 1.9 Hz, 1H), 5.69 (dd, *J* = 12.0, 4.9 Hz, 1H), 5.14 (m, 1H), 3.74 (s, 3H), 2.77 (m, 1H), 2.42 (dd, *J* = 13.6, 5.0 Hz, 1H), 2.30 (s, 1H), 2.30 (m, 1H), 2.22 (m, 2H), 2.14 (s, 3H), 2.13 (m, 1H), 1.82 (m, 1H), 1.66 (m, 3H), 1.46 (s, 3H), 1.12 (s, 3H). $^{13}$C NMR (126 MHz, $CDCl_3$) δ 201.87, 171.54, 171.04, 169.96, 162.95 (d, $^{1}J_{CF}$ = 246.35 Hz), 150.24 (d, $^{4}J_{CF}$ = 2.61 Hz), 142.52, 131.98 (d, $^{3}J_{CF}$ = 8.47 Hz), 130.49 (d, $^{3}J_{CF}$ = 8.48 Hz), 122.58 (d, $^{4}J_{CF}$ = 2.89 Hz), 120.14, 115.38 (d, $^{2}J_{CF}$ = 21.24 Hz), 113.89 (d, $^{2}J_{CF}$ = 23.18 Hz), 110.39, 75.00, 71.66, 64.03, 53.61, 52.02, 51.68, 43.17, 42.12, 38.20, 35.56, 30.75, 20.56, 18.18, 16.47, 15.09. $^{19}$F NMR (376 MHz, $CDCl_3$) δ -113.49. HRMS calculated for $C_{29}H_{31}FO_8$: $[M+Na]^+$: 549.1920 (found); 549.1901 (calc). Melting point 230-232°C.

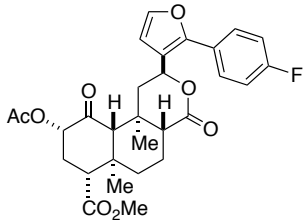

26

**(2*S*,4a*R*,6a*R*,7*R*,9*S*,10a*S*,10b*R*)-Methyl 9-acetoxy-2-(2-(4-fluorophenyl)furan-3-yl)-6a,10b-dimethyl-4,10-dioxododecahydro-1*H*-benzo[*f*]isochromene-7-carboxylate.** $^{1}$H NMR (500 MHz, $CDCl_3$) δ 7.54 (dd, *J* = 8.9, 5.3 Hz, 2H), 7.43 (d, *J* = 1.9 Hz, 1H), 7.15 (t, *J* = 8.7 Hz, 2H), 6.48 (d, *J* = 2.0 Hz, 1H),

5.61 (dd, $J$ = 12.0, 5.0 Hz, 1H), 5.14 (m, 1H), 3.74 (s, 3H), 2.77 (m, 1H), 2.40 (dd, $J$ = 13.6, 5.0 Hz, 1H), 2.30 (s, 1H), 2.30 (m, 1H), 2.16 (m, 3H), 2.14 (s, 3H), 1.81 (m, 1H), 1.66 (m, 3H), 1.44 (s, 3H), 1.12 (s, 3H). $^{13}$C NMR (126 MHz, $CDCl_3$) δ 201.93, 171.54, 171.14, 169.97, 162.79 (d, $^1J_{CF}$ = 248.79 Hz), 150.97, 142.15, 129.06 (d, $^3J_{CF}$ = 8.25 Hz), 126.26 (d, $^4J_{CF}$ = 3.29), 119.04, 115.96 (d, $^2J_{CF}$ = 21.82 Hz), 110.15, 75.01, 71.86, 64.03, 53.61, 52.03, 51.65, 43.19, 42.13, 38.20, 35.53, 30.75, 20.56, 18.18, 16.46, 15.06. $^{19}$F NMR (376 MHz, $CDCl_3$) δ -114.01. HRMS calculated for $C_{29}H_{31}FO_8$: $[M+Na]^+$: 549.1907 (found); 549.1901 (calc). Melting point 200-201°C.

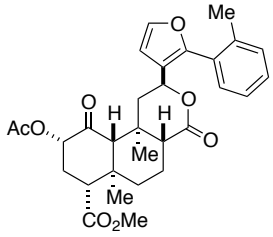

27

**(2*S*,4a*R*,6a*R*,7*R*,9*S*,10a*S*,10b*R*)-Methyl 9-acetoxy-6a,10b-dimethyl-4,10-dioxo-2-(2-(*o*-tolyl)furan-3-yl)dodecahydro-1*H*-benzo[*f*]isochromene-7-carboxylate.** $^1$H NMR (500 MHz, $CDCl_3$) δ 7.46 (d, $J$ = 1.95 Hz, 1H), 7.33 (m, 1H), 7.29 (dd, $J$ = 1.62, 5.81 Hz, 2H), 7.26 (m, 1H), 6.47 (d, $J$ = 1.99 Hz, 1H), 5.38 (dd, $J$ = 5.17, 11.90 Hz, 1H), 5.13 (dd, $J$ = 8.84, 11.26 Hz, 1H), 3.73 (s, 3H), 2.76 (dd, $J$ = 5.51, 11.36 Hz, 1H), 2.32 (m, 3H), 2.29 (s, 3H), 2.17 (m, 2H), 2.15 (s, 3H), 2.06 (m, 1H), 1.79 (dd, $J$ = 2.93, 10.00 Hz, 1H), 1.64 (m, 3H), 1.34 (s, 3H), 1.09 (s, 3H). $^{13}$C NMR (126 MHz, $CDCl_3$) δ 201.94, 171.58, 171.28, 169.97, 152.35, 142.17, 138.36, 130.76, 130.47, 129.33, 129.05, 125.74, 120.36, 109.29, 75.00, 72.07, 64.05, 53.59, 52.01, 51.47, 43.53, 42.11, 38.20, 35.50, 30.75, 20.59, 20.30, 18.16, 16.39, 14.95. HRMS calculated for $C_{30}H_{34}O_8$: $[M+Na]^+$: 545.2157 (found); 545.2151 (calc). Melting point: 166-167 °C (dec.).

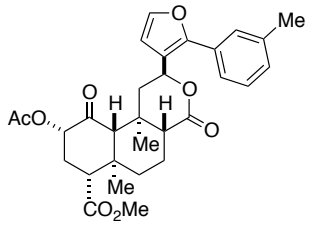

28

**(2*S*,4a*R*,6a*R*,7*R*,9*S*,10a*S*,10b*R*)-Methyl 9-acetoxy-6a,10b-dimethyl-4,10-dioxo-2-(2-(*m*-tolyl)furan-3-yl)dodecahydro-1*H*-benzo[*f*]isochromene-7-carboxylate.** $^{1}$H NMR (500 MHz, $CDCl_3$) δ 7.43 (d, *J* = 1.87 Hz, 1H), 7.37 (m, 1H), 7.34 (d, *J* = 4.11 Hz, 2H), 7.19 (m, 1H), 6.47 (d, *J* = 1.96 Hz, 1H), 5.70 (dd, *J* = 4.95, 12.03 Hz, 1H), 5.14 (m, 1H), 3.74 (s, 3H), 2.77 (m, 1H), 2.41 (dd, *J* = 5.12, 13.50 Hz, 1H), 2.41 (s, 3H), 2.30 (m, 2H), 2.17 (m, 3H), 2.14 (s, 3H), 1.81 (m, 1H), 1.66 (m, 3H), 1.44 (s, 3H), 1.12 (s, 3H). $^{13}$C NMR (126 MHz, $CDCl_3$) δ 201.86, 171.58, 171.25, 169.94, 151.79, 142.05, 138.54, 129.97, 129.28, 128.73, 127.75, 124.28, 119.16, 110.14, 74.98, 72.07, 64.04, 53.61, 52.01, 51.67, 43.36, 42.12, 38.23, 35.55, 30.77, 21.51, 20.57, 18.19, 16.46, 15.05. HRMS calculated for $C_{30}H_{34}O_8$: $[M+Na]^+$: 545.2157 (found); 545.2151 (calc). Melting point: 172-175 °C (dec.).

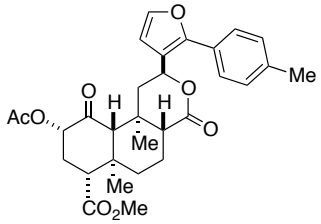

29

**(2*S*,4a*R*,6a*R*,7*R*,9*S*,10a*S*,10b*R*)-Methyl 9-acetoxy-6a,10b-dimethyl-4,10-dioxo-2-(2-(*p*-tolyl)furan-3-yl)dodecahydro-1*H*-benzo[*f*]isochromene-7-carboxylate.** $^{1}$H NMR (500 MHz, $CDCl_3$) δ 7.43 (dd, *J* = 4.99, 10.86 Hz, 3H), 7.26 (d, *J* = 6.26 Hz, 2H), 6.47 (d, *J* = 1.96 Hz, 1H), 5.67 (dd, *J* = 4.98, 12.02 Hz, 1H), 5.14 (m, 1H), 3.74 (s, 3H), 2.77 (dd, *J* = 5.67, 11.17 Hz, 1H), 2.41 (m, 1H), 2.40 (s, 3H), 2.30 (m, 2H), 2.19 (m, 3H), 2.14 (s, 3H), 1.81 (m, 1H), 1.66 (m, 3H), 1.44 (s, 3H), 1.12 (s, 3H).

$^{13}$C NMR (126 MHz, $CDCl_3$) δ 201.89, 171.58, 171.28, 169.93, 151.99, 141.88, 138.47, 129.53, 127.24, 127.07, 118.65, 110.05, 74.99, 72.08, 64.05, 53.61, 52.01, 51.63, 43.31, 42.12, 38.22, 35.54, 30.76, 21.34, 20.56, 18.19, 16.45, 15.04. HRMS calculated for $C_{30}H_{34}O_8$: $[M+Na]^+$: 545.2142 (found); 545.2151 (calc). Melting point: 204-206 °C (dec.).

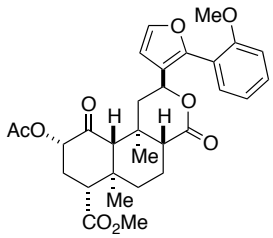

**30**

**(2*S*,4a*R*,6a*R*,7*R*,9*S*,10a*S*,10b*R*)-Methyl 9-acetoxy-2-(2-(2-methoxyphenyl)furan-3-yl)-6a,10b-dimethyl-4,10-dioxododecahydro-1*H*-benzo[*f*]isochromene-7-carboxylate.** $^1$H NMR (500 MHz, $CDCl_3$) δ 7.48 (d, *J* = 1.9 Hz, 1H), 7.42 (dd, *J* = 7.6, 1.7 Hz, 1H), 7.38 (ddd, *J* = 8.4, 7.5, 1.7 Hz, 1H), 7.04 (td, *J* = 7.5, 0.9 Hz, 1H), 6.98 (d, *J* = 8.3 Hz, 1H), 6.46 (d, *J* = 2.0 Hz, 1H), 5.54 (dd, *J* = 11.9, 4.8 Hz, 1H), 5.14 (dd, *J* = 11.4, 8.7 Hz, 1H), 3.89 (s, 3H), 3.73 (s, 3H), 2.77 (dd, *J* = 11.4, 5.4 Hz, 1H), 2.52 (dd, *J* = 13.7, 4.8 Hz, 1H), 2.29 (m, 2H), 2.19 (s, 1H), 2.15 (s, 3H), 2.13 (m, 2H), 1.80 (m, 1H), 1.62 (m, 3H), 1.39 (s, 3H), 1.11 (s, 3H). $^{13}$C NMR (126 MHz, $CDCl_3$) δ 202.06, 171.63, 171.48, 169.78, 156.32, 147.77, 142.83, 131.01, 130.34, 121.16, 120.75, 119.12, 111.10, 109.66, 75.00, 72.79, 64.08, 55.39, 53.61, 51.99, 51.74, 43.21, 42.13, 38.28, 35.43, 30.84, 20.58, 18.14, 16.45, 14.95. HRMS calculated for $C_{30}H_{34}O_9$: $[M+Na]^+$: 561.2076 (found); 561.2101 (calc). Melting point: 165-167°C.

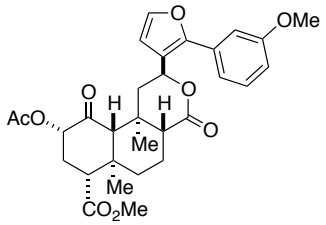

31

**(2*S*,4a*R*,6a*R*,7*R*,9*S*,10a*S*,10b*R*)-Methyl 9-acetoxy-2-(2-(3-methoxyphenyl)furan-3-yl)-6a,10b-dimethyl-4,10-dioxododecahydro-1*H*-benzo[*f*]isochromene-7-carboxylate.** $^{1}$H NMR (500 MHz, $CDCl_3$) δ 7.44 (d, *J* = 1.9 Hz, 1H), 7.36 (t, *J* = 8.0 Hz, 1H), 7.14 (dd, *J* = 7.6, 0.9 Hz, 1H), 7.10 (m, 1H), 6.93 (ddd, *J* = 8.3, 2.6, 0.8 Hz, 1H), 6.48 (d, *J* = 1.9 Hz, 1H), 5.72 (dd, *J* = 12.1, 4.9 Hz, 1H), 5.14 (m, 1H), 3.86 (s, 3H), 3.74 (s, 3H), 2.77 (dd, *J* = 10.8, 6.1 Hz, 1H), 2.43 (dd, *J* = 13.6, 4.9 Hz, 1H), 2.30 (m, 2H), 2.21 (m, 1H), 2.20 (s, 1H), 2.14 (s, 3H), 2.13 (m, 1H), 1.81 (m, 1H), 1.66 (m, 3H), 1.45 (s, 3H), 1.12 (s, 3H). $^{13}$C NMR (126 MHz, $CDCl_3$) δ 201.87, 171.57, 171.17, 169.94, 159.85, 151.47, 142.11, 131.25, 129.91, 119.46, 114.88, 111.86, 110.21, 74.99, 71.96, 64.03, 55.36, 53.61, 52.02, 51.68, 43.29, 42.12, 38.22, 35.56, 30.76, 20.56, 18.18, 16.47, 15.09. HRMS calculated for $C_{30}H_{34}O_9$: $[M+Na]^+$: 561.2092 (found); 561.2101 (calc). Melting point 165-167°C.

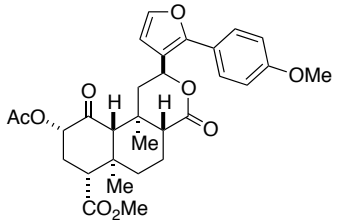

32

**(2*S*,4a*R*,6a*R*,7*R*,9*S*,10a*S*,10b*R*)-Methyl 9-acetoxy-2-(2-(4-methoxyphenyl)furan-3-yl)-6a,10b-dimethyl-4,10-dioxododecahydro-1*H*-benzo[*f*]isochromene-7-carboxylate.** $^{1}$H NMR (500 MHz, $CDCl_3$) δ 7.49 (d, *J* = 8.9 Hz, 2H), 7.40 (d, *J* = 2.0 Hz, 1H), 6.98 (d, *J* = 8.8 Hz, 2H), 6.46 (d, *J* = 2.0 Hz, 1H), 5.63 (dd, *J* = 12.0, 5.0 Hz, 1H), 5.14 (m, 1H), 3.86 (s, 3H), 3.73 (s, 3H), 2.77 (m, 1H), 2.40 (dd, *J* =

13.6, 5.0 Hz, 1H), 2.30 (s, 1H), 2.29 (m, 1H), 2.20 (m, 2H), 2.14 (s, 3H), 2.12 (m, 1H), 1.81 (dd, *J* = 10.1, 2.9 Hz, 1H), 1.66 (m, 3H), 1.43 (s, 3H), 1.12 (s, 3H). $^{13}$C NMR (126 MHz, $CDCl_3$) δ 201.93, 171.59, 171.30, 169.94, 159.79, 151.96, 141.63, 128.62, 122.76, 118.03, 114.29, 109.99, 75.00, 72.15, 64.04, 55.36, 53.59, 52.01, 51.61, 43.26, 42.13, 38.21, 35.53, 30.76, 20.56, 18.19, 16.45, 15.05. HRMS calculated for $C_{30}H_{34}O_9$: $[M+K]^+$: 577.1863 (found); 577.1840 (calc). Melting point: 118-121°C.

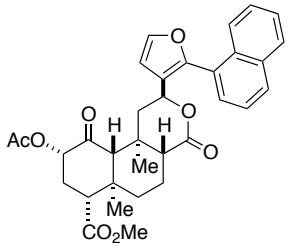


**33**

**(2*S*,4a*R*,6a*R*,7*R*,9*S*,10a*S*,10b*R*)-Methyl 9-acetoxy-6a,10b-dimethyl-2-(2-(naphthalen-1-yl)furan-3-yl)-4,10-dioxododecahydro-1*H*-benzo[*f*]isochromene-7-carboxylate.** $^1$H NMR (500 MHz, $CDCl_3$) δ 7.94 (m, 1H), 7.91 (m, 1H), 7.85 (m, 1H), 7.59 (d, *J* = 2.0 Hz, 1H), 7.54 (m, 4H), 6.58 (d, *J* = 2.0 Hz, 1H), 5.43 (dd, *J* = 11.7, 5.2 Hz, 1H), 5.09 (dd, *J* = 11.7, 8.4 Hz, 1H), 3.72 (s, 3H), 2.71 (dd, *J* = 11.8, 5.0 Hz, 1H), 2.36 (dd, *J* = 13.7, 5.2 Hz, 1H), 2.27 (m, 2H), 2.16 (m, 1H), 2.14 (s, 3H), 2.10 (s, 1H), 2.05 (dd, *J* = 11.1, 3.1 Hz, 1H), 1.77 (dd, *J* = 10.1, 3.0 Hz, 1H), 1.69 (m, 1H), 1.58 (m, 2H), 1.27 (s, 3H), 1.06 (s, 3H). $^{13}$C NMR (126 MHz, $CDCl_3$) δ 201.80, 171.56, 171.27, 169.92, 151.36, 142.79, 133.77, 132.15, 129.91, 128.84, 128.30, 127.01, 126.86, 126.31, 125.83, 125.20, 121.70, 109.71, 74.96, 72.05, 64.01, 53.54, 51.99, 51.40, 43.41, 42.06, 38.16, 35.47, 30.73, 20.58, 18.14, 16.35, 14.99. HRMS calculated for $C_{33}H_{34}O_9$: $[M+Na]^+$: 581.2131 (found); 581.2151 (calc). Melting point: 137-140°C.

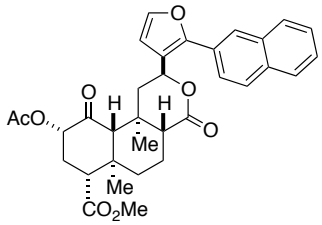

34

**(2*S*,4a*R*,6a*R*,7*R*,9*S*,10a*S*,10b*R*)-Methyl 9-acetoxy-6a,10b-dimethyl-2-(2-(naphthalen-2-yl)furan-3-yl)-4,10-dioxododecahydro-1*H*-benzo[*f*]isochromene-7-carboxylate.** $^{1}$H NMR (500 MHz, $CDCl_3$) δ 8.02 (d, *J* = 0.8 Hz, 1H), 7.92 (d, *J* = 8.8 Hz, 2H), 7.87 (m, 1H), 7.69 (dd, *J* = 8.5, 1.6 Hz, 1H), 7.52 (m, 2H), 7.50 (d, *J* = 1.9 Hz, 1H), 6.53 (d, *J* = 1.9 Hz, 2H), 5.79 (dd, *J* = 12.0, 4.9 Hz, 1H), 5.14 (m, 1H), 3.73 (s, 3H), 2.77 (m, 1H), 2.47 (dd, *J* = 13.7, 4.9 Hz, 1H), 2.29 (m, 2H), 2.17 (m, 3H), 2.13 (s, 3H), 1.81 (m, 1H), 1.74 (m, 1H), 1.65 (m, 2H), 1.46 (s, 3H), 1.12 (s, 3H). $^{13}$C NMR (126 MHz, $CDCl_3$) δ 201.85, 171.56, 171.24, 169.93, 151.68, 142.37, 133.23, 132.99, 128.60, 128.46, 127.73, 127.46, 126.61, 126.60, 126.38, 124.68, 119.72, 110.39, 74.98, 72.12, 64.02, 53.60, 52.01, 51.72, 43.34, 42.12, 38.22, 35.57, 30.76, 20.56, 18.20, 16.48, 15.10. HRMS calculated for $C_{33}H_{34}O_8$: $[M+K]^+$: 597.1896 (found); 597.1891 (calc). Melting point: 160-163°C.

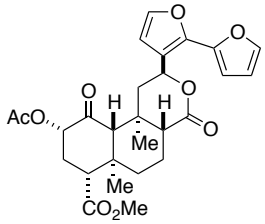

35

**(2*S*,4a*R*,6a*R*,7*R*,9*S*,10a*S*,10b*R*)-Methyl 2-([2,2'-bifuran]-3-yl)-9-acetoxy-6a,10b-dimethyl-4,10-dioxododecahydro-1*H*-benzo[*f*]isochromene-7-carboxylate.** $^{1}$H NMR (500 MHz, $CDCl_3$) δ 7.47 (dd, *J* = 1.7, 0.7 Hz, 1H), 7.36 (d, *J* = 1.9 Hz, 1H), 6.60 (dd, *J* = 3.4, 0.6 Hz, 1H), 6.48 (dd, *J* = 3.4, 1.8 Hz, 1H), 6.43 (d, *J* = 1.9 Hz, 1H), 6.04 (dd, *J* = 12.0, 5.0 Hz, 1H), 5.12 (m, 1H), 3.73 (s, 3H), 2.76 (m, 1H), 2.48

(dd, *J* = 13.6, 5.1 Hz, 1H), 2.30 (m, 2H), 2.20 (m, 2H), 2.15 (m, 1H), 2.14 (s, 3H), 1.81 (m, 1H), 1.64 (m, 3H), 1.51 (s, 3H), 1.13 (s, 3H). $^{13}$C NMR (126 MHz, $CDCl_3$) δ 201.91, 171.59, 171.31, 169.91, 145.77, 142.62, 142.53, 142.01, 119.81, 111.38, 110.18, 107.45, 74.99, 71.75, 64.04, 53.61, 52.00, 51.62, 43.67, 42.13, 38.26, 35.61, 30.78, 20.57, 18.19, 16.47, 15.09. HRMS calculated for $C_{27}H_{30}O_9$: $[M+Na]^+$: 521.1804 (found); 521.1788 (calc). Melting point: 240-245°C.

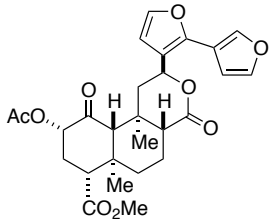

**36**

**(2*S*,4a*R*,6a*R*,7*R*,9*S*,10a*S*,10b*R*)-Methyl 2-([2,3'-bifuran]-3-yl)-9-acetoxy-6a,10b-dimethyl-4,10-dioxododecahydro-1*H*-benzo[*f*]isochromene-7-carboxylate.** $^1$H NMR (500 MHz, $CDCl_3$) δ 7.71 (m, 1H), 7.49 (t, *J* = 1.7 Hz, 1H), 7.37 (d, *J* = 2.0 Hz, 1H), 6.65 (dd, *J* = 1.8, 0.7 Hz, 1H), 6.43 (d, *J* = 2.0 Hz, 1H), 5.61 (dd, *J* = 12.0, 4.9 Hz, 1H), 5.14 (m, 1H), 3.74 (s, 3H), 2.77 (m, 1H), 2.40 (dd, *J* = 13.6, 4.9 Hz, 1H), 2.30 (m, 2H), 2.16 (m, 3H), 2.15 (s, 3H), 1.81 (m, 1H), 1.64 (m, 3H), 1.48 (s, 3H), 1.13 (s, 3H). $^{13}$C NMR (126 MHz, $CDCl_3$) δ 201.91, 171.56, 171.14, 169.96, 145.23, 143.66, 141.72, 139.85, 119.03, 116.20, 109.73, 108.84, 74.99, 71.68, 64.03, 53.60, 52.02, 51.64, 43.02, 42.11, 38.19, 35.51, 30.75, 20.57, 18.16, 16.48, 15.13. HRMS calculated for $C_{27}H_{30}O_9$: $[M+Na]^+$: 521.1793 (found); 521.1788 (calc). Melting point: 235°C (dec.).

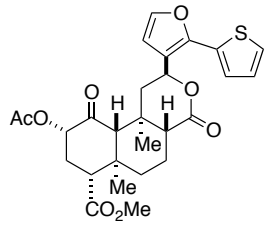

37

**(2*S*,4a*R*,6a*R*,7*R*,9*S*,10a*S*,10b*R*)-Methyl 9-acetoxy-6a,10b-dimethyl-4,10-dioxo-2-(2-(thiophen-2-yl)furan-3-yl)dodecahydro-1*H*-benzo[*f*]isochromene-7-carboxylate.** An oven-dried conical vial was cooled under a stream of argon and charged with **4** (60 mg, 0.117 mmol), $Pd(OAc)_2$ (1.3 mg, 0.0059 mmol), SPhos (4.8 mg, 0.012 mmol), and 2-thiopheneboronic acid MIDA ester (33.7 mg, 0.141 mmol). The vial was sealed with a Biotage Reseal cap and flushed with argon for 5 min before adding toluene (1.6 mL) through the septum. After stirring at room temperature for 10 min., a solution of $K_3PO_4$ (aq., 3.0 M, 0.880 mmol) the reaction was heated to 65°C for 24 hrs. The reaction was cooled to room temperature, diluted with a 10% NaOH solution (1 mL) and extracted with $Et_2O$ (3 x 10 mL). Combined organic layers were dried over $Na_2SO_4$ and concentrated in vacuo. The resulting residue was purified by FCC eluting with 35% EtOAc/Pent to yield **37** as a white solid (28.3 mg, 47%) and **4** (13.2 mg, 22%). $^1$H NMR (500 MHz, $CDCl_3$) δ 7.38 (d, *J* = 1.9 Hz, 1H), 7.36 (dd, *J* = 5.1, 1.1 Hz, 1H), 7.27 (m, 1H), 7.10 (dd, *J* = 5.1, 3.7 Hz, 1H), 6.46 (d, *J* = 1.9 Hz, 1H), 5.80 (dd, *J* = 12.1, 4.9 Hz, 1H), 5.14 (m, 1H), 3.73 (s, 3H), 2.77 (m, 1H), 2.45 (dd, *J* = 13.6, 4.9 Hz, 1H), 2.30 (m, 2H), 2.20 (m, 2H), 2.14 (s, 3H), 2.14 (m, 1H), 1.81 (m, 1H), 1.65 (m, 3H), 1.49 (s, 3H), 1.13 (s, 3H). $^{13}$C NMR (126 MHz, $CDCl_3$) δ 200.85, 170.55, 170.15, 168.90, 145.18, 140.92, 130.52, 126.65, 125.01, 124.35, 118.35, 109.26, 73.93, 70.84, 62.97, 52.56, 50.98, 50.66, 42.10, 41.08, 37.17, 34.57, 29.74, 19.55, 17.14,

15.47, 14.09. HRMS calculated for $C_{27}H_{30}O_8S$: $[M+MeOH+Na]^+$: 569.1830 (found); 569.1821 (calc). Melting point: 230-232°C.

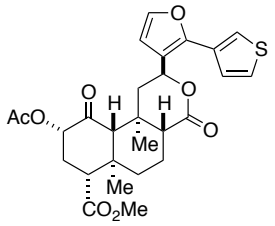

**38**

**(2*S*,4a*R*,6a*R*,7*R*,9*S*,10a*S*,10b*R*)-Methyl 9-acetoxy-6a,10b-dimethyl-4,10-dioxo-2-(2-(thiophen-3-yl)furan-3-yl)dodecahydro-1*H*-benzo[*f*]isochromene-7-carboxylate.** $^1$H NMR (500 MHz, $CDCl_3$) δ 7.49 (dd, *J* = 2.9, 1.2 Hz, 1H), 7.41 (dd, *J* = 5.0, 3.0 Hz, 1H), 7.38 (d, *J* = 1.9 Hz, 1H), 7.33 (dd, *J* = 5.0, 1.2 Hz, 1H), 6.45 (d, *J* = 1.9 Hz, 1H), 5.71 (dd, *J* = 12.0, 4.9 Hz, 1H), 5.14 (m, 1H), 3.74 (s, 3H), 2.77 (m, 1H), 2.42 (dd, *J* = 13.7, 5.0 Hz, 1H), 2.30 (m, 2H), 2.19 (m, 3H), 2.15 (s, 3H), 1.81 (m, 1H), 1.66 (m, 3H), 1.47 (s, 3H), 1.13 (s, 3H). $^{13}$C NMR (126 MHz, $CDCl_3$) δ 201.91, 171.57, 171.19, 169.94, 148.17, 141.53, 130.94, 126.47, 126.10, 122.58, 118.70, 109.88, 74.98, 71.83, 64.05, 53.60, 52.02, 51.65, 43.06, 42.12, 38.20, 35.54, 30.76, 20.57, 18.18, 16.48, 15.13. HRMS HRMS calculated for $C_{27}H_{30}O_8S$: $[M+K]^+$: 553.1292 (found); 553.1299. Melting point: 244-245°C (dec.).

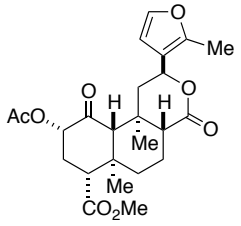

**39**

**(2*S*,4a*R*,6a*R*,7*R*,9*S*,10a*S*,10b*R*)-Methyl 9-acetoxy-6a,10b-dimethyl-2-(2-methylfuran-3-yl)-4,10-dioxododecahydro-1*H*-benzo[*f*]isochromene-7-carboxylate.** $^1$H NMR (500 MHz, $CDCl_3$) δ 7.24 (d, *J* = 1.9 Hz, 1H), 6.25 (d, *J* = 1.9 Hz, 1H), 5.45 (dd, *J* = 12.0, 5.1 Hz, 1H), 5.13 (m, 1H), 3.73 (s, 3H), 2.77 (dd, *J* = 9.7, 7.1 Hz,

1H), 2.32 (m, 3H), 2.27 (s, 3H), 2.18 (m, 2H), 2.16 (s, 3H), 2.08 (m, 1H), 1.80 (m, 1H), 1.63 (m, 3H), 1.47 (s, 3H), 1.12 (s, 3H). $^{13}$C NMR (126 MHz, $CDCl_3$) δ 202.06, 171.57, 171.32, 169.97, 149.48, 140.92, 118.25, 108.64, 75.07, 72.08, 64.03, 53.61, 52.01, 51.55, 43.66, 42.16, 38.21, 35.50, 30.76, 20.57, 18.16, 16.42, 15.04, 11.89. HRMS calculated for $C_{24}H_{30}O_8$: $[M+Na]^+$: 485.1584 (found); 485.1578 (calc). Melting point: 112-116°C.

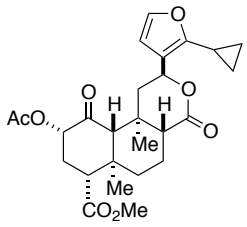


**40**

**(2*S*,4a*R*,6a*R*,7*R*,9*S*,10a*S*,10b*R*)-Methyl 9-acetoxy-2-(2-cyclopropylfuran-3-yl)-6a,10b-dimethyl-4,10-dioxododecahydro-1*H*-benzo[*f*]isochromene-7-carboxylate.** $^1$H NMR (500 MHz, $CDCl_3$) δ 7.14 (d, *J* = 1.9 Hz, 1H), 6.24 (d, *J* = 2.0 Hz, 1H), 5.63 (dd, *J* = 12.0, 5.1 Hz, 1H), 5.14 (m, 1H), 3.73 (s, 3H), 2.77 (m, 1H), 2.39 (dd, *J* = 13.6, 5.1 Hz, 1H), 2.31 (s, 1H), 2.30 (dd, *J* = 13.5, 7.0 Hz, 1H), 2.18 (m, 2H), 2.16 (s, 3H), 2.09 (dd, *J* = 11.5, 3.0 Hz, 1H), 1.83 (m, 2H), 1.64 (m, 3H), 1.48 (s, 3H), 1.12 (s, 3H), 0.89 (m, 4H). $^{13}$C NMR (126 MHz, $CDCl_3$) δ 202.08, 171.59, 171.43, 169.97, 153.32, 140.03, 118.27, 108.91, 75.07, 71.91, 64.05, 53.61, 52.01, 51.55, 43.70, 42.16, 38.22, 35.53, 30.77, 20.58, 18.18, 16.43, 15.06, 7.41, 6.61, 6.50. HRMS calculated for $C_{26}H_{32}O_8$: $[M+K]^+$: 549.0499 (found); 549.0526 (calc). Melting point: 130-133°C.

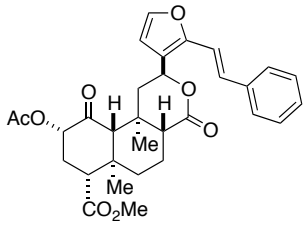

41

**(2*S*,4a*R*,6a*R*,7*R*,9*S*,10a*S*,10b*R*)-Methyl 9-acetoxy-6a,10b-dimethyl-4,10-dioxo-2-(2-((*E*)-styryl)furan-3-yl)dodecahydro-1*H*-benzo[*f*]isochromene-7-carboxylate.** $^{1}$H NMR (500 MHz, $CDCl_3$) δ 7.49 (d, *J* = 7.3 Hz, 2H), 7.36 (dd, *J* = 8.5, 6.7 Hz, 3H), 7.10 (d, *J* = 16.1 Hz, 1H), 6.89 (d, *J* = 16.1 Hz, 1H), 6.38 (d, *J* = 1.9 Hz, 1H), 5.67 (dd, *J* = 11.9, 5.1 Hz, 1H), 5.14 (m, 1H), 3.73 (s, 3H), 2.77 (dd, *J* = 9.7, 7.1 Hz, 1H), 2.44 (dd, *J* = 13.6, 5.1 Hz, 1H), 2.30 (s, 1H), 2.30 (dd, *J* = 13.5, 7.1 Hz, 1H), 2.16 (m, 3H), 2.15 (s, 3H), 1.81 (m, 1H), 1.61 (m, 3H), 1.51 (s, 3H), 1.13 (s, 3H). $^{13}$C NMR (126 MHz, $CDCl_3$) δ 201.99, 171.56, 171.11, 169.93, 149.68, 142.19, 136.65, 128.92, 128.72, 127.97, 126.63, 121.01, 113.66, 110.07, 75.02, 71.58, 63.99, 53.59, 52.02, 51.58, 43.73, 42.14, 38.17, 35.61, 30.76, 20.56, 18.17, 16.44, 15.15. HRMS calculated for $C_{31}H_{34}O_8$: $[M+K]^+$: 573.1876 (found); 573.1891 (calc). Melting point: 170-172°C.

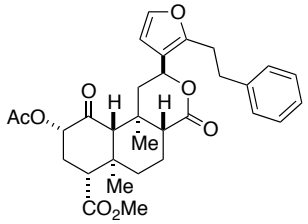

42

**(2*S*,4a*R*,6a*R*,7*R*,9*S*,10a*S*,10b*R*)-Methyl 9-acetoxy-6a,10b-dimethyl-4,10-dioxo-2-(2-phenethylfuran-3-yl)dodecahydro-1*H*-benzo[*f*]isochromene-7-carboxylate.** $^{1}$H NMR (500 MHz, $CDCl_3$) δ 7.27 (m, 5H), 7.05 (d, *J* = 8.3 Hz, 1H), 6.20 (d, *J* = 2.0 Hz, 1H), 5.13 (m, 2H), 3.73 (s, 3H), 2.91 (m, 4H), 2.73 (dd, *J* = 11.7, 5.1 Hz, 1H), 2.29 (m, 2H), 2.19 (s, 3H), 2.15 (m, 1H), 2.04 (s, 1H),

1.94 (ddd, *J* = 13.5, 12.4, 3.8 Hz, 2H), 1.77 (m, 1H), 1.59 (m, 3H), 1.32 (s, 3H), 1.08 (s, 3H). $^{13}$C NMR (126 MHz, $CDCl_3$) δ 201.67, 171.59, 171.27, 169.94, 151.92, 141.14, 140.86, 128.52, 128.49, 126.40, 119.11, 108.64, 75.01, 71.96, 63.82, 53.62, 51.99, 51.35, 43.48, 42.11, 38.17, 35.34, 34.63, 30.79, 28.74, 20.61, 18.09, 16.34, 14.88. HRMS calculated for $C_{31}H_{36}O_8$: $[M+K]^+$: 575.2057 (found); 575.2047 (calc). Melting point: 149-151°C.

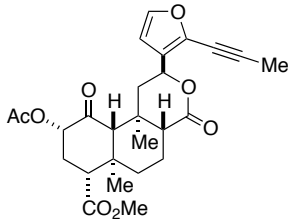

**43**

**(2*S*,4a*R*,6a*R*,7*R*,9*S*,10a*S*,10b*R*)-Methyl 9-acetoxy-6a,10b-dimethyl-4,10-dioxo-2-(2-(prop-1-yn-1-yl)furan-3-yl)dodecahydro-1*H*-benzo[*f*]isochromene-7-carboxylate**. A conical vial was charged with **4** (50.0 mg, 0.0978 mmol), potassium propynyltrifluoroborate (15.7 mg, 0.108 mmol), $Cs_2CO_3$ (95.6 mg, 0.293 mmol), and $PdCl_2(dppf)\cdot CH_2Cl_2$ (7.2 mg, 0.0088 mmol). The vial was fitted with a Biotage Reseal cap and flushed with argon for 5 min before the addition of THF (1.0 mL) and argon-sparged $H_2O$ (0.05 mL). The reaction was heated to 65 °C for 16 h and then cooled to room temperature. The layers were separated, and the organic layer was filtered through a thin pad of silica, with rinsing with EtOAc. Solvent was removed in vacuo and residue purified by FCC eluting with 30% EtOAc/Pent to yield **43** (20.7 mg, 45%) as a white solid. $^1$H NMR (500 MHz, $CDCl_3$) δ 7.26 (d, *J* = 2.0 Hz, 1H), 6.35 (d, *J* = 2.0 Hz, 1H), 5.57 (dd, *J* = 11.7, 5.3 Hz, 1H), 5.13 (m, 1H), 3.73 (s, 3H), 2.76 (m, 1H), 2.48 (dd, *J* = 13.6, 5.4 Hz, 1H), 2.31 (m, 1H), 2.30 (s, 1H), 2.18 (m, 2H), 2.16 (s, 3H), 2.11 (s, 3H), 2.10 (m, 1H), 1.80 (m, 1H), 1.62 (m, 3H), 1.47 (s, 3H), 1.12 (s, 3H). $^{13}$C

NMR (126 MHz, $CDCl_3$) δ 201.98, 171.56, 171.11, 169.90, 142.89, 127.10, 109.16, 94.61, 75.02, 72.02, 68.53, 64.01, 53.60, 52.01, 51.50, 43.22, 42.12, 38.21, 35.53, 30.75, 20.56, 18.16, 16.39, 15.07, 4.67. HRMS calculated for $C_{26}H_{30}O_8$: $[M+Na]^+$: 493.1828 (found); 493.1838 (calc). Melting point: 210-212 °C (dec.)

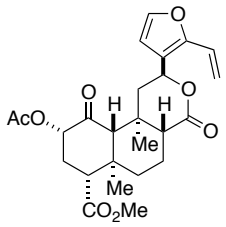

**5**

**(2*S*,4a*R*,6a*R*,7*R*,9*S*,10a*S*,10b*R*)-Methyl 9-acetoxy-6a,10b-dimethyl-4,10-dioxo-2-(2-vinylfuran-3-yl)dodecahydro-1*H*-benzo[*f*]isochromene-7-carboxylate.** A conical vial was charged with **4** (50.0 mg, 0.0978 mmol), potassium vinyltrifluoroborate (14.4 mg, 0.108 mmol), $Cs_2CO_3$ (95.6 mg, 0.293 mmol), and $PdCl_2(dppf)\cdot CH_2Cl_2$ (7.2 mg, 0.0088 mmol). The vial was fitted with a Biotage Reseal cap and flushed with argon for 5 min before the addition of THF (1.0 mL) and argon-sparged $H_2O$ (0.05 mL). The reaction was heated to 65 °C for 16 h and then cooled to room temperature. The layers were separated, and the organic layer was filtered through a thin pad of silica, with rinsing with EtOAc. Solvent was removed in vacuo and residue purified by FCC eluting with 30% EtOAc/Pent to yield **43** (10.5 mg, 23%) as a white solid that was spectroscopically identical to that prepared by Beguin *et. al*.[4]

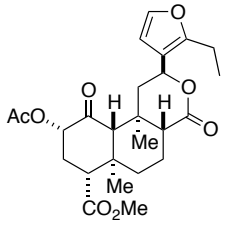

**44**

**(2*S*,4a*R*,6a*R*,7*R*,9*S*,10a*S*,10b*R*)-Methyl 9-acetoxy-2-(2-ethylfuran-3-yl)-6a,10b-dimethyl-4,10-dioxododecahydro-1*H*-benzo[*f*]isochromene-7-carboxylate.**

Synthesized from **5** (23.0 mg, 0.0502 mmol) using general procedure for reduction to yield **44** (20.3 mg, 88%) as a white solid. $^{1}$H NMR (500 MHz, $CDCl_3$): δ 7.26 (d, J = 1.96 Hz, 1H), 6.25 (d, J = 1.96 Hz, 1H), 5.47 (dd, J = 5.10, 11.97 Hz, 1H), 5.13 (m, 1H), 3.73 (s, 3H), 2.77 (m, 1H), 2.63 (ddd, J = 4.66, 7.57, 15.09 Hz, 2H), 2.32 (m, 3H), 2.17 (m, 2H), 2.16 (s, 3H), 2.09 (dd, J = 2.98, 11.41 Hz, 1H), 1.80 (m, 1H), 1.61 (m, 3H), 1.46 (s, 3H), 1.22 (t, J = 7.56 Hz, 3H), 1.12 (s, 3H). $^{13}$C NMR (126 MHz, CDCl3): δ 202.05, 171.58, 171.34, 169.94, 154.47, 140.96, 117.41, 108.51, 75.04, 71.89, 64.01, 53.58, 52.00, 51.50, 43.83, 42.14, 38.20, 35.50, 30.76, 20.57, 19.69, 18.16, 16.41, 15.04, 12.94. HRMS calculated for $C_{25}H_{32}O_8$: $[M+Na]^+$: 483.1973 (found); 483.1995 (calc). Melting point: 160–162 °C (dec).

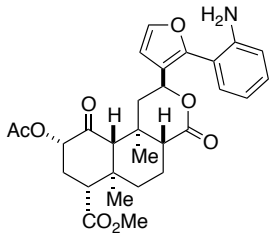

**45**

**(2*S*,4a*R*,6a*R*,7*R*,9*S*,10a*S*,10b*R*)-Methyl 9-acetoxy-2-(2-(2-aminophenyl)furan-3-yl)-6a,10b-dimethyl-4,10-dioxododecahydro-1*H*-benzo[*f*]isochromene-7-carboxylate.** Synthesized from **21** (34.9 mg, 0.0630 mmol) using general reduction procedure to yield **45** (20.1 mg, 61%) as a white solid. 1H NMR (500 MHz, CDCl3): δ 7.48 (d, J = 1.87 Hz, 1H), 7.20 (m, 2H), 6.80 (td, J = 1.05, 7.53 Hz, 1H), 6.76 (d, J = 7.99 Hz, 1H), 6.49 (d, J = 1.99 Hz, 1H), 5.54 (dd, J = 5.15, 11.84 Hz, 1H), 5.12 (dd, J = 9.67, 10.47 Hz, 1H), 4.07 (s, 2H), 3.73 (s, 3H), 2.75 (m, 1H), 2.36 (dd, J = 5.18, 13.62 Hz, 1H), 2.29 (s, 1H), 2.29 (m, 1H), 2.15 (m, 2H), 2.14 (s, 3H), 2.08 (dd, J = 2.86, 11.31 Hz, 1H), 1.79 (dd, J = 2.97, 10.10 Hz, 1H), 1.62 (m, 3H), 1.37 (s, 3H), 1.09 (s, 3H). 13C NMR (126 MHz, $CDCl_3$): δ 201.85, 171.57, 171.29, 169.96,

150.43, 145.32, 142.41, 130.84, 130.44, 120.69, 118.17, 116.08, 114.58, 109.87, 75.00, 72.00, 64.03, 53.59, 52.00, 51.47, 43.28, 42.11, 38.21, 35.52, 30.74, 20.58, 18.16, 16.39, 15.03. HRMS calculated for $C_{29}H_{33}O_8$: $[M+Na]^+$: 546.2097 (found); 546.2104 (calc). Melting point: 200– 202 °C (dec).

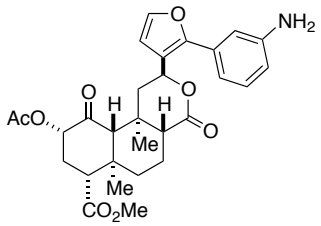

**46**

**(2*S*,4a*R*,6a*R*,7*R*,9*S*,10a*S*,10b*R*)-Methyl 9-acetoxy-2-(2-(3-aminophenyl)furan-3-yl)-6a,10b-dimethyl-4,10-dioxododecahydro-1*H*-benzo[*f*]isochromene-7-carboxylate.** Synthesized from **22** (30.3 mg, 0.0547 mmol) using general reduction procedure to yield **46** (17.8 mg, 62%) as a solid. $^1$H NMR (500 MHz, $CDCl_3$): δ 7.41 (d, J = 1.90 Hz, 1H), 7.23 (t, J = 7.83 Hz, 1H), 6.92 (m, 1H), 6.88 (m, 1H), 6.69 (ddd, J = 0.88, 2.36, 8.02 Hz, 1H), 6.46 (d, J = 1.95 Hz, 1H), 5.70 (dd, J = 5.00, 12.01 Hz, 1H), 5.14 (m, 1H), 3.73 (s, 3H), 2.77 (m, 1H), 2.40 (dd, J = 5.02, 13.66 Hz, 1H), 2.29 (m, 2H), 2.21 (m, 2H), 2.14 (s, 3H), 2.12 (m, 1H), 1.80 (m, 1H), 1.65 (m, 3H), 1.44 (s, 3H), 1.11 (s, 3H). $^{13}$C NMR (126 MHz, $CDCl_3$): δ 201.90, 171.59, 171.33, 169.94, 151.91, 146.77, 141.92, 130.98, 129.79, 119.12, 117.48, 115.26, 113.49, 110.15, 74.98, 72.05, 64.01, 53.58, 52.00, 51.62, 43.28, 42.11, 38.20, 35.53, 30.76, 20.57, 18.18, 16.45, 15.09. HRMS calculated for $C_{29}H_{33}O_8$: $[M+Na]^+$: 546.2089 (found); 546.2104 (calc). Melting point: 123–127 °C.

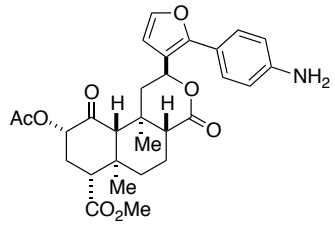

47

**(2*S*,4a*R*,6a*R*,7*R*,9*S*,10a*S*,10b*R*)-Methyl 9-acetoxy-2-(2-(4-aminophenyl)furan-3-yl)-6a,10b-dimethyl-4,10-dioxododecahydro-1*H*-benzo[*f*]isochromene-7-carboxylate.** Synthesized from **23** (63.2 mg, 0.114 mmol) using general reduction procedure to yield **47** (49.6 mg, 83%) as a white solid. $^{1}$H NMR (500 MHz, $CDCl_3$): δ 7.36 (m, 3H), 6.74 (d, J = 8.65 Hz, 2H), 6.43 (d, J = 1.98 Hz, 1H), 5.62 (dd, J = 5.00, 11.99 Hz, 1H), 5.14 (m, 1H), 3.83 (s, 2H), 3.73 (s, 3H), 2.77 (m, 1H), 2.39 (dd, J = 5.01, 13.66 Hz, 1H), 2.29 (m, 2H), 2.21 (m, 2H), 2.14 (s, 3H), 2.12 (m, 1H), 1.80 (m, 1H), 1.64 (m, 3H), 1.43 (s, 3H), 1.11 (s, 3H). $^{13}$C NMR (126 MHz, $CDCl_3$): δ 201.92, 171.60, 171.40, 169.92, 152.62, 146.79, 141.22, 128.58, 120.46, 117.24, 115.08, 109.90, 74.99, 72.31, 64.06, 53.59, 52.00, 51.59, 43.25, 42.12, 38.22, 35.52, 30.77, 20.57, 18.19, 16.44, 15.05. HRMS calculated for $C_{29}H_{33}O_8$: $[M+Na]^+$: 546.2112 (found); 546.2104 (calc). Melting point: 222– 223 °C (dec).

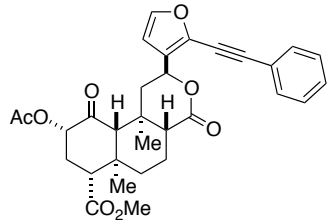

48

**(2*S*,4a*R*,6a*R*,7*R*,9*S*,10a*S*,10b*R*)-Methyl 9-acetoxy-6a,10b-dimethyl-4,10-dioxo-2-(2-(phenylethynyl)furan-3-yl)dodecahydro-1*H*-benzo[*f*]isochromene-7-carboxylate.** $^{1}$H NMR (500 MHz, $CDCl_3$) δ 7.53 (m, 2H), 7.37 (dd, *J* = 6.4, 2.6 Hz, 4H), 6.42 (d, *J* = 1.9 Hz, 1H), 5.66 (dd, *J* = 11.8, 5.4 Hz, 1H), 5.11 (m, 1H), 3.72 (s, 3H), 2.72 (m, 1H), 2.55 (dd, *J* = 13.6, 5.4 Hz, 1H), 2.29 (s, 1H), 2.29

(dd, *J* = 13.6, 6.7 Hz, 1H), 2.17 (m, 3H), 2.15 (s, 3H), 1.79 (dt, *J* = 13.3, 2.9 Hz, 1H), 1.65 (m, 3H), 1.49 (s, 3H), 1.12 (s, 3H). $^{13}$C NMR (126 MHz, $CDCl_3$) δ 201.95, 171.55, 171.08, 169.89, 143.77, 134.58, 131.58, 129.05, 128.90, 128.48, 121.85, 109.72, 97.20, 77.64, 75.01, 72.13, 63.95, 53.55, 52.00, 51.53, 43.33, 42.09, 38.15, 35.59, 30.74, 20.56, 18.17, 16.39, 15.06. HRMS calculated for $C_{31}H_{32}O_8$: $[M+Na]^+$: 555.1982 (found); 555.1995 (calc). Melting point 110-113°C.

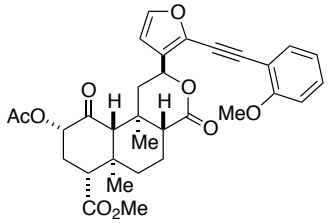


**49**

**(2*S*,4a*R*,6a*R*,7*R*,9*S*,10a*S*,10b*R*)-Methyl 9-acetoxy-2-(2-((2-methoxyphenyl)ethynyl)furan-3-yl)-6a,10b-dimethyl-4,10-dioxododecahydro-1*H*-benzo[*f*]isochromene-7-carboxylate.** $^{1}$H NMR (500 MHz, $CDCl_3$) δ 7.48 (dd, *J* = 7.6, 1.7 Hz, 1H), 7.35 (m, 2H), 6.96 (td, *J* = 7.5, 0.9 Hz, 1H), 6.92 (d, *J* = 8.3 Hz, 1H), 6.41 (d, *J* = 1.9 Hz, 1H), 5.69 (dd, *J* = 11.7, 5.4 Hz, 1H), 5.10 (m, 1H), 3.92 (s, 3H), 3.72 (s, 3H), 2.71 (dd, *J* = 10.2, 6.7 Hz, 1H), 2.50 (dd, *J* = 13.6, 5.4 Hz, 1H), 2.28 (s, 1H), 2.28 (m, 1H), 2.16 (m, 4H), 2.14 (s, 3H), 1.78 (dt, *J* = 13.4, 3.1 Hz, 1H), 1.72 (m, 1H), 1.64 (m, 1H), 1.49 (s, 3H), 1.11 (s, 3H). $^{13}$C NMR (126 MHz, $CDCl_3$) δ 201.93, 171.58, 171.21, 169.85, 160.17, 143.54, 135.11, 133.29, 130.57, 128.56, 120.54, 111.22, 110.74, 109.82, 93.88, 81.46, 75.00, 72.20, 63.92, 55.87, 53.55, 51.99, 51.38, 43.17, 42.10, 38.15, 35.61, 30.77, 20.56, 18.20, 16.38, 15.07. HRMS calculated for $C_{32}H_{34}O_9$: $[M+K]^+$: 639.1611 (found); 639.1608 (calc). Melting point: 108-110°C.

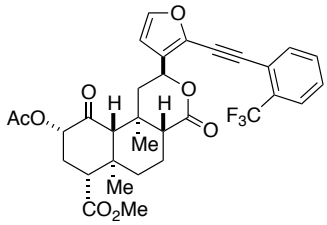

50

**(2*S*,4a*R*,6a*R*,7*R*,9*S*,10a*S*,10b*R*)-Methyl 9-acetoxy-6a,10b-dimethyl-4,10-dioxo-2-(2-((2-(trifluoromethyl)phenyl)ethynyl)furan-3-yl)dodecahydro-1*H*-benzo[*f*]isochromene-7-carboxylate.** $^{1}$H NMR (500 MHz, $CDCl_3$) δ 7.69 (t, *J* = 6.8 Hz, 2H), 7.55 (t, *J* = 7.7 Hz, 1H), 7.46 (t, *J* = 7.7 Hz, 1H), 7.41 (d, *J* = 1.9 Hz, 1H), 6.45 (d, *J* = 1.9 Hz, 1H), 5.72 (dd, *J* = 12.0, 5.1 Hz, 1H), 5.12 (m, 1H), 3.73 (s, 3H), 2.74 (m, 1H), 2.50 (dd, *J* = 13.6, 5.1 Hz, 1H), 2.29 (s, 1H), 2.29 (m, 1H), 2.16 (m, 3H), 2.14 (s, 3H), 1.80 (m, 1H), 1.65 (m, 3H), 1.51 (s, 3H), 1.13 (s, 3H). $^{13}$C NMR (126 MHz, $CDCl_3$) δ 201.68, 171.59, 171.07, 169.90, 144.48, 134.09, 133.68, 131.59, 131.01 (q, $^{2}J_{CF}$=30.64 Hz), 130.13, 128.59, 125.97 ($^{3}J_{CF}$=5.03 Hz), 123.48 ($^{1}J_{CF}$=273.47 Hz), 120.16 ($^{3}J_{CF}$=2.08), 109.84, 93.15, 82.89, 74.98, 71.87, 63.91, 53.63, 51.99, 51.57, 43.36, 42.08, 38.20, 35.65, 30.77, 20.56, 18.14, 16.44, 14.85. $^{19}$F NMR (376 MHz, $CDCl_3$) δ -61.50. HRMS calculated for $C_{32}H_{31}F_3O_8$: $[M+Na]^+$: 585.2113 (found); 585.2101 (calc). Melting point: 112-114°C.

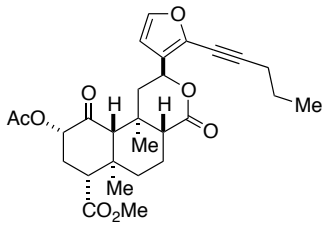

51

**(2*S*,4a*R*,6a*R*,7*R*,9*S*,10a*S*,10b*R*)-Methyl 9-acetoxy-6a,10b-dimethyl-4,10-dioxo-2-(2-(pent-1-yn-1-yl)furan-3-yl)dodecahydro-1*H*-benzo[*f*]isochromene-7-carboxylate.** $^{1}$H NMR (500 MHz, $CDCl_3$) δ 7.26 (d, *J* = 2.2 Hz, 1H), 6.35 (d, *J* = 2.0 Hz, 1H), 5.57 (dd, *J* = 11.8, 5.3 Hz, 1H), 5.13 (m, 1H), 3.73 (s, 3H),

2.75 (m, 1H), 2.47 (dd, *J* = 13.6, 5.2 Hz, 1H), 2.44 (t, *J* = 7.0 Hz, 2H), 2.30 (s, 1H), 2.30 (dd, *J* = 13.5, 7.2 Hz, 1H), 2.18 (m, 2H), 2.16 (s, 3H), 2.10 (dd, *J* = 11.7, 2.9 Hz, 1H), 1.80 (m, 1H), 1.63 (m, 5H), 1.47 (s, 3H), 1.12 (s, 3H), 1.05 (t, *J* = 7.4 Hz, 3H). $^{13}$C NMR (126 MHz, $CDCl_3$) δ 201.93, 171.56, 171.14, 169.89, 142.81, 135.21, 127.13, 109.18, 98.90, 75.00, 72.14, 69.39, 64.00, 53.62, 52.01, 51.54, 43.26, 42.11, 38.22, 35.54, 30.76, 21.77, 21.54, 20.56, 18.16, 16.40, 15.01, 13.59. HRMS calculated for $C_{28}H_{34}O_8$: $[M+Na]^+$: 521.2162 (found); 521.2151 (calc). Melting point: 87-91°C.

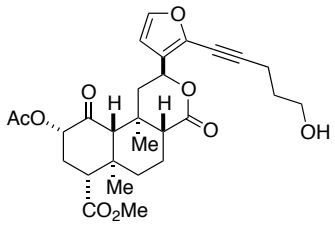

**52**

**(2*S*,4a*R*,6a*R*,7*R*,9*S*,10a*S*,10b*R*)-Methyl 9-acetoxy-2-(2-(5-hydroxypent-1-yn-1-yl)furan-3-yl)-6a,10b-dimethyl-4,10-dioxododecahydro-1*H*-benzo[*f*]isochromene-7-carboxylate.** $^1$H NMR (500 MHz, $CDCl_3$) δ 7.26 (d, *J* = 2.2 Hz, 1H), 6.37 (d, *J* = 1.9 Hz, 1H), 5.58 (dd, *J* = 11.7, 5.4 Hz, 1H), 5.14 (m, 1H), 3.78 (dd, *J* = 10.3, 5.0 Hz, 2H), 3.73 (s, 3H), 2.76 (m, 1H), 2.60 (td, *J* = 6.7, 1.4 Hz, 2H), 2.55 (dd, *J* = 13.6, 5.4 Hz, 1H), 2.30 (s, 1H), 2.30 (dd, *J* = 13.5, 6.7 Hz, 1H), 2.18 (m, 2H), 2.17 (s, 3H), 2.11 (dd, *J* = 11.6, 2.9 Hz, 1H), 1.85 (m, 3H), 1.63 (m, 3H), 1.46 (s, 3H), 1.12 (s, 3H). $^{13}$C NMR (126 MHz, $CDCl_3$) δ 202.37, 171.55, 171.28, 170.19, 142.79, 134.21, 127.95, 109.38, 98.28, 75.04, 72.36, 69.98, 63.94, 61.13, 53.51, 52.01, 51.48, 43.10, 42.11, 38.15, 35.46, 30.80, 30.74, 20.58, 18.16, 16.42, 16.00, 15.12. HRMS calculated for $C_{28}H_{34}O_9$: $[M+Na]^+$: 537.2090 (found); 537.2101 (calc). Melting point 80-84°C.

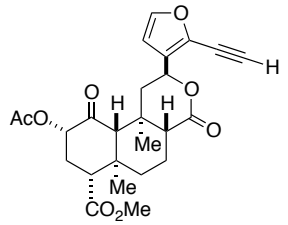

**53**

**(2*S*,4a*R*,6a*R*,7*R*,9*S*,10a*S*,10b*R*)-Methyl 9-acetoxy-2-(2-ethynylfuran-3-yl)-6a,10b-dimethyl-4,10-dioxododecahydro-1*H*-benzo[*f*]isochromene-7-carboxylate.** The silyl-protected alkyne was prepared according to general Sonogashira proceduring using **4** (75 mg, 0.147 mmol), $PdCl_2(PPh_3)_2$ (5.1 mg, 0.0073 mmol), CuI (2.8 mg, 0.015 mmol), and ethynyltrimethylsilane (0.03 mL, 0.22 mmol) in THF/$NEt_3$ (1:1, 2 mL). Reaction residue was purified by column chromatography (30% EtOAc/Pent.) to produce an inseparable mixture (42.8 mg). The resulting mixture was dissolved in $CH_2Cl_2$ (10 mL) and a solution of TBAF in THF (0.16 mL, 0.16 mmol) was added dropwise. After stirring for 30 min., reaction concentrated in vacuo. The residue was purified by column chromatography (30 to 33% EtOAc/Pent.) to yield **53** as a white solid (11 mg, 16%). $^1$H NMR (500 MHz, $CDCl_3$) δ 7.33 (d, *J* = 1.9 Hz, 1H), 6.40 (d, *J* = 1.9 Hz, 1H), 5.59 (dd, *J* = 11.6, 5.3 Hz, 1H), 5.13 (m, 1H), 3.73 (s, 3H), 3.61 (s, 1H), 2.76 (dd, *J* = 9.5, 7.4 Hz, 1H), 2.50 (dd, *J* = 13.6, 5.4 Hz, 1H), 2.30 (m, 2H), 2.17 (m, 2H), 2.16 (s, 3H), 2.11 (dd, *J* = 11.6, 2.8 Hz, 1H), 1.80 (m, 1H), 1.63 (m, 3H), 1.47 (s, 3H), 1.12 (s, 3H). $^{13}$C NMR (126 MHz, $CDCl_3$) δ 201.95, 171.55, 171.01, 169.94, 143.97, 133.53, 130.11, 109.52, 85.97, 75.04, 72.30, 71.80, 63.96, 53.60, 52.01, 51.42, 43.01, 42.14, 38.17, 35.52, 30.74, 20.57, 18.13, 16.40, 15.19. HRMS calculated for $C_{25}H_{28}O_8$: $[M+K]^+$: 495.1407 (found); 495.1421 (calc). Melting point: 170-173°C.

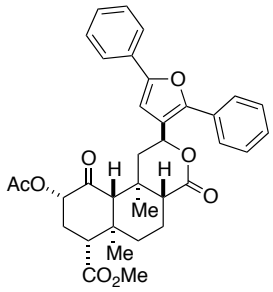


**54**

**(2*S*,4a*R*,6a*R*,7*R*,9*S*,10a*S*,10b*R*)-Methyl 9-acetoxy-2-(2,5-diphenylfuran-3-yl)-6a,10b-dimethyl-4,10-dioxododecahydro-1*H*-benzo[*f*]isochromene-7-carboxylate.** Prepared according to general procedure for Suzuki-Miyaura reaction using 1**5** (60.5 mg, 0.103 mmol), $PhB(OH)_2$ (12.5 mg, 0.103 mmol), $Pd_2dba_3$ (3.8 mg, 0.0041 mmol), SPhos (6.7 mg, 0.016 mmol), and $K_3PO_4$ (65.3 mg, 0.308 mmol). Purification of the reaction mixture by column chromatography yielded **15** (19.2 mg, 32%) and **54** (24.4 mg, 40%) as white solids. $^1$H NMR (500 MHz, $CDCl_3$) δ 7.71 (m, 2H), 7.64 (dd, *J* = 8.1, 1.0 Hz, 2H), 7.48 (t, *J* = 7.6 Hz, 2H), 7.40 (m, 3H), 7.29 (m, 1H), 6.76 (s, 1H), 5.73 (dd, *J* = 12.0, 5.0 Hz, 1H), 5.15 (m, 1H), 3.74 (s, 3H), 2.78 (dd, *J* = 10.6, 6.3 Hz, 1H), 2.48 (dd, *J* = 13.7, 5.0 Hz, 1H), 2.30 (m, 2H), 2.19 (m, 3H), 2.13 (s, 3H), 1.81 (m, 2H), 1.64 (m, 2H), 1.47 (s, 3H), 1.13 (s, 3H). $^{13}$C NMR (126 MHz, $CDCl_3$) δ 201.90, 171.56, 171.18, 169.89, 153.31, 150.91, 130.19, 130.02, 128.90, 128.72, 128.44, 127.79, 127.00, 123.91, 121.44, 105.48, 74.98, 72.04, 64.10, 53.65, 52.02, 51.71, 43.29, 42.14, 38.25, 35.62, 30.78, 20.55, 18.21, 16.47, 15.09. HRMS calculated for $C_{35}H_{36}O_8$: $[M+Na]^+$: 607.2328 (found); 607.2308 (calc). Melting point: 210-215°C.

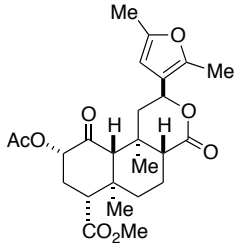

55

**(2*S*,4a*R*,6a*R*,7*R*,9*S*,10a*S*,10b*R*)-Methyl 9-acetoxy-2-(2,5-dimethylfuran-3-yl)-6a,10b-dimethyl-4,10-dioxododecahydro-1*H*-benzo[*f*]isochromene-7-carboxylate.** Prepared according to general Suzuki-Miyaura procedure using **15** (50.0 mg, 0.0847 mmol), $MeB(OH)_2$ (20.3 mg, 0.339 mmol), $Pd_2dba_3$ (3.1 mg, 0.0034 mmol), SPhos (5.6 mg, 0.014 mmol), and $K_3PO_4$ (89.8 mg, 0.254 mmol) to yield **55** (17.9 mg, 46%) as a white solid. $^1$H NMR (500 MHz, $CDCl_3$) δ 5.84 (s, 1H), 5.39 (dd, *J* = 5.12, 11.93 Hz, 1H), 5.12 (m, 1H), 3.73 (s, 3H), 2.76 (m, 1H), 2.30 (m, 2H), 2.22 (s, 3H), 2.20 (s, 3H), 2.17 (m, 3H), 2.16 (s, 3H), 2.06 (dd, *J* = 3.04, 11.52 Hz, 1H), 1.80 (m, 1H), 1.61 (m, 3H), 1.45 (s, 3H), 1.11 (s, 3H). $^{13}$C NMR (126 MHz, $CDCl_3$) δ 202.07, 171.59, 171.43, 169.97, 150.47, 147.51, 118.72, 104.36, 75.08, 72.28, 64.06, 53.63, 52.01, 51.49, 43.65, 42.16, 38.24, 35.46, 30.76, 20.57, 18.16, 16.39, 15.02, 13.38, 11.77. HRMS calculated for $C_{25}H_{32}O_8$: $[M+Na]^+$: 483.1987 (found); 483.1995 (calc). Melting point: 125-128 °C (dec.).

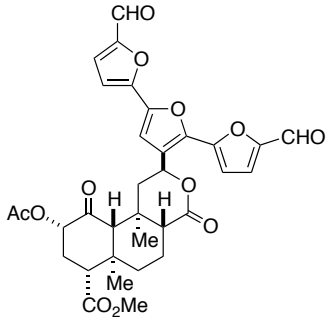

56

**(2*S*,4a*R*,6a*R*,7*R*,9*S*,10a*S*,10b*R*)-Methyl 9-acetoxy-2-(5,5''-diformyl-[2,2':5',2''-terfuran]-3'-yl)-6a,10b-dimethyl-4,10-dioxododecahydro-1*H*-benzo[*f*]isochromene-7-carboxylate.** Prepared according to general Suzuki-Miyaura

procedure using **15** (125 mg, 0.212 mmol), 2-formyl-5-furanylboronic acid (119 mg, 0.847 mmol), $Pd_2dba_3$ (7.8 mg, 0.0085 mmol), SPhos (13.9 mg, 0.0334 mmol), and $K_3PO_4$ (270 mg, 1.272 mmol) to yield **55** (18.8 mg, 14%) as a white solid. $^1$H NMR (500 MHz, $CDCl_3$) δ 9.67 (s, 1H), 9.65 (s, 1H), 7.33 (dd, *J* = 3.78, 8.38 Hz, 2H), 6.95 (d, *J* = 3.78 Hz, 1H), 6.85 (d, *J* = 3.75 Hz, 1H), 5.90 (dd, *J* = 4.95, 12.26 Hz, 1H), 5.11 (m, 1H), 2.82 (dd, *J* = 6.96, 9.89 Hz, 1H), 2.77 (d, *J* = 10.67 Hz, 1H), 2.53 (dd, *J* = 4.98, 13.46 Hz, 1H), 2.29 (m, 4H), 2.17 (s, 1H), 2.14 (s, 3H), 1.94 (t, *J* = 12.88 Hz, 1H), 1.83 (m, 2H), 1.55 (s, 3H), 1.15 (s, 3H).$^{13}$C NMR (126 MHz, $CDCl_3$) δ 202.15, 177.14, 176.72, 171.73, 171.38, 170.04, 152.43, 152.23, 149.72, 149.40, 145.08, 141.88, 126.74, 123.41 (broad), 122.80 (broad), 111.41, 110.42, 109.18, 75.12, 71.92, 63.76, 53.52, 51.98, 50.61, 42.63, 42.23, 38.00, 35.82, 30.79, 20.58, 18.10, 16.49, 15.22. HRMS calculated for $C_{33}H_{32}O_{12}$: $[M+Na]^+$: 643.1803 (found); 643.1791 (calc).

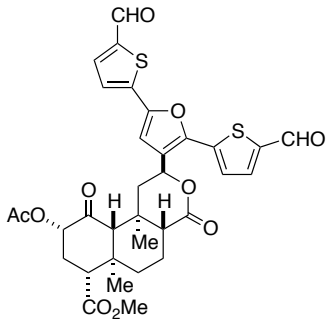


**57**

**(2*S*,4a*R*,6a*R*,7*R*,9*S*,10a*S*,10b*R*)-Methyl 9-acetoxy-2-(5,5''-diformyl-[2,2':5',2''-terfuran]-3'-yl)-6a,10b-dimethyl-4,10-dioxododecahydro-1*H*-benzo[*f*]isochromene-7-carboxylate.** Prepared according to general Suzuki-Miyaura procedure using **15** (125 mg, 0.212 mmol), 2-formyl-5-thienylboronic acid (132 mg, 0.847 mmol), $Pd_2dba_3$ (7.8 mg, 0.0085 mmol), SPhos (13.9 mg, 0.0334 mmol), and $K_3PO_4$ (270 mg, 1.272 mmol) to yield **55** (17.6 mg, 13%) as a white solid. $^1$H NMR (500 MHz, $CDCl_3$) δ 9.95 (s, 1H), 9.91 (s, 1H), 7.78 (d, *J* = 4.01 Hz, 1H), 7.72 (d, *J* = 3.98 Hz,

1H), 7.46 (d, *J* = 4.00 Hz, 1H), 7.42 (d, *J* = 3.96 Hz, 1H), 6.86 (s, 1H), 5.86 (dd, *J* = 4.82, 12.09 Hz, 1H), 5.14 (m, 1H), 3.74 (s, 3H), 2.78 (m, 1H), 2.53 (dd, *J* = 4.85, 13.60 Hz, 1H), 2.31 (dd, *J* = 7.23, 13.58 Hz, 2H), 2.23 (d, *J* = 8.62 Hz, 2H), 2.19 (m, 1H), 2.14 (s, 3H), 1.84 (m, 1H), 1.69 (dt, *J* = 13.31, 25.58 Hz, 3H), 1.54 (s, 3H), 1.15 (s, 3H). $^{13}$C NMR (126 MHz, $CDCl_3$) δ 201.75, 182.64, 182.62, 171.47, 170.55, 169.97, 148.58, 145.25, 143.39, 142.79, 140.50, 139.32, 137.04, 136.75, 126.03, 125.31, 124.46, 109.57, 74.96, 71.02, 63.92, 53.60, 52.06, 51.79, 42.71, 42.10, 38.13, 35.71, 30.71, 20.58, 18.13, 16.54, 15.23. HRMS calculated for $C_{33}H_{32}O_{10}S_2$: $[M+Na]^+$: 675.1328 (found); 675.1335 (calc).

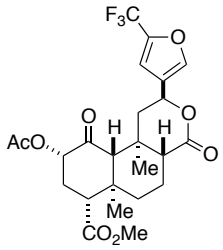

**58**

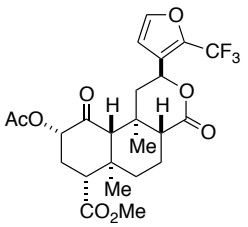

**59**

**(2*S*,4a*R*,6a*R*,7*R*,9*S*,10a*S*,10b*R*)-Methyl 9-acetoxy-2-(5,5''-diformyl-[2,2':5',2''-terfuran]-3'-yl)-6a,10b-dimethyl-4,10-dioxododecahydro-1*H*-benzo[*f*]isochromene-7-carboxylate** (**58**) and **(2*S*,4a*R*,6a*R*,7*R*,9*S*,10a*S*,10b*R*)-Methyl 9-acetoxy-2-(5,5''-diformyl-[2,2':5',2''-terfuran]-3'-yl)-6a,10b-dimethyl-4,10-dioxododecahydro-1*H*-benzo[*f*]isochromene-7-carboxylate** (**59**). An oven-dried glass tube was charged with 1 (200 mg, 1.0 equiv), $K_2HPO_4$ (238 mg, 3.0 equiv), and $Ru(phen)_3Cl_2{\cdot}H_2O$ (6.6 mg, 0.02 equiv) and fitted with a Teflon screwcap. The reaction vessel was flushed with argon. Dry, degassed acetonitrile (4 mL) was added. After stirring for 10 min, triflyl chloride (0.10 mL, 2.0 equiv) was added and the reaction vessel was placed next to a fluorescent light bulb. Two additional portions of 0.05 mL of triflyl chloride were added after 3 and 24 h. After 48 h,

the reaction was quenched by the addition of $H_2O$ (10 mL) and extracted with $Et_2O$ (3 × 10 mL) and $CH_2Cl_2$ (3 × 10 mL). The combined organic layers were dried over $Na_2SO_4$ and decanted, and the solvent was removed in vacuo. The resulting residue was purified by flash column chromatography (30–45% EtOAc/pentane) to yield **59** (70.6 mg, 31%) and **58** (74.8 mg, 32%) as white solids. **58**: $^1$H NMR (500 MHz, CDCl3): δ 7.51 (s, 1H), 6.80 (s, 1H), 5.52 (dd, *J* = 4.98, 11.87 Hz, 1H), 5.14 (m, 1H), 3.73 (s, 3H), 2.75 (m, 1H), 2.52 (dd, *J* = 5.10, 13.39 Hz, 1H), 2.30 (s, 1H), 2.30 (dd, *J* = 6.28, 14.49 Hz, 1H), 2.17 (s, 3H), 2.16 (m, 2H), 2.08 (dd, *J* = 2.87, 11.62 Hz, 1H), 1.80 (m, 1H), 1.60 (m, 3H), 1.46 (s, 3H), 1.12 (s, 3H). $^{13}$C NMR (126 MHz, CDCl3): δ 202.02, 171.48, 170.63, 170.00, 143.02 (q, *J* = 43.05 Hz), 141.41, 126.42, 118.68 (q, *J* = 267.33 Hz), 110.18 (q, *J* = 2.69 Hz), 75.01, 71.28, 63.88, 53.56, 52.02, 51.47, 43.18, 42.07, 38.08, 35.48, 30.72, 20.57, 18.09, 16.43, 15.15. HRMS calculated for $C_{24}H_{27}F_3O_8$: $[M+Na]^+$: 523.1570 (found); 523.1556 (calc). Melting point: 104–106 °C. **59**: $^1$H NMR (500 MHz, $CDCl_3$): δ 7.48 (s, 1H), 6.48 (s, 1H), 5.73 (dd, *J* = 5.03, 12.04 Hz, 1H), 5.12 (m, 1H), 3.73 (s, 3H), 2.76 (m, 1H), 2.41 (dd, *J* = 5.07, 13.56 Hz, 1H), 2.29 (s, 1H), 2.29 (dd, *J* = 6.37, 14.59 Hz, 1H), 2.16 (s, 3H), 2.15 (m, 3H), 1.80 (m, 1H), 1.60 (m, 3H), 1.46 (s, 3H), 1.12 (s, 3H). $^{13}$C NMR (126 MHz, $CDCl_3$): δ 201.78, 171.53, 170.62, 169.94, 144.58, 137.20 (q, *J* = 41.81 Hz), 126.83 (q, *J* = 1.97 Hz), 119.33 (q, *J* = 268.22 Hz), 110.21, 74.94, 70.45, 63.75, 53.52, 52.01, 51.45, 43.76, 42.05, 38.06, 35.63, 30.74, 20.58, 18.11, 16.46, 15.01. HRMS calculated for $C_{24}H_{27}F_3O_8$: $[M+Na]^+$: 523.1539 (found); 523.1556 (calc). Melting point: 147–150 °C.

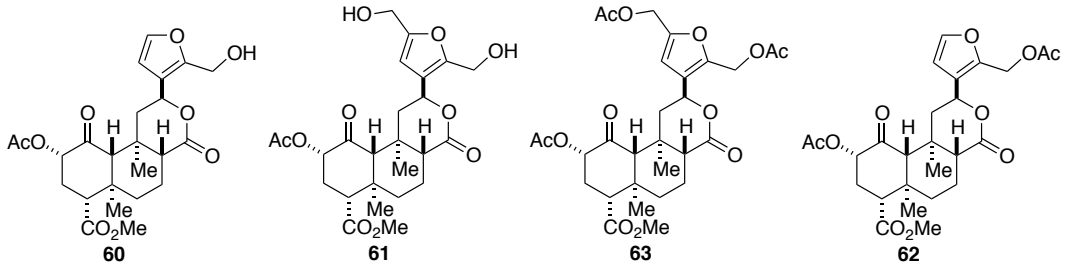


**(2*S*,4a*R*,6a*R*,7*R*,9*S*,10a*S*,10b*R*)-Methyl 9-acetoxy-2-(2-(hydroxymethyl)furan-3-yl)-6a,10b-dimethyl-4,10-dioxododecahydro-1*H*-benzo[*f*]isochromene-7-carboxylate** (**60**), **(2*S*,4a*R*,6a*R*,7*R*,9*S*,10a*S*,10b*R*)-Methyl 9-acetoxy-2-(2,5-bis(hydroxymethyl)furan-3-yl)-6a,10b-dimethyl-4,10-dioxododecahydro-1*H*-benzo[*f*]isochromene-7-carboxylate** (**61**), **(2*S*,4a*R*,6a*R*,7*R*,9*S*,10a*S*,10b*R*)-Methyl 9-acetoxy-2-(2-(acetoxymethyl)furan-3-yl)-6a,10b-dimethyl-4,10-dioxododecahydro-1*H*-benzo[*f*]isochromene-7-carboxylate** (**62**), and **(3-((2*S*,4a*R*,6a*R*,7*R*,9*S*,10a*S*,10b*R*)-9-Acetoxy-7-(methoxycarbonyl)-6a,10b-dimethyl-4,10-dioxododecahydro-1*H*-benzo[*f*]isochromen-2-yl)furan-2,5-diyl)bis(methylene) diacetate** (**63**). A mixture of **1** (305 mg, 1.0 equiv) and paraformaldehyde (115 mg, 5.43 equiv) was dissolved in glacial acetic acid (5 mL) under an atmosphere of argon. The reaction was slowly warmed to 75 °C. After 20 h, reaction was cooled to room temperature and the solvent removed in vacuo. The resulting residue was purified by flash column chromatography (40 → 100% EtOAc/pentane) to yield **1** (60.9 mg, 20%), **62** (51.4 mg, 14%), and **63** (45.2 mg, 11%), as well as the previously described **60** (42.2 mg, 13%) and **61** (14.7 mg, 4%). Compounds **60** and **61** were identical to that reported by Munro *et. al.*[5] **62**: $^1$H NMR (500 MHz, $CDCl_3$): δ 7.38 (d, *J* = 1.88 Hz, 1H), 6.33 (d, *J* = 1.89 Hz, 1H), 5.65 (dd, *J* = 5.01, 11.99 Hz, 1H), 5.10 (dd, *J* = 19.97, 28.28 Hz, 1H), 5.08 (d, *J* = 9.32 Hz, 2H), 3.73 (s, 3H), 2.76 (m, 1H), 2.37 (dd, *J* = 5.02, 13.53 Hz, 1H), 2.29 (dd, *J* = 6.36, 13.55 Hz, 2H), 2.16 (m,

3H), 2.15 (s, 3H), 2.08 (s, 3H), 1.80 (m, 1H), 1.62 (m, 3H), 1.48 (s, 3H), 1.12 (s, 3H). 13C NMR (126 MHz, CDCl3): δ 201.85, 171.56, 171.09, 170.57, 169.95, 146.17, 143.25, 123.77, 109.19, 75.03, 71.61, 63.91, 56.08, 53.57, 52.00, 51.42, 43.73, 42.09, 38.17, 35.52, 30.72, 20.78, 20.57, 18.12, 16.45, 15.06. HRMS calculated for $C_{26}H_{32}O_{10}$: $[M+Na]^+$: 527.1867 (found); 527.1893 (calc). Melting point: 81–85 °C. **63**: $^1$H NMR (500 MHz, $CDCl_3$): δ 6.36 (s, 1H), 5.62 (dd, *J* = 5.02, 12.00 Hz, 1H), 5.06 (d, *J* = 5.29 Hz, 2H), 5.05 (m, 1H), 4.99 (d, *J* = 4.53 Hz, 2H), 3.73 (s, 3H), 2.76 (dd, *J* = 7.38, 9.44 Hz, 1H), 2.36 (dd, *J* = 5.07, 13.59 Hz, 1H), 2.30 (dd, *J* = 6.87, 13.52 Hz, 2H), 2.16 (m, 3H), 2.15 (s, 3H), 2.09 (s, 3H), 2.09 (s, 3H), 1.80 (m, 1H), 1.59 (m, 3H), 1.47 (s, 3H), 1.12 (s, 3H). $^{13}$C NMR (126 MHz, $CDCl_3$): δ 201.81, 171.55, 170.94, 170.57, 170.53, 169.99, 150.34, 146.62, 124.73, 110.05, 75.07, 71.40, 63.92, 57.71, 56.01, 53.62, 52.01, 51.44, 43.66, 42.12, 38.20, 35.52, 30.71, 20.87, 20.79, 20.57, 18.11, 16.43, 15.03. HRMS calculated for $C_{29}H_{36}O_{12}$: $[M+Na]^+$: 599.2110 (found); 599.2105 (calc). Melting point: 78–81 °C.

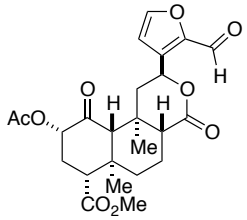

**64**

**(2*S*,4a*R*,6a*R*,7*R*,9*S*,10a*S*,10b*R*)-Methyl 9-acetoxy-2-(2-formylfuran-3-yl)-6a,10b-dimethyl-4,10-dioxododecahydro-1*H*-benzo[*f*]isochromene-7-carboxylate.** A solution DMSO (0.08 mL, 27 equiv) in $CH_2Cl_2$ (0.5 mL) was added to a solution of oxalyl chloride (0.05 mL, 14 equiv) in $CH_2Cl_2$ (2 mL) at –78 °C. After 40 min, a solution of **60** (19.0 mg, 1.0 equiv) in $CH_2Cl_2$ (0.4 mL) was added slowly. After an additional 30 min, $Et_3N$ (0.03 mL, 5.2 equiv) was added

dropwise and the reaction slowly warmed to room temperature and stirred for 3 h. Reaction was quenched with the addition of $H_2O$ and extracted with $CH_2Cl_2$ (3 × 10 mL). Combined organic layers were washed sequentially with HCl (2M), saturated $NaHCO_3$, and brine and then dried over $Na_2SO_4$. Solvent was removed in vacuo and the resulting residue purified by flash column chromatography (55% EtOAc/pentane) to yield **64** (15.3 mg, 81%) as a solid. $^1$H NMR (500 MHz, $CDCl_3$) δ 9.83 (s, 1H), 7.59 (d, *J* = 1.70 Hz, 1H), 6.58 (d, *J* = 1.63 Hz, 1H), 5.97 (dd, *J* = 5.13, 11.99 Hz, 1H), 5.09 (m, 1H), 3.73 (s, 3H), 2.74 (m, 1H), 2.52 (dd, *J* = 5.15, 13.34 Hz, 1H), 2.29 (s, 1H), 2.29 (m, 2H), 2.22 (m, 1H), 2.15 (s, 1H), 2.15 (s, 3H), 1.81 (m, 1H), 1.62 (m, 3H), 1.50 (s, 3H), 1.13 (s, 3H). $^{13}$C NMR (126 MHz, $CDCl_3$) δ 201.65, 179.50, 171.54, 170.78, 169.98, 147.88, 147.17, 134.31, 112.10, 74.98, 71.65, 63.85, 53.59, 52.01, 51.31, 42.79, 42.09, 38.14, 35.71, 30.73, 20.59, 18.09, 16.45, 15.06. HRMS calculated for $C_{24}H_{28}O_9$: $[M+Na]^+$: 483.1623 (found); 483.1631 (calc). Melting point: 215-220 °C (dec.).

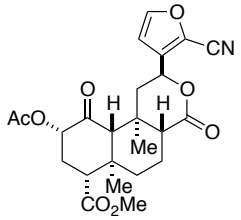

**65**

**(2*S*,4a*R*,6a*R*,7*R*,9*S*,10a*S*,10b*R*)-Methyl 9-acetoxy-2-(2-cyanofuran-3-yl)-6a,10b-dimethyl-4,10-dioxododecahydro-1*H*-benzo[*f*]isochromene-7-carboxylate.** To a solution of **64** (30.5 mg, 1.0 equiv) in MeOH (5 mL) was added $NH_2OH{\cdot}HCl$ (18.4 mg, 4.0 equiv) and pyridine (0.05 mL, 9.3 equiv). The resulting solution was heated to reflux for 5 h and then cooled to room temperature. Solvent was removed in vacuo, the resulting residue was extracted with $CH_2Cl_2$ (20 mL) and $H_2O$ (10 mL), and the layers were separated. The aqueous layer was extracted with $CH_2Cl_2$ (2 × 20

mL). The combined organic layers were washed sequentially with 2 N HCl and brine and then dried over $Na_2SO_4$. The solvent was removed in vacuo, and the resulting residue was placed under an atmosphere of argon and dissolved in dry $CH_2Cl_2$ (5 mL). To this solution were added TsCl (13.9 mg, 1.1 equiv) and DIPEA (0.03 mL, 2.6 equiv). The reaction was stirred at room temperature overnight before being diluted with $CH_2Cl_2$ (10 mL) and HCl (6 M, 10 mL). The layers were separated, and the aqueous layer was extracted with $CH_2Cl_2$ (3 × 10 mL). Combined organic layers were washed sequentially with saturated NaHCO3 and brine and then dried over $Na_2SO_4$. The solvent was removed in vacuo and the resulting residue was purified by flash column chromatography (45→50% EtOAc/pentane) to give **65** (23.8 mg, 79%) as a solid. $^1$H NMR (500 MHz, $CDCl_3$): δ 7.53 (d, J = 1.86 Hz, 1H), 6.50 (d, J = 1.88 Hz, 1H), 5.61 (dd, J = 5.17, 12.04 Hz, 1H), 5.12 (m, 1H), 3.73 (s, 3H), 2.75 (m, 1H), 2.51 (dd, J = 5.18, 13.52 Hz, 1H), 2.31 (s, 1H), 2.31 (m, 1H), 2.17 (m, 3H), 2.17 (s, 3H), 1.81 (m, 1H), 1.63 (m, 3H), 1.48 (s, 3H), 1.13 (s, 3H). $^{13}$C NMR (126 MHz, $CDCl_3$): δ 201.83, 171.46, 170.01, 169.99, 147.51, 137.13, 123.63, 110.51, 110.45, 75.00, 70.98, 63.72, 53.53, 52.04, 51.50, 43.29, 42.09, 37.99, 35.71, 30.69, 20.57, 18.06, 16.43, 14.99. HRMS calculated for $C_{24}H_{27}NO_8$: $[M+Na]^+$: 480.1626 (found); 480.1634 (calc). Melting point: 108–114 °C.

*Experimentals for Chapter III*

Compounds **1**,[6] **2**,[7] **3**,[8] **9**-**11a**,[7] **21a**-**23a**,[7] **25a**,[7] **27a**-**29a**,[7] **32**,[9] and **33**[10] were synthesized according to published procedures. Compounds **9a**-**31a** were synthesized according to the general acylation procedure using MiniBlock XT Parallel synthesizer and compounds **9b**-

**31b** and **36**-**44** were synthesized using general acylation procedure using standard glassware.

**General acylation procedure using MiniBlock XT Parallel Synthesizer.** To 24 plastic tubes in a MiniBlock XT system, was added **3** (40 mg, 0.103 mmol) and the appropriate benzoic acid (0.154 mmol). The tubes were placed under an atmosphere of argon and to each was added a solution of EDC·HCl (29.5 mg, 0.154 mmol) and DMAP (18.8 mg, 0.154 mmol) in $CH_2Cl_2$ (8 mL). After 5 h, reactions were concentrated to ~4 mL and rinsed sequentially with HCl (1 M, 4 mL), saturated NaHCO3 (4 mL), and brine (4 mL). The reaction mixtures were concentrated using a Genevac DD-4 evaporator. The concentrated samples were purified using mass-directed reverse phase HPLC.

**General acylation procedure using standard benchtop glassware.** An oven-dried flask was charged with **6** (40 mg, 0.103 mmo), EDC·HCl (29.5 mg, 0.154 mmol), DMAP (18.8 mg, 0.154 mmol), and the appropriate benzoic acid (0.154 mmol). To the flask was added CH2Cl2 (8 mL). After stirring overnight at RT the reaction was quenched with HCl (1 M, 8 mL) and the organic layer rinsed sequentially with saturaded NaHCO3 (8 mL) and brine (8 mL) then dried over Na2SO4. The solvent was removed in vacuo and the resulting residue purified by FCC eluting with 30-35% EtOAc/Pent. Compounds <95% pure as indicated by HPLC were further purified by reverse phase semi-preparatory HPLC.

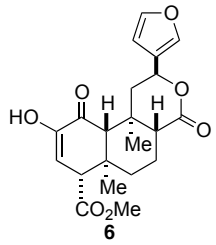

**6**

**(2*S*,4a*R*,6a*R*,7*R*,10a*R*,10b*R*)-methyl 2-(furan-3-yl)-9-hydroxy-6a,10b-dimethyl-4,10-dioxo-2,4,4a,5,6,6a,7,10,10a,10b-decahydro-1*H*-benzo[*f*]isochromene-7-carboxylate.** A combination of $CH_2Cl_2$ (40 mL) and MeOH (40 mL) was added to a flask containing **3** (250 mg, 0.640 mmol) and $Cu(OAc)_2$ (349 mg, 1.92 mmol). After stirring overnight at RT the reaction was concentrated in vacuo. The residue was redissovled in $CH_2Cl_2$ (40 mL) and $H_2O$ (40 mL). The aqueous layer was reextracted with $CH_2Cl_2$ (2 ×40 mL). The combined organic layers were washed with saturated $NH_4Cl$ (50 mL) and brine (50 mL) then dried over $Na_2SO_4$. The solvent was removed in vacuo and the residue purified FCC eluting with 12.5% EtOAc/$CH_2Cl_2$ to yield **3** (43 mg, 17%) and an inseparable mixture of **5**, **6**, and **7** (139 mg, 52%). $^1$H NMR (500 MHz, $CDCl_3$) δ 7.44 (m, 1H), 7.42 (m, 1H), 6.41 (dd, *J* = 0.80, 1.79 Hz, 1H), 6.02 (d, *J* = 2.50 Hz, 1H), 5.59 (dd, *J* = 5.25, 11.62 Hz, 1H), 3.76 (s, 3H), 3.41 (d, *J* = 2.49 Hz, 1H), 3.14 (dd, *J* = 5.13, 13.35 Hz, 1H), 2.33 (s, 1H), 2.18 (m, 2H), 2.01 (m, 1H), 1.67 (m, 3H), 1.36 (s, 3H), 1.11 (s, 3H). $^{13}$C NMR (126 MHz, $CDCl_3$) δ 194.70, 171.32, 171.25, 146.69, 143.77, 139.38, 125.46, 112.18, 108.42, 71.92, 62.70, 55.98, 52.24, 51.27, 44.67, 43.88, 38.20, 35.78, 17.86, 16.64, 14.72. HRMS calculated for $C_{21}H_{24}O_7$: $[M+Na]^+$: 411.1409 (found); 411.1420 (calc). Melting point: 165-170 °C (dec).

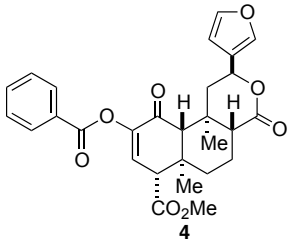

**4**

**(2*S*,4a*R*,6a*R*,7*R*,10a*R*,10b*R*)-Methyl 9-((2-chlorobenzoyl)oxy)-2-(furan-3-yl)-6a,10b-dimethyl-4,10-dioxo-2,4,4a,5,6,6a,7,10,10a,10b-decahydro-1*H*-benzo[*f*]isochromene-7-carboxylate.** A mixture of **5**, **6**, and **7** (40 mg, 0.103 mmol) in $CH_2Cl_2$ (8 mL) was treated with benzoyl chloride (24 μL, 0.206 mmol), DIPEA (36 μL, 0.206 mmol), and DMAP (1.3 mg, 0.206 mmol). After stirring overningt the reaction mixture was rinsed with HCl (1 M, 8 mL), saturated $NaHCO_3$ (8 mL), and brine (8 mL). The organic layer was dried over $Na_2SO_4$ and concentrated in vacuo. The resulting residue was purified by FCC 30%EtOAc/Pent. to yield **4** as a white solid (26.4 mg, 52%). $^1$H NMR (400 MHz, $CDCl_3$) δ 8.11 (d, *J* = 7.14 Hz, 2H), 7.62 (t, *J* = 7.45 Hz, 1H), 7.48 (t, *J* = 7.74 Hz, 2H), 7.41 (s, 1H), 7.39 (t, *J* = 1.66 Hz, 1H), 6.66 (d, *J* = 2.15 Hz, 1H), 6.39 (d, *J* = 0.95 Hz, 1H), 5.54 (dd, *J* = 5.28, 11.47 Hz, 1H), 3.80 (s, 3H), 3.60 (d, *J* = 2.13 Hz, 1H), 3.07 (dd, *J* = 5.34, 13.66 Hz, 1H), 2.47 (s, 1H), 2.20 (dd, *J* = 5.66, 8.50 Hz, 2H), 2.12 (m, 1H), 1.69 (m, 3H), 1.38 (s, 3H), 1.25 (s, 3H). $^{13}$C NMR (126 MHz, $CDCl_3$) δ 190.91, 171.39, 170.41, 164.61, 145.47, 143.67, 139.37, 133.94, 130.28, 129.98, 128.63, 128.28, 125.43, 108.45, 72.07, 63.47, 56.51, 52.48, 51.39, 44.20, 43.81, 38.46, 35.85, 17.95, 16.83, 14.86. HRMS calculated for $C_{28}H_{28}O_8$: $[M-H]^-$: 491.1704 (found); 491.1711 (calc). Melting point 104-108 °C.

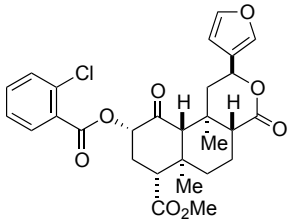

**12a**

**(2*S*,4a*R*,6a*R*,7*R*,9*S*,10a*S*,10b*R*)-Methyl 9-((2-chlorobenzoyl)oxy)-2-(furan-3-yl)-6a,10b-dimethyl-4,10-dioxododecahydro-1*H*-benzo[*f*]isochromene-7-carboxylate.** $^{1}$H NMR (500 MHz, $CDCl_3$) δ 7.99 (m, 1H), 7.47 (m, 2H), 7.42 (m, 1H), 7.40 (t, *J* = 1.70 Hz, 1H), 7.35 (ddd, *J* = 2.10, 6.53, 7.81 Hz, 1H), 6.39 (dd, *J* = 0.78, 1.79 Hz, 1H), 5.52 (dd, *J* = 5.09, 11.69 Hz, 1H), 5.41 (m, 1H), 3.74 (s, 3H), 2.84 (m, 1H), 2.53 (dd, *J* = 5.17, 13.49 Hz, 1H), 2.45 (m, 1H), 2.45 (s, 1H), 2.28 (s, 1H), 2.18 (m, 1H), 2.11 (dd, *J* = 2.97, 11.36 Hz, 1H), 1.82 (m, 1H), 1.63 (dt, *J* = 7.15, 20.47 Hz, 3H), 1.47 (s, 3H), 1.16 (s, 3H). $^{13}$C NMR (126 MHz, $CDCl_3$) δ 201.60, 171.55, 171.15, 164.35, 143.73, 139.50, 134.09, 133.13, 131.92, 131.19, 128.87, 126.72, 125.14, 108.44, 75.78, 72.04, 64.07, 53.55, 52.04, 51.36, 43.33, 42.19, 38.15, 35.48, 30.80, 18.15, 16.49, 15.22. HRMS calculated for $C_{28}H_{29}ClO_8$: $[M-H]^-$: 535.1434 (found), 527.1449 (calc). Melting point: 175-178 °C.

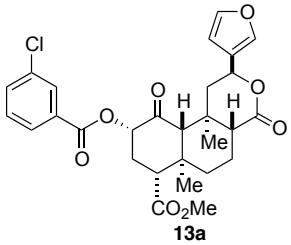

**13a**

**(2*S*,4a*R*,6a*R*,7*R*,9*S*,10a*S*,10b*R*)-Methyl 9-((3-chlorobenzoyl)oxy)-2-(furan-3-yl)-6a,10b-dimethyl-4,10-dioxododecahydro-1*H*-benzo[*f*]isochromene-7-carboxylate.** $^{1}$H NMR (500 MHz, $CDCl_3$) δ 8.06 (t, *J* = 1.75 Hz, 1H), 7.97 (m, 1H), 7.57 (ddd, *J* = 1.08, 2.16, 8.01 Hz, 1H), 7.42 (m, 2H), 7.40 (m, 1H), 6.39 (s, 1H), 5.52 (dd, *J* = 5.09, 11.69 Hz, 1H), 5.39 (dd, *J* = 8.47, 11.69 Hz, 1H), 3.75 (s,

3H), 2.84 (dd, *J* = 5.16, 11.66 Hz, 1H), 2.52 (m, 1H), 2.46 (m, 1H), 2.46 (d, *J* = 11.76 Hz, 1H), 2.26 (s, 1H), 2.19 (m, 1H), 2.11 (dd, *J* = 2.96, 11.42 Hz, 1H), 1.83 (m, 1H), 1.64 (m, 3H), 1.46 (s, 3H), 1.17 (s, 3H). $^{13}$C NMR (126 MHz, $CDCl_3$) δ 201.57, 171.50, 171.12, 164.35, 143.73, 139.46, 134.67, 133.55, 130.81, 129.94, 129.84, 128.03, 125.18, 108.40, 75.78, 72.04, 64.10, 53.58, 52.06, 51.40, 43.39, 42.22, 38.20, 35.49, 30.85, 18.15, 16.51, 15.22. HRMS calculated for $C_{28}H_{29}ClO_8$: $[M-H]^-$: 527.1453 (found), 527.1478 (calc). Melting point: 211-213 °C.

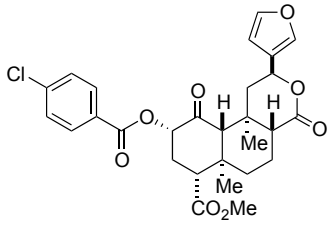

**14a**

**(2*S*,4a*R*,6a*R*,7*R*,9*S*,10a*S*,10b*R*)-Methyl 9-((4-chlorobenzoyl)oxy)-2-(furan-3-yl)-6a,10b-dimethyl-4,10-dioxododecahydro-1*H*-benzo[*f*]isochromene-7-carboxylate.** $^1$H NMR (400 MHz, $CDCl_3$) δ 8.02 (d, *J* = 8.21 Hz, 2H), 7.42 (dd, *J* = 7.54, 12.72 Hz, 4H), 6.38 (s, 1H), 5.52 (dd, *J* = 5.06, 11.68 Hz, 1H), 5.38 (t, *J* = 10.01 Hz, 1H), 3.75 (s, 3H), 2.83 (m, 1H), 2.54 (dd, *J* = 5.00, 13.45 Hz, 1H), 2.46 (m, 2H), 2.25 (s, 1H), 2.19 (d, *J* = 12.77 Hz, 1H), 2.10 (d, *J* = 10.90 Hz, 1H), 1.83 (d, *J* = 12.43 Hz, 1H), 1.61 (m, 3H), 1.46 (s, 3H), 1.17 (s, 3H). $^{13}$C NMR (126 MHz, $CDCl_3$) δ 201.71, 171.53, 171.10, 164.67, 143.74, 140.04, 139.45, 131.28, 128.87, 127.53, 125.17, 108.39, 75.64, 72.04, 64.13, 53.59, 52.06, 51.42, 43.42, 42.22, 38.21, 35.50, 30.90, 18.15, 16.51, 15.22. HRMS calculated for $C_{28}H_{29}ClO_8$: $[M-H]^-$: 527.1452 (found), 527.1478 (calc). Melting point: 187-189 °C.

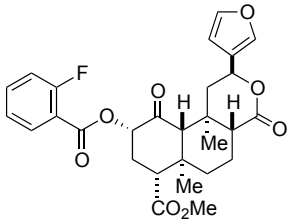

**15a**

**(2*S*,4a*R*,6a*R*,7*R*,9*S*,10a*S*,10b*R*)-Methyl 9-((2-fluorobenzoyl)oxy)-2-(furan-3-yl)-6a,10b-dimethyl-4,10-dioxododecahydro-1*H*-benzo[*f*]isochromene-7-carboxylate.** $^{1}$H NMR (500 MHz, $CDCl_3$) δ 8.01 (td, *J* = 1.81, 7.61 Hz, 1H), 7.56 (m, 1H), 7.42 (m, 1H), 7.40 (t, *J* = 1.70 Hz, 1H), 7.23 (td, *J* = 1.03, 7.79 Hz, 1H), 7.16 (ddd, *J* = 0.78, 8.37, 10.74 Hz, 1H), 6.39 (dd, *J* = 0.76, 1.76 Hz, 1H), 5.51 (dd, *J* = 5.09, 11.70 Hz, 1H), 5.41 (m, 1H), 3.75 (s, 3H), 2.84 (m, 1H), 2.53 (dd, *J* = 5.15, 13.46 Hz, 1H), 2.46 (m, 1H), 2.46 (m, 1H), 2.29 (s, 1H), 2.20 (dd, *J* = 3.52, 6.22 Hz, 1H), 2.11 (dd, *J* = 2.95, 11.37 Hz, 1H), 1.82 (m, 1H), 1.63 (m, 3H), 1.46 (s, 3H), 1.17 (s, 3H). $^{13}$C NMR (126 MHz, $CDCl_3$) δ 201.60, 171.57, 171.18, 163.01 (d, *J* = 3.66 Hz), 162.25 (d, *J* = 261.26 Hz), 143.73, 139.51, 135.11 (d, *J* = 9.09 Hz),132.25, 125.15, 124.08 (d, *J* = 3.92 Hz), 117.68 (d, *J* = 9.12 Hz), 117.11 (d, *J* = 22.02 Hz), 108.44, 75.65, 72.05, 64.03, 53.59, 52.03, 51.38, 43.31, 42.21, 38.18, 35.48, 30.84, 18.16, 16.49, 15.21. HRMS calculated for $C_{28}H_{29}FO_8$: $[M-H]^-$: 535.1756 (found), 535.1744 (calc). Melting point: 203-205 °C.

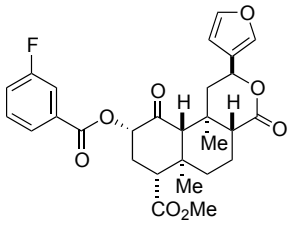

**16a**

**(2*S*,4a*R*,6a*R*,7*R*,9*S*,10a*S*,10b*R*)-Methyl 9-((3-fluorobenzoyl)oxy)-2-(furan-3-yl)-6a,10b-dimethyl-4,10-dioxododecahydro-1*H*-benzo[*f*]isochromene-7-carboxylate.** $^{1}$H NMR (400 MHz, $CDCl_3$) δ 7.88 (d, *J* = 7.68

Hz, 1H), 7.76 (d, *J* = 9.24 Hz, 1H), 7.45 (dd, *J* = 7.84, 13.65 Hz, 1H), 7.41 (d, *J* = 6.85 Hz, 2H), 7.30 (t, *J* = 8.42 Hz, 1H), 6.39 (s, 1H), 5.52 (dd, *J* = 5.05, 11.64 Hz, 1H), 5.39 (m, 1H), 3.75 (s, 3H), 2.84 (dd, *J* = 6.66, 10.10 Hz, 1H), 2.54 (m, 1H), 2.47 (dd, *J* = 8.03, 13.38 Hz, 2H), 2.26 (s, 1H), 2.19 (d, *J* = 11.76 Hz, 1H), 2.10 (d, *J* = 11.31 Hz, 1H), 1.84 (d, *J* = 12.48 Hz, 1H), 1.65 (m, 3H), 1.46 (s, 3H), 1.17 (s, 3H). $^{13}$C NMR (126 MHz, $CDCl_3$) δ 201.60, 171.51, 171.11, 164.41 (d, *J* = 3.05 Hz), 162.54 (d, *J* = 247.45 Hz), 143.74, 139.46, 131.21 (d, *J* = 7.54 Hz), 130.19 (d, *J* = 7.75 Hz), 125.66 (d, *J* = 3.05 Hz), 125.18, 120.63 (d, *J* = 21.24 Hz), 116.80 (d, *J* = 23.20 Hz)108.40, 75.76, 72.05, 64.12, 53.59, 52.07, 51.41, 43.41, 42.22, 38.21, 35.50, 30.86, 18.16, 16.51, 15.22. HRMS calculated for $C_{28}H_{29}FO_8$: $[M-H]^-$: 511.1755 (found), 511.1774 (calc). Melting point: 168-170 °C.

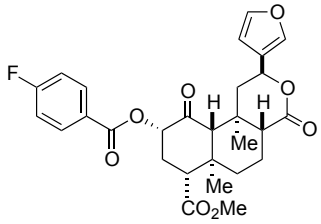

**17a**

**(2*S*,4a*R*,6a*R*,7*R*,9*S*,10a*S*,10b*R*)-Methyl 9-((4-fluorobenzoyl)oxy)-2-(furan-3-yl)-6a,10b-dimethyl-4,10-dioxododecahydro-1*H*-benzo[*f*]isochromene-7-carboxylate.** $^{1}$H NMR (400 MHz, $CDCl_3$) δ 8.11 (dd, *J* = 5.56, 8.04 Hz, 2H), 7.41 (d, *J* = 6.28 Hz, 2H), 7.13 (t, *J* = 8.38 Hz, 2H), 6.38 (s, 1H), 5.52 (dd, *J* = 5.26, 11.68 Hz, 1H), 5.38 (t, *J* = 9.93 Hz, 1H), 3.75 (s, 3H), 2.83 (m, 1H), 2.54 (dd, *J* = 5.02, 13.46 Hz, 1H), 2.47 (dd, *J* = 7.18, 13.51 Hz, 1H), 2.45 (d, *J* = 9.27 Hz, 1H), 2.25 (s, 1H), 2.19 (d, *J* = 12.23 Hz, 1H), 2.10 (d, *J* = 10.65 Hz, 1H), 1.83 (d, *J* = 12.13 Hz, 1H), 1.65 (m, 3H), 1.46 (s, 3H), 1.17 (s, 3H). $^{13}$C NMR (126 MHz, $CDCl_3$) δ 201.60, 171.51, 171.11, 166.11 (d, *J* = 254.86 Hz), 143.74, 139.46, 132.53 (d, *J* = 9.47 Hz),

125.32 (d, *J* = 2.92 Hz), 125.18, 115.72 (d, *J* = 22.06 Hz), 108.40, 75.76, 72.05, 64.12, 53.59, 52.07, 51.41, 43.41, 42.22, 38.21, 35.50, 30.86, 18.16, 16.51, 15.22. HRMS calculated for $C_{28}H_{29}FO_8$: $[M-H]^-$: 511.1757 (found), 511.1774 (calc). Melting point: 139-142 °C.

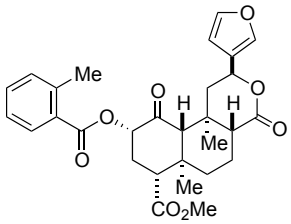

**18a**

**(2*S*,4a*R*,6a*R*,7*R*,9*S*,10a*S*,10b*R*)-Methyl 2-(furan-3-yl)-6a,10b-dimethyl-9-((2-methylbenzoyl)oxy)-4,10-dioxododecahydro-1*H*-benzo[*f*]isochromene-7-carboxylate.** $^1$H NMR (500 MHz, $CDCl_3$) δ 8.01 (m, 1H), 7.43 (m, 2H), 7.40 (t, *J* = 1.71 Hz, 1H), 7.26 (m, 2H), 6.39 (dd, *J* = 0.80, 1.81 Hz, 1H), 5.53 (dd, *J* = 5.09, 11.68 Hz, 1H), 5.39 (m, 1H), 3.75 (s, 3H), 2.83 (dd, *J* = 7.74, 9.10 Hz, 1H), 2.60 (s, 3H), 2.55 (dd, *J* = 5.17, 13.49 Hz, 1H), 2.45 (td, *J* = 2.09, 9.61 Hz, 2H), 2.25 (s, 1H), 2.19 (m, 1H), 2.11 (dd, *J* = 2.98, 11.54 Hz, 1H), 1.82 (m, 1H), 1.65 (m, 3H), 1.48 (s, 3H), 1.17 (s, 3H). $^{13}$C NMR (126 MHz, $CDCl_3$) δ 201.96, 171.63, 171.16, 166.41, 143.73, 140.52, 139.46, 132.50, 131.72, 130.93, 128.55, 125.84, 125.19, 108.42, 75.26, 72.07, 64.16, 53.69, 52.03, 51.45, 43.46, 42.18, 38.20, 35.49, 30.96, 21.72, 18.16, 16.49, 15.23. HRMS calculated for $C_{29}H_{32}O_8$: $[M-H]^-$: 507.2002 (found), 507.2024 (calc). Melting point: 108-112 °C.

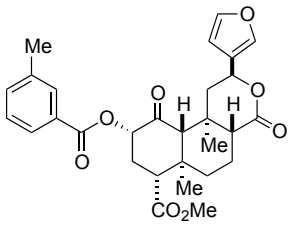

**19a**

**(2*S*,4a*R*,6a*R*,7*R*,9*S*,10a*S*,10b*R*)-Methyl 2-(furan-3-yl)-6a,10b-dimethyl-9-((3-methylbenzoyl)oxy)-4,10-dioxododecahydro-1*H*-benzo[*f*]isochromene-7-carboxylate.** $^{1}$H NMR (400 MHz, $CDCl_3$) δ 7.82 (m, 2H), 7.40 (m, 3H), 7.34 (t, *J* = 7.52 Hz, 1H), 6.39 (d, *J* = 0.97 Hz, 1H), 5.52 (dd, *J* = 5.12, 11.62 Hz, 1H), 5.40 (m, 1H), 3.75 (s, 3H), 2.83 (dd, *J* = 5.79, 11.05 Hz, 1H), 2.55 (dd, *J* = 5.15, 13.45 Hz, 1H), 2.47 (m, 2H), 2.41 (s, 3H), 2.26 (s, 1H), 2.19 (m, 1H), 2.10 (dd, *J* = 2.95, 11.29 Hz, 1H), 1.83 (dd, *J* = 2.81, 10.10 Hz, 1H), 1.61 (m, 3H), 1.47 (s, 3H), 1.18 (s, 3H).$^{13}$C NMR (126 MHz, $CDCl_3$) δ 201.91, 171.62, 171.18, 165.71, 143.72, 139.46, 138.32, 134.30, 130.38, 128.96, 128.40, 127.07, 125.20, 108.41, 75.41, 72.08, 64.11, 53.66, 52.03, 51.44, 43.41, 42.22, 38.23, 35.49, 30.95, 21.26, 18.17, 16.51, 15.22. HRMS calculated for $C_{29}H_{32}O_8$: $[M-H]^-$: 507.2001 (found), 507.2024 (calc). Melting point: 147-149 °C.

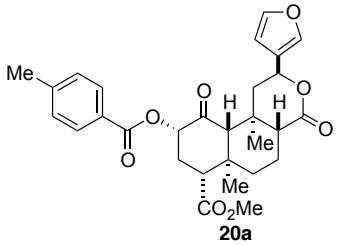

**20a**

**(2*S*,4a*R*,6a*R*,7*R*,9*S*,10a*S*,10b*R*)-Methyl 2-(furan-3-yl)-6a,10b-dimethyl-9-((4-methylbenzoyl)oxy)-4,10-dioxododecahydro-1*H*-benzo[*f*]isochromene-7-carboxylate**. $^{1}$H NMR (500 MHz, $CDCl_3$) δ 7.97 (d, *J* = 8.20 Hz, 2H), 7.41 (m, 2H), 7.25 (d, *J* = 0.56 Hz, 2H), 6.39 (dd, *J* = 0.82, 1.80 Hz, 1H), 5.52 (dd, *J* = 5.09, 11.68 Hz, 1H), 5.38 (dd, *J* = 9.70, 10.47 Hz, 1H), 3.75 (s, 3H), 2.83 (m,

1H), 2.55 (dd, *J* = 5.19, 13.46 Hz, 1H), 2.45 (m, 2H), 2.42 (s, 3H), 2.25 (s, 1H), 2.18 (m, 1H), 2.10 (dd, *J* = 2.94, 11.53 Hz, 1H), 1.82 (m, 1H), 1.60 (dd, *J* = 11.58, 23.61 Hz, 3H), 1.46 (s, 3H), 1.17 (s, 3H). $^{13}$C NMR (126 MHz, $CDCl_3$) δ 201.96, 171.63, 171.18, 165.58, 144.31, 143.71, 139.45, 129.94, 129.20, 126.31, 125.20, 108.41, 75.29, 72.08, 64.12, 53.67, 52.02, 51.45, 43.42, 42.20, 38.22, 35.49, 30.98, 21.75, 18.17, 16.50, 15.22. HRMS calculated for $C_{29}H_{32}O_8$: $[M-H]^-$: 507.2002 (found), 507.2024 (calc). Melting point: 188-190 °C.

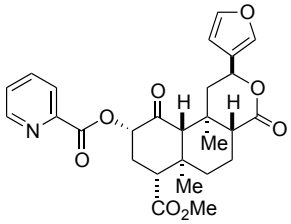

**24a**

**(2*S*,4a*R*,6a*R*,7*R*,9*S*,10a*S*,10b*R*)-2-(Furan-3-yl)-7-(methoxycarbonyl)-6a,10b-dimethyl-4,10-dioxododecahydro-1H-*b*enzo[f]*i*sochromen-9-yl picolinate.** $^1$H NMR (500 MHz, $CDCl_3$) δ 8.82 (ddd, *J* = 0.79, 1.58, 4.71 Hz, 1H), 8.17 (dt, *J* = 0.97, 7.85 Hz, 1H), 7.87 (td, *J* = 1.74, 7.74 Hz, 1H), 7.52 (ddd, *J* = 1.17, 4.74, 7.63 Hz, 1H), 7.42 (m, 1H), 7.40 (t, *J* = 1.70 Hz, 1H), 6.38 (dd, *J* = 0.79, 1.76 Hz, 1H), 5.50 (m, 2H), 3.74 (s, 3H), 2.85 (dd, *J* = 3.64, 13.09 Hz, 1H), 2.53 (m, 3H), 2.28 (s, 1H), 2.19 (m, 1H), 2.11 (dd, *J* = 2.97, 11.45 Hz, 1H), 1.83 (m, 1H), 1.63 (m, 3H), 1.46 (s, 3H), 1.17 (s, 3H). $^{13}$C NMR (126 MHz, $CDCl_3$) δ 201.24, 171.45, 171.15, 164.07, 150.23, 147.13, 143.72, 139.39, 137.09, 127.30, 125.58, 125.23, 108.38, 76.24, 72.09, 64.14, 53.69, 52.03, 51.41, 43.34, 42.27, 38.22, 35.51, 30.85, 18.17, 16.54, 15.21. HRMS calculated for $C_{27}H_{29}O_8$: $[M-H]^-$: 494.1804 (found), 494.1820 (calc). Melting point: 243 °C (dec).

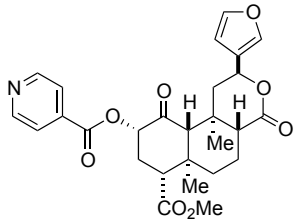

**26a**

**(2*S*,4a*R*,6a*R*,7*R*,9*S*,10a*S*,10b*R*)-2-(Furan-3-yl)-7-(methoxycarbonyl)-6a,10b-dimethyl-4,10-dioxododecahydro-1*H*-benzo[*f*]isochromen-9-yl isonicotinate.** $^{1}$H NMR (500 MHz, $CDCl_3$) δ 8.82 (s, 2H), 7.89 (d, *J* = 5.48 Hz, 2H), 7.42 (m, 1H), 7.40 (t, *J* = 1.70 Hz, 1H), 6.39 (dd, *J* = 0.81, 1.78 Hz, 1H), 5.53 (dd, *J* = 5.09, 11.69 Hz, 1H), 5.40 (dd, *J* = 8.49, 11.65 Hz, 1H), 3.76 (s, 3H), 2.85 (dd, *J* = 5.19, 11.64 Hz, 1H), 2.52 (dd, *J* = 5.04, 13.53 Hz, 1H), 2.47 (m, 2H), 2.27 (s, 1H), 2.20 (m, 1H), 2.11 (dd, *J* = 2.94, 11.38 Hz, 1H), 1.83 (m, 1H), 1.65 (ddd, *J* = 7.44, 17.21, 30.97 Hz, 3H), 1.46 (s, 3H), 1.17 (s, 3H). $^{13}$C NMR (126 MHz, $CDCl_3$) δ 201.21, 171.43, 171.02, 164.15, 150.74, 143.76, 139.46, 136.32, 125.16, 123.00, 108.38, 76.12, 72.00, 64.14, 53.51, 52.11, 51.38, 43.40, 42.25, 38.20, 35.51, 30.76, 18.15, 16.52, 15.22. HRMS calculated for $C_{27}H_{29}O_8$: $[M-H]^-$: 494.1807 (found), 494.1820 (calc). Melting point: 110-116 °C.

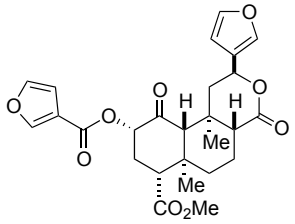

**30a**

**(2*S*,4a*R*,6a*R*,7*R*,9*S*,10a*S*,10b*R*)-Methyl 9-((furan-3-carbonyl)oxy)-2-(furan-3-yl)-6a,10b-dimethyl-4,10-dioxododecahydro-1*H*-benzo[*f*]isochromene-7-carboxylate.** $^{1}$H NMR (500 MHz, $CDCl_3$) δ 8.10 (dd, *J* = 0.76, 1.51 Hz, 1H), 7.45 (m, 1H), 7.41 (dt, *J* = 0.84, 1.59 Hz, 1H), 7.40 (t, *J* = 1.71 Hz, 1H), 6.77 (dd, *J* = 0.75, 1.90 Hz, 1H), 6.38 (dd, *J* = 0.82, 1.80 Hz, 1H), 5.52 (dd, *J* = 5.09,

11.70 Hz, 1H), 5.32 (m, 1H), 3.74 (s, 3H), 2.81 (m, 1H), 2.53 (dd, *J* = 5.17, 13.46 Hz, 1H), 2.42 (m, 1H), 2.40 (d, *J* = 10.04 Hz, 1H), 2.24 (s, 1H), 2.18 (m, 1H), 2.10 (dd, *J* = 2.94, 11.60 Hz, 1H), 1.82 (m, 1H), 1.63 (m, 3H), 1.46 (s, 3H), 1.15 (s, 3H). $^{13}$C NMR (126 MHz, $CDCl_3$) δ 201.88, 171.57, 171.13, 161.90, 148.44, 143.97, 143.73, 139.45, 125.18, 118.28, 109.84, 108.40, 74.99, 72.05, 64.08, 53.61, 52.04, 51.42, 43.40, 42.19, 38.21, 35.48, 30.86, 18.16, 16.49, 15.21. HRMS calculated for $C_{26}H_{28}O_9$: $[M-H]^-$: 494.1641 (found), 483.1661 (calc). Melting point: 214-215 °C.

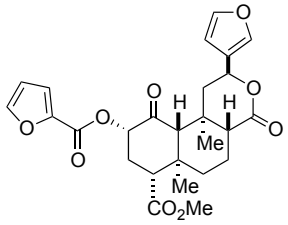

**31a**

**(2*S*,4a*R*,6a*R*,7*R*,9*S*,10a*S*,10b*R*)-Methyl 9-((furan-2-carbonyl)oxy)-2-(furan-3-yl)-6a,10b-dimethyl-4,10-dioxododecahydro-1*H*-benzo[*f*]isochromene-7-carboxylate.** $^1$H NMR (500 MHz, $CDCl_3$) δ 7.62 (dd, *J* = 0.82, 1.71 Hz, 1H), 7.41 (dt, *J* = 0.81, 1.58 Hz, 1H), 7.39 (t, *J* = 1.71 Hz, 1H), 7.29 (dd, *J* = 0.81, 3.52 Hz, 1H), 6.55 (dd, *J* = 1.73, 3.52 Hz, 1H), 6.38 (dd, *J* = 0.82, 1.80 Hz, 1H), 5.52 (dd, *J* = 5.07, 11.69 Hz, 1H), 5.37 (dd, *J* = 8.55, 11.64 Hz, 1H), 3.74 (s, 3H), 2.82 (dd, *J* = 5.21, 11.60 Hz, 1H), 2.53 (dd, *J* = 5.17, 13.46 Hz, 1H), 2.45 (m, 1H), 2.44 (d, *J* = 11.30 Hz, 1H), 2.25 (s, 1H), 2.18 (m, 1H), 2.10 (dd, *J* = 2.93, 11.51 Hz, 1H), 1.82 (m, 1H), 1.63 (m, 3H), 1.46 (s, 3H), 1.16 (s, 3H). $^{13}$C NMR (126 MHz, $CDCl_3$) δ 201.58, 171.49, 171.14, 157.44, 147.05, 143.72, 143.60, 139.42, 125.19, 119.22, 112.10, 108.39, 75.28, 72.07, 64.06, 53.59, 52.04, 51.38, 43.32, 42.20, 38.19, 35.48, 30.84, 18.15, 16.50, 15.21. HRMS calculated for $C_{26}H_{28}O_9$: $[M-H]^-$: 494.1641 (found), 483.1661 (calc). Melting point: 140-145 °C.

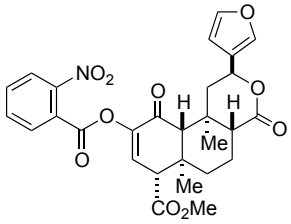

**9b**

**(2*S*,4a*R*,6a*R*,7*R*,10a*R*,10b*R*)-Methyl 2-(furan-3-yl)-6a,10b-dimethyl-9-((2-nitrobenzoyl)oxy)-4,10-dioxo-2,4,4a,5,6,6a,7,10,10a,10b-decahydro-1*H*-benzo[*f*]isochromene-7-carboxylate.** $^{1}$H NMR (500 MHz, $CDCl_3$) δ 8.01 (dd, *J* = 1.13, 7.99 Hz, 1H), 7.95 (m, 1H), 7.75 (td, *J* = 1.34, 7.55 Hz, 1H), 7.70 (m, 1H), 7.43 (dt, *J* = 0.80, 1.57 Hz, 1H), 7.40 (t, *J* = 1.71 Hz, 1H), 6.76 (d, *J* = 2.17 Hz, 1H), 6.40 (dd, *J* = 0.79, 1.82 Hz, 1H), 5.57 (dd, *J* = 5.27, 11.50 Hz, 1H), 3.80 (s, 3H), 3.59 (d, *J* = 2.17 Hz, 1H), 3.07 (dd, *J* = 5.34, 13.66 Hz, 1H), 2.47 (s, 1H), 2.20 (dt, *J* = 2.62, 5.97 Hz, 2H), 2.13 (m, 1H), 1.70 (m, 3H), 1.39 (s, 3H), 1.21 (s, 3H). $^{13}$C NMR (126 MHz, $CDCl_3$) δ 190.65, 171.30, 170.03, 163.26, 147.79, 144.66, 143.72, 139.44, 133.33, 132.39, 130.97, 130.36, 126.32, 125.39, 124.17, 108.48, 71.99, 63.50, 56.42, 52.54, 51.31, 44.20, 43.72, 38.35, 35.83, 17.91, 16.77, 14.84. HRMS calculated for $C_{28}H_{27}NO_{10}$: $[M-H]^-$: 536.1539 (found), 536.1562 (calc). Melting point: 114-118 °C.

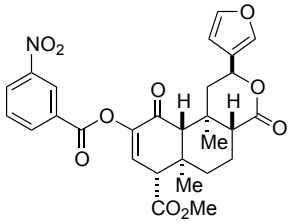

**10b**

**(2*S*,4a*R*,6a*R*,7*R*,10a*R*,10b*R*)-Methyl 2-(furan-3-yl)-6a,10b-dimethyl-9-((3-nitrobenzoyl)oxy)-4,10-dioxo-2,4,4a,5,6,6a,7,10,10a,10b-decahydro-1*H*-benzo[*f*]isochromene-7-carboxylate.** $^{1}$H NMR (500 MHz, $CDCl_3$) δ 8.95 (m, 1H), 8.49 (ddd, *J* = 1.08, 2.27, 8.22 Hz, 1H), 8.43 (m, 1H), 7.72 (t, *J* = 8.01 Hz, 1H), 7.42 (d, *J* = 0.73 Hz, 1H), 7.39 (t, *J* = 1.69 Hz, 1H), 6.73 (d, *J* = 2.15 Hz, 1H), 6.39 (dd, *J* = 0.73,

1.71 Hz, 1H), 5.55 (dd, *J* = 5.27, 11.54 Hz, 1H), 3.81 (s, 3H), 3.62 (d, *J* = 2.14 Hz, 1H), 3.05 (dd, *J* = 5.35, 13.65 Hz, 1H), 2.50 (s, 1H), 2.22 (m, 2H), 2.14 (m, 1H), 1.71 (m, 3H), 1.38 (s, 3H), 1.25 (s, 3H). $^{13}$C NMR (126 MHz, $CDCl_3$) δ 190.55, 171.28, 170.21, 162.48, 148.32, 145.11, 143.71, 139.38, 135.84, 130.56, 130.14, 129.98, 128.29, 125.40, 125.24, 108.44, 71.99, 63.45, 56.42, 52.56, 51.29, 44.29, 43.77, 38.41, 35.87, 17.94, 16.82, 14.85. HRMS calculated for $C_{28}H_{27}NO_{10}$: $[M-H]^-$: 536.1553 (found), 536.1562 (calc). Melting point: 117-121 °C.

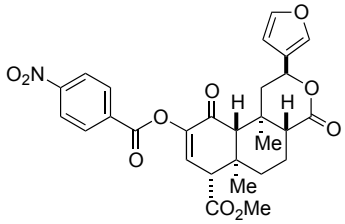

**11b**

**(2*S*,4a*R*,6a*R*,7*R*,10a*R*,10b*R*)-Methyl 2-(furan-3-yl)-6a,10b-dimethyl-9-((4-nitrobenzoyl)oxy)-4,10-dioxo-2,4,4a,5,6,6a,7,10,10a,10b-decahydro-1*H*-benzo[*f*]isochromene-7-carboxylate.** $^1$H NMR (500 MHz, $CDCl_3$) δ 8.34 (d, *J* = 8.82 Hz, 2H), 8.29 (d, *J* = 8.81 Hz, 2H), 7.41 (d, *J* = 9.79 Hz, 2H), 6.72 (d, *J* = 2.00 Hz, 1H), 6.39 (s, 1H), 5.55 (dd, *J* = 5.26, 11.50 Hz, 1H), 3.81 (s, 3H), 3.62 (d, *J* = 1.92 Hz, 1H), 3.05 (dd, *J* = 5.31, 13.62 Hz, 1H), 2.49 (s, 1H), 2.22 (m, 2H), 2.13 (d, *J* = 13.50 Hz, 1H), 1.71 (m, 3H), 1.38 (s, 3H), 1.25 (s, 3H). $^{13}$C NMR (126 MHz, $CDCl_3$) δ 190.55, 171.24, 170.23, 162.69, 151.02, 145.12, 143.72, 139.39, 133.73, 131.41, 130.56, 125.39, 123.76, 108.43, 71.98, 63.49, 56.42, 52.57, 51.31, 44.29, 43.80, 38.43, 35.88, 17.93, 16.82, 14.85. HRMS calculated for $C_{28}H_{27}NO_{10}$: $[M-H]^-$: 536.1551 (found), 536.1562 (calc). Melting point: 125 °C (dec).

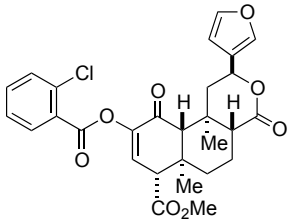

**12b**

**(2*S*,4a*R*,6a*R*,7*R*,10a*R*,10b*R*)-Methyl 9-((2-chlorobenzoyl)oxy)-2-(furan-3-yl)-6a,10b-dimethyl-4,10-dioxo-2,4,4a,5,6,6a,7,10,10a,10b-decahydro-1*H*-benzo[*f*]isochromene-7-carboxylate.** $^{1}$H NMR (500 MHz, $CDCl_3$) δ 8.06 (m, 1H), 7.50 (m, 2H), 7.42 (dt, *J* = 0.86, 1.62 Hz, 1H), 7.39 (t, *J* = 1.73 Hz, 1H), 7.37 (ddd, *J* = 2.71, 5.96, 7.87 Hz, 1H), 6.69 (d, *J* = 2.18 Hz, 1H), 6.39 (dd, *J* = 0.81, 1.81 Hz, 1H), 5.55 (dd, *J* = 5.24, 11.52 Hz, 1H), 3.80 (s, 3H), 3.59 (d, *J* = 2.18 Hz, 1H), 3.08 (dd, *J* = 5.33, 13.67 Hz, 1H), 2.46 (s, 1H), 2.20 (ddd, *J* = 2.78, 6.26, 9.64 Hz, 2H), 2.12 (m, 1H), 1.69 (m, 3H), 1.39 (s, 3H), 1.24 (s, 3H). $^{13}$C NMR (126 MHz, $CDCl_3$) δ 190.73, 171.35, 170.30, 163.02, 145.20, 143.69, 139.39, 134.79, 133.65, 132.39, 131.41, 130.30, 127.73, 126.78, 125.40, 108.45, 72.06, 63.53, 56.50, 52.49, 51.37, 44.20, 43.82, 38.43, 35.85, 17.94, 16.85, 14.85. HRMS calculated for $C_{28}H_{27}ClO_8$: $[M-H]^-$: 525.1306 (found), 525.1322 (calc). Melting point: 93-96 °C.

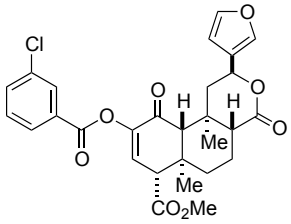

**13b**

**(2*S*,4a*R*,6a*R*,7*R*,10a*R*,10b*R*)-Methyl 9-((3-chlorobenzoyl)oxy)-2-(furan-3-yl)-6a,10b-dimethyl-4,10-dioxo-2,4,4a,5,6,6a,7,10,10a,10b-decahydro-1*H*-benzo[*f*]isochromene-7-carboxylate.** $^{1}$H NMR (500 MHz, $CDCl_3$) δ 8.09 (s, 1H), 7.99 (m, 1H), 7.60 (ddd, *J* = 1.07, 2.15, 8.02 Hz, 1H), 7.44 (d, *J* = 7.97 Hz, 1H), 7.41 (dd, *J* = 0.86, 1.60 Hz, 1H), 7.39 (t, *J* = 1.71 Hz, 1H), 6.67 (d, *J* = 2.18 Hz, 1H), 6.39 (dd, *J* =

0.81, 1.80 Hz, 1H), 5.54 (dd, *J* = 5.26, 11.51 Hz, 1H), 3.80 (s, 3H), 3.60 (d, *J* = 2.18 Hz, 1H), 3.05 (dd, *J* = 5.33, 13.66 Hz, 1H), 2.47 (s, 1H), 2.21 (m, 2H), 2.12 (m, 1H), 1.69 (m, 3H), 1.37 (s, 3H), 1.24 (s, 3H). $^{13}$C NMR (126 MHz, $CDCl_3$) δ 190.73, 171.33, 170.30, 163.38, 145.26, 143.68, 139.37, 134.80, 133.96, 130.28, 130.21, 130.03, 129.97, 128.38, 125.42, 108.45, 72.03, 63.43, 56.45, 52.50, 51.33, 44.23, 43.78, 38.43, 35.85, 17.94, 16.81, 14.84. HRMS calculated for $C_{28}H_{27}ClO_8$: $[M-H]^-$: 525.1309 (found), 525.1322 (calc). Melting point: 103-108 °C.

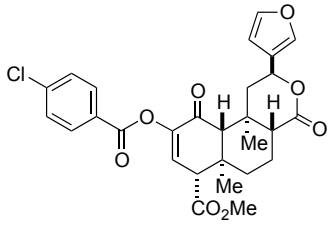

**14b**

**(2*S*,4a*R*,6a*R*,7*R*,10a*R*,10b*R*)-Methyl 9-((4-chlorobenzoyl)oxy)-2-(furan-3-yl)-6a,10b-dimethyl-4,10-dioxo-2,4,4a,5,6,6a,7,10,10a,10b-decahydro-1*H*-benzo[*f*]isochromene-7-carboxylate.** $^1$H NMR (400 MHz, $CDCl_3$) δ 8.04 (d, *J* = 8.25 Hz, 2H), 7.46 (d, *J* = 8.10 Hz, 2H), 7.40 (d, *J* = 7.59 Hz, 2H), 6.67 (s, 1H), 6.39 (s, 1H), 5.54 (dd, *J* = 5.28, 11.34 Hz, 1H), 3.80 (s, 3H), 3.59 (s, 1H), 3.06 (dd, *J* = 5.25, 13.62 Hz, 1H), 2.46 (s, 1H), 2.20 (m, 2H), 2.12 (d, *J* = 13.38 Hz, 1H), 1.71 (m, 3H), 1.38 (s, 3H), 1.24 (s, 3H). $^{13}$C NMR (126 MHz, $CDCl_3$) δ 190.82, 171.32, 170.34, 163.73, 145.31, 143.69, 140.53, 139.38, 131.64, 130.16, 129.02, 126.75, 125.42, 108.44, 72.03, 63.48, 56.48, 52.50, 51.37, 44.23, 43.82, 38.46, 35.86, 17.94, 16.82, 14.86. HRMS calculated for $C_{28}H_{27}ClO_8$: $[M-H]^-$: 525.1307 (found), 525.1322 (calc). Melting point: 165-167 °C.

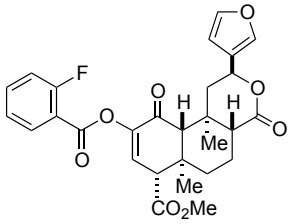

**15b**

**(2*S*,4a*R*,6a*R*,7*R*,9*S*,10a*S*,10b*R*)-Methyl 9-((2-fluorobenzoyl)oxy)-2-(furan-3-yl)-6a,10b-dimethyl-4,10-dioxododecahydro-1*H*-benzo[*f*]isochromene-7-carboxylate.** $^{1}$H NMR (500 MHz, $CDCl_3$) δ 8.05 (td, *J* = 1.80, 7.60 Hz, 1H), 7.60 (m, 1H), 7.41 (m, 1H), 7.39 (t, *J* = 1.71 Hz, 1H), 7.25 (dd, *J* = 0.92, 7.60 Hz, 1H), 7.19 (ddd, *J* = 0.83, 8.39, 10.75 Hz, 1H), 6.68 (d, *J* = 2.17 Hz, 1H), 6.39 (dd, *J* = 0.78, 1.78 Hz, 1H), 5.54 (dd, *J* = 5.24, 11.50 Hz, 1H), 3.80 (s, 3H), 3.59 (d, *J* = 2.18 Hz, 1H), 3.07 (dd, *J* = 5.34, 13.67 Hz, 1H), 2.46 (s, 1H), 2.20 (m, 2H), 2.12 (m, 1H), 1.69 (m, 3H), 1.38 (s, 3H), 1.24 (s, 3H). $^{13}$C NMR (126 MHz, $CDCl_3$) δ 190.69, 171.38, 170.31, 162.45 (d, *J* = 262.15 Hz), 161.86 (d, *J* = 3.97 Hz), 145.22, 143.68, 139.37, 135.66 (d, *J* = 9.16 Hz), 132.63, 130.20, 125.42, 124.21 (d, *J* = 3.85 Hz, H), 117.21 (d, *J* = 22.01 Hz), 116.81 (d, *J* = 9.10 Hz), 108.45, 72.05, 63.47, 56.48, 52.47, 51.34, 44.19, 43.81, 38.41, 35.85, 17.94, 16.83, 14.84. HRMS calculated for $C_{28}H_{27}FO_8$: $[M-H]^-$: 509.1601 (found), 509.1617 (calc). Melting point: 99-102 °C.

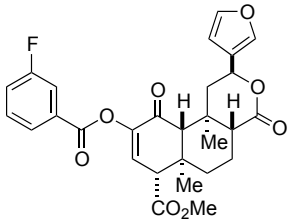

**16b**

**(2*S*,4a*R*,6a*R*,7*R*,10a*R*,10b*R*)-Methyl 9-((3-fluorobenzoyl)oxy)-2-(furan-3-yl)-6a,10b-dimethyl-4,10-dioxo-2,4,4a,5,6,6a,7,10,10a,10b-decahydro-1*H*-benzo[*f*]isochromene-7-carboxylate.** $^{1}$H NMR (500 MHz, $CDCl_3$) δ 7.91 (m, 1H), 7.79 (ddd, *J* = 1.54, 2.51, 9.11 Hz, 1H), 7.47 (td, *J* = 5.47, 8.03 Hz, 1H), 7.41 (m, 1H), 7.39 (t,

*J* = 1.70 Hz, 1H), 7.33 (tdd, *J* = 0.95, 2.64, 8.31 Hz, 1H), 6.68 (d, *J* = 2.17 Hz, 1H), 6.39 (dd, *J* = 0.79, 1.78 Hz, 1H), 5.54 (dd, *J* = 5.26, 11.54 Hz, 1H), 3.80 (s, 3H), 3.60 (d, *J* = 2.17 Hz, 1H), 3.06 (dd, *J* = 5.34, 13.66 Hz, 1H), 2.47 (s, 1H), 2.20 (m, 2H), 2.12 (m, 1H), 1.69 (m, 3H), 1.38 (s, 3H), 1.24 (s, 3H).[13]C NMR (126 MHz, $CDCl_3$) δ 190.74, 171.33, 170.31, 163.45 (d, *J* = 3.07 Hz), 162.54 (d, *J* = 247.83 Hz), 145.29, 143.69, 139.37, 130.37 (d, *J* = 15.18 Hz), 130.28 (d, *J* = 21.81 Hz), 126.05 (d, *J* = 3.05 Hz), 125.42, 121.07 (d, *J* = 21.24 Hz), 117.15 (d, *J* = 23.33 Hz)108.44, 72.03, 63.46, 56.46, 52.50, 51.35, 44.23, 43.80, 38.44, 35.86, 17.94, 16.81, 14.85. HRMS calculated for $C_{28}H_{27}FO_8$: $[M-H]^-$: 509.1610 (found), 509.1617 (calc). Melting point: 101-105 °C.

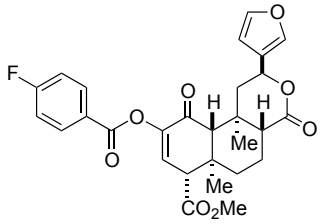

**17b**

**(2*S*,4a*R*,6a*R*,7*R*,10a*R*,10b*R*)-Methyl 9-((4-fluorobenzoyl)oxy)-2-(furan-3-yl)-6a,10b-dimethyl-4,10-dioxo-2,4,4a,5,6,6a,7,10,10a,10b-decahydro-1*H*-benzo[*f*]isochromene-7-carboxylate.** [1]H NMR (500 MHz, $CDCl_3$) δ 8.13 (m, 2H), 7.41 (m, 1H), 7.39 (t, *J* = 1.70 Hz, 1H), 7.16 (t, *J* = 8.66 Hz, 2H), 6.66 (d, *J* = 2.17 Hz, 1H), 6.39 (dd, *J* = 0.79, 1.76 Hz, 1H), 5.54 (dd, *J* = 5.27, 11.53 Hz, 1H), 3.80 (s, 3H), 3.60 (d, *J* = 2.16 Hz, 1H), 3.06 (dd, *J* = 5.34, 13.66 Hz, 1H), 2.47 (s, 1H), 2.21 (m, 2H), 2.12 (m, 1H), 1.70 (m, 3H), 1.38 (s, 3H), 1.24 (s, 3H). [13]C NMR (126 MHz, $CDCl_3$) δ 190.91, 171.35, 170.37, 166.34 (d, *J* = 255.72 Hz),163.58, 145.35, 143.68, 139.38, 132.96 (d, *J* = 9.55 Hz), 130.12, 125.43, 124.55 (d, *J* = 2.94 Hz), 115.90 (d, *J* = 22.11 Hz), 108.45, 72.03, 63.46, 56.47, 52.49, 51.36, 44.22,

43.81, 38.45, 35.85, 17.95, 16.82, 14.85. HRMS calculated for $C_{28}H_{27}FO_8$: $[M-H]^-$: 509.1611 (found), 509.1617 (calc). Melting point: 98-101 °C.

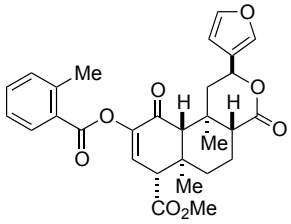

**18b**

**(2*S*,4a*R*,6a*R*,7*R*,10a*R*,10b*R*)-Methyl 2-(furan-3-yl)-6a,10b-dimethyl-9-((2-methylbenzoyl)oxy)-4,10-dioxo-2,4,4a,5,6,6a,7,10,10a,10b-decahydro-1*H*-benzo[*f*]isochromene-7-carboxylate.** $^1$H NMR (500 MHz, $CDCl_3$) δ 8.07 (dd, *J* = 1.35, 8.12 Hz, 1H), 7.46 (td, *J* = 1.39, 7.54 Hz, 1H), 7.42 (m, 1H), 7.39 (t, *J* = 1.70 Hz, 1H), 7.29 (m, 2H), 6.64 (d, *J* = 2.18 Hz, 1H), 6.39 (dd, *J* = 0.79, 1.78 Hz, 1H), 5.55 (dd, *J* = 5.25, 11.54 Hz, 1H), 3.80 (s, 3H), 3.59 (d, *J* = 2.17 Hz, 1H), 3.08 (dd, *J* = 5.31, 13.68 Hz, 1H), 2.61 (s, 3H), 2.46 (s, 1H), 2.20 (m, 2H), 2.11 (m, 1H), 1.68 (m, 3H), 1.38 (s, 3H), 1.25 (d, *J* = 3.55 Hz, 3H). $^{13}$C NMR (126 MHz, $CDCl_3$) δ 191.04, 171.40, 170.45, 165.16, 145.51, 143.66, 141.37, 139.39, 133.01, 131.86, 131.35, 129.94, 127.46, 125.94, 125.44, 108.48, 72.06, 63.50, 56.52, 52.45, 51.39, 44.16, 43.80, 38.43, 35.84, 21.72, 17.95, 16.85, 14.85. HRMS calculated for $C_{29}H_{30}O_8$: $[M-H]^-$: 505.1859 (found), 505.1868 (calc). Melting point: 94-101 °C.

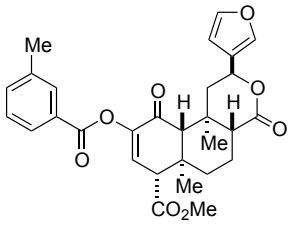

**19b**

**(2*S*,4a*R*,6a*R*,7*R*,10a*R*,10b*R*)-Methyl 2-(furan-3-yl)-6a,10b-dimethyl-9-((3-methylbenzoyl)oxy)-4,10-dioxo-2,4,4a,5,6,6a,7,10,10a,10b-decahydro-1*H*-benzo[*f*]isochromene-7-carboxylate.** $^1$H NMR (500 MHz, $CDCl_3$) δ 7.93 (m, 1H),

7.91 (d, *J* = 8.09 Hz, 1H), 7.43 (d, *J* = 7.49 Hz, 1H), 7.41 (dt, *J* = 0.86, 1.60 Hz, 1H), 7.39 (t, *J* = 1.71 Hz, 1H), 7.37 (t, *J* = 7.63 Hz, 1H), 6.65 (d, *J* = 2.18 Hz, 1H), 6.39 (dd, *J* = 0.78, 1.79 Hz, 1H), 5.54 (dd, *J* = 5.29, 11.58 Hz, 1H), 3.80 (s, 3H), 3.60 (d, *J* = 2.18 Hz, 1H), 3.07 (dd, *J* = 5.34, 13.67 Hz, 1H), 2.48 (s, 1H), 2.41 (s, 3H), 2.20 (m, 2H), 2.12 (m, 1H), 1.69 (m, 3H), 1.38 (s, 3H), 1.24 (s, 3H). $^{13}$C NMR (126 MHz, $CDCl_3$) δ 190.95, 171.41, 170.42, 164.79, 145.50, 143.66, 139.38, 138.48, 134.72, 130.76, 129.89, 128.53, 128.17, 127.44, 125.44, 108.47, 72.06, 63.42, 56.49, 52.45, 51.36, 44.19, 43.78, 38.45, 35.84, 21.25, 17.95, 16.82, 14.85. HRMS calculated for $C_{29}H_{30}O_8$: $[M-H]^-$: 505.1856 (found), 505.1868 (calc). Melting point: 96-102 °C.

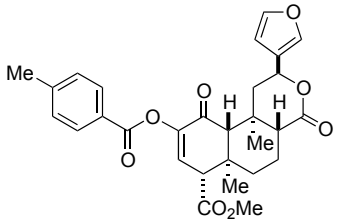

**20b**

**(2*S*,4a*R*,6a*R*,7*R*,10a*R*,10b*R*)-Methyl 2-(furan-3-yl)-6a,10b-dimethyl-9-((4-methylbenzoyl)oxy)-4,10-dioxo-2,4,4a,5,6,6a,7,10,10a,10b-decahydro-1*H*-benzo[*f*]isochromene-7-carboxylate.** $^{1}$H NMR (500 MHz, $CDCl_3$) δ 7.99 (d, *J* = 8.21 Hz, 2H), 7.41 (m, 1H), 7.39 (t, *J* = 1.70 Hz, 1H), 7.28 (d, *J* = 7.99 Hz, 2H), 6.64 (d, *J* = 2.18 Hz, 1H), 6.39 (dd, *J* = 0.78, 1.77 Hz, 1H), 5.54 (dd, *J* = 5.25, 11.54 Hz, 1H), 3.80 (s, 3H), 3.59 (d, *J* = 2.18 Hz, 1H), 3.07 (dd, *J* = 5.34, 13.67 Hz, 1H), 2.47 (s, 1H), 2.43 (s, 3H), 2.20 (m, 2H), 2.12 (m, 1H), 1.69 (m, 3H), 1.38 (s, 3H), 1.24 (s, 3H). $^{13}$C NMR (126 MHz, $CDCl_3$) δ 190.99, 171.41, 170.43, 164.66, 145.50, 144.84, 143.66, 139.38, 130.32, 129.87, 129.34, 125.51, 125.44, 108.47, 72.07, 63.45, 56.51, 52.45, 51.38, 44.18, 43.80, 38.46, 35.84, 21.80, 17.96, 16.82, 14.86. HRMS calculated for $C_{29}H_{30}O_8$: $[M-H]^-$: 505.1856 (found), 505.1868 (calc). Melting point: 184-185 °C (dec).

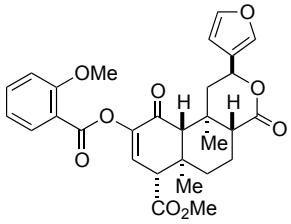

**21b**

**(2*S*,4a*R*,6a*R*,7*R*,10a*R*,10b*R*)-Methyl 2-(furan-3-yl)-9-((2-methoxybenzoyl)oxy)-6a,10b-dimethyl-4,10-dioxo-2,4,4a,5,6,6a,7,10,10a,10b-decahydro-1*H*-benzo[*f*]isochromene-7-carboxylate.** $^{1}$H NMR (500 MHz, $CDCl_3$) δ 8.03 (dd, *J* = 1.81, 8.14 Hz, 1H), 7.55 (m, 1H), 7.41 (dt, *J* = 0.80, 1.54 Hz, 1H), 7.39 (t, *J* = 1.71 Hz, 1H), 7.02 (dd, *J* = 4.45, 11.25 Hz, 2H), 6.62 (d, *J* = 2.19 Hz, 1H), 6.39 (dd, *J* = 0.78, 1.79 Hz, 1H), 5.54 (dd, *J* = 5.23, 11.55 Hz, 1H), 3.92 (s, 3H), 3.79 (s, 3H), 3.57 (d, *J* = 2.19 Hz, 1H), 3.08 (dd, *J* = 5.32, 13.69 Hz, 1H), 2.44 (s, 1H), 2.19 (dt, *J* = 2.79, 8.76 Hz, 2H), 2.11 (m, 1H), 1.69 (m, 3H), 1.38 (s, 3H), 1.24 (s, 3H). $^{13}$C NMR (126 MHz, $CDCl_3$) δ 191.03, 171.46, 170.44, 163.24, 160.28, 145.48, 143.66, 139.37, 134.93, 132.71, 129.88, 125.43, 120.22, 117.30, 112.04, 108.47, 72.10, 63.49, 56.57, 56.03, 52.41, 51.40, 44.13, 43.86, 38.44, 35.83, 17.96, 16.85, 14.84. HRMS calculated for $C_{29}H_{30}O_9$: $[M-H]^-$: 505.1802 (found), 521.1817 (calc). Melting point: 110-114 °C.

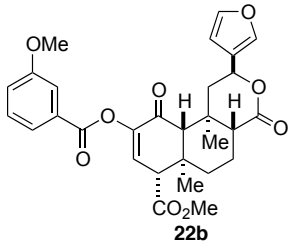

**22b**

**(2*S*,4a*R*,6a*R*,7*R*,10a*R*,10b*R*)-Methyl 2-(furan-3-yl)-9-((3-methoxybenzoyl)oxy)-6a,10b-dimethyl-4,10-dioxo-2,4,4a,5,6,6a,7,10,10a,10b-decahydro-1*H*-benzo[*f*]isochromene-7-carboxylate.** $^{1}$H NMR (500 MHz, $CDCl_3$) δ 7.71 (m, 1H), 7.60 (dd, *J* = 1.53, 2.55 Hz, 1H), 7.41 (m, 1H), 7.39 (m, 2H), 7.17 (ddd, *J* = 0.93, 2.68, 8.29 Hz, 1H), 6.66 (d, *J* = 2.18 Hz, 1H), 6.39 (dd, *J* = 0.77, 1.77 Hz, 1H), 5.55

(dd, *J* = 5.25, 11.53 Hz, 1H), 3.86 (s, 3H), 3.80 (s, 3H), 3.60 (d, *J* = 2.18 Hz, 1H), 3.07 (dd, *J* = 5.34, 13.67 Hz, 1H), 2.47 (s, 1H), 2.21 (m, 2H), 2.12 (m, 1H), 1.69 (m, 3H), 1.38 (s, 3H), 1.25 (s, 3H). $^{13}$C NMR (126 MHz, $CDCl_3$) δ 190.85, 171.38, 170.41, 164.50, 159.67, 145.48, 143.68, 139.38, 129.95, 129.66, 129.48, 125.43, 122.74, 120.78, 114.31, 108.46, 72.06, 63.47, 56.50, 55.50, 52.48, 51.38, 44.21, 43.82, 38.47, 35.85, 17.96, 16.82, 14.86. HRMS calculated for $C_{29}H_{30}O_9$: $[M-H]^-$: 505.1799 (found), 521.1817 (calc). Melting point: 106-108 °C.

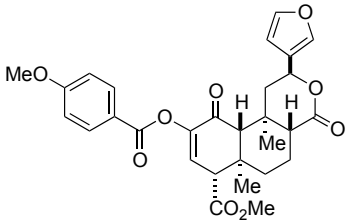

**23b**

**(2*S*,4a*R*,6a*R*,7*R*,10a*R*,10b*R*)-Methyl 2-(furan-3-yl)-9-((4-methoxybenzoyl)oxy)-6a,10b-dimethyl-4,10-dioxo-2,4,4a,5,6,6a,7,10,10a,10b-decahydro-1*H*-benzo[*f*]isochromene-7-carboxylate.** $^1$H NMR (500 MHz, $CDCl_3$) δ 8.06 (d, *J* = 9.01 Hz, 2H), 7.41 (dt, *J* = 0.85, 1.61 Hz, 1H), 7.39 (t, *J* = 1.71 Hz, 1H), 6.95 (d, *J* = 9.01 Hz, 2H), 6.63 (d, *J* = 2.19 Hz, 1H), 6.39 (dd, *J* = 0.81, 1.80 Hz, 1H), 5.54 (dd, *J* = 5.24, 11.53 Hz, 1H), 3.88 (s, 3H), 3.80 (s, 3H), 3.59 (d, *J* = 2.19 Hz, 1H), 3.07 (dd, *J* = 5.34, 13.67 Hz, 1H), 2.47 (s, 1H), 2.20 (m, 2H), 2.12 (m, 1H), 1.70 (m, 3H), 1.38 (s, 3H), 1.24 (s, 3H). $^{13}$C NMR (126 MHz, $CDCl_3$) δ 191.11, 171.42, 170.46, 164.30, 164.15, 145.53, 143.66, 139.37, 132.46, 129.82, 125.44, 120.54, 113.90, 108.46, 72.08, 63.46, 56.53, 55.53, 52.45, 51.41, 44.18, 43.82, 38.48, 35.84, 17.96, 16.82, 14.87. HRMS calculated for $C_{29}H_{30}O_9$: $[M-H]^-$: 505.1801 (found), 521.1817 (calc). Melting point: 192-195 °C.

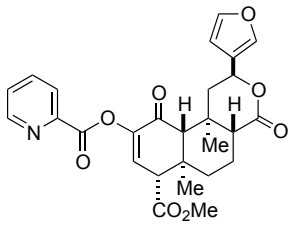

**24b**

**(2*S*,4a*R*,6a*R*,7*R*,10a*R*,10b*R*)-2-(Furan-3-yl)-7-(methoxycarbonyl)-6a,10b-dimethyl-4,10-dioxo-2,4,4a,5,6,6a,7,10,10a,10b-decahydro-1H-*b*enzo[f]*i*sochromen-9-yl picolinate.** $^{1}$H NMR (500 MHz, $CDCl_3$) δ 8.82 (ddd, *J* = 0.87, 1.69, 4.72 Hz, 1H), 8.20 (dt, *J* = 1.00, 7.85 Hz, 1H), 7.90 (td, *J* = 1.74, 7.75 Hz, 1H), 7.55 (ddd, *J* = 1.18, 4.73, 7.66 Hz, 1H), 7.41 (m, 1H), 7.39 (t, *J* = 1.71 Hz, 1H), 6.75 (d, *J* = 2.17 Hz, 1H), 6.38 (dd, *J* = 0.80, 1.77 Hz, 1H), 5.54 (dd, *J* = 5.28, 11.52 Hz, 1H), 3.79 (s, 3H), 3.61 (d, *J* = 2.17 Hz, 1H), 3.07 (dd, *J* = 5.35, 13.67 Hz, 1H), 2.49 (s, 1H), 2.20 (m, 2H), 2.14 (m, 1H), 1.69 (m, 3H), 1.38 (s, 3H), 1.24 (s, 3H). $^{13}$C NMR (126 MHz, $CDCl_3$) δ 190.40, 171.38, 170.21, 163.14, 150.19, 146.40, 145.41, 143.69, 139.32, 137.24, 130.33, 127.70, 125.99, 125.45, 108.43, 72.07, 63.40, 56.51, 52.46, 51.34, 44.22, 43.72, 38.45, 35.85, 17.95, 16.81, 14.85. HRMS calculated for $C_{27}H_{27}NO_8$: $[M+Na]^+$: 516.1619 (found), 516.1634 (calc). Melting point: 185-190 °C (dec).

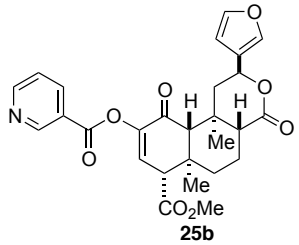

**25b**

**(2*S*,4a*R*,6a*R*,7*R*,10a*R*,10b*R*)-2-(Furan-3-yl)-7-(methoxycarbonyl)-6a,10b-dimethyl-4,10-dioxo-2,4,4a,5,6,6a,7,10,10a,10b-decahydro-1*H*-benzo[*f*]isochromen-9-yl nicotinate.** $^{1}$H NMR (500 MHz, $CDCl_3$) δ 9.31 (s, 1H), 8.85 (d, *J* = 3.16 Hz, 1H), 8.37 (dt, *J* = 1.90, 7.97 Hz, 1H), 7.45 (dd, *J* = 4.89, 7.94 Hz, 1H), 7.42 (m, 1H), 7.40 (t, *J* = 1.71 Hz, 1H), 6.71 (d, *J* = 2.17 Hz, 1H), 6.39 (dd,

*J* = 0.80, 1.78 Hz, 1H), 5.55 (dd, *J* = 5.28, 11.52 Hz, 1H), 3.81 (s, 3H), 3.61 (d, *J* = 2.17 Hz, 1H), 3.06 (dd, *J* = 5.35, 13.65 Hz, 1H), 2.48 (s, 1H), 2.21 (m, 2H), 2.13 (m, 1H), 1.70 (m, 3H), 1.38 (s, 3H), 1.25 (s, 3H). $^{13}$C NMR (126 MHz, $CDCl_3$) δ 190.65, 171.29, 170.26, 163.28, 154.29, 151.45, 145.15, 143.71, 139.38, 137.67, 130.45, 125.41, 124.48, 123.50, 108.43, 72.02, 63.50, 56.46, 52.54, 51.35, 44.26, 43.83, 38.44, 35.88, 17.94, 16.83, 14.86. HRMS calculated for $C_{27}H_{27}NO_8$: $[M-H]^-$: 492.1640 (found), 492.1664 (calc). Melting point: 109-112 °C.

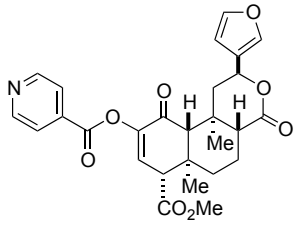

**26b**

**(2*S*,4a*R*,6a*R*,7*R*,10a*R*,10b*R*)-2-(Furan-3-yl)-7-(methoxycarbonyl)-6a,10b-dimethyl-4,10-dioxo-2,4,4a,5,6,6a,7,10,10a,10b-decahydro-1*H*-benzo[*f*]isochromen-9-yl isonicotinate.** $^1$H NMR (500 MHz, $CDCl_3$) δ 8.84 (dd, *J* = 1.39, 4.55 Hz, 2H), 7.91 (dd, *J* = 1.61, 4.42 Hz, 2H), 7.42 (m, 1H), 7.40 (t, *J* = 1.69 Hz, 1H), 6.71 (d, *J* = 2.15 Hz, 1H), 6.39 (dd, *J* = 0.73, 1.69 Hz, 1H), 5.55 (dd, *J* = 5.27, 11.53 Hz, 1H), 3.81 (s, 3H), 3.61 (d, *J* = 2.14 Hz, 1H), 3.05 (dd, *J* = 5.35, 13.65 Hz, 1H), 2.47 (s, 1H), 2.21 (m, 2H), 2.14 (m, 1H), 1.69 (m, 3H), 1.38 (s, 3H), 1.24 (s, 3H). $^{13}$C NMR (126 MHz, $CDCl_3$) δ 190.47, 171.24, 170.22, 163.18, 150.87, 145.12, 143.72, 139.38, 135.59, 130.49, 125.40, 123.19, 108.42, 72.00, 63.52, 56.44, 52.56, 51.34, 44.28, 43.83, 38.45, 35.88, 17.94, 16.82, 14.85. HRMS calculated for $C_{27}H_{27}NO_8$: $[M+Na]^+$: 492.1624 (found), 492.1664 (calc). Melting point: 112-114 °C.

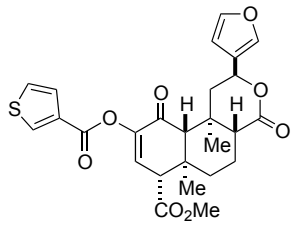

**27b**

**(2*S*,4a*R*,6a*R*,7*R*,10a*R*,10b*R*)-Methyl 2-(furan-3-yl)-6a,10b-dimethyl-4,10-dioxo-9-((thiophene-3-carbonyl)oxy)-2,4,4a,5,6,6a,7,10,10a,10b-decahydro-1*H*-benzo[*f*]isochromene-7-carboxylate.** $^{1}$H NMR (500 MHz, $CDCl_3$) δ 8.26 (dd, *J* = 1.20, 3.03 Hz, 1H), 7.58 (dd, *J* = 1.20, 5.10 Hz, 1H), 7.41 (dd, *J* = 0.76, 1.52 Hz, 1H), 7.39 (t, *J* = 1.71 Hz, 1H), 7.36 (dd, *J* = 3.05, 5.10 Hz, 1H), 6.64 (d, *J* = 2.17 Hz, 1H), 6.39 (dd, *J* = 0.80, 1.78 Hz, 1H), 5.54 (dd, *J* = 5.25, 11.52 Hz, 1H), 3.80 (s, 3H), 3.59 (d, *J* = 2.16 Hz, 1H), 3.07 (dd, *J* = 5.33, 13.66 Hz, 1H), 2.47 (s, 1H), 2.20 (m, 2H), 2.12 (m, 1H), 1.70 (m, 3H), 1.38 (s, 3H), 1.23 (s, 3H). $^{13}$C NMR (126 MHz, $CDCl_3$) δ 190.98, 171.39, 170.39, 160.29, 145.19, 143.67, 139.37, 134.68, 131.42, 130.05, 128.13, 126.56, 125.43, 108.45, 72.06, 63.43, 56.48, 52.47, 51.36, 44.20, 43.80, 38.45, 35.84, 17.95, 16.81, 14.86. HRMS calculated for $C_{26}H_{26}O_8S$: $[M+Na]^+$: 521.1231 (found), 521.1246 (calc). Melting point: 175-176 °C (dec).

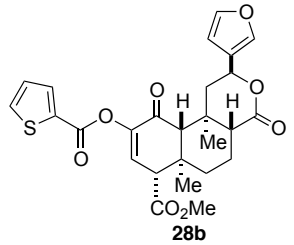

**28b**

**(2*S*,4a*R*,6a*R*,7*R*,10a*R*,10b*R*)-Methyl 2-(furan-3-yl)-6a,10b-dimethyl-4,10-dioxo-9-((thiophene-2-carbonyl)oxy)-2,4,4a,5,6,6a,7,10,10a,10b-decahydro-1*H*-benzo[*f*]isochromene-7-carboxylate.** $^{1}$H NMR (500 MHz, $CDCl_3$) δ 7.92 (dd, *J* = 1.26, 3.79 Hz, 1H), 7.67 (dd, *J* = 1.25, 4.96 Hz, 1H), 7.41 (dt, *J* = 0.81, 1.58 Hz, 1H), 7.39 (t, *J* = 1.71 Hz, 1H), 7.16 (dd, *J* = 3.81, 4.97 Hz, 1H), 6.67 (d, *J* = 2.18 Hz,

1H), 6.39 (dd, *J* = 0.79, 1.79 Hz, 1H), 5.54 (dd, *J* = 5.25, 11.52 Hz, 1H), 3.80 (s, 3H), 3.59 (d, *J* = 2.17 Hz, 1H), 3.07 (dd, *J* = 5.34, 13.66 Hz, 1H), 2.46 (s, 1H), 2.20 (ddd, *J* = 2.73, 6.71, 11.74 Hz, 2H), 2.12 (m, 1H), 1.68 (m, 3H), 1.38 (s, 3H), 1.23 (s, 3H). $^{13}$C NMR (126 MHz, $CDCl_3$) δ 190.83, 171.37, 170.33, 159.89, 145.06, 143.68, 139.37, 135.24, 134.08, 131.34, 130.25, 128.14, 125.43, 108.44, 72.07, 63.46, 56.48, 52.48, 51.37, 44.21, 43.82, 38.45, 35.85, 17.95, 16.82, 14.86. HRMS calculated for $C_{26}H_{26}O_8S$: $[M-H]^-$: 521.1254 (found), 521.1246 (calc). Melting point: 150-152 °C (dec).

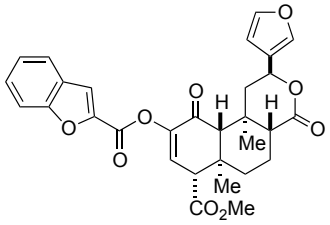

**29b**

**(2*S*,4a*R*,6a*R*,7*R*,10a*R*,10b*R*)-Methyl 9-((benzofuran-2-carbonyl)oxy)-2-(furan-3-yl)-6a,10b-dimethyl-4,10-dioxo-2,4,4a,5,6,6a,7,10,10a,10b-decahydro-1*H*-benzo[*f*]isochromene-7-carboxylate.**

$^1$H NMR (500 MHz, $CDCl_3$) δ 7.72 (dd, *J* = 0.91, 7.76 Hz, 1H), 7.70 (d, *J* = 0.93 Hz, 1H), 7.61 (dd, *J* = 0.79, 8.45 Hz, 1H), 7.50 (ddd, *J* = 1.25, 7.22, 8.46 Hz, 1H), 7.41 (m, 1H), 7.39 (t, *J* = 1.70 Hz, 1H), 7.34 (td, *J* = 0.89, 7.62 Hz, 1H), 6.73 (d, *J* = 2.17 Hz, 1H), 6.39 (dd, *J* = 0.79, 1.77 Hz, 1H), 5.55 (dd, *J* = 5.27, 11.51 Hz, 1H), 3.80 (s, 3H), 3.61 (d, *J* = 2.17 Hz, 1H), 3.06 (dd, *J* = 5.36, 13.67 Hz, 1H), 2.50 (s, 1H), 2.20 (dt, *J* = 6.36, 14.91 Hz, 2H), 2.13 (m, 1H), 1.70 (m, 3H), 1.38 (s, 3H), 1.23 (s, 3H).$^{13}$C NMR (126 MHz, $CDCl_3$) δ 190.54, 171.35, 170.24, 157.05, 156.17, 144.73, 143.69, 143.64, 139.36, 130.48, 128.41, 126.76, 125.41, 124.11, 123.13, 116.22, 112.49, 108.44, 72.06, 63.40, 56.46, 52.51, 51.31, 44.23, 43.71, 38.45, 35.84, 17.95, 16.82, 14.85. HRMS calculated for $C_{30}H_{28}O_9$: $[M+Na]^+$: 555.1611 (found), 555.1631 (calc). Melting point: 126-130 °C.

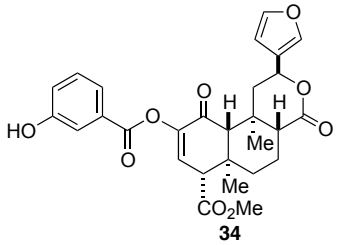

**34**

**(2*S*,4a*R*,6a*R*,7*R*,10a*R*,10b*R*)-Methyl 2-(furan-3-yl)-9-((3-hydroxybenzoyl)oxy)-6a,10b-dimethyl-4,10-dioxo-2,4,4a,5,6,6a,7,10,10a,10b-decahydro-1*H*-benzo[*f*]isochromene-7-carboxylate.** Synthesized according to general acylation procedure using standard benchtop glassware using **6** (40.0 mg, 0.103 mmol) and 3-((*tert*-butyldimethylsilyl)oxy)benzoic acid (39.0 mg, 0.154 mmol). The resulting silyl-protected phenol was dissolved in THF (5 mL) and treated with a solution of TBAF (1.0 M, 0.12 mmol) at 0 °C. After 10 min, the reaction was quenched with saturated NH4Cl and extracted with EtOAc (3 x 10 mL). The combined organic layers were washed with brine and dried over Na2SO4 then concentrated in vacuo. The residue was purified by FCC eluting with 50% EtOAc/Pent. to yield **34** as white solid (26.7mg, 51%). $^{1}$H NMR (500 MHz, $CDCl_3$) δ 7.66 (m, 1H), 7.55 (dd, *J* = 1.56, 2.49 Hz, 1H), 7.39 (dt, *J* = 0.82, 1.58 Hz, 1H), 7.38 (t, *J* = 1.71 Hz, 1H), 7.33 (t, *J* = 7.94 Hz, 1H), 7.10 (ddd, *J* = 0.86, 2.61, 8.13 Hz, 1H), 6.65 (d, *J* = 2.16 Hz, 1H), 6.37 (dd, *J* = 0.81, 1.80 Hz, 1H), 6.02 (s, 1H), 5.54 (dd, *J* = 5.25, 11.47 Hz, 1H), 3.80 (s, 3H), 3.59 (d, *J* = 2.16 Hz, 1H), 3.04 (dd, *J* = 5.36, 13.68 Hz, 1H), 2.47 (s, 1H), 2.20 (m, 2H), 2.11 (m, 1H), 1.70 (m, 3H), 1.36 (s, 3H), 1.23 (s, 3H).$^{13}$C NMR (126 MHz, $CDCl_3$) δ 190.91, 171.83, 170.43, 164.51, 156.09, 145.40, 143.67, 139.43, 130.13, 129.95, 129.49, 125.34, 122.52, 121.35, 116.82, 108.47, 72.19, 63.40, 56.44, 52.50, 51.31, 44.20, 43.69, 38.39, 35.84, 17.93, 16.80, 14.86. HRMS calculated for $C_{28}H_{28}O_9$: $[M+Na]^+$: 531.1611 (found), 531.1631 (calc). Melting point: 124-126 °C.

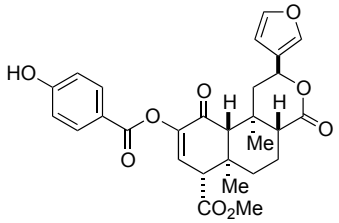

**35**

**(2*S*,4a*R*,6a*R*,7*R*,10a*R*,10b*R*)-Methyl 2-(furan-3-yl)-9-((4-hydroxybenzoyl)oxy)-6a,10b-dimethyl-4,10-dioxo-2,4,4a,5,6,6a,7,10,10a,10b-decahydro-1*H*-benzo[*f*]isochromene-7-carboxylate.** Synthesized according to general acylation procedure using standard benchtop glassware using **6** (40.0 mg, 0.103 mmol) and 4-((*tert*-butyldimethylsilyl)oxy)benzoic acid (39.0 mg, 0.154 mmol). The resulting silyl-protected phenol was dissolved in THF (5 mL) and treated with a solution of TBAF (1.0 M, 0.12 mmol) at 0 °C. After 10 min, the reaction was quenched with saturated NH4Cl and extracted with EtOAc (3 x 10 mL). The combined organic layers were washed with brine and dried over Na2SO4 then concentrated in vacuo. The residue was purified by FCC eluting with 45% EtOAc/Pent. to yield **35** as white solid (12.6 mg, 24%). $^{1}$H NMR (500 MHz, $CDCl_3$) δ 8.00 (d, *J* = 8.84 Hz, 2H), 7.40 (dd, *J* = 0.75, 1.50 Hz, 1H), 7.39 (t, *J* = 1.70 Hz, 1H), 6.88 (d, *J* = 8.85 Hz, 2H), 6.64 (d, *J* = 2.18 Hz, 1H), 6.38 (dd, *J* = 0.79, 1.77 Hz, 1H), 6.02 (s, 1H), 5.54 (dd, *J* = 5.25, 11.52 Hz, 1H), 3.80 (s, 3H), 3.59 (d, *J* = 2.18 Hz, 1H), 3.06 (dd, *J* = 5.35, 13.69 Hz, 1H), 2.47 (s, 1H), 2.20 (m, 2H), 2.12 (m, 1H), 1.69 (m, 3H), 1.37 (s, 3H), 1.23 (s, 3H). $^{13}$C NMR (126 MHz, $CDCl_3$) δ 191.22, 171.66, 170.52, 164.34, 160.82, 145.48, 143.69, 139.40, 132.78, 129.99, 125.37, 120.56, 115.51, 108.45, 72.17, 63.42, 56.51, 52.49, 51.38, 44.21, 43.76, 38.47, 35.83, 17.94, 16.83, 14.88. HRMS calculated for $C_{28}H_{28}O_9$: $[M+Na]^+$: 531.1625 (found), 531.1631 (calc). Melting point: 136-139 °C.

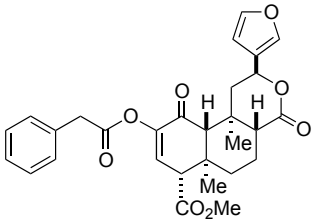

**36**

**(2*S*,4a*R*,6a*R*,7*R*,10a*R*,10b*R*)-Methyl 2-(furan-3-yl)-6a,10b-dimethyl-4,10-dioxo-9-(2-phenylacetoxy)-2,4,4a,5,6,6a,7,10,10a,10b-decahydro-1*H*-benzo[*f*]isochromene-7-carboxylate.** $^{1}$H NMR (500 MHz, $CDCl_3$) δ 7.41 (d, *J* = 0.65 Hz, 1H), 7.39 (t, *J* = 1.65 Hz, 1H), 7.32 (m, 5H), 6.50 (d, *J* = 2.15 Hz, 1H), 6.39 (d, *J* = 0.96 Hz, 1H), 5.55 (dd, *J* = 5.25, 11.53 Hz, 1H), 3.83 (s, 2H), 3.76 (s, 3H), 3.50 (d, *J* = 2.12 Hz, 1H), 3.04 (dd, *J* = 5.32, 13.63 Hz, 1H), 2.37 (s, 1H), 2.16 (m, 2H), 2.06 (m, 1H), 1.65 (m, 3H), 1.35 (s, 3H), 1.16 (s, 3H). $^{13}$C NMR (126 MHz, $CDCl_3$) δ 190.72, 171.37, 170.30, 169.55, 145.26, 143.67, 139.43, 132.89, 129.89, 129.42, 128.70, 127.41, 125.40, 108.50, 71.99, 63.38, 56.34, 52.42, 51.29, 44.10, 43.69, 40.30, 38.35, 35.79, 17.90, 16.71, 14.81. HRMS calculated for $C_{29}H_{30}O_8$: $[M+Na]^+$: 529.1826 (found), 529.1838 (calc). Melting point: 157-159 °C.

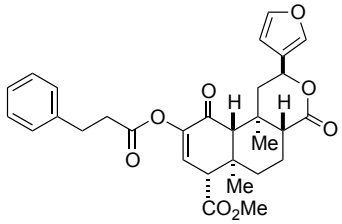

**37**

**(2*S*,4a*R*,6a*R*,7*R*,10a*R*,10b*R*)-Methyl 2-(furan-3-yl)-6a,10b-dimethyl-4,10-dioxo-9-((3-phenylpropanoyl)oxy)-2,4,4a,5,6,6a,7,10,10a,10b-decahydro-1*H*-benzo[*f*]isochromene-7-carboxylate.** $^{1}$H NMR (500 MHz, $CDCl_3$) δ 7.42 (m, 1H), 7.39 (t, *J* = 1.70 Hz, 1H), 7.30 (m, 2H), 7.22 (m, 3H), 6.47 (d, *J* = 2.18 Hz, 1H), 6.40 (dd, *J* = 0.78, 1.78 Hz, 1H), 5.56 (dd, *J* = 5.25, 11.49 Hz, 1H), 3.78 (s, 3H), 3.51 (d, *J* = 2.17 Hz, 1H), 3.03 (m, 3H), 2.83 (m, 2H), 2.39 (s, 1H), 2.17 (m, 2H), 2.08

(m, 1H), 1.66 (m, 3H), 1.36 (s, 3H), 1.17 (s, 3H). $^{13}$C NMR (126 MHz, $CDCl_3$) δ 190.95, 171.37, 170.78, 170.32, 145.17, 143.69, 139.96, 139.41, 129.84, 128.59, 128.28, 126.43, 125.42, 108.48, 72.01, 63.35, 56.36, 52.42, 51.30, 44.12, 43.72, 38.38, 35.80, 35.16, 30.69, 17.91, 16.73, 14.82. HRMS calculated for $C_{30}H_{32}O_8$: $[M+Na]^+$: 543.1973 (found), 543.1995 (calc). Melting point: 162-165 °C.

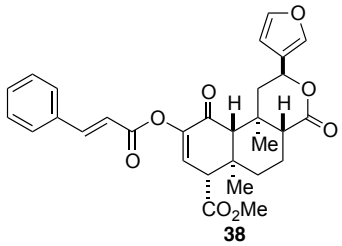

**38**

**(2*S*,4a*R*,6a*R*,7*R*,10a*R*,10b*R*)-Methyl 9-(cinnamoyloxy)-2-(furan-3-yl)-6a,10b-dimethyl-4,10-dioxo-2,4,4a,5,6,6a,7,10,10a,10b-decahydro-1*H*-benzo[*f*]isochromene-7-carboxylate.** $^1$H NMR (500 MHz, $CDCl_3$) δ 7.82 (d, *J* = 16.01 Hz, 1H), 7.55 (m, 2H), 7.42 (m, 4H), 7.39 (t, *J* = 1.71 Hz, 1H), 6.61 (d, *J* = 2.19 Hz, 1H), 6.55 (d, *J* = 15.99 Hz, 1H), 6.39 (dd, *J* = 0.78, 1.81 Hz, 1H), 5.56 (dd, *J* = 5.26, 11.49 Hz, 1H), 3.80 (s, 3H), 3.57 (d, *J* = 2.19 Hz, 1H), 3.08 (dd, *J* = 5.34, 13.68 Hz, 1H), 2.45 (s, 1H), 2.20 (m, 2H), 2.11 (m, 1H), 1.69 (dd, *J* = 7.09, 17.84 Hz, 3H), 1.38 (s, 3H), 1.21 (s, 3H). $^{13}$C NMR (126 MHz, $CDCl_3$) δ 191.07, 171.40, 170.40, 164.66, 147.64, 145.29, 143.68, 139.38, 133.92, 130.93, 129.83, 129.00, 128.39, 125.44, 115.75, 108.46, 72.07, 63.42, 56.47, 52.45, 51.38, 44.19, 43.78, 38.47, 35.85, 17.95, 16.79, 14.86. HRMS calculated for $C_{30}H_{30}O_8$: $[M+Na]^+$: 541.1824 (found), 541.1838 (calc). Melting point: 178 °C (dec).

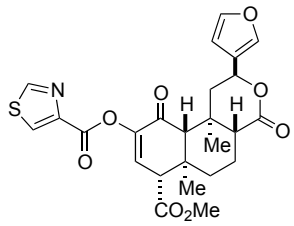

**39**

**(2*S*,4a*R*,6a*R*,7*R*,10a*R*,10b*R*)-2-(Furan-3-yl)-7-(methoxycarbonyl)-6a,10b-dimethyl-4,10-dioxo-2,4,4a,5,6,6a,7,10,10a,10b-decahydro-1*H*-benzo[*f*]isochromen-9-yl thiazole-4-carboxylate.** $^{1}$H NMR (500 MHz, $CDCl_3$) δ 8.90 (d, *J* = 2.08 Hz, 1H), 8.41 (d, *J* = 2.07 Hz, 1H), 7.41 (m, 1H), 7.39 (t, *J* = 1.71 Hz, 1H), 6.72 (d, *J* = 2.17 Hz, 1H), 6.38 (dd, *J* = 0.79, 1.77 Hz, 1H), 5.54 (dd, *J* = 5.30, 11.51 Hz, 1H), 3.80 (s, 3H), 3.60 (d, *J* = 2.17 Hz, 1H), 3.06 (dd, *J* = 5.35, 13.68 Hz, 1H), 2.49 (s, 1H), 2.20 (ddd, *J* = 2.69, 6.54, 9.86 Hz, 2H), 2.13 (m, 1H), 1.69 (m, 3H), 1.37 (s, 3H), 1.22 (s, 3H). $^{13}$C NMR (126 MHz, $CDCl_3$) δ 190.54, 171.36, 170.25, 158.78, 153.91, 146.10, 145.02, 143.70, 139.33, 130.34, 129.45, 125.43, 108.42, 72.07, 63.38, 56.47, 52.48, 51.33, 44.23, 43.71, 38.47, 35.84, 17.95, 16.81, 14.86. HRMS calculated for $C_{25}H_{25}O_8S$: $[M+Na]^+$: 522.1205 (found), 522.1199 (calc). Melting point: 186 °C (dec).

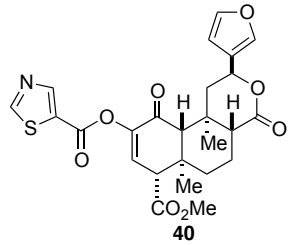

**40**

**(2*S*,4a*R*,6a*R*,7*R*,10a*R*,10b*R*)-2-(Furan-3-yl)-7-(methoxycarbonyl)-6a,10b-dimethyl-4,10-dioxo-2,4,4a,5,6,6a,7,10,10a,10b-decahydro-1*H*-benzo[*f*]isochromen-9-yl thiazole-5-carboxylate.** $^{1}$H NMR (500 MHz, $CDCl_3$) δ 9.05 (s, 1H), 8.63 (d, *J* = 4.73 Hz, 1H), 7.42 (m, 1H), 7.39 (t, *J* = 1.68 Hz, 1H), 6.71 (d, *J* = 2.17 Hz, 1H), 6.39 (dd, *J* = 0.79, 1.79 Hz, 1H), 5.55 (dd, *J* = 5.43, 11.47 Hz, 1H), 3.81 (s, 2H), 3.60 (d, *J* = 2.16 Hz, 1H), 3.05 (dd, *J* = 5.30, 13.61 Hz, 1H), 2.46 (s,

1H), 2.20 (m, 2H), 2.12 (m, 1H), 1.71 (m, 4H), 1.37 (s, 3H), 1.23 (s, 3H).[13]C NMR (126 MHz, $CDCl_3$) δ 190.55, 171.29, 170.56, 170.19, 159.33, 158.86, 150.53, 144.76, 143.71, 139.38, 130.68, 125.39, 108.43, 72.01, 63.44, 56.40, 52.55, 51.30, 44.26, 43.79, 38.41, 35.86, 17.92, 16.81, 14.84. HRMS calculated for $C_{25}H_{25}O_8S$: $[M+Na]^+$: 522.1181 (found), 522.1199 (calc). Melting point: 211-212°C (dec).

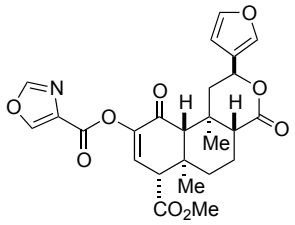

**41**

**(2*S*,4a*R*,6a*R*,7*R*,10a*R*,10b*R*)-2-(Furan-3-yl)-7-(methoxycarbonyl)-6a,10b-dimethyl-4,10-dioxo-2,4,4a,5,6,6a,7,10,10a,10b-decahydro-1*H*-benzo[*f*]isochromen-9-yl oxazole-4-carboxylate.** [1]H NMR (500 MHz, $CDCl_3$) δ 8.41 (d, *J* = 0.96 Hz, 1H), 8.00 (d, *J* = 0.96 Hz, 1H), 7.41 (dd, *J* = 0.83, 1.50 Hz, 1H), 7.39 (t, *J* = 1.70 Hz, 1H), 6.69 (d, *J* = 2.17 Hz, 1H), 6.39 (dd, *J* = 0.77, 1.76 Hz, 1H), 5.54 (dd, *J* = 5.18, 11.47 Hz, 1H), 3.79 (s, 3H), 3.59 (d, *J* = 2.16 Hz, 1H), 3.04 (dd, *J* = 5.35, 13.67 Hz, 1H), 2.48 (s, 1H), 2.19 (m, 2H), 2.12 (m, 1H), 1.70 (m, 3H), 1.37 (s, 3H), 1.21 (s, 3H). [13]C NMR (126 MHz, $CDCl_3$) δ 190.51, 171.35, 170.22, 158.42, 151.75, 145.50, 144.66, 143.69, 139.35, 131.69, 130.52, 125.42, 108.44, 72.04, 63.32, 56.40, 52.49, 51.27, 44.21, 43.66, 38.42, 35.82, 29.70, 17.93, 16.79, 14.84. HRMS calculated for $C_{25}H_{25}O_9$: $[M+Na]^+$: 506.1424 (found), 506.1427 (calc). Melting point: 209-213 °C (dec.).

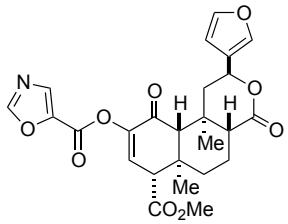

**42**

**(2*S*,4a*R*,6a*R*,7*R*,10a*R*,10b*R*)-2-(Furan-3-yl)-7-(methoxycarbonyl)-6a,10b-dimethyl-4,10-dioxo-2,4,4a,5,6,6a,7,10,10a,10b-decahydro-1*H*-benzo[*f*]isochromen-9-yl oxazole-5-carboxylate.** $^{1}$H NMR (500 MHz, $CDCl_3$) δ 8.09 (s, 1H), 7.94 (s, 1H), 7.42 (dt, *J* = 0.82, 1.60 Hz, 1H), 7.40 (t, *J* = 1.71 Hz, 1H), 6.72 (d, *J* = 2.17 Hz, 1H), 6.39 (dd, *J* = 0.81, 1.79 Hz, 1H), 5.55 (dd, *J* = 5.30, 11.50 Hz, 1H), 3.80 (s, 3H), 3.59 (d, *J* = 2.17 Hz, 1H), 3.05 (dd, *J* = 5.35, 13.65 Hz, 1H), 2.46 (s, 1H), 2.20 (m, 2H), 2.13 (m, 1H), 1.69 (m, 3H), 1.37 (s, 3H), 1.22 (s, 3H). $^{13}$C NMR (126 MHz, $CDCl_3$) δ 190.37, 171.24, 170.11, 154.90, 154.13, 144.35, 143.73, 141.26, 139.36, 135.43, 130.85, 125.39, 108.41, 72.01, 63.47, 56.41, 52.57, 51.30, 44.28, 43.77, 38.43, 35.86, 17.92, 16.80, 14.84. HRMS calculated for $C_{25}H_{25}O_9$: $[M+Na]^+$: 506.1426 (found), 506.1427 (calc). Melting point: 213-215 °C (dec.).

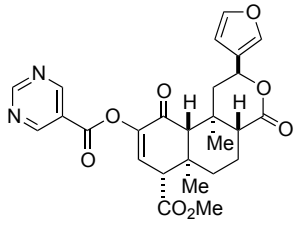

**43**

**(2*S*,4a*R*,6a*R*,7*R*,10a*R*,10b*R*)-2-(Furan-3-yl)-7-(methoxycarbonyl)-6a,10b-dimethyl-4,10-dioxo-2,4,4a,5,6,6a,7,10,10a,10b-decahydro-1*H*-benzo[*f*]isochromen-9-yl pyrimidine-5-carboxylate.** $^{1}$H NMR (500 MHz, $CDCl_3$) δ 9.44 (s, 1H), 9.36 (s, 2H), 7.42 (dt, *J* = 0.84, 1.62 Hz, 1H), 7.40 (t, *J* = 1.70 Hz, 1H), 6.74 (d, *J* = 2.16 Hz, 1H), 6.39 (dd, *J* = 0.79, 1.78 Hz, 1H), 5.56 (dd, *J* = 5.33, 11.50 Hz, 1H), 3.82 (s, 3H), 3.61 (d, *J* = 2.16 Hz, 1H), 3.04 (dd, *J* = 5.35, 13.61 Hz,

1H), 2.48 (s, 1H), 2.21 (m, 2H), 2.14 (dd, *J* = 6.46, 9.54 Hz, 1H), 1.71 (m, 3H), 1.38 (s, 3H), 1.25 (s, 3H). $^{13}$C NMR (126 MHz, $CDCl_3$) δ 190.38, 171.20, 170.13, 162.10, 161.60, 158.48, 144.85, 143.75, 139.39, 130.87, 125.38, 122.91, 108.41, 71.98, 63.53, 56.43, 52.60, 51.31, 44.32, 43.83, 38.43, 35.90, 17.93, 16.83, 14.86. HRMS calculated for $C_{26}H_{26}N_2O_8$: $[M+Na]^+$: 517.1587 (found), 517.1587 (calc). Melting point: 121-124 °C.

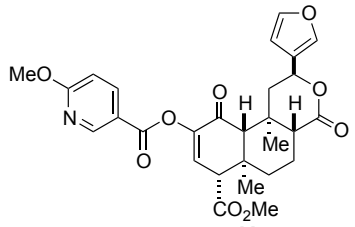

**44**

**(2*S*,4a*R*,6a*R*,7*R*,10a*R*,10b*R*)-2-(furan-3-yl)-7-(methoxycarbonyl)-6a,10b-dimethyl-4,10-dioxo-2,4,4a,5,6,6a,7,10,10a,10b-decahydro-1*H*-benzo[*f*]isochromen-9-yl 6-methoxynicotinate.** $^1$H NMR (500 MHz, $CDCl_3$) δ 8.91 (dd, *J* = 0.64, 2.40 Hz, 1H), 8.19 (dd, *J* = 2.41, 8.74 Hz, 1H), 7.42 (dt, *J* = 0.81, 1.58 Hz, 1H), 7.39 (t, *J* = 1.71 Hz, 1H), 6.80 (dd, *J* = 0.65, 8.74 Hz, 1H), 6.66 (d, *J* = 2.18 Hz, 1H), 6.39 (dd, *J* = 0.81, 1.80 Hz, 1H), 5.55 (dd, *J* = 5.25, 11.51 Hz, 1H), 4.02 (s, 3H), 3.80 (s, 3H), 3.59 (d, *J* = 2.18 Hz, 1H), 3.06 (dd, *J* = 5.34, 13.66 Hz, 1H), 2.46 (s, 1H), 2.20 (m, 2H), 2.12 (m, 1H), 1.68 (m, 3H), 1.38 (s, 3H), 1.24 (s, 3H). $^{13}$C NMR (126 MHz, $CDCl_3$) δ 190.91, 171.36, 170.36, 167.42, 163.42, 151.05, 145.26, 143.69, 139.93, 139.38, 130.20, 125.43, 117.84, 110.99, 108.45, 72.04, 63.48, 56.49, 54.22, 52.49, 51.36, 44.21, 43.82, 38.44, 35.86, 17.95, 16.83, 14.86. HRMS calculated for $C_{28}H_{29}NO_9$: $[M+Na]^+$: 546.1735 (found), 546.1740 (calc). Melting point: 192-195°C (dec.).

*Experimentals for Chapter IV*

Specific rotations were recorded on an Autopol IV automatic polarimeter at λ=589 nm and corrected to 20 °C. Enantiomeric ratios were measured on an Agilent 1100 series HPLC system with diode array detection at 209.4 nm using a CHIRALCEL OD-H column (4.6 x 150 mm) eluting with an isocratic mixture of 2-propanol (IPA) and hexanes (2% IPA/hexanes for **51** and 5% IPA/hexanes for **1**). Compounds **10**,[11] **13**,[12]**14**,[12] **15**,[12] **27**,[13] **50**,[14] **54**,[15] were prepared according to previous reports.

**General MOMO-ether Protection Procedure**: To a solution of phenol (1.0 equiv) in $CH_2Cl_2$ under an atmosphere of argon at 0 °C, was added, sequentially, DIPEA (2.0 equiv) and MOMCl (2.5 equiv). The reaction was allowed to warm to room temperature and stirred until complete by TLC. The reaction was quenched with the addition of saturated aqueous $NH_4Cl$ and the layers allowed to separate. The aqueous layer was further extracted with $CH_2Cl_2$ (3x) and the combined organic layers washed with brine then dried over $Na_2SO_4$. The organic layer was concentrated in vacuo and the resulting residue purified by FCC.

**General Wittig Olefination Procedure**: To a suspension of $[Ph_3PCH_3]^+I^-$ (1.5 equiv) in THF under an atmosphere of argon was added a solution of *n*-BuLi (1.4 equiv) at 0 °C. The resulting bright yellow solution was stirred for 1 h at this temperature. The benzaldehyde (1.0 equiv) was added as a solution in THF and the reaction stirred for an additional hour before being quenched with saturated aqueous $NH_4Cl$ until the color had faded from the reaction. The mixture was extracted with $Et_2O$ (3x) and the combined organic layers were washed with brine then dried over $Na_2SO_4$. The solvent was removed in vacuo and the resulting residue was purified by FCC.

**General Saponification Procedure**: A solution of the ester (2-3 g) dissolved in MeOH (40 mL) was treated with NaOH (3 M, 20 mL) and stirred at RT for 3 h. The MeOH was removed in vacuo and the resulting aqueous layer rinsed with $CH_2Cl_2$ (25 mL). The aqueous was layer was acidified to pH<4 with HCl (6 M) and extracted with $CH_2Cl_2$ (3x30 mL). The combined organic layers were dried over $Na_2SO_4$ and concentrated in vacuo.

**General Amidation Procedure 1**: A solution of propionic acid (1.0 equiv) in THF was treated with CDMT (1.2 equiv) under argon at RT. NMM (3.0 equiv) was added to the reaction and allowed to stir for 1 h before the addition of *N*,*O*-dimethylhydroxylamine·HCl (1.1 equiv). The reaction was allowed to stir overnight then quenched with $H_2O$. The mixture was extracted with $Et_2O$ (3x). The combined organic layers were washed with saturated aqueous $Na_2CO_3$ (2x), HCl (2 M, 2x), and brine (1x). The organic layer was dried over $Na_2SO_4$ and concentrated in vacuo the residue purified by FCC.

**General Amidation Procedure 2**: A solution of $^{i}$PrMgCl (2 M, 3.0 equiv) was added dropwise to a heterogeneous mixture of ethyl ester (1.0 equiv) and *N*,*O*-dimethylhydroxylamine·HCl (1.55 equiv) in THF at -20 °C under argon. After the reaction was complete by TLC (~30 min) the reaction was quenched by the careful addition of HCl (2M) and mixture extracted with $Et_2O$ (3x). The combined organic layer was washed with brine, dried over $Na_2SO_4$, and concentrated in vacuo. The residue was purified by FCC.

**General Borylation Procedure**: Dry, degassed $Et_3N$ (3.0 equiv) was added to a solution of aryl bromide (1.0 equiv), $PdCl_2(CH_3CN)_2$ (0.02 equiv), and SPhos (0.04 equiv) in 1,4-

diox (1.6 M). After vigorous stirring for 10 min, HBPin (1.5 equiv) was added to the reaction resulting in vigorous bubbling. The reaction tube was sealed with a teflon screw cap and heated to 110 °C for 4.5 h. Th reaction was then cooled to RT, diluted with EtOAc and filtered through a pad of Celite. The solvent was removed in vacuo and the residue purified by FCC.

**General Intermolecular Suzuki-Miyaura Procedure**: A reaction tube fitted with a septum was charged with $Pd(OAc)_2$ (0.01 equiv), SPhos (0.02 equiv), and $K_3PO_4$ (2.0 equiv). A solution of boronate ester (1.5 equiv) and arylboromide (1.0 equiv) dissolved in toluene (0.6 M based on aryl bromide) was added. Argon sparged $H_2O$ was added and the reaction vessel sealed with a teflon screwcap. The reaction was heated to 100 °C for 16 h then cooled to RT, diluted with EtOAc, and filtered through a thin pad of Celite. The filtrate was concentrated in vacuo and the resulting residue purified by FCC.

**General Grignard Reaction Procedure**: A three-neck flask fitted with a septum, reflux condenser and slow addition funnel filled with a solution of 4-bromo-1-butene (3.5 M, 3.5 equiv) was charged with magnesium (3.8 equiv) and a crystal of $I_2$. Approximately one tenth of the 4-bromo-1-butene solution was added to the magnesium/$I_2$ mixture and heated until the reaction changed from brown to clear. The remaining solution 4-bromo-1-butene solution was added to the reaction at a rate to maintain a gentle reflux. Upon complete addition, the reaction was heated to reflux for an additional 20 min and cooled to RT. The Grignard solution was added slowly to a solution of Weinreb amide (1.0 equiv) in THF at 0 °C. After the reaction was complete by TLC, it was quenched with saturated aqueous $NH_4Cl$ and extracted with $Et_2O$ (3x). The combined organic layers were

washed with HCl (2 M, 2x) and brine (1x) then dried over $Na_2SO_4$. The solvent was removed in vacuo and the residue purified by FCC.

**General RCM/Reduction Procedure**: A solution of the diene (1.0 equiv) dissolved in $CH_2Cl_2$ (3 mM) was degassed by argon spargining for 15 min. G II (0.10 equiv) was added and the reaction heated to reflux for 24 h then cooled to RT and concentrated in vacuo. The residue was redissolved in THF and treated with 10% Pd/C and placed under an atmosphere of $H_2$ by evacuating and backfilling with $H_2$. The reaction was stirred vigorously overnight then filtered through Celite. The solvent was removed from the filtrate and the residue purified by FCC.

**General Cross-Metathesis Procedure.** A mixture of the two olefins (1:1) was dissolved in anhydrous and degassed $CH_2Cl_2$ (0.1 M) and degassed by argon sparging for 15 min. Grubbs II catalyst (10 mol%) was added and the reaction heated to reflux for 24 h, cooled to RT, treated with DMSO (50 equiv), and stirred at RT for an additional 24 h. The reaction mixture was purified by adsorbing onto silica gel and chromatographed by FCC eluting with 6% EtOAc/Pent. for **51** and 12% EtOAc/Pent. for **58**.

**General Intramolecular Suzuki-Miyaura Reaction Procedure.** A vial was charged with $PdCl_2$(dppf) (20 mol%) and base (10.0 equiv) under an atmosphere of argon and sealed with a teflon coated cap. A solution of **51** in the appropriate solvent was degassed by evacuating and back filling with argon (3x). The solution was transferred to the reaction vessel and degassed $H_2O$ (argon sparged) was added. The reaction was heated in an oil bath at 90 °C for the indicated time then cooled to RT. The reaction was diluted with EtOAc and filtered through Celite. The solvent was removed in vacuo and residue purified by FCC eluting with 5% EtOAc/Pent.

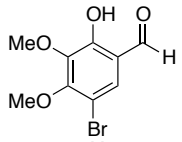

**11**

**5-Bromo-2-hydroxy-3,4-dimethioxybenzaldehyde.** Bromine (1.48 mL, 28.8 mmol) was slowly added to a solution of **10** (5.00 g, 27.4 mmol) in glacial AcOH (50 mL) and stirred for 1.5 h at RT. The reaction was diluted with $CH_2Cl_2$ (75 mL) and washed with $Na_2S_2O_3$ (30 mL), $H_2O$ (3 x 30 mL) and brine (30 mL). The organic layer was dried over $Na_2SO_4$ and concentrated in vacuo. The resulting residue was purified by FCC eluting with 8% EtOAc/Pent. to yield **11** as a white solid (5.80 g, 81%). Melting point: 66-68 °C. $^1$H NMR (500 MHz, $CDCl_3$) δ 11.20 (s, 1H), 9.75 (s, 1H), 7.51 (s, 1H), 4.07 (s, 3H), 3.94 (s, 3H). $^{13}$C NMR (126 MHz, $CDCl_3$) δ 194.50, 156.67, 156.25, 141.30, 131.50, 118.15, 106.84, 61.40, 61.13. HRMS calculated for $C_9H_9BrO_4$: $[M-H]^-$: 258.9594 (found); 258.9606 (calc.).

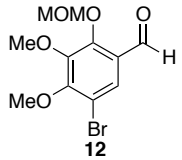

**12**

**5-Bromo-3,4-dimethoxy-2-(methoxymethoxy)benzaldehyde**. Prepared from **11** (1.500 g, 5.745 mmol) in $CH_2Cl_2$ (20 mL) according to general MOM-ether protection procedure and purified via FCC eluting with 10% EtOAc/Hex. to yield **12** as a clear oil (1.631 g, 93%).$^1$H NMR (400 MHz, $CDCl_3$) δ 10.30 (s, 1H), 7.84 (s, 1H), 5.29 (s, 2H), 4.01 (s, 4H), 3.92 (s, 4H), 3.60 (s, 1H). $^{13}$C NMR (126 MHz, $CDCl_3$) δ 187.98, 156.57, 153.74, 146.79, 126.73, 126.69, 113.05, 99.99, 99.98, 99.94, 61.18, 58.02. HRMS calculated for $C_{11}H_{13}BrO_5$: $[M+Na]^+$: 326.9853 (found); 326.9844 (calc).

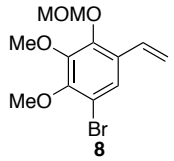

**8**

**1-Bromo-2,3-dimethoxy-4-(methoxymethoxy)-5-vinylbenzene**. Prepared from **12** (1.631 g, 5.346 mmol) according to general Wittig olefination procedure and purified via FCC eluting with 5% EtOAc/Hex. to yield a **8** as a clear oil (1.345 g, 83%). $^{1}$H NMR (500 MHz, $CDCl_3$) δ 7.47 (s, 1H), 6.97 (dd, *J* = 11.06, 17.70 Hz, 1H), 5.69 (dd, *J* = 0.92, 17.70 Hz, 1H), 5.32 (dd, *J* = 0.89, 11.05 Hz, 1H), 5.14 (s, 2H), 3.92 (s, 3H), 3.91 (s, 3H), 3.59 (s, 3H). $^{13}$C NMR (126 MHz, $CDCl_3$) δ 150.71, 147.86, 147.21, 130.18, 129.19, 124.01, 115.47, 112.38, 99.34, 61.05, 61.00, 57.75. HRMS calculated for $C_{12}H_{15}BrO_4$: $[M+Na]^+$: 325.0054 (found); 325.0051 (calc).

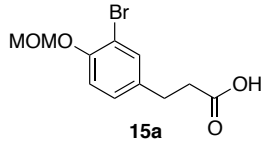

**15a**

**3-(3-Bromo-4-(methoxymethoxy)phenyl)propanoic acid.** Prepared from **15**[12] (2.41 g, 8.34 mmol) according to general saponification procedure to yield **15a** as a white solid (2.14 g, 98%). $^{1}$H NMR (400 MHz, $CDCl_3$) δ 7.42 (s, 1H), 7.10 (d, *J* = 2.83 Hz, 2H), 5.24 (s, 2H), 3.54 (s, 3H), 2.91 (t, *J* = 7.67 Hz, 2H), 2.68 (t, *J* = 7.67 Hz, 2H). $^{13}$C NMR (126 MHz, $CDCl_3$) δ 178.06, 152.28, 135.20, 133.09, 128.30, 116.30, 112.84, 95.16, 56.38, 35.39, 29.38. HRMS calculated for $C_{11}H_{13}BrO_4$: $[M-H]^-$:286.9937 (found), 286.9924 (calc).

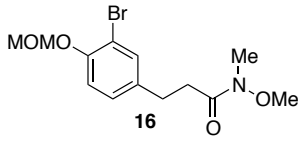

**16**

**3-(3-Bromo-4-(methoxymethoxy)phenyl)-*N*-methoxy-*N*-methylpropanamide**. Prepared from **15a** (2.136 g, 7.389 mmol) using general amidation procedure 1 or from **15** (1.016 g, 3.204 mmol) using general amidation procedure 2.

Purified by FCC eluting with 35% EtOAc/Hex. to yield **16** as a clear oil (90% and 91%, respectively). $^{1}$H NMR (500 MHz, $CDCl_3$) δ 7.44 (d, *J* = 1.84 Hz, 1H), 7.14 (dd, *J* = 1.91, 8.37 Hz, 1H), 7.09 (d, *J* = 8.36 Hz, 1H), 5.24 (s, 2H), 3.66 (s, 3H), 3.54 (d, *J* = 0.82 Hz, 3H), 3.21 (s, 3H), 2.91 (m, 2H), 2.73 (m, 2H). $^{13}$C NMR (126 MHz, $CDCl_3$) δ 173.34, 152.04, 136.51, 133.13, 128.50, 116.32, 112.76, 95.22, 61.26, 56.36, 33.64, 32.20, 29.42. HRMS calculated for $C_{13}H_{18}BrNO_4$: $[M]^+$: 331.0416 (found); 331.0419 (calc).

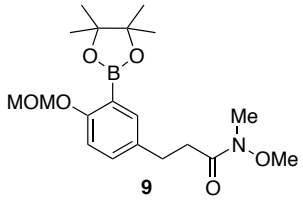

**9**

***N*-Methoxy-3-(4-(methoxymethoxy)-3-(4,4,5,5-tetramethyl-1,3,2-dioxaborolan-2-yl)phenyl)-*N*-methylpropanamide.** Prepared from **16** (964.9 mg, 2.905 mmol) according to general borylation procedure and purified via FCC eluting with 30-35% EtOAc/Pent. to yield **9** as a clear yellow oil (1.095 g, 99%). $^{1}$H NMR (500 MHz, $CDCl_3$) δ 7.54 (d, *J* = 2.36 Hz, 1H), 7.24 (dd, *J* = 2.44, 8.40 Hz, 1H), 6.96 (d, *J* = 8.40 Hz, 1H), 5.16 (s, 2H), 3.62 (s, 3H), 3.51 (s, 3H), 3.18 (s, 3H), 2.90 (m, 2H), 2.71 (m, 2H), 1.35 (s, 12H). $^{13}$C NMR (126 MHz, $CDCl_3$) δ 173.80, 160.14, 136.40, 134.66, 132.36, 116.11, 95.55, 83.49, 75.01, 61.24, 56.10, 34.06, 32.18, 29.84, 24.84. HRMS calculated for $C_{19}H_{30}BNO_6$: $[M]^+$: 379.2146 (found); 379.2166 (calc).

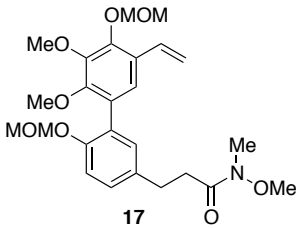

**17**

**3-(2',3'-Dimethoxy-4',6-bis(methoxymethoxy)-5'-vinyl-[1,1'-biphenyl]-3-yl)-*N*-methoxy-*N*-methylpropanamide.** Prepared from **8** (345 mg, 1.14 mmol) and **9** (561 mg, 1.48 mmol) according to the general intermolecular Suzuki-

Miyaura reaction conditions and purified by FCC eluting with 45% EtOAc/Hex. to yield **17** as a clear yellow oil (526 mg, 97%). $^{1}$H NMR (500 MHz, $CDCl_3$) δ 7.21 (dd, *J* = 2.23, 8.41 Hz, 1H), 7.18 (s, 1H), 7.16 (d, *J* = 8.39 Hz, 1H), 7.13 (d, *J* = 2.16 Hz, 1H), 7.07 (dd, *J* = 11.11, 17.79 Hz, 1H), 5.67 (dd, *J* = 1.21, 17.73 Hz, 1H), 5.26 (dd, *J* = 1.20, 11.09 Hz, 1H), 5.21 (s, 2H), 5.09 (s, 2H), 3.92 (s, 3H), 3.69 (s, 3H), 3.66 (s, 3H), 3.65 (s, 3H), 3.38 (s, 3H), 3.21 (s, 3H), 2.97 (m, 2H), 2.77 (t, *J* = 7.52 Hz, 2H). $^{13}$C NMR (126 MHz, $CDCl_3$) δ 173.78, 153.15, 151.61, 147.75, 145.77, 134.69, 131.23, 131.19, 128.73, 128.70, 128.59, 127.02, 122.67, 115.65, 114.14, 99.44, 95.35, 61.26, 60.80, 60.76, 57.67, 55.94, 33.88, 29.87, 24.87. HRMS calculated for $C_{25}H_{33}NO_8$: $[M]^+$: 475.2226 (found); 475.2206 (calc).

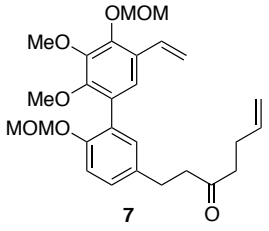

7

**1-(2',3'-Dimethoxy-4',6-bis(methoxymethoxy)-5'-vinyl-[1,1'-biphenyl]-3-yl)hept-6-en-3-one.** Prepared from **17** (700 mg, 1.472 mmol) according to general Grignard reaction condition. Purified by FCC eluting with 15% EtOAc/Hex. to yield **7** as a clear oil (636 mg, 92%). $^{1}$H NMR (500 MHz, $CDCl_3$) δ 7.14 (s, 1H), 7.12 (d, *J* = 1.30 Hz, 2H), 7.04 (m, 2H), 5.78 (ddt, *J* = 6.50, 10.20, 16.78 Hz, 1H), 5.64 (dd, *J* = 1.28, 17.72 Hz, 1H), 5.24 (dd, *J* = 1.25, 11.09 Hz, 1H), 5.18 (s, 2H), 5.06 (s, 2H), 4.99 (ddq, *J* = 1.47, 10.21, 19.36 Hz, 2H), 3.90 (s, 3H), 3.65 (s, 3H), 3.62 (s, 3H), 3.35 (s, 3H), 2.88 (t, *J* = 7.64 Hz, 2H), 2.74 (t, *J* = 7.62 Hz, 2H), 2.50 (t, *J* = 7.38 Hz, 2H), 2.32 (ddd, *J* = 4.07, 7.36, 12.34 Hz, 2H). $^{13}$C NMR (126 MHz, $CDCl_3$) δ 209.31, 153.13, 151.58, 147.76, 145.78, 137.05, 134.34, 131.17, 131.11, 128.65, 128.60, 127.04, 122.63, 115.64,

115.26, 114.16, 99.43, 95.31, 60.79, 60.77, 57.66, 55.94, 44.46, 42.01, 28.89, 27.71. HRMS calculated for $C_{27}H_{34}O_7$: $[M+Na]^+$: 493.2221(found); 493.2202 (calc).

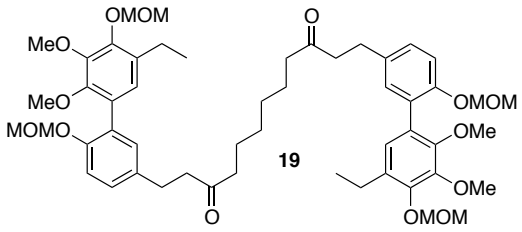

**19**

**1,12-Bis(5'-ethyl-2',3'-dimethoxy-4',6-bis(methoxymethoxy)-[1,1'-biphenyl]-3-yl)dodecane-3,10-dione.** Prepared from **7** according to general RCM/reduction procedure and purified by FCC to yield **19** as a clear oil. $^1$H NMR (500 MHz, $CDCl_3$) δ 7.10 (s, 4H), 7.05 (s, 2H), 6.81 (s, 2H), 5.17 (s, 4H), 5.05 (s, 4H), 3.89 (s, 6H), 3.63 (s, 6H), 3.61 (s, 6H), 3.34 (s, 6H), 2.86 (t, *J* = 7.63 Hz, 4H), 2.70 (m, 8H), 2.38 (td, *J* = 3.75, 7.39 Hz, 4H), 1.55 (dd, *J* = 5.77, 9.35 Hz, 4H), 1.24 (dt, *J* = 5.48, 15.13 Hz, 10H). $^{13}$C NMR (126 MHz, $CDCl_3$) δ 210.25, 153.08, 149.74, 148.16, 145.50, 134.39, 132.49, 131.21, 128.91, 128.36, 128.18, 125.43, 115.78, 99.34, 95.37, 60.73, 60.69, 57.36, 55.90, 44.44, 42.87, 42.66, 28.95, 23.40, 22.81, 14.71. HRMS calculated for $C_{52}H_{70}O_{14}$: $[M+Na]^+$: 941.4648 (found), 941.4663 (calc).

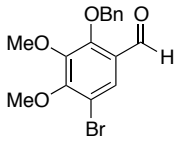

**26**

**2-(Benzyloxy)-5-bromo-3,4-dimethoxybenzaldehyde.** A solution of **11** (5.30 g, 20.30 mmol) in anhydrous DMF (50 mL) was treated sequentially with BnBr (2.53 mL, 21.32 mmol) and $K_2CO_3$ and stirred overnight at RT. The reaction was diluted with $Et_2O$ (150 mL) and $H_2O$ (100 mL). The organic layer was rinsed with additional $H_2O$ (2 x 100 mL) and brine (100 mL), dried over $Na_2SO_4$ and solvent removed in vacuo to yield **26** as a white solid (7.08 g, 99%). Melting point: 48-50 °C. $^1$H NMR (500 MHz, $CDCl_3$) δ 10.05 (s, 1H), 7.76 (s, 1H), 7.38 (m, 5H), 5.21 (s, 2H), 4.03 (s, 3H), 3.96 (s,

3H). $^{13}$C NMR (126 MHz, $CDCl_3$) δ 187.81, 156.60, 155.33, 147.21, 135.81, 128.82, 128.76, 128.65, 126.62, 126.41, 112.80, 61.37, 61.28. HRMS calculated for $C_{16}H_{15}BrO_4$: $[M+Na]^+$: 373.0034(found); 373.0051(calc.).

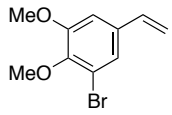

**28**

**1-Bromo-2,3-dimethoxy-5-vinylbenzene**. Prepared from 3-bromo-4,5-dimethoxybenzaldehyde (526 mg, 2.15 mmol) using the general Wittig olefin procedure and purified by FCC eluting with 5% EtOAc/Hex. to yield **28** as colorless oil (402 mg, 77%). $^1$H NMR (500 MHz, $CDCl_3$) δ 7.19 (d, *J* = 1.89 Hz, 1H), 6.89 (d, *J* = 1.88 Hz, 1H), 6.59 (dd, *J* = 10.84, 17.51 Hz, 1H), 5.67 (d, *J* = 17.50 Hz, 1H), 5.25 (d, *J* = 10.83 Hz, 1H), 3.89 (s, 3H), 3.85 (s, 3H). $^{13}$C NMR (126 MHz, $CDCl_3$) δ 153.62, 146.14, 135.32, 134.82, 122.77, 117.80, 114.46, 109.23, 60.67, 56.06. HRMS calculated for $C_{10}H_{11}BrO_2$: $[M+Na]^+$: 264.9825 (found); 264.9840 (calc.).

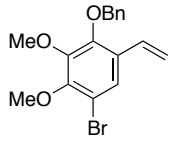

**29**

**2-(Benzyloxy)-5-bromo-3,4-dimethoxy-1-vinylbenzene**. Prepared from **26** (1.021 g, 2.906 mmol) using the general Wittig olefin procedure and purified by FCC eluting with 2% EtOAc/Hex to yield **29** as a colorless oil (786 mg, 77%). $^1$H NMR (500 MHz, $CDCl_3$) δ 7.45 (dd, *J* = 3.79, 10.51 Hz, 3H), 7.39 (m, 2H), 7.35 (m, 1H), 6.87 (dd, *J* = 11.10, 17.77 Hz, 1H), 5.65 (dd, *J* = 1.02, 17.70 Hz, 1H), 5.24 (dd, *J* = 1.01, 11.06 Hz, 1H), 4.99 (s, 2H), 3.92 (s, 3H), 3.92 (s, 3H). $^{13}$C NMR (126 MHz, $CDCl_3$) δ 150.69, 149.72, 147.71, 137.03, 129.97, 129.17, 128.51, 128.26, 128.21, 123.84, 115.34, 112.26, 75.66, 61.26, 61.15. HRMS calculated for $C_{17}H_{17}BrO_3$: $[M+Na]^+$: 371.0257 (found); 371.0259 (calc).

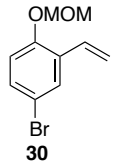

**30**

**4-Bromo-1-(methoxymethoxy)-2-vinylbenzene.** Prepared from **27** (1.09 g, 4.45 mmol) using the general Wittig olefin procedure and purified by FCC eluting with 2% EtOAc/Hex. to yield **30** as a colorless oil (963 mg, 89%). $^{1}$H NMR (500 MHz, $CDCl_3$) δ 7.59 (d, *J* = 2.48 Hz, 1H), 7.29 (dd, *J* = 2.50, 8.78 Hz, 1H), 6.98 (m, 2H), 5.73 (dd, *J* = 1.15, 17.72 Hz, 1H), 5.31 (dd, *J* = 1.14, 11.12 Hz, 1H), 5.18 (s, 2H), 3.47 (s, 3H). $^{13}$C NMR (126 MHz, $CDCl_3$) δ 153.34, 131.33, 130.30, 129.55, 129.05, 116.50, 115.83, 114.52, 94.74, 56.18. HRMS calculated for $C_{10}H_{11}BrO_2$: $[M+H]^+$: 243.0018 (found); 243.0021 (calc).

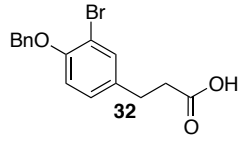

**32**

**3-(4-(Benzyloxy)-3-bromophenyl)propanoic acid.** Prepared from **54** (3.01 g, 8.29 mmol) using general saponification procedure to yield **32** as a white solid (2.53 g, 91%) Melting point: 102-104 °C. $^{1}$H NMR (500 MHz, $CDCl_3$) δ 7.47 (m, 2H), 7.42 (d, *J* = 2.18 Hz, 1H), 7.38 (m, 2H), 7.32 (m, 1H), 7.06 (dd, *J* = 2.20, 8.37 Hz, 1H), 6.85 (d, *J* = 8.40 Hz, 1H), 5.13 (s, 2H), 2.87 (t, *J* = 7.67 Hz, 2H), 2.64 (t, *J* = 7.69 Hz, 2H). $^{13}$C NMR (126 MHz, $CDCl_3$) δ 178.20, 153.59, 136.56, 134.13, 133.17, 128.57, 128.18, 127.92, 126.99, 113.93, 112.44, 70.89, 35.45, 29.34. HRMS calculated for $C_{16}H_{15}BrO_3$: $[M-H]^-$ : 334.0124 (found), 333.0126 (calc).

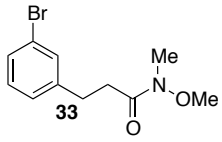

**33**

**3-(3-Bromophenyl)-*N*-methoxy-*N*-methylpropanamide**. Prepared from 3-(3-bromophenyl)propionic acid (1.000 g, 4.365 mmol) according to general

amidation procedure 1 to yield **33** as an oil (1.180 g, 99%). $^{1}$H NMR (500 MHz, $CDCl_3$) δ 7.38 (m, 1H), 7.33 (m, 1H), 7.16 (m, 2H), 3.63 (s, 3H), 3.18 (s, 3H), 2.93 (m, 2H), 2.73 (t, *J* = 7.56 Hz, 2H). $^{13}$C NMR (126 MHz, $CDCl_3$) δ 173.22, 143.71, 131.47, 130.02, 129.24, 127.20, 122.45, 61.26, 33.41, 32.20, 30.22. HRMS calculated for $C_{11}H_{14}BrNO_2$: $[M+Na]^+$: 294.0113 (found), 294.0106 (calc).

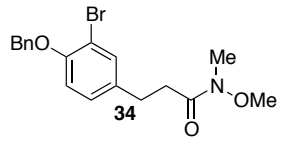

**34**

**3-(4-(Benzyloxy)-3-bromophenyl)-*N*-methoxy-*N*-methylpropanamide**. Prepared from **32** (3.000 g, 8.952 mmol) according to general amidation procedure 1 to yield **34** as a clear oil (3.35 g, 99%). $^{1}$H NMR (400 MHz, $CDCl_3$) δ 7.49 (d, *J* = 7.46 Hz, 2H), 7.45 (t, *J* = 2.40 Hz, 1H), 7.40 (t, *J* = 7.34 Hz, 2H), 7.34 (d, *J* = 7.17 Hz, 1H), 7.10 (m, 1H), 6.87 (d, *J* = 8.38 Hz, 1H), 3.63 (s, 2H), 3.19 (s, 2H), 2.90 (t, *J* = 7.75 Hz, 2H), 2.68 (m, 2H). $^{13}$C NMR (126 MHz, $CDCl_3$) δ 173.63, 153.36, 136.64, 135.41, 133.21, 128.56, 128.40, 127.90, 127.00, 113.93, 112.35, 70.90, 61.25, 33.66, 32.18, 29.42. HRMS calculated for $C_{18}H_{20}BrNO_3$: $[M+Na]^+$: 400.0536 (found); 400.0524 (calc).

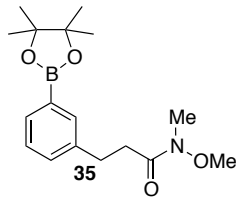

**35**

***N*-Methoxy-*N*-methyl-3-(3-(4,4,5,5-tetramethyl-1,3,2-dioxaborolan-2-yl)phenyl)propanamide**. Prepared from **33** (1.500 g, 5.511 mmol) according to general borylation procedure and purified by FCC eluting with 30% EtOAc/Hex. to yield **35** as a yellow oil (1.202 g, 68%). $^{1}$H NMR (500 MHz, $CDCl_3$) δ 7.66 (m, 2H), 7.33 (m, 2H), 3.61 (s, 3H), 3.18 (s, 3H), 2.95 (m, 2H), 2.75 (m, 2H), 1.35 (s, 12H). $^{13}$C NMR (126

MHz, $CDCl_3$) δ 173.74, 143.71, 140.64, 134.68, 132.60, 131.53, 131.47, 130.02, 129.24, 127.92, 127.20, 122.45, 83.78, 61.24, 33.93, 33.41, 32.19, 24.87. HRMS calculated for $C_{17}H_{26}BNO_4$: $[M+Na]^+$: 3421865 (found); 342.1853 (calc).

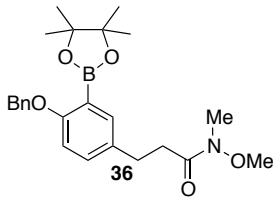

**36**

**3-(4-(Benzyloxy)-3-(4,4,5,5-tetramethyl-1,3,2-dioxaborolan-2-yl)phenyl)-*N*-methoxy-*N*-methylpropanamide**. Prepared from **34** (2.085 g, 5.512 mmol) according to general borylation procedure and purified by FCC eluting with 33% EtOAc/Hex. to yield **36** as yellow oil (2.347 g, 100%). $^1$H NMR (500 MHz, $CDCl_3$) δ 7.62 (d, *J* = 7.51 Hz, 2H), 7.57 (d, *J* = 2.26 Hz, 1H), 7.39 (t, *J* = 7.57 Hz, 2H), 7.31 (t, *J* = 6.36 Hz, 2H), 6.89 (d, *J* = 8.41 Hz, 1H), 5.12 (s, 2H), 3.63 (s, 3H), 3.20 (s, 3H), 2.93 (m, 2H), 2.74 (m, 2H), 1.39 (s, 12H). $^{13}$C NMR (126 MHz, $CDCl_3$) δ 171.21, 161.79, 137.73, 136.49, 133.26, 132.52, 129.44, 128.13, 127.29, 126.79, 112.27, 83.48, 75.03, 70.12, 34.09, 32.15, 29.83, 24.85. HRMS calculated for $C_{24}H_{32}BNO_5$: $[M+Na]^+$: 448.2245 (found), 448.2271 (calc).

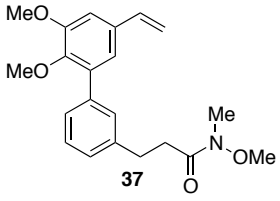

**37**

**3-(2',3'-Dimethoxy-5'-vinyl-[1,1'-biphenyl]-3-yl)-*N*-methoxy-*N*-methylpropanamide.** Synthesized according to general intermolecular Suzuki-Miyaura reaction procedure with **28** (143 mg, 0.588 mmol) and **35** (282 mg, 0.882 mmol) and purified by FCC eluting with 30-35% EtOAc/Hex. to yield **37** as a thick oil (178 mg, 84%). $^1$H NMR (500 MHz, $CDCl_3$) δ 7.39 (m, 2H), 7.34 (t, *J* = 7.52 Hz, 1H), 7.22 (dt, *J* = 1.46, 7.39 Hz, 1H), 6.98 (s, 2H), 6.69 (dd, *J* = 10.84, 17.54 Hz, 1H), 5.69 (dd, *J* = 0.72,

17.54 Hz, 1H), 5.23 (dd, *J* = 0.66, 10.84 Hz, 1H), 3.93 (s, 3H), 3.62 (s, 3H), 3.59 (s, 3H), 3.19 (s, 3H), 3.02 (m, 2H), 2.78 (m, 2H). $^{13}$C NMR (126 MHz, $CDCl_3$) δ 173.74, 153.08, 146.39, 141.11, 138.30, 136.43, 135.78, 133.53, 129.22, 128.23, 127.39, 127.01, 121.08, 113.33, 108.77, 61.24, 60.73, 55.95, 33.80, 32.19, 30.76. HRMS calculated for $C_{21}H_{25}NO_4$: [M+Na]+: 355.1754 (found), 355.1784 (calc).

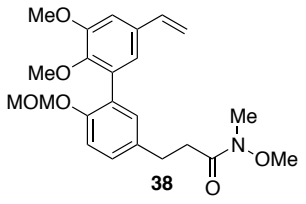

**38**

**3-(2',3'-Dimethoxy-6-(methoxymethoxy)-5'-vinyl-[1,1'-biphenyl]-3-yl)-*N*-methoxy-*N*-methylpropanamide**. Synthesized according to general intermolecular Suzuki-Miyaura reaction procedure with **28** (100 mg, 0.411 mmol) and **9** (222 mg, 0.585 mmol) and purified by FCC eluting with 40% EtOAc/Hex to yield **38** as a clear oil (138 mg, 81%). $^1$H NMR (400 MHz, $CDCl_3$) δ 7.18 (ddd, *J* = 2.11, 9.48, 18.89 Hz, 3H), 7.01 (d, *J* = 2.00 Hz, 1H), 6.93 (d, *J* = 2.00 Hz, 1H), 6.69 (dd, *J* = 10.86, 17.55 Hz, 1H), 5.68 (d, *J* = 17.52 Hz, 1H), 5.23 (d, *J* = 10.87 Hz, 1H), 5.09 (s, 2H), 3.95 (s, 3H), 3.64 (s, 3H), 3.62 (s, 3H), 3.37 (s, 3H), 3.20 (s, 3H), 2.96 (m, 2H), 2.76 (m, 2H). $^{13}$C NMR (126 MHz, $CDCl_3$) δ 173.76, 153.10, 152.61, 146.91, 136.51, 134.52, 132.98, 132.95, 131.12, 128.75, 128.63, 121.78, 115.59, 113.02, 108.95, 95.22, 61.25, 60.64, 55.91, 55.86, 33.89, 32.18, 29.89. HRMS calculated for $C_{23}H_{29}NO_6$: $[M+Na]^+$: 415.1966 (found), 415.1995 (calc).

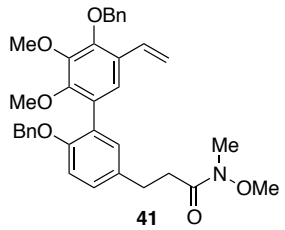

**41**

**3-(4',6-Bis(benzyloxy)-2',3'-dimethoxy-5'-vinyl-[1,1'-biphenyl]-3-yl)-*N*-methoxy-*N*-methylpropanamide**. Prepared from **29** (1.137 g, 3.256 mmol) and **36** (2.077 g, 4.883 mmol) according to general intramolecular Suzuki-Miyaura reaction conditions and purified by FCC eluting with 33% EtOAc/Hex. to yield **41** as an oil (1.687 g, 91%).$^{1}$H NMR (500 MHz, $CDCl_3$) δ 7.52 (dd, *J* = 0.92, 7.74 Hz, 2H), 7.41 (m, 2H), 7.36 (m, 1H), 7.27 (m, 4H), 7.20 (m, 4H), 6.99 (dd, *J* = 11.21, 17.85 Hz, 1H), 6.95 (d, *J* = 8.25 Hz, 1H), 5.63 (dd, *J* = 1.32, 17.73 Hz, 1H), 5.18 (dd, *J* = 1.29, 11.11 Hz, 1H), 5.06 (s, 2H), 5.04 (s, 2H), 3.92 (s, 3H), 3.67 (s, 3H), 3.62 (s, 3H), 3.18 (s, 3H), 2.95 (m, 2H), 2.75 (t, *J* = 7.37 Hz, 2H).$^{13}$C NMR (126 MHz, $CDCl_3$) δ 173.84, 154.50, 151.71, 149.69, 146.26, 137.60, 137.46, 133.61, 131.33, 131.04, 128.57, 128.55, 128.48, 128.29, 128.23, 128.19, 128.03, 127.49, 126.90, 126.87, 122.68, 113.94, 113.14, 75.66, 70.55, 61.26, 61.04, 60.97, 33.92, 32.17, 29.90. HRMS calculated for $C_{35}H_{37}NO_6$: $[M+Na]^+$: 590.2557 (found), 590.2519 (calc).

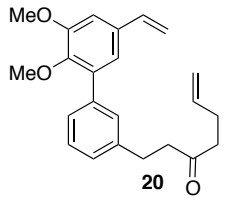

**20**

**1-(2',3'-Dimethoxy-5'-vinyl-[1,1'-biphenyl]-3-yl)hept-6-en-3-one.** Prepared from **37** (178 mg, 0.473 mmol) according to general Grignard reaction procedure and purified by FCC eluting with 10% EtOAc/Hex. to yield **20** as a clear oil (134 mg, 76%). $^{1}$H NMR (500 MHz, $CDCl_3$) δ 7.37 (m, 2H), 7.33 (t, *J* = 7.45 Hz, 1H), 7.17 (dt, *J* = 1.42, 7.41 Hz, 1H), 6.97 (dd, *J* = 1.99, 7.89 Hz, 2H), 6.69 (dd, *J* = 10.85,

17.54 Hz, 1H), 5.78 (ddt, *J* = 6.50, 10.20, 16.79 Hz, 1H), 5.69 (dd, *J* = 0.71, 17.54 Hz, 1H), 5.23 (dd, *J* = 0.66, 10.84 Hz, 1H), 4.98 (ddq, *J* = 1.47, 10.20, 19.24 Hz, 2H), 3.93 (s, 3H), 3.58 (s, 3H), 2.95 (t, *J* = 7.68 Hz, 2H), 2.78 (t, *J* = 7.68 Hz, 2H), 2.50 (t, *J* = 7.38 Hz, 2H), 2.33 (m, 2H). $^{13}$C NMR (126 MHz, $CDCl_3$) δ 209.27, 153.09, 146.37, 140.78, 138.31, 137.04, 136.42, 135.74, 133.56, 129.12, 128.26, 127.27, 126.98, 121.03, 115.28, 113.35, 108.79, 60.72, 55.96, 44.32, 42.03, 29.74, 27.72. HRMS calculated for $C_{23}H_{26}O_3$: $[M+Na]^+$: 373.1756 (found), 373.1780 (calc).

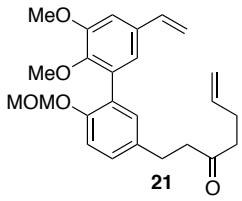

**21**

**1-(2',3'-Dimethoxy-6-(methoxymethoxy)-5'-vinyl-[1,1'-biphenyl]-3-yl)hept-6-en-3-one**. Prepared from **38** (131 mg, 0.316 mmol) according to general Grignard reaction procedure and purified by FCC eluting with 10% EtOAc/Hex. to yield **21** as a clear oil (99 mg, 76%). $^1$H NMR (500 MHz, $CDCl_3$) δ 7.13 (d, *J* = 2.02 Hz, 2H), 7.06 (d, *J* = 1.14 Hz, 1H), 6.98 (d, *J* = 2.02 Hz, 1H), 6.89 (d, *J* = 1.97 Hz, 1H), 6.67 (dd, *J* = 10.85, 17.54 Hz, 1H), 5.78 (ddt, *J* = 6.50, 10.20, 16.78 Hz, 1H), 5.66 (dd, *J* = 0.75, 17.53 Hz, 1H), 5.20 (dd, *J* = 0.69, 10.84 Hz, 1H), 5.06 (s, 2H), 4.98 (ddq, *J* = 1.47, 10.21, 18.85 Hz, 2H), 3.93 (s, 3H), 3.58 (s, 3H), 3.35 (s, 3H), 2.87 (t, *J* = 7.63 Hz, 2H), 2.73 (t, *J* = 7.62 Hz, 2H), 2.49 (t, *J* = 7.38 Hz, 2H), 2.32 (tdd, *J* = 3.52, 4.60, 8.28 Hz, 2H). $^{13}$C NMR (126 MHz, $CDCl_3$) δ 209.35, 153.08, 152.62, 146.88, 137.05, 136.76, 136.50, 134.17, 133.00, 132.89, 131.01, 128.62, 121.73, 115.59, 115.25, 113.03, 108.95, 95.20, 60.63, 55.91, 55.86, 44.46, 42.02, 28.91, 27.71. HRMS calculated for $C_{25}H_{30}O_5$: $[M+Na]^+$: 433.1986 (found); 433.1991 (calc).

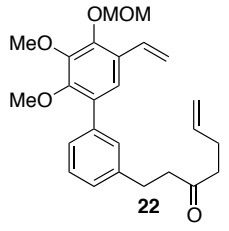


**1-(2',3'-Dimethoxy-4'-(methoxymethoxy)-5'-vinyl-[1,1'-biphenyl]-3-yl)hept-6-en-3-one.** Prepared from **39** (233 mg, 0.561 mmol) according to general Grignard reaction procedure and purified by FCC eluting with 10% EtOAc/Hex. to yield **22** as a clear oil (190 mg, 83%). $^{1}$H NMR (500 MHz, $CDCl_3$) δ 7.32 (m, 3H), 7.21 (s, 1H), 7.16 (ddd, *J* = 2.09, 3.72, 5.12 Hz, 1H), 7.05 (dd, *J* = 11.18, 17.83 Hz, 1H), 5.79 (ddt, *J* = 6.50, 10.20, 16.78 Hz, 1H), 5.70 (dd, *J* = 1.24, 17.74 Hz, 1H), 5.27 (dd, *J* = 1.21, 11.09 Hz, 1H), 5.18 (s, 2H), 4.99 (ddq, *J* = 1.47, 10.21, 19.62 Hz, 2H), 3.92 (s, 3H), 3.65 (s, 3H), 3.61 (s, 3H), 2.96 (t, *J* = 7.66 Hz, 2H), 2.78 (t, *J* = 7.68 Hz, 2H), 2.51 (t, *J* = 7.38 Hz, 2H), 2.33 (m, 2H).$^{13}$C NMR (126 MHz, $CDCl_3$) δ 209.22, 151.08, 147.72, 146.24, 140.89, 138.23, 137.04, 131.72, 131.13, 129.09, 128.32, 127.65, 127.13, 126.93, 122.00, 115.28, 114.54, 99.41, 60.97, 60.89, 57.72, 44.37, 42.02, 29.74, 27.72. HRMS calculated for $C_{25}H_{30}O_5$: $[M+Na]^+$: 433.1976 (found); 433.1991 (calc).

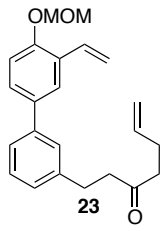


**1-(4'-(Methoxymethoxy)-3'-vinyl-[1,1'-biphenyl]-3-yl)hept-6-en-3-one.** Prepared from **40** (168 mg, 0.473 mmol) according to general Grignard reaction procedure and purified by FCC eluting with 5% EtOAc/Hex. to yield **23** as a clear oil (110 mg, 66%). $^{1}$H NMR (500 MHz, $CDCl_3$) δ 7.68 (d, *J* = 2.34 Hz, 1H), 7.40 (m, 3H), 7.34 (t, *J* = 7.58 Hz, 1H), 7.15 (t, *J* = 8.01 Hz, 2H), 7.11 (dd, *J* = 11.09, 17.71 Hz, 1H), 5.80 (m, 2H), 5.33 (dd, *J* = 1.36, 11.14 Hz, 1H), 5.25 (s, 2H), 4.99 (ddq, *J* = 1.46, 10.21,

19.51 Hz, 2H), 3.52 (s, 3H), 2.96 (t, *J* = 7.67 Hz, 2H), 2.79 (t, *J* = 7.68 Hz, 2H), 2.51 (t, *J* = 7.37 Hz, 2H), 2.33 (m, 2H). $^{13}$C NMR (126 MHz, $CDCl_3$) δ 209.23, 153.88, 141.56, 141.55, 141.05, 137.03, 134.95, 131.52, 128.90, 127.72, 127.55, 126.93, 126.90, 125.21, 124.75, 115.30, 115.01, 94.72, 56.20, 44.42, 42.02, 29.78, 27.72. HRMS calculated for $C_{23}H_{26}O_3$: $[M+Na]^+$: 373.1768 (found); 373.1780 (calc).

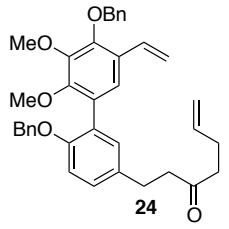

24

**1-(4',6-Bis(benzyloxy)-2',3'-dimethoxy-5'-vinyl-[1,1'-biphenyl]-3-yl)hept-6-en-3-one**. Prepared from **41** (316 mg, 0.556 mmol) according to general Grignard reaction procedure and purified by FCC eluting with 7.5% EtOAc/Hex. to yield **24** as a clear oil (261 mg, 83%). $^1$H NMR (500 MHz, $CDCl_3$) δ 7.52 (d, *J* = 6.92 Hz, 2H), 7.41 (t, *J* = 7.26 Hz, 2H), 7.36 (d, *J* = 7.26 Hz, 1H), 7.27 (d, *J* = 3.57 Hz, 5H), 7.19 (s, 1H), 7.11 (d, *J* = 7.18 Hz, 2H), 6.99 (dd, *J* = 11.16, 17.81 Hz, 1H), 6.93 (dd, *J* = 1.56, 7.32 Hz, 1H), 5.78 (ddt, *J* = 6.50, 10.20, 16.80 Hz, 1H), 5.63 (dd, *J* = 1.28, 17.73 Hz, 1H), 5.18 (dd, *J* = 1.26, 11.12 Hz, 1H), 5.06 (s, 2H), 5.04 (s, 2H), 4.98 (dddd, *J* = 1.47, 3.13, 10.21, 19.40 Hz, 2H), 3.92 (s, 3H), 3.65 (s, 3H), 2.88 (dd, *J* = 5.44, 9.77 Hz, 2H), 2.75 (t, *J* = 7.57 Hz, 2H), 2.50 (t, *J* = 7.39 Hz, 2H), 2.32 (m, 2H). $^{13}$C NMR (126 MHz, $CDCl_3$) δ 209.43, 154.47, 151.68, 149.68, 146.26, 137.58, 137.41, 137.05, 133.26, 131.19, 131.00, 128.48, 128.44, 128.29, 128.22, 128.18, 128.03, 127.49, 126.88, 122.63, 115.26, 113.95, 113.13, 75.65, 70.53, 61.05, 60.96, 44.52, 42.03, 28.89, 27.71.

HRMS calculated for $C_{35}H_{34}O_3$: $[M+Na]^+$: 585.2599 (found); 585.2617 (calc).

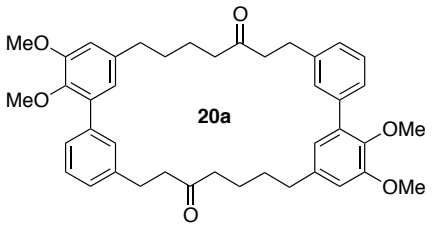


Prepared from **20** (133 mg, 0.380 mmol) according to general RCM/reduction procedure to yield **20a** as a white solid (38 mg, 31%). $^{1}$H NMR (500 MHz, $CDCl_3$) δ 7.41 (m, 2H), 7.29 (d, *J* = 7.62 Hz, 2H), 7.25 (d, *J* = 1.50 Hz, 2H), 7.14 (d, *J* = 7.66 Hz, 2H), 6.76 (d, *J* = 2.00 Hz, 2H), 6.71 (d, *J* = 2.02 Hz, 2H), 3.90 (s, 6H), 3.56 (s, 6H), 2.93 (m, 8H), 2.76 (t, *J* = 7.44 Hz, 4H), 2.33 (t, *J* = 7.28 Hz, 4H), 1.52 (dd, *J* = 4.64, 9.49 Hz, 4H), 1.18 (m, 4H). $^{13}$C NMR (126 MHz, $CDCl_3$) δ 210.52, 152.84, 144.71, 140.99, 138.49, 137.42, 137.32, 135.46, 128.83, 128.04, 127.25, 122.76, 111.72, 60.67, 55.97, 44.27, 42.86, 38.15, 29.91, 28.40, 23.43. HRMS calculated for $C_{42}H_{48}O_6$: $[M+Na]^+$: 671.3322 (found), 671.3349 (calc).

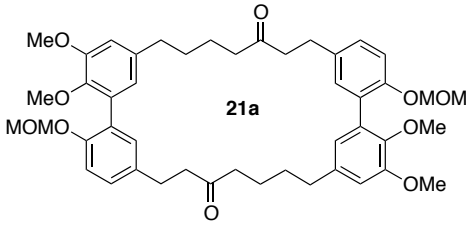


Prepared from **21** (98.1 mg, 0.239 mmol) according to general RCM/reduction procedure to yield **21a** as a white solid (31 mg, 34%). $^{1}$H NMR (500 MHz, $CDCl_3$) δ 7.11 (m, 4H), 6.99 (s, 2H), 6.75 (m, 2H), 6.60 (m, 2H), 5.01 (s, 4H), 3.89 (s, 6H), 3.57 (s, 6H), 3.33 (s, 6H), 2.91 (s, 4H), 2.85 (t, *J* = 7.22 Hz, 4H), 2.72 (t, *J* = 7.26 Hz, 4H), 2.30 (t, *J* = 7.36 Hz, 4H), 1.51 (m, 4H), 1.18 (m, 4H). $^{13}$C NMR (126 MHz, $CDCl_3$) δ 210.63, 153.25, 152.22, 145.22, 136.99, 134.41, 132.94, 130.88, 129.13, 128.70, 123.20, 115.66, 111.90, 95.35, 60.58, 55.89, 55.83, 44.27, 43.05, 38.10, 29.01, 28.57, 23.49. HRMS calculated for $C_{46}H_{56}O_{10}$: $[M+Na]^+$: 791.3802 (found), 791.3771 (calc).

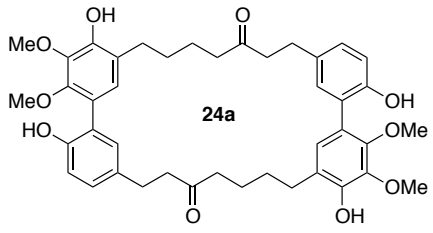

**24a**

Prepared from **24** (120 mg, 0.213 mmol) according to general RCM/reduction procedure to yield **24a** as a white solid (16 mg, 21%). $^{1}$H NMR (500 MHz, $CDCl_3$) δ 7.08 (dt, *J* = 2.85, 5.46 Hz, 4H), 6.95 (d, *J* = 8.83 Hz, 2H), 6.83 (s, 2H), 6.68 (s, 2H), 5.88 (s, 2H), 4.00 (s, 6H), 3.66 (s, 6H), 2.87 (t, *J* = 7.61 Hz, 4H), 2.73 (dd, *J* = 5.55, 9.67 Hz, 4H), 2.67 (m, 4H), 2.38 (t, *J* = 7.39 Hz, 4H), 1.54 (m, 4H), 1.23 (t, *J* = 7.55 Hz, 4H). $^{13}$C NMR (126 MHz, $CDCl_3$) δ 210.44, 151.64, 147.10, 146.71, 139.24, 133.46, 130.72, 128.76, 127.50, 126.25, 125.84, 122.91, 117.81, 61.56, 61.39, 44.55, 42.95, 29.07, 28.98, 23.54, 22.94, 14.09. HRMS calculated for $C_{42}H_{48}O_{10}$: $[M+Na]^+$: 735.3112 (found), 735.3145 (calc).

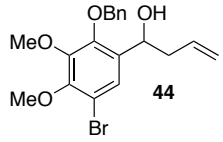

**44**

**1-(2-(Benzyloxy)-5-bromo-3,4-dimethoxyphenyl)but-3-en-1-ol. 26** (7.08 g, 20.16 mmol) was dissolved in a mixture of THF (56 mL) and saturated aqueous $NH_4Cl$ (112 mL). To the reaction was added allyl bromide (3.5 mL, 40.32 mmol) and Zn dust (2.637 g, 40.32 mmol). The biphasic reaction was stirred vigorously for 6 h over which time the solid Zn was consumed. The two layers were separated and the aqueous layer extracted with $Et_2O$ (3 x 50 mL). The combined organic layers were washed with $H_2O$ (100 mL) and brine (100 mL). The organic layer was dried over $Na_2SO_4$ and concentrated in vacuo. The residue was purified by FCC eluting with 8% EtOAc/Pent. to yield **44** as a clear oil (7.33 g, 92%). $^{1}$H NMR (500 MHz, CDCl3) δ 7.37 (m, 6H), 5.74 (dddd, *J* = 6.55, 7.62, 10.76, 16.98 Hz, 1H), 5.11 (m, 4H), 4.85 (dt, *J* = 4.26, 8.38 Hz,

1H), 3.94 (s, 3H), 3.92 (s, 3H), 2.40 (m, 2H), 1.98 (d, *J* = 4.00 Hz, 1H). $^{13}$C NMR (126 MHz, CDCl3) δ 150.45, 148.93, 147.23, 137.04, 134.47, 134.39, 128.62, 128.36, 128.24, 124.70, 118.37, 111.93, 75.38, 67.80, 61.15, 61.06, 42.45. HRMS calculated for $C_{19}H_{21}BrO_4$: $[M+Na]^+$: 415.0521(found); 415.0533 (calc.).

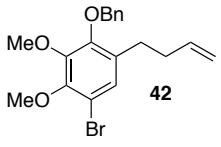

**42**

**2-(Benzyloxy)-5-bromo-1-(but-3-en-1-yl)-3,4-dimethoxybenzene.** A solution of **44** (3.50 g, 8.90 mmol) in $MeNO_2$ (50 mL) under an atmosphere of argon was treated with $Et_3SiH$ (3.13 mL, 19.6 mmol) followed by $FeCl_3$ (144 mg, 0.890 mmol). After 4 h, the solvent was removed in vacuo and residue purified by FCC eluting with 2% EtOAc/Pent.) to yield **42** as a clear oil (2.93 g, 87%). $^1$H NMR (500 MHz, $CDCl_3$) δ 7.45 (dd, *J* = 1.02, 7.77 Hz, 2H), 7.39 (dd, *J* = 6.43, 8.00 Hz, 2H), 7.35 (dt, *J* = 4.32, 9.74 Hz, 1H), 7.09 (s, 1H), 5.80 (ddt, *J* = 6.60, 10.21, 16.88 Hz, 1H), 5.03 (s, 2H), 4.98 (m, 2H), 3.93 (s, 3H), 3.91 (s, 3H), 2.59 (dd, *J* = 6.79, 9.05 Hz, 2H), 2.26 (m, 2H). $^{13}$C NMR (126 MHz, $CDCl_3$) δ 150.20, 149.40, 147.61, 137.86, 137.45, 132.72, 128.50, 128.09, 128.03, 127.38, 115.05, 111.31, 75.15, 61.12, 61.06, 34.43, 29.25. HRMS calculated for $C_{19}H_{21}BrO_3$: $[M+Na]^+$: 399.0579 (found); 399.0572 (calc.)

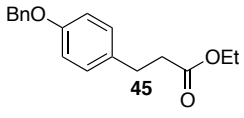

**45**

**Ethyl 3-(4-(benzyloxy)phenyl)propanoate**. A solution of **13** (1.93 g, 9.94 mmol) in DMF (5 mL) was treated with BnBr (1.3 mL, 1.1 equiv) and $K_2CO_3$ (4.12 g, 29.8 mmol). The reaction was stirred overnight at RT then quenched with $H_2O$ (70 mL). The mixture was extracted with $Et_2O$ (3x50 mL). The combined organic layers were washed with HCl (2 M, 1x) and brine (1x) then dried over $Na_2SO_4$ and concentrated in

vacuo. The residue was purified by FCC eluting with 5% EtOAc/Pent. to yield **45** as a clear oil (2.288 g, 81%) that matched the literature values.[16]

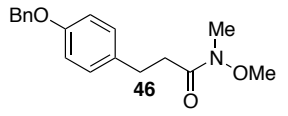

**46**

**3-(4-(Benzyloxy)phenyl)-*N*-methoxy-*N*-methylpropanamide**. Prepared from **45** (643 mg, 2.26 mmol) according to general amidation procedure 2 to provide **46** as a clear oil (582 mg, 86%). $^{1}$H NMR (500 MHz, $CDCl_3$) δ 7.43 (d, *J* = 7.07 Hz, 2H), 7.38 (t, *J* = 7.40 Hz, 2H), 7.32 (t, *J* = 7.21 Hz, 1H), 7.15 (d, *J* = 8.57 Hz, 2H), 6.91 (m, 2H), 5.04 (s, 2H), 3.60 (s, 3H), 3.17 (s, 3H), 2.90 (m, 2H), 2.71 (t, *J* = 7.32 Hz, 2H). $^{13}$C NMR (126 MHz, $CDCl_3$) δ 157.18, 137.14, 133.71, 129.40, 129.26, 128.56, 127.91, 127.46, 114.83, 70.02, 61.21, 36.20, 34.00, 32.16. HRMS calculated for $C_{18}H_{21}NO_3$: [M+Na]+: 322.1419 (found); 322.1404 (calc).

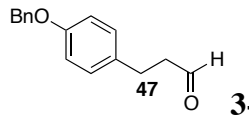

**47**

**3-(4-(Benzyloxy)phenyl)propanal**. A solution of **46** (584 mg, 1.95 mmol) in THF (15 mL) was cooled to -78 °C and treated with $LiAlH_4$ (148 mg, 3.90 mmol) in two portions. The reaction was stirred at this temperature for 3 h and quenched by pouring into ice. The mixture was filtered through Celite and the filterate extracted with $CH_2Cl_2$ (3x25 mL). The combined organic layers were washed with brine (1x) and dried over $Na_2SO_4$. The solvent was removed in vacuo and the resulting residue purified by FCC eluting with 10% EtOAc/Pent. to yield **47** that solidified upon standing (355 mg, 76%).

Alternate method: A solution of DIBAlH (1 M, 4.0 mL) was added dropwise to a solution of **45** (1071 mg, 3.765 mmol) in PhMe (20 mL) cooled to -78 °C. After stirring at this temperature for 2 h, the reaction was quenched with ~1mL MeOH and warmed to RT.

After 20 min, 20 mL of concentrated Rochelle salt solution was added and the mixture stirred vigorously for 30 min. The two layers were separated and the aqueous layer extracted with EtOAc (3x). The combined organic layers were washed with brine, dried over $Na_2SO_4$, and concentrated in vacuo. The residue was purified by FCC eluting with 10% EtOAc/Pent. to yield a white solid (859 mg, 95%).

Material prepared by either method was spectroscopically identical to literature values.[17]

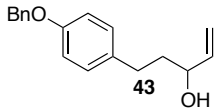

**43** **5-(4-(Benzyloxy)phenyl)pent-1-en-3-ol**. A solution of **47** (277 mg, 1.156 mmol) cooled to 0 °C was treated with a solution of vinyl magnesium bromide (1 M, 2.3 mL). The reaction was allowed to warm to RT over 5 h then quenched with HCl (2 M). The reaction mixture was extracted with $Et_2O$ (3x) and the combined organic layers were washed with brine and dried over $Na_2SO_4$. The solvent was removed in vacuo and the residue purified by FCC eluting with 10% EtOAc/Pent. to yield **43** as a clear oil (292 mg, 94%). $^1$H NMR (500 MHz, $CDCl_3$) δ 7.42 (d, *J* = 6.93 Hz, 2H), 7.37 (t, *J* = 7.41 Hz, 2H), 7.31 (ddd, *J* = 1.33, 4.48, 8.58 Hz, 1H), 7.11 (d, *J* = 8.67 Hz, 2H), 6.90 (d, *J* = 8.66 Hz, 2H), 5.89 (ddd, *J* = 6.17, 10.41, 17.11 Hz, 1H), 5.23 (dt, *J* = 1.40, 17.21 Hz, 1H), 5.12 (dt, *J* = 1.31, 10.41 Hz, 1H), 5.03 (s, 2H), 4.11 (dd, *J* = 6.14, 12.82 Hz, 1H), 2.65 (m, 2H), 1.81 (m, 2H), 1.62 (s, 1H). $^{13}$C NMR (126 MHz, $CDCl_3$) δ 157.00, 141.01, 137.14, 134.16, 129.34, 128.54, 127.88, 127.46, 114.86, 114.74, 72.41, 70.00, 38.67, 30.70. HRMS calculated for $C_{18}H_{20}O_2$: $[M+Na]^+$: 291.1366 (found); 291.1361 (calc).

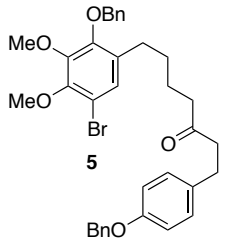


**5**

**7-(2-(Benzyloxy)-5-bromo-3,4-dimethoxyphenyl)-1-(4-(benzyloxy)phenyl)heptan-3-one.** Synthesized from **42** (150 mg, 0.397 mmol) and **43** (107 mg, 0.397 mmol) by general cross-metathesis procedure and purified by FCC eluting with 5% EtOAc/Hex. to yield **5** as a clear oil (56 mg, 23%) $^{1}$H NMR (500 MHz, $CDCl_3$) δ 7.42 (m, 4H), 7.37 (t, *J* = 7.47 Hz, 4H), 7.32 (tdd, *J* = 1.40, 3.15, 6.15 Hz, 2H), 7.07 (m, 3H), 6.89 (m, 2H), 5.03 (s, 2H), 5.00 (s, 2H), 3.91 (s, 3H), 3.90 (s, 3H), 2.80 (t, *J* = 7.65 Hz, 2H), 2.63 (t, *J* = 7.55 Hz, 2H), 2.47 (m, 2H), 2.32 (t, *J* = 7.25 Hz, 2H), 1.53 (dd, *J* = 7.50, 14.64 Hz, 2H), 1.46 (m, 2H).$^{13}$C NMR (126 MHz, $CDCl_3$) δ 210.17, 157.13, 150.14, 149.31, 147.56, 137.44, 137.08, 133.41, 133.07, 129.25, 128.56, 128.50, 128.10, 128.07, 127.91, 127.45, 127.26, 114.83, 114.81, 111.36, 69.99, 61.11, 61.05, 44.48, 42.68, 29.95, 29.42, 28.89, 23.40. HRMS calculated for $C_{35}H_{37}O_5$: $[M+Na]^+$: 639.1753 (found); 639.1722 (calc).

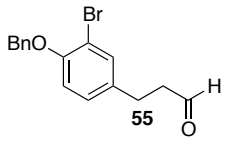


**55**

**3-(4-(Benzyloxy)-3-bromophenyl)propanal.** A solution of **54** (9.84 g, 27.0 mmol) in toluene (150 mL) was cooled in a dry-ice/acetone bath under an atmosphere of argon. A solution of DIBAlH (1.0 M in hex., 28 mL, 28 mmol) was added dropwise to the quickly stirring solution. After 2 h, the reaction was quenched with MeOH (1 mL) and warmed to RT. A concentrated solution of Rochelle's salt was added and the reaction was stirred vigorously for 1 hr. The organic layer was separated and the aqueous layer extracted with EtOAc (2 x 50 mL). The combined organic layers were

washed with $H_2O$ (3 x 50 mL) and brine (2 x 50 mL), then dried over $Na_2SO_4$ and concentrated in vacuo. The residue was purified by FCC (12-17.5%) EtOAc to yield **55** (7.46 g, 87%) as a clear oil that was spectroscopically identical to that prepared by Mori *et al*.[18]

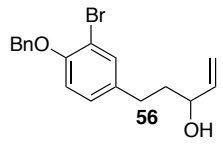


**5-(4-(Benzyloxy)-3-bromophenyl)pent-1-en-3-ol**. A solution of **55** (7.46 g, 23.4 mmol) dissolved in THF was cooled to 0 °C and treated with a solution of vinyl magnesium bromide (1.0 M in THF, 35.1 mL, 35.1 mmol). The reaction was slowly warmed to RT over 3 h and then quenched with aqueous HCl (6M, 10 mL). Th reaction was extracted with $Et_2O$ (4 x 60 mL) and the combined ethereal layers were washed with brine (2 x 100 mL), dried over $Na_2SO_4$, and concentrated in vacuo. The residue was purified by FCC eluting with 12% EtOAc/Pent.) to yield **16** as a clear oil (6.90 g, 85%).

**Enzymatic kinetic resolution.** A solution of (±)-**56** (4.42 g, 12.7 mmol) dissolved in diisopropyl ether (65 mL) with ~100 mg 4 Å molecular sieves was treated with vinyl acetate (1.76 mL, 19.1 mmol) and amano lipase from *Pseudomonas fluorescens* (50 w/w%). The reaction was stirred until half complete as observed by $^1$H-NMR (~24 hr). Reaction was filtered through celite and concentrated in vacuo. Residue purified by FCC (15%-20% EtOAc/Pent.) to yield **57** (2.186 g, 44%) as a clear oil and (*R*)-**56** (1.998 g, 45%) as a white solid.

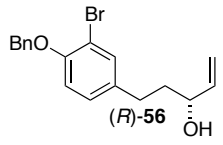


**(*R*)-5-(4-(Benzyloxy)-3-bromophenyl)pent-1-en-3-ol.** Melting point: 42-45 °C. $^1$H NMR (500 MHz, $CDCl_3$) δ 7.47 (dd, *J* = 0.96, 7.93 Hz, 2H), 7.41 (d, *J* =

2.14 Hz, 1H), 7.39 (t, *J* = 7.47 Hz, 2H), 7.32 (t, *J* = 7.33 Hz, 1H), 7.05 (dd, *J* = 2.16, 8.34 Hz, 1H), 6.85 (d, *J* = 8.36 Hz, 1H), 5.89 (ddd, *J* = 6.18, 10.41, 17.12 Hz, 1H), 5.24 (dt, *J* = 1.37, 17.20 Hz, 1H), 5.14 (td, *J* = 1.36, 2.80 Hz, 1H), 5.13 (s, 2H), 4.11 (m, 1H), 2.64 (m, 2H), 1.80 (m, 2H), 1.48 (d, *J* = 4.22 Hz, 1H). $^{13}$C NMR (126 MHz, $CDCl_3$) δ 153.21, 140.87, 136.68, 135.93, 133.27, 128.56, 128.26, 127.89, 127.01, 115.07, 113.93, 112.35, 72.27, 70.94, 38.41, 30.39. HRMS calculated for $C_{18}H_{19}BrO_2$: $[M+Na]^+$: 346.0588 (found); 346.0568 (calc.). $[\alpha]^{20}_D$=+4.4 (*c* 1.00, $CHCl_3$). Chiral HPLC: $t_r$ = 25.195 min, e.r. = 95:5.

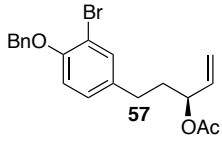


**(*S*)-5-(4-(Benzyloxy)-3-bromophenyl)pent-1-en-3-yl acetate.** $^1$H NMR (500 MHz, $CDCl_3$) δ 7.47 (dd, *J* = 0.59, 7.56 Hz, 2H), 7.39 (t, *J* = 7.45 Hz, 3H), 7.32 (t, *J* = 7.33 Hz, 1H), 7.02 (dd, *J* = 2.17, 8.34 Hz, 1H), 6.85 (d, *J* = 8.37 Hz, 1H), 5.79 (m, 1H), 5.23 (m, 3H), 5.13 (s, 2H), 2.57 (dt, *J* = 6.21, 9.25 Hz, 2H), 2.06 (s, 3H), 1.90 (m, 2H). $^{13}$C NMR (126 MHz, $CDCl_3$) δ 170.31, 153.29, 136.64, 136.11, 135.37, 133.15, 128.56, 128.16, 127.90, 127.01, 117.09, 113.93, 112.39, 74.13, 70.92, 35.74, 30.23, 21.21. HRMS calculated for $C_{20}H_{21}BrO_3$: $[M+Na]^+$: 441.0576 (found); 441.0572 (calc.). $[\alpha]^{20}_D$=+2.1 (*c* 1.00, $CHCl_3$).

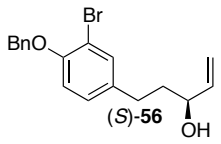


**(*S*)-5-(4-(Benzyloxy)-3-bromophenyl)pent-1-en-3-ol.** A solution of **57** (1.060 g, 2.723 mmol) in MeOH (30 mL) was cooled to 0 °C was treated with $K_2CO_3$ (1.129 g, 8.168 mmol) and stirred for 3 h. The reaction was diluted with $CH_2Cl_2$ (30 mL) and $H_2O$ (30 mL). The aqueous layer was extracted with additional $CH_2Cl_2$ (4 x 30 mL)

and the combined organic layers were dried over $Na_2SO_4$ and concentrated. The residue was purified by FCC eluting with 25% EtOAc/Pent. to yield (*S*)-**56** (0.946 g, 100%).$^1$H NMR (500 MHz, $CDCl_3$) δ 7.47 (m, 2H), 7.39 (m, 3H), 7.32 (m, 1H), 7.05 (dd, *J* = 2.17, 8.34 Hz, 1H), 6.85 (d, *J* = 8.36 Hz, 1H), 5.89 (ddd, *J* = 6.19, 10.41, 17.13 Hz, 1H), 5.20 (m, 2H), 5.13 (s, 2H), 4.11 (m, 1H), 2.64 (m, 2H), 1.80 (m, 2H), 1.49 (d, *J* = 4.22 Hz, 1H). $^{13}$C NMR (126 MHz, $CDCl_3$) δ 153.21, 140.87, 136.68, 135.93, 133.27, 128.56, 128.26, 127.89, 127.01, 115.07, 113.93, 112.35, 72.27, 70.94, 38.41, 30.39. HRMS calculated for $C_{18}H_{19}BrO_2$: $[M+Na]^+$: 369.0472 (found); 369.0466 (calc). $[\alpha]^{20}_D$= -4.5 (*c* 1.00, $CHCl_3$). Chiral HPLC: $t_r$ = 22.424 min, e.r. = 96:4.

**Mitsunobu procedures**

A solution of (*R*)-**56** (150 mg, 0.432 mmol) in THF was treated with AcOH (0.03 mL, 0.518 mmol) and $PPh_3$ (135.9 mg, 0.518 mmol). DIAD (0.10 mL, 0.518 mmol) was slowly added and reaction stirred overnight at RT. Reaction diluted with EtOAc (30 mL) and rinsed with aqueous HCl (2 M, 20 mL), sat. $NaHCO_3$ (20 mL), and brine (20 mL). Organic layer dried over $Na_2SO_4$ and concentrated in vacuo. The residue was purified by FCC eluting with 6-8% EtOAc/Pent. **57** as a clear oil (104.8 mg, 62%). $[\alpha]^{20}_D$= +2.1 (*c* 1.00, $CHCl_3$).

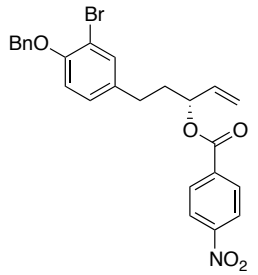


**(*R*)-5-(4-(Benzyloxy)-3-bromophenyl)pent-1-en-3-yl 4-nitrobenzoate.** A solution of (*S*)-**56** (149 mg, 0.429 mmol) in THF was treated with 4-nitrobenzoic acid (85.9 mg, 0.514 mmol) and $PPh_3$ (134.9 mg, 0.514 mmol). DIAD (0.11

mL, 0.53 mmol) was slowly added and the reaction stirred overnight at RT. The reaction was diluted with EtOAc (30 mL) and rinsed with aqueous HCl (2 M, 20 mL), sat. $NaHCO_3$ (20 mL), and brine (20 mL). The organic layer was dried over $Na_2SO_4$ and concentrated in vacuo. The residue was purified by FCC eluting with 7.5% EtOAc/Pent. to yield the title compound as a faint yellow oil (195 mg, 92%). $^1$H NMR (500 MHz, $CDCl_3$) δ 8.29 (d, *J* = 8.98 Hz, 2H), 8.17 (d, *J* = 9.01 Hz, 2H), 7.45 (d, *J* = 6.97 Hz, 2H), 7.39 (m, 3H), 7.32 (t, *J* = 7.30 Hz, 1H), 7.02 (dd, *J* = 2.17, 8.35 Hz, 1H), 6.82 (d, *J* = 8.38 Hz, 1H), 5.91 (ddd, *J* = 6.50, 10.52, 17.13 Hz, 1H), 5.53 (dd, *J* = 6.50, 12.89 Hz, 1H), 5.33 (ddt, *J* = 1.11, 10.52, 31.82 Hz, 2H), 5.09 (m, 2H), 2.66 (t, *J* = 7.83 Hz, 2H), 2.08 (m, 2H). $^{13}$C NMR (126 MHz, $CDCl_3$) δ 163.85, 153.39, 150.54, 136.53, 135.65, 135.46, 134.97, 133.14, 130.68, 128.58, 128.16, 127.93, 126.97, 123.53, 118.01, 113.88, 112.48, 75.98, 70.89, 35.61, 30.32. HRMS calculated for $C_{25}H_{22}BrNO_5$: $[M+Na]^+$: 518.0567 (found); 518.0579 (calc.) $[\alpha]^{20}_D$ = +0.7 (*c* 1.00, $CHCl_3$).

(*R*)-5-(4-(benzyloxy)-3-bromophenyl)pent-1-en-3-yl 4-nitrobenzoate (86.5 mg, 0.174 mmol) was dissolved in a combination of MeOH (5 mL) and THF (0.5 mL). $K_2CO_3$ (72.1 mg, 0.522 mmol) was added and the reaction was stirred at RT for 1 h. The solvent was removed in vacuo and the residue redissolved in $CH_2Cl_2$ (10 mL) and $H_2O$ (10 mL). The aqueous layer was extracted with additional $CH_2Cl_2$ (2 x 20 mL). The combined organic layers were washed with aqueous HCl (2 M, 10 mL) and brine (10 mL) then dried over $Na_2SO_4$ and concentrated in vacuo. The residue was purified by FCC eluting with 20 % EtOAc/Pent. to yield (*R*)-**56** (51.9 mg, 86%).

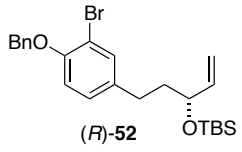


**(*R*)-((5-(4-(Benzyloxy)-3-bromophenyl)pent-1-en-3-yl)oxy)(*tert*-butyl)dimethylsilane (7).** A solution of (*R*)-**56** (1.596 g, 4.597 mmol) in $CH_2Cl_2$ (30 mL) was cooled in a dry-ice/acetone bath and treated sequentially with anhydrous $Et_3N$ (1.0 mL, 7.2 mmol) and TBSOTf (1.1 mL, 4.8 mmol). After 1 h, the reaction was warmed to RT and quenched with sat. $NaHCO_3$ (15 mL). The aqueous layer was separated and extracted with additional $CH_2Cl_2$ (3 x 25 mL). The combined organic layers were washed with $NaHCO_3$ and dried over $Na_2SO_4$. The solvent was removed in vacuo and the residue purified by FCC eluting with 5% EtOAc/Pent. to yield (*R*)-**52** as a clear oil (2.015 g, 95%). $^1$H NMR (500 MHz, $CDCl_3$) δ 7.47 (m, 2H), 7.38 (t, *J* = 7.48 Hz, 3H), 7.31 (m, 1H), 7.02 (dd, *J* = 2.13, 8.34 Hz, 1H), 6.84 (d, *J* = 8.36 Hz, 1H), 5.82 (ddd, *J* = 6.09, 10.37, 16.99 Hz, 1H), 5.16 (m, 1H), 5.13 (s, 2H), 5.06 (m, 1H), 4.13 (q, *J* = 6.21 Hz, 1H), 2.57 (m, 2H), 1.75 (m, 2H), 0.91 (s, 9H), 0.05 (s, 3H), 0.03 (s, 3H). $^{13}$C NMR (126 MHz, $CDCl_3$) δ 153.05, 141.32, 136.72, 136.60, 133.19, 128.54, 128.14, 127.86, 127.01, 114.10, 113.95, 112.29, 73.17, 70.96, 39.72, 30.23, 25.89, 18.26, -4.30, -4.83. HRMS calculated for $C_{24}H_{33}BrO_2Si$: $[M+Na]^+$: 346.0558 (found); 346.0568 (calc.) $[\alpha]^{20}_D$ = -7.8 (*c* 1.00, $CHCl_3$).

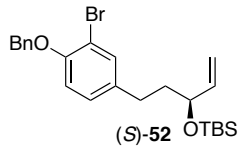


**(*S*)-((5-(4-(Benzyloxy)-3-bromophenyl)pent-1-en-3-yl)oxy)(*tert*-butyl)dimethylsilane ((*S*)-52).** Prepared from **(*S*)-56** (876 mg, 2.52 mmol) in 95% yield using the same procedure described for **(*R*)-52**. $^1$H NMR (500 MHz, $CDCl_3$) δ 7.47 (d, *J* = 6.97 Hz, 2H), 7.41 (d, *J* = 2.14 Hz, 1H), 7.39 (t, *J* = 7.47 Hz, 2H), 7.32 (t, *J* = 7.33 Hz,

1H), 7.05 (dd, *J* = 2.17, 8.34 Hz, 1H), 6.85 (d, *J* = 8.36 Hz, 1H), 5.89 (ddd, *J* = 6.19, 10.41, 17.13 Hz, 1H), 5.20 (m, 2H), 5.13 (s, 2H), 4.11 (m, 1H), 2.64 (m, 2H), 1.80 (m, 2H), 1.49 (d, *J* = 4.22 Hz, 1H). $^{13}$C NMR (126 MHz, $CDCl_3$) δ 153.21, 140.87, 136.68, 135.93, 133.27, 128.56, 128.26, 127.89, 127.01, 115.07, 113.93, 112.35, 72.27, 70.94, 38.41, 30.39. HRMS calculated for $C_{24}H_{33}BrO_2Si$: $[M+Na]^+$: 369.0472 (found); 369.0466 (calc). $[\alpha]^{20}_D$ = +7.8 (*c* 1.00, $CHCl_3$).

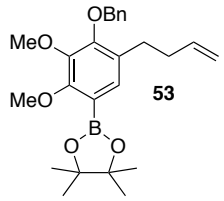

**53**

**2-(4-(Benzyloxy)-5-(but-3-en-1-yl)-2,3-dimethoxyphenyl)-4,4,5,5-tetramethyl-1,3,2-dioxaborolane.** In a glove box, $Pd(dba)_2$ (68.6 mg, 0.119 mmol) and $PCy_3$ (80.2 mg, 0.286 mmol) were combined in a Schlenk flask. The reaction vessel was removed from the glove box and 1,4-dioxane (24 mL) was added. The reaction was stirred at RT for 30 min before being treated with KOAc (585.3 mg, 5.964 mmol), $B_2Pin_2$ (1.211 g, 4.771 mmol), and **42** (1.500 g, 3.976 mmol). The reaction was heated to 80 °C for 24 h. The reaction was cooled to RT and treated with CuCl (15 mg, 0.15 mmol) to remove excess $PCy_3$ and stirred for 20 min before diluted with EtOAc (30 mL) and $H_2O$ (25 mL). The aqueous layer was extracted with additional EtOAc (3 x 30 mL). The combined organic layers were washed with brine (40 mL) and dried over $Na_2SO_4$. The solvent was removed in vacuo and the residue purified by FCC eluting with 5% EtOAc/Pent. to yield **53** as a faint yellow oil (1.110 g, 66%) $^1$H NMR (500 MHz, $CDCl_3$) δ 7.46 (d, *J* = 7.23 Hz, 2H), 7.38 (t, *J* = 7.29 Hz, 2H), 7.33 (t, *J* = 7.27 Hz, 1H), 7.25 (s, 1H), 5.83 (ddt, *J* = 6.60, 10.20, 16.87 Hz, 1H), 5.09 (s, 2H), 4.97 (m, 2H), 3.91 (s, 3H), 3.87 (s, 3H), 2.62 (dd, *J* = 6.76, 9.47 Hz, 2H), 2.28 (dd, *J* = 6.73, 16.08 Hz, 2H), 1.36 (s,

12H). $^{13}$C NMR (126 MHz, $CDCl_3$) δ 157.89, 153.51, 146.17, 138.53, 137.84, 131.36, 131.27, 128.43, 128.41, 127.96, 127.91, 114.52, 83.43, 75.02, 62.03, 61.02, 34.90, 29.71, 24.82. HRMS calculated for $C_{25}H_{33}BO_5$: $[M+Na]^+$: 447.2325(found); 447.2319 (calc.).

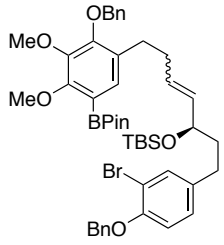


(*R*)-**51**

**(*R*)-((7-(2-(Benzyloxy)-3,4-dimethoxy-5-(4,4,5,5-tetramethyl-1,3,2-dioxaborolan-2-yl)phenyl)-1-(4-(benzyloxy)-3-bromophenyl)hept-4-en-3-yl)oxy)(*tert*-butyl)dimethylsilane.** Synthesized according to General Cross-Metathesis Procedure using **53** (364 mg, 0.858 mmol) and (*R*)-**52** (396 mg, 0.858 mmol) to yield (*R*)-**51** as a clear oil (644 mg, 88%). $^1$H NMR (500 MHz, $CDCl_3$) δ 7.47 (m, 4H), 7.37 (m, 5H), 7.31 (m, 2H), 7.24 (s, 1H), 7.00 (dd, *J* = 2.14, 8.37 Hz, 1H), 6.83 (d, *J* = 8.39 Hz, 1H), 5.55 (dt, *J* = 8.73, 13.51 Hz, 1H), 5.41 (m, 1H), 5.13 (s, 2H), 5.09 (s, 2H), 4.03 (m, 1H), 3.90 (s, 3H), 3.86 (s, 3H), 2.54 (m, 4H), 2.25 (dd, *J* = 7.57, 15.10 Hz, 2H), 1.69 (m, 2H), 1.34 (s, 12H), 0.88 (s, 9H), 0.02 (s, 3H), -0.02 (s, 3H). $^{13}$C NMR (126 MHz, $CDCl_3$) δ 157.94, 153.50, 153.00, 146.18, 137.80, 136.75, 134.44, 133.50, 133.21, 131.36, 131.17, 130.28, 128.54, 128.45, 128.18, 128.02, 127.98, 127.95, 127.85, 127.02, 113.95, 112.26, 83.42, 75.03, 73.00, 70.97, 62.03, 61.02, 40.09, 33.15, 30.46, 30.04, 25.95, 24.82, 18.25, -3.99, -4.74. HRMS calculated for $C_{47}H_{62}BBrO_7Si$: $[M+Na]^+$: 879.3440 (found); 879.3439 (calc.) $[\alpha]^{20}_D$ = +2.7 (*c* 1.0, $CHCl_3$).

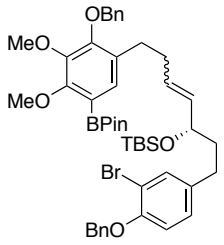


(*S*)-**51**

**(*S*)-((7-(2-(Benzyloxy)-3,4-dimethoxy-5-(4,4,5,5-tetramethyl-1,3,2-dioxaborolan-2-yl)phenyl)-1-(4-(benzyloxy)-3-bromophenyl)hept-4-en-3-yl)oxy)(*tert*-butyl)dimethylsilane.** Prepared from **53** (142 mg, 0.336 mmol) and **(*S*)-52** (155 mg, 0.336 mmol) in 79% yield using the same procedure described for (*R*)-**51**. $^{1}$H NMR (400 MHz, $CDCl_3$) δ 7.46 (m, 4H), 7.34 (m, 7H), 7.24 (s, 1H), 6.99 (t, *J* = 8.86 Hz, 1H), 6.82 (t, *J* = 8.49 Hz, 1H), 5.56 (m, 1H), 5.40 (m, 1H), 5.13 (s, 2H), 5.09 (s, 2H), 4.02 (m, 1H), 3.90 (s, 3H), 3.86 (s, 3H), 2.54 (ddd, *J* = 5.24, 9.46, 22.56 Hz, 4H), 2.25 (dd, *J* = 7.25, 15.43 Hz, 2H), 1.71 (m, 2H), 1.34 (s, 12H), 0.89 (s, 9H), 0.02 (s, 3H), -0.01 (s, 3H). $^{13}$C NMR (126 MHz, $CDCl_3$) δ 157.94, 153.50, 152.99, 146.18, 137.80, 136.74, 134.44, 133.50, 133.20, 131.36, 131.17, 130.28, 128.54, 128.45, 128.18, 128.02, 127.98, 127.95, 127.85, 127.02, 113.94, 112.25, 83.41, 75.03, 72.99, 70.96, 62.03, 61.01, 40.09, 33.15, 30.46, 30.04, 25.95, 24.82, 18.25, -3.99, -4.74. HRMS calculated for $C_{47}H_{62}BBrO_7Si$: $[M+Na]^+$: 879.3440 (found); 879.3439 (calc.) $[\alpha]^{20}_D$ = -2.7 (*c* 1.0, $CHCl_3$).

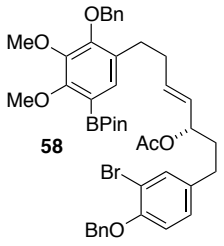


**58**

**(*S*)-7-(2-(Benzyloxy)-3,4-dimethoxy-5-(4,4,5,5-tetramethyl-1,3,2-dioxaborolan-2-yl)phenyl)-1-(4-(benzyloxy)-3-bromophenyl)hept-4-en-3-yl acetate.** Synthesized according to General Cross-Methathesis Procedure using **53** (236 mg, 0.557 mmol) and **57** (217 mg, 0.557 mmol) to yield **58** as a tan oil (217 mg, 50%). $^{1}$H NMR

(500 MHz, $CDCl_3$) δ 7.46 (ddd, *J* = 3.67, 7.90, 13.87 Hz, 4H), 7.37 (m, 5H), 7.32 (ddd, *J* = 1.97, 4.48, 7.79 Hz, 2H), 7.22 (s, 1H), 6.98 (dd, *J* = 2.14, 8.36 Hz, 1H), 6.83 (d, *J* = 8.38 Hz, 1H), 5.72 (m, 1H), 5.38 (m, 1H), 5.18 (dd, *J* = 6.94, 13.88 Hz, 1H), 5.13 (s, 2H), 5.08 (s, 2H), 3.90 (s, 3H), 3.86 (s, 3H), 2.60 (m, 2H), 2.49 (ddd, *J* = 2.44, 6.46, 8.93 Hz, 2H), 2.27 (m, 2H), 2.02 (s, 3H), 1.88 (m, 1H), 1.77 (m, 1H), 1.34 (s, 12H). $^{13}C$ NMR (126 MHz, $CDCl_3$) δ 170.30, 157.97, 153.50, 153.22, 146.15, 137.82, 136.68, 135.55, 134.17, 133.15, 131.38, 130.89, 128.56, 128.45, 128.19, 128.16, 127.98, 127.95, 127.92, 127.88, 127.01, 113.92, 112.35, 83.44, 75.03, 74.19, 70.93, 62.03, 61.02, 36.05, 33.32, 30.34, 29.75, 24.81, 21.34. HRMS calculated for $C_{43}H_{50}BBrO_8$: $[M+Na]^+$: 807.2704 (found); 807.2680 (calc.) $[\alpha]^{20}_D$ = -1.1 (*c* 1.0, $CHCl_3$).

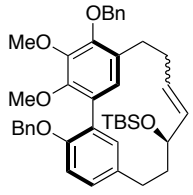

(*R*)-**59**

Synthesized according to general intramolecular Suzuki-Miyaura reaction procedure with (*R*)-**51** (415 mg, 0.483 mmol), $K_3PO_4$, and 1,4-dioxane/$H_2O$ (30:1, 24.2 mL) to yield (*R*)-**59** as a clear oil (88.0 mg, 26%). $^1H$ NMR (500 MHz, $CDCl_3$) δ 7.49 (m, 4H), 7.41 (m, 3H), 7.34 (m, 4H), 7.03 (d, *J* = 7.36 Hz, 2H), 6.85 (m, 1H), 5.56 (t, *J* = 10.56 Hz, 2H), 5.17 (s, 2H), 5.06 (s, 2H), 4.22 (m, 1H), 3.95 (s, 3H), 3.79 (s, 3H), 2.98 (s, 2H), 2.79 (dd, *J* = 12.18, 16.32 Hz, 2H), 2.53 (s, 2H), 2.19 (d, *J* = 15.88 Hz, 1H), 2.07 (dd, *J* = 10.89, 16.92 Hz, 1H), 0.87 (s, 9H), 0.07 (s, 3H), 0.03 (s, 3H). $^{13}C$ NMR (126 MHz, $CDCl_3$) δ 153.43, 149.71, 145.99, 140.47, 137.93, 137.70, 131.96, 128.87, 128.49, 128.46, 128.40, 128.31, 128.26, 128.14, 128.11, 127.99, 127.80, 127.64, 127.48, 127.37, 127.16, 112.66, 75.51, 74.78, 70.48, 60.87, 60.49, 37.92, 37.82, 29.71, 26.14, 25.90,

18.17, -4.03, -4.39. HRMS calculated for $C_{41}H_{50}O_5Si$: $[M+Na]^+$: 673.3342 (found); 673.3325 (calc.) $[\alpha]^{20}_D$=-2.0 (*c* 1.0, $CHCl_3$).

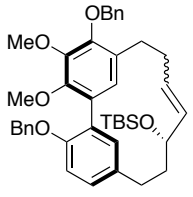

(*S*)-**59**

Prepared from **(*S*)-51** (175 mg) in 25% yield using the same procedure described for **(*R*)-1**.$^1$H NMR (500 MHz, $CDCl_3$) δ 7.50 (dd, *J* = 0.86, 7.75 Hz, 2H), 7.47 (m, 2H), 7.40 (m, 3H), 7.33 (m, 4H), 7.03 (m, 2H), 6.85 (d, *J* = 8.46 Hz, 1H), 5.54 (m, 2H), 5.17 (s, 2H), 5.06 (s, 2H), 4.22 (m, 1H), 3.95 (s, 3H), 3.79 (s, 3H), 2.98 (m, 2H), 2.79 (dd, *J* = 12.14, 16.24 Hz, 2H), 2.53 (d, *J* = 6.16 Hz, 2H), 2.21 (d, *J* = 8.34 Hz, 1H), 2.06 (m, 1H), 0.87 (s, 9H), 0.07 (s, 3H), 0.03 (s, 3H). $^{13}$C NMR (126 MHz, $CDCl_3$) δ 153.42, 149.71, 145.98, 140.46, 137.93, 137.69, 136.73, 135.79, 134.44, 131.95, 128.86, 128.48, 128.45, 128.39, 128.31, 128.25, 127.98, 127.80, 127.48, 127.36, 127.15, 112.66, 75.48, 74.77, 70.47, 60.86, 60.48, 37.85, 33.49, 30.37, 26.13, 25.90, 18.16, -4.03, -4.39. HRMS calculated for $C_{41}H_{50}O_5Si$: $[M+Na]^+$: 673.3351 (found); 673.3325 (calc.) $[\alpha]^{20}_D$=+2.0 (*c* 1.0, $CHCl_3$).

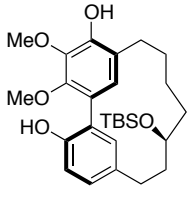

(*S*)-**60**

A solution of (*R*)-**59** (82.9 mg, 0.127 mmol) dissolved in EtOAc (25 mM) was treated with 10% Pd/C (20 w/w%) and placed under and atmosphere of $H_2$ by evacuating and backfilling with $H_2$ (3x). The reaction was stirred for 48 h then filtered through Celite. The filtrate was concentrated in vacuo and purified by FCC eluting with 10% EtOAc/Pent. to yield **(*S*)-60** as a white solid (47.2 mg, 78%). Melting point: 159-

162 °C. $^{1}$H NMR (500 MHz, $CDCl_3$) δ 7.65 (s, 1H), 7.19 (d, *J* = 1.93 Hz, 1H), 7.06 (dd, *J* = 2.27, 8.27 Hz, 1H), 6.94 (s, 1H), 6.90 (d, *J* = 8.20 Hz, 1H), 5.84 (s, 1H), 4.01 (m, 1H), 4.00 (s, 3H), 3.89 (s, 3H), 2.83 (m, 3H), 2.54 (ddd, *J* = 3.09, 11.58, 17.76 Hz, 1H), 2.25 (m, 1H), 1.91 (m, 3H), 1.73 (m, 1H), 1.65 (t, *J* = 12.48 Hz, 1H), 1.53 (m, 2H), 0.86 (s, 9H), -0.10 (s, 3H), -0.21 (s, 3H). $^{13}$C NMR (126 MHz, $CDCl_3$) δ 151.28, 147.64, 145.80, 138.66, 133.27, 130.98, 130.05, 129.39, 124.65, 123.59, 122.73, 116.74, 68.99, 61.46, 61.43, 39.38, 35.13, 27.00, 25.89, 25.85, 25.45, 23.25, 17.98, -4.33, -4.59. HRMS calculated for $C_{27}H_{40}O_5Si$: $[M+Na]^+$: 495.2996 (found); 495.2989 (calc.) $[\alpha]^{20}_D$= +26 (*c* 0.69, $CHCl_3$).

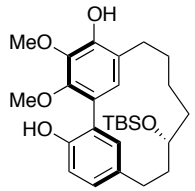

(*R*)-**60**

Prepared from **(*S*)-59** (30.5 mg, 0.0469 mmol) in 71% yield using the same procedure described for **(*S*)-60**. Melting point: 159-162 °C. $^{1}$H NMR (400 MHz, $CDCl_3$) δ 7.63 (s, 1H), 7.19 (s, 1H), 7.06 (d, *J* = 8.09 Hz, 1H), 6.91 (m, 2H), 5.84 (s, 1H), 4.03 (m, 1H), 3.99 (s, 3H), 3.89 (s, 3H), 2.83 (m, 3H), 2.53 (ddd, *J* = 3.26, 11.54, 17.75 Hz, 1H), 2.25 (m, 1H), 1.90 (m, 3H), 1.71 (m, 2H), 1.53 (m, 2H), 0.86 (s, 9H), -0.10 (s, 3H), -0.21 (s, 3H). $^{13}$C NMR (126 MHz, $CDCl_3$) δ 151.28, 147.65, 145.80, 138.67, 133.27, 130.98, 130.05, 129.39, 124.65, 123.59, 122.74, 116.74, 68.99, 61.46, 61.43, 39.38, 35.13, 27.01, 25.89, 25.85, 25.45, 23.25, 17.98, -4.33, -4.59. HRMS calculated for $C_{27}H_{40}O_5Si$: $[M-H]^-$: 471.2557 (found); 471.2567 (calc.) $[\alpha]^{20}_D$= -26 (*c* 0.69, $CHCl_3$).

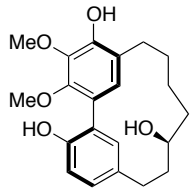

(+)-**1**

**(+)-Myricanol**. A solution of (*S*)-**60** (18.7 mg) in EtOH (5 mL) was acidified with conc. HCl (90 μL) and stirred at room temperature for 30 min. The reaction mixture was neutralized with aqueous $NaHCO_3$ and extracted with $CH_2Cl_2$ (4×20 mL). The combined organic layers were washed with brine, dried over $Na_2SO_4$ and concentrated in vacuo. The resulting residue was purified by FCC eluting with 33% EtOAc/Pent to yield a (+)-**1** as a white solid (11.3 mg, 80%). Melting point 100-103°C. $^1$H NMR (400 MHz, $CDCl_3$) δ 7.67 (s, 1H), 7.17 (s, 1H), 7.09 (dd, *J* = 2.26, 8.20 Hz, 1H), 6.90 (m, 2H), 5.86 (s, 1H), 4.09 (t, *J* = 9.76 Hz, 1H), 4.00 (s, 3H), 3.88 (s, 3H), 2.91 (m, 2H), 2.80 (dt, *J* = 3.31, 18.14 Hz, 1H), 2.54 (m, 1H), 2.34 (m, 1H), 1.92 (m, 3H), 1.70 (m, 2H), 1.57 (dd, *J* = 10.54, 14.25 Hz, 2H), 1.50 (s, 1H). $^{13}$C NMR (126 MHz, $CDCl_3$) δ 151.40, 147.71, 145.85, 138.63, 133.10, 130.64, 129.91, 129.37, 124.67, 123.42, 122.61, 116.86, 68.57, 61.43, 61.40, 39.44, 34.72, 26.89, 25.75, 25.41, 22.90. HRMS calculated for $C_{21}H_{26}O_5$: $[M\text{-}H]^-$: 357.1702 (found); 357.1702 (calc). $[\alpha]^{20}_D$=+51 (*c* 0.10, $CHCl_3$). Chiral HPLC: $t_r$=17.586 min, e.r. = 96:4.

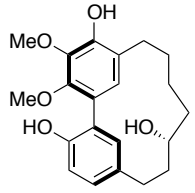

(-)-**1**

**(-)-Myricanol**. Prepared from **(*R*)-17** (9.7 mg) in 80% using the same procedure described for **(+)-1**. Melting point 100-103°C $^1$H NMR (500 MHz, $CDCl_3$) δ 7.66 (s, 1H), 7.17 (d, *J* = 1.85 Hz, 1H), 7.09 (dd, *J* = 2.33, 8.22 Hz, 1H), 6.90 (m, 2H), 5.83 (s, 1H), 4.09 (t, *J* = 9.83 Hz, 1H), 3.99 (s, 3H), 3.87 (s, 3H), 2.91 (m, 2H), 2.80 (dt, *J*

= 3.16, 18.07 Hz, 1H), 2.54 (m, 1H), 2.33 (m, 1H), 1.93 (m, 3H), 1.69 (m, 2H), 1.55 (m, 2H), 1.43 (s, 1H). $^{13}$C NMR (126 MHz, $CDCl_3$) δ 151.43, 147.71, 145.85, 138.63, 133.11, 130.62, 129.92, 129.38, 124.68, 123.44, 122.61, 116.87, 68.60, 61.43, 61.41, 39.44, 34.74, 26.90, 25.77, 25.41, 22.91. HRMS calculated for $C_{21}H_{26}O_5$: $[M-H]^-$: 357.1699 (found); 357.1702 (calc). $[\alpha]^{20}_D$=-51 (*c* 0.1, $CHCl_3$). Chiral HPLC: $t_r$=22.164 min, e.r. = 97:3.

**Reference**s:


(1) Simpson, D. S.; Lovell, K. M.; Lozama, A.; Han, N.; Day, V. W.; Dersch, C. M.; Rothman, R. B.; Prisinzano, T. E. Synthetic studies of neoclerodane diterpenes from Salvia divinorum: role of the furan in affinity for opioid receptors. *Org. Biomol. Chem.* **2009**, *7*, 3748.

(2) Riley, A. P.; Day, V. W.; Navarro, H. A.; Prisinzano, T. E. Palladium-catalyzed transformations of salvinorin A, a neoclerodane diterpene from *Salvia divinorum*. *Org. Lett.* **2013**, *15*, 5936.

(3) Riley, A. P.; Groer, C. E.; Young, D.; Ewald, A. W.; Kivell, B. M.; Prisinzano, T. E. Synthesis and kappa-opioid receptor activity of furan–substituted salvinorin A analogues. *J. Med. Chem.* **2014**, *57*, 10464.

(4) Beguin, C.; Duncan, K. K.; Munro, T. A.; Ho, D. M.; Xu, W.; Liu-Chen, L. Y.; Carlezon, W. A., Jr.; Cohen, B. M. Modification of the furan ring of salvinorin A: identification of a selective partial agonist at the kappa opioid receptor. *Bioorg. Med. Chem.* **2009**, *17*, 1370.

(5) Munro, T. A.; Xu, W.; Ho, D. M.; Liu-Chen, L. Y.; Cohen, B. M. Studies toward bivalent kappa opioids derived from salvinorin A: Heteromethylation of the furan ring reduces affinity. *Beilstein J. Org. Chem.* **2013**, *9*, 2916.

(6) Harding, W. W.; Tidgewell, K.; Byrd, N.; Cobb, H.; Dersch, C. M.; Butelman, E. R.; Rothman, R. B.; Prisinzano, T. E. Neoclerodane diterpenes as a novel scaffold for mu opioid receptor ligands. *J. Med. Chem.* **2005**, *48*, 4765.

(7) Tidgewell, K.; Groer, C. E.; Harding, W. W.; Lozama, A.; Schmidt, M.; Marquam, A.; Hiemstra, J.; Partilla, J. S.; Dersch, C. M.; Rothman, R. B.; Bohn, L. M.; Prisinzano, T. E. Herkinorin analogues with differential beta-arrestin-2 interactions. *J. Med. Chem.* **2008**, *51*, 2421.

(8) Tidgewell, K.; Harding, W. W.; Schmidt, M.; Holden, K. G.; Murry, D. J.; Prisinzano, T. E. A facile method for the preparation of deuterium labeled salvinorin A: Synthesis of [2,2,2-$^{2}H_{3}$]-salvinorin A. *Bioorg. Med. Chem. Lett.* **2004**, *14*, 5099.

(9) Beguin, C.; Richards, M. R.; Li, J. G.; Wang, Y. L.; Xu, W.; Liu-Chen, L. Y.; Carlezon, W. A.; Cohen, B. M. Synthesis and in vitro evaluation of salvinorin A analogues: Effect of configuration at C(2) and substitution at C(18). *Bioorg. Med. Chem. Lett.* **2006**, *16*, 4679.

(10) Harding, W. W.; Schmidt, M.; Tidgewell, K.; Kannan, P.; Holden, K. G.; Gilmour, B.; Navarro, H.; Rothman, R. B.; Prisinzano, T. E. Synthetic studies of neoclerodane diterpenes from *Salvia divinorum*: Semisynthesis of salvinicins A and B and other chemical transformations of salvinorin A. *J. Nat. Prod.* **2006**, *69*, 107.

(11) Chan, B. K.; Ciufolini, M. A. Total synthesis of streptonigrone. *J. Org. Chem.* **2007**, *72*, 8489.

(12) Dandepally, S. R.; Williams, A. L. Liebeskind-Srogl cross coupling mediated synthesis of verbenachalcone. *Tetrahedron Lett.* **2010**, *51*, 5753.

(13) Pilkington, L. I.; Barker, D. Total synthesis of (-)-isoamericanin A and (+)-isoamericanol A. *Eur J. Org. Chem.* **2014**, *2014*, 1037.

(14) Whiting, D. A.; Wood, A. F. Total syntheses of the *meta,meta*-bridged biphenyls (±)-myricanol and myricanone, and of an isomeric biphenyl ether, a 14-Oxa-[7,1]-metapara-cyclophane. *J. Chem. So.c Perk., Trans. 1* **1980**, 623.

(15) Xing, X. C.; Padmanaban, D.; Yeh, L. A.; Cuny, G. D. Utilization of a copper-catalyzed diaryl ether synthesis for the preparation of verbenachalcone. *Tetrahedron* **2002**, *58*, 7903.

(16) Bennie, L. S.; Fraser, C. J.; Irvine, S.; Kerr, W. J.; Andersson, S.; Nilsson, G. N. Highly active iridium(I) complexes for the selective hydrogenation of carbon-carbon multiple bonds. *Chem. Comm.* **2011**, *47*, 11653.

(17) Frost, C. G.; Hartley, B. C. Lewis base-promoted hydrosilylation of cyclic malonates: Synthesis of β-substituted aldehydes and γ-substituted amines. *J. Org. Chem.* **2009**, *74*, 3599.

(18) Mori, K.; Yamamura, S.; Nishiyama, S. Synthesis of spirodienone derivatives and their conversion into dihydrobenzopyrans. *Tetrahedron* **2001**, *57*, 5533.